# A STUDY OF FLUIDISED BED GRANULATION

A thesis submitted for the degree of Ph.D.

in the University of London

by

Peter Geoffrey Smith B.Sc. (Eng.)

February 1980

Ramsay Laboratory of
Chemical Engineering

University College London

ABSTRACT

An experimental study of fluidised bed granulation is presented. Preliminary experiments establish the main variables in the granulation process and enable a systematic experimental programme to be devised.

In this programme, either glass powder or porous alumina are used as the bed material. The effects of the fundamental fluidised bed granulation parameters on particle growth are established from a series of batch experiments conducted in a 0·15 m diameter, glass-walled bed. Together with measurements of the physical properties of the product granules and the binder solutions (carbowax or benzoic acid, in methanol) and with supporting studies of the bed structure (in the form of X-ray photography and measurement of temperature profiles), this information is also used to propose a mechanism of particle growth.

Two types of product granule are identified; agglomerates which consist of two or more, and usually several, initial particles: and layered granules, which consist of single initial particles with dried feed material adhering to the surface. The effects of varying the excess fluidising gas velocity, the binder concentration and the initial particle size are quantified. A bed can be prevented from quenching (a defluidisation phenomenon leading to the failure of the process) by increasing the fluidising gas rate. For a given bed particle / binder combination, successively higher excess gas velocities allow an otherwise quenching bed to be operated firstly so as to produce agglomerates and subsequently layered granules. Similar effects are observed with increases in initial bed particle size and decreases in binder concentration.

A particle growth mechanism is proposed in which the initial stages of both desirable particle growth (irrespective of the type of granule) and of bed quenching, are considered to be exactly the same. Beyond the initial formation of liquid bonds between adjacent bed particles, the strength of the inter-particle bridges (which is a function of the binder material and relates to growth) and the extent of fluid drag and inertial forces on particles (which are functions of gas velocity and particle size respectively, and relate to granule breakdown) determine the equilibrium granule form and size. However, if the particles are porous the above mechanism may break down since the liquid can enter the pores and not be available for the initial formation of liquid bonds.

X-ray photography shows that the mode of entry of atomising air into the bed is by periodic bubbling, rather than by continuous issue from a jet of air, thus throwing considerable doubt upon the traditionally proposed mechanism of growth by particle circulation through a high voidage zone. Nevertheless, the temperature measurements indicate that a substantial portion of the bed below the atomising nozzle is at a significantly lower temperature than the remainder.

The experimental particle growth data for both types of product granule fit simple geometrical models. In the case of agglomeration, a relationship is established between average granule size and binder content.

TO MY PARENTS

"Human history becomes more and more a race
between education and catastrophe."

H.G. Wells

"For in much wisdom is much grief: and
he that increaseth knowledge increaseth sorrow."

Ecclesiastes 1.18

ACKNOWLEDGEMENTS

I wish to thank the following:

Dr. A.W. Nienow for his supervision of the project and his constant encouragement,

Professor P.N. Rowe for provision of the facilities for research and for many helpful discussions,

Mr. H.J. MacGillivray and Mr. D.J. Cheesman for their technical assistance and help with the design of apparatus,

Mr. D.F. Montgomery, Mr. L.J.Coates and the technical staff of the Department for construction of apparatus.

My wife Liz for her constant support,

The Science Research Council for financial assistance.

TABLE OF CONTENTS

LIST OF FIGURES

ADDENDUM

page

LIST OF TABLES

# CHAPTER ONE

# INTRODUCTION

## 1.1 FLUIDISATION

When a fluid is passed upwards through a bed of particles, the bed remains packed at low fluid velocities. However, if the velocity is increased sufficiently a point will be reached at which the drag force on a particle is balanced by the net gravitational force. This is the point of incipient fluidisation, at and beyond which the bed is said to be fluidised. The superficial fluid velocity at the point of incipient fluidisation is called the minimum fluidising velocity. At velocities in excess of that required for minimum fluidisation, one of two phenomena will occur. The bed may continue to expand, and the particles space themselves uniformly, or alternatively excess fluid may pass through the bed as bubbles, giving rise to the analogy of a boiling liquid. The former is known as particulate fluidisation and in general occurs with liquid-solid systems. The latter, with which the present work is concerned, occurs with most gas-solid systems and is called aggregative fluidisation.[1] Throughout this thesis the term fluidisation is taken to mean gas-solid fluidisation.

A fluidised bed is characterised by rapid particle movement, caused by the rising bubbles, and consequently good particle mixing, high rates of heat transfer and uniform temperature profiles are possible.[2] These properties have led to the use of fluidised beds in a wide range of physical and chemical processes, including drying, roasting, calcination, particle mixing and catalytic chemical reactions. A review of some of the uses of fluidisation is given by Priestley.[3]

## 1.2 FLUIDISED BED GRANULATION

Fluidised bed granulation is a term that has been applied to processes which produce granules or dry powder from a solution or slurry in a fluidised bed to which sensible heat is applied. Growth of bed particles, creation of new particles and drying of the product may all take place. Heat for evaporation of the solvent or for removal of moisture from bed particles can be supplied either in the fluidising air or through the bed walls, and the wet feed material may be introduced under, or sprayed onto the bed surface.

The word "granulation" is taken to cover all forms of particle growth and not a specific mechanism; "particle" refers to the bed material at any stage of the process, "initial particle" refers specifically to particles charged to the fluidised bed, before growth takes place and the word "granule" is used to mean any product particle. Terms such as agglomeration and layering are used to describe individual modes of growth. Since the terminology used in the literature is often contradictory, in the survey which follows, the above definitions have been adhered to.

Free liquid, at first sight, would seem to be incompatible with a fluidised bed and indeed severe practical problems can result from their interaction. An excess of liquid feed, either over the whole bed or in a localised region, produces excessive and uncontrollable particle agglomeration and leads to a loss of fluidisation, or what Nienow and Rowe[4] have called "wet quenching". The defluidisation phenomenon, which results in the failure of the process (see Section 3.1.2), has been called simply "bed quenching" in this work. The term "dry quenching" has been adopted when defluidisation is the result of the excessive formation of dry granular material and "wet quenching" has been reserved for the cases where failure is caused by excessive free liquid. Despite the apparent incompatibility, the use of a fluidised bed for granu-

lation offers several advantages over more traditional methods such as spray drying for inorganic chemicals, prilling for fertilisers and pan, or rotary drum, granulation for pharmaceuticals. Good heat transfer, uniform bed temperatures and close temperature control are advantages which are particularly important when heat sensitive materials are being handled. In comparison with a spray drier in particular, a fluidised bed represents a large reduction in plant volume for the same throughput. Closer control of the physical properties of the product, such as particle size, flow characteristics, bulk density, is possible: a fluidised bed relies not only on the fine atomisation of the feed liquid but also its interaction with existing bed particles in the complex hydrodynamic regime of the bed. For example, the formation of particles of a larger mean size (perhaps by an order of magnitude) is possible in a fluidised bed.

The type of particle produced, and its properties, is important in its subsequent use - for example the high voidage of agglomerates enables the quick dissolution and distribution of active compounds in a pharmaceutical granulation. Applications of fluidised bed granulation techniques in nuclear technology (the production of uranium trioxide and the calcination of radioactive waste) have been possible because of the lack of moving parts in a fluidised bed and the ability to build an enclosed system.

Some large scale industrial applications have been reported[5,6] and commercial fluid bed granulators are available.[7,8,9] Improvements to such systems have been the subject of a number of patents.[10,11,12]

## 1.3 OBJECTS OF THE CURRENT WORK

Introducing a liquid into a fluidised bed immediately creates problems and, as will be apparent from the survey of available literature, is often responsible for the failure of fluid bed granulation devices. Also apparent is the lack of a clear understanding of exactly how particle growth occurs - a process which ultimately determines the product properties. The objects of this experimental study can be summarised, therefore, as follows:

(i) to gain an understanding of the particle growth mechanism or mechanisms which take place in what is known as a fluidised bed granulator;

(ii) to discover why fluidised bed granulators sometimes "quench" and defluidise when liquid feed is introduced;

(iii) to ascertain the operating limits, and optimum operating conditions of, a fluidised bed granulator.

# CHAPTER TWO

# LITERATURE SURVEY

## 2.1 INTRODUCTION

This chapter surveys the reported work on granulation within a fluidised bed, together with that on other relevant particle growth processes. The applications of fluidised bed granulation fall into three groups:

(i) the calcination of uranyl nitrate and the granulation of the resultant uranium trioxide; the calcination of radioactive aluminium nitrate wastes;[13,14,15]

(ii) the drying and granulation of solutions or melts of inorganic chemicals, for example sodium chloride;[16]

(iii) pharmaceutical granulation, in which particles are agglomerated by the addition of a binding agent.[17]

However, despite these well-defined areas of application, the following sections will deal with the fluidised bed granulation literature according to the various mechanisms commonly governing the granulation process and the effect of various process parameters.

Very little experimental work has been reported which attempts to explain, comprehensively, the underlying principles of fluidised bed granulation. The physics of fluidisation has been largely ignored; this is reflected in the fact that not a single paper reports on the variation of the most fundamental fluidisation parameter - relative gas velocity. The effect of using different materials, either bed particles or feed solution, and the effect of their physical properties is obscured by work which is geared to development of a particular process. An exception to the general lack of systematic study is the series of papers by Ormos and his co-workers.[18,19,20,21,22] The literature contains only one extensive review[4] and little has been published since it appeared in 1975.

## 2.2 MASS AND ENERGY BALANCES

Several workers[5,14,23,24,25] have described the technique, outlined in the previous chapter, of producing particle growth by introducing a solution into a bed fluidised with hot air. The fundamental mass and thermal energy balance equations have been set out by Scott et al.[25] and, in summary, by Nienow and Rowe[4] and are reproduced here. Referring to Fig. 2.1, the mass balance is:

$$w + W_a = W_a + w(1 - x_s) + x_s w \qquad (2.1)$$

liquid in + air in = aid out + vapour out + solids out

Consequently the heat balance is:

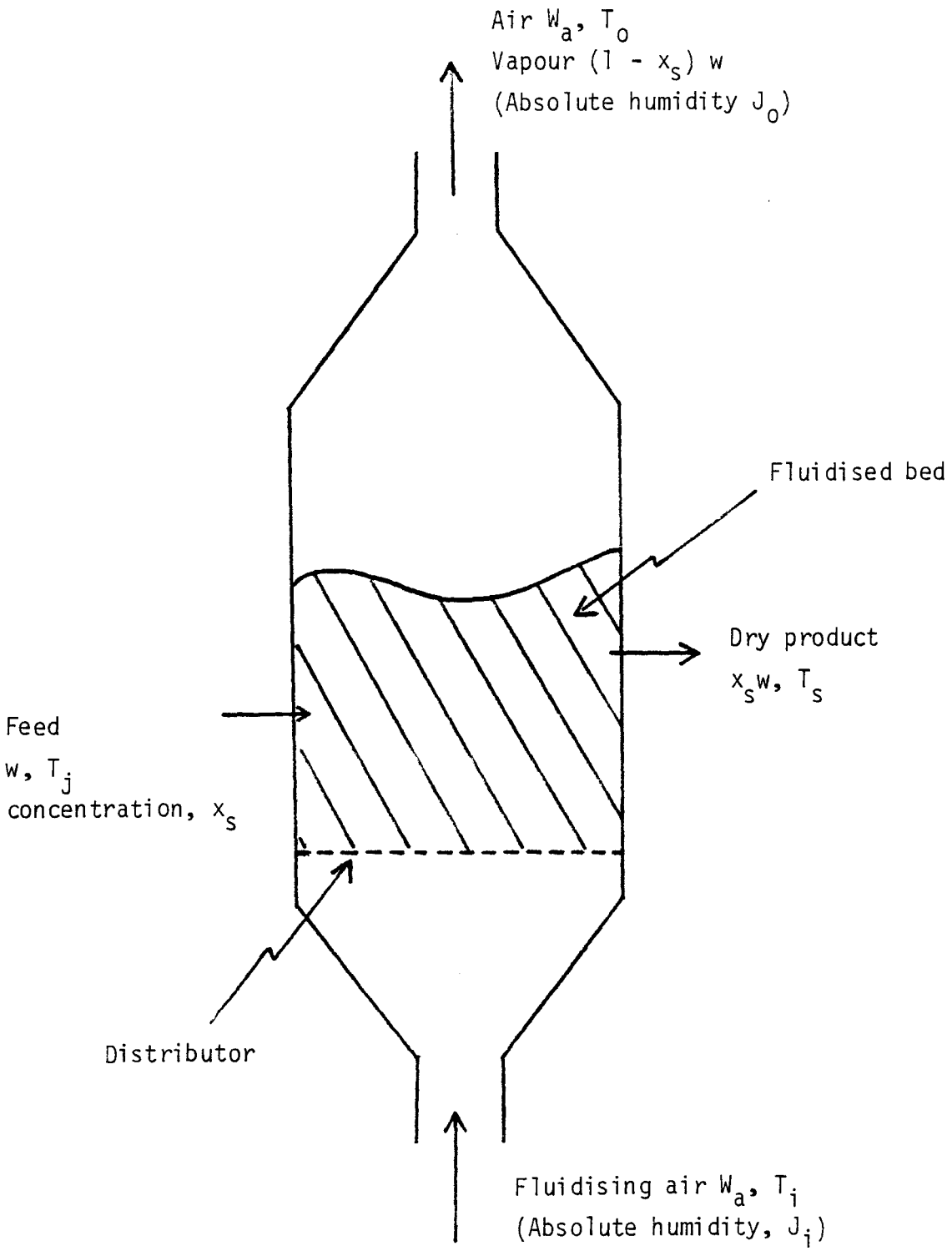


Fig. 2.1 Schematic diagram of a fluidised bed granulator

$$\frac{Wa}{w} c_a(T_i - T_o) + c_j T_j + \frac{q_w}{w}$$

$$= (1 - x_s)(c_v T_o + \lambda) + x_s c_s T_s + \frac{q_L}{w} \qquad (2.2)$$

In a fluidised bed, $T_s$ is very close to $T_o$. A moisture balance may also be written:

$$w = \frac{W_a(J_o - J_i)}{(1 - x_s)} \qquad (2.3)$$

In these equations it is assumed that the solid product has an acceptable moisture content (which could be zero). Equ. 2.3 stipulates that,[25] for a given bed outlet temperature, the liquid feed rate must not exceed that which will saturate the outlet air stream. Scott et al.[25] point out that, if Equ. 2.3 is not obeyed, the bed material will become increasingly over-wet. Continued operation under these conditions will rapidly lead to wet quenching and the failure of the process (see Section 3.1.2).

Nienow and Rowe[4] use the heat balance (Equ. 2.2) to illustrate a possible fundamental difference between fluid bed granulation and spray drying. For a spray drier $q_w = o$, but with a fluidised bed a considerable amount of the required heat may be put in through the bed walls. The term $q_w$ must be substantial if the fluidising air flowrate is to be reduced significantly.[26]

## 2.3 BATCH AND CONTINUOUS OPERATION; PARTICLE SIZE AND ITS CONTROL

It is possible to operate a fluidised bed granulator in either a batch or a continuous mode. Batch operation, often associated with pharmaceutical applications,[27] produces a continuous increase in bed weight and therefore, if attrition and particle breakdown effects are not dominant, a continuous increase in bed particle size. This necessitates a gradual increase in the volumetric air flow through the bed, to compensate for the increasing minimum fluidising velocity and thus maintain the "degree" or "quality" of fluidisation.[19]

With continuous operation it is desirable to maintain a stable particle size distribution. Clearly, in order that granules do not grow to be too large, seed particles or nuclei must be added to the bed, together with the removal of large particles. Dunlop et al.,[23] in an investigation of the fluid-coking process, assumed that the equilibrium particle size distribution (PSD) was determined by the size of, and the rate of, both seed addition and product removal. Equations predicting the equilibrium PSD are presented for both the cases of non-selective withdrawal and selective withdrawal of coarse particles. Metheney and Vance[28] controlled the particle size distribution by adjusting the size of seed particles, the liquid to solid feed ratio and by means of an in-bed classification device. Control of the PSD can be effected by external grinding and crushing of the oversize and by recycle to the bed of nuclei.[5] In some cases particle size reduction has been achieved inside the fluidised bed by grinding with high velocity air jets.[23,29,30] Jonke et al.[14] found that it was possible to control the particle size distribution by a proper choice of operating conditions, for example bed temperature, and therefore the need to recycle ground product as seed particles was eliminated.

Control of PSD in a particle growth process, particularly by means of adjusting the product removal stream, is better understood in the

unit operation of crystallisation, and is well-documented.[31] It has been suggested[4] that much may be learnt about the operation of fluidised bed granulators by studying the crystallisation literature.

## 2.4 BED QUENCHING

### 2.4.1 Introduction

It has been claimed[4] that the capacity of a fluidised bed granulator is limited by the amount of free liquid that can be tolerated in the bed. Certainly defluidisation due to bed quenching is one of the major reasons for unsuccessful operation of fluidised bed granulators, a proportion of papers in the literature report such problems, although whether wet or dry quenching is the cause is not clear. Bed quenching, however, is not confined to fluidised bed granulation. Similar phenomena have been reported in the high temperature reduction of beds of fine iron ore,[32] the carbonising or combustion of coal particles[33,34] and high temperature sintering of copper and glass beads.[32] In all of these processes bed quenching can be disastrous unless it is anticipated and controlled.

Very early in experimental studies it was realised that good liquid distribution would prevent bed quenching and serious caking problems, and consequently atomising spray nozzles were used,[14] with the idea of reducing the amount of liquid feed associated with each bed particle. Rapid particle mixing will prevent the build-up of localised moisture and it has been suggested[4] that the mixing obtained in a fluidised bed, being a good approximation to perfect mixing, combined with top-spraying of feed, enables granulation to be carried out without bed quenching. Further, a much more ordered particle circulation pattern, as in for example a spouted bed[35] (see Section 2.5.2) or vortex bed,[36] is likely to prevent agglomeration and hence quenching.

### 2.4.2 Feed methods

In most of the reported work in which a liquid feed is introduced into a fluidised bed two-fluid atomising nozzles have been employed, either entering through the bed wall and below the bed surface, or positioned in the freeboard region with feed being sprayed onto the

fluidised surface. The principle of operation of a two-fluid nozzle is that an annulus of compressed air is mixed, either in the nozzle or externally, with a central stream of liquid which produces finely divided droplets of liquid. Early work in the United States[14,16] showed that this type of nozzle gave rise to fewer practical problems than single-fluid, pressure nozzles; for example Markvart et al.[37] report the use of a mechanical (single-fluid) nozzle to be a failure due to blockage by bed particles, an observation confirmed by Mortensen and Hovmand.[5] Despite the weight of opinion it has been claimed[38] that pneumo-mechanical sprays are more effective and allow stable granulation without the formation of lumps or coarse agglomerates. Detailed discussion of the selection of nozzles for fluidised bed applications is given by Legler,[39] who concludes that two-fluid nozzles are the most satisfactory.

However, although its use is widespread, the literature contains several references to severe problems encountered with this form of liquid injection. These include caking of the nozzle,[40] bed walls and distributor plate,[17] nozzle blockage (prevention of which often requires elaborate start-up procedures[41]), nozzle erosion[39] and severe agglomeration or quenching of the fluidised solids.[5,30] Several workers[5,28,30,40] have varied the atomising nozzle geometry and position in an attempt to improve performance or eliminate caking problems. Jonke et al.[14] report that positioning the nozzle in the freeboard and spraying liquid feed onto the fluidised surface results in caking of feed material on both nozzle and in the bed. There is also a danger of overspraying onto the bed walls with this arrangement.[28] Nozzle caking was still a problem when the nozzle was mounted in a hole cut in the distributor plate with the spray directed upwards.[14] In a study of pharmaceutical granulation Davies and Gloor[27] found that the number of large agglomerates formed in the bed increased as the

atomising nozzle was lowered towards the bed surface.

Of the groups of applications listed in Section 2.1, it can be said that, in most cases, the processes in groups (i) and (ii) (calcination and solution granulation) adopt side entry of the atomising nozzle through the bed wall, and that those in group (iii) (pharmaceutical granulation) locate the nozzle in the freeboard of the bed. When side entry is used the vertical position within the fluidised layer has variously been claimed to be either of only minor importance,[14] or to be critical in preventing bed quenching.[30,40] A detailed study of problems encountered with this nozzle geometry is reported by Otero and Garcia[42] who present expressions to describe the extent of formation of lumps and cakes of feed material as a function of operating variables. They and other sets of workers[41,43,44] conclude that projection of the nozzle tip, or the liquid duct of the nozzle, into the fluidised bed (by distances up to 0·004 m) dramatically reduces such problems.

The degree of atomisation of the feed is reported to have considerable effect on the product granule size (see Section 2.6.2), although little has been determined about its effect on bed quenching. Feeding sodium sulphate solutions through a hyperdermic needle,[45] and thus without atomisation, resulted in large agglomerates which segregated and formed a defluidised layer on the distributor. At the other extreme, Ormos et al.[21] found that increasing the flow of atomising air beyond a certain point caused liquid to penetrate too deeply into the bed and clog the distributor plate.

The literature also contains references[7,22] to purely mechanical methods of preventing bed quenching, by means of rotating blades which break up agglomerated material at the bottom of the bed.

2.4.3 The effect of operating parameters on bed quenching

In an early attempt to remove mists from a gas stream, by using a fluidised bed as a kind of filter,[46] it was found that the operation

worked well if the bed particles had a porous structure, and that when non-porous particles were used fluidisation ceased (i.e. the bed quenched) at very low moisture contents. McCarthy et al.,[47] in a similar study, report that liquid aerosols are best collected with fluidised beds of porous particles in order to increase bed capacity, and that non-porous particles have shorter useful "lives", because bed quenching may occur after a period of collection. This view is supported in recent work on the effect of bed moisture on the fluidisation characteristics of fine powders,[48] in which it was shown that porous materials can tolerate considerably more liquid than non-porous particles (such as glass ballotini, sand and limestone) before what these workers call "bed compaction" occurs. All of this work indicates that problems such as bed quenching are less likely to arise with bed materials which have some intra-particle porosity. It is interesting to note that several of the successful applications of fluidised bed granulation, covering a range of materials, give rise to porous product particles; calcination of uranyl nitrate[40,49] and aluminium nitrate[50] solutions, the granulation of ammonium nitrate[38] and the fluid-coking process.[23]

Of the other parameters mentioned in the literature which determine whether fluidised beds quench or operate in a stable condition, fluidising gas velocity would seem to be the most important. The superficial gas velocities required to give sufficient mixing to avoid caking or lump formation in the bed have been quoted for particular systems,[5,50] although no indication of the relative gas velocities involved are given. Similarly it is reported that lumps form in the bed "when the gas velocity is too low",[14] and that "it is necessary to exceed the normal fluidising velocity to maintain good fluidisation of wet agglomerates".[28] Gluckmann et al.[32] report that beds of iron ore, of sticky coke particles and of sintering copper particles, are all governed by well-defined operating limits. Precise temperature and velocity boundaries could be drawn between normal fluidisation and a

"slumped", or quenched, condition in which gas passed through the bed in channels. Fluidisation could usually be recovered if the gas velocity was increased. These authors also carried out experiments in which a viscous liquid ($\mu$ = 4·1 Pa s) was added to beds of cracking catalyst at room temperature. The defluidisation velocity was found to be directly proportional to the amount of liquid introduced, in other words at a higher velocity more liquid was required to produce bed quenching. An increase in the minimum fluidising velocity has been noted when liquid bonds exist in the bed,[51] and water on the surface of (non-porous) particles smaller than 335 $\mu$m is stated as making fluidisation impossible. It has been observed that the chances of bed quenching are greater at high liquid feed rates,[14,52,53] and low bed temperatures,[14] and the granulation of pharmaceutical powders at room temperature[27] also failed due to "overwetting" of the bed material. In both cases it is unclear whether this is a result of insufficient heat being supplied to the bed, or is a genuine temperature effect. The former seems more likely.

A single instance is reported[52] of severe agglomeration problems with a bed of narrow particle size distribution, the degree of fluidisation being improved by using a wider distribution.

## 2.5 PARTICLE GROWTH MECHANISMS

### 2.5.1 Fluidised bed granulation

There has been much speculation about the precise mechanism by which particles grow in a fluidised bed granulator, and some supporting experimental evidence, although much of the latter is contradictory. Several authors have put forward particle growth schemes,[5,14,23,37,40] the essence of which is as follows:

> when the liquid feed is sprayed through an atomising nozzle into, or onto the surface of, a fluidised bed, discrete liquid droplets are formed which may either dry and form new discrete particles, or combine with existing bed particles in one of two ways:
>
> (i) the liquid coats the particle surface, dries before a collision with a second particle is possible and consequently produces a growth layer, or crust, of the dissolved feed substance;
>
> (ii) wet particles coalesce and the liquid between them dries to form solid bridges and thus produces an agglomerate of two or more primary particles.

In a continuous granulation system the equilibrium particle size will be determined by the balance between growth mechanisms, like those outlined above, and mechanisms which lead to particle breakdown,[19,43,44] of which the most important are attrition and thermal shock.[30,49,50,54] Attrition is variously reported to be insignificant,[44] independent of major operating parameters (gas velocity, feed concentration and atomising air rate),[43] or alternatively to be very significant and due largely to the effects of feed spraying[50] or of the fluidising gas.[5,37,41,55]

Direct comparison of different experimental studies is difficult because, usually, each is concerned with a single feed material or bed material and the work is designed to gain understanding of a particular process, for example the drying of sodium sulphate solutions.[45] Only

one systematic study is reported[18,19,20,21,22] and thus, from a study of the literature, it is not easy to identify which growth mechanisms are important and how they are influenced by operating parameters and the physical properties of the materials used. The idea has been proposed[43,44,56] of specific "spray zones" of atomised liquid existing within a fluidised bed, through which the bed particles pass in a regular and ordered manner and thus are regularly and evenly coated with the feed liquid. This, it is suggested, gives rise to concentric growth rings around a core consisting of the original particle. This type of growth appears to be restricted to the work on high temperature calcination and solution granulation. Pharmaceutical granulation, in which the object is to combine several different powders in the final granule, is concerned only with growth by agglomeration (with the exception of applying final coats to large drug particles[57,58,59]). Here the feed liquid is a binder solution prepared specifically to promote agglomeration[60] whereas, for example, in radioactive waste calcination the emphasis is on treating and processing a given liquid stream rather than a bed of particulate material.

Dunlop and his co-workers[23] have shown, with photographic evidence, that coke particles grow by the addition of uniformly thick layers and similar results have been described for aluminium nitrate calcination.[44] In both cases growth rates are independent of particle size. Other papers, describing the formation of porous alumina from aluminium nitrate, have reported spherical, layered particles but with size-dependent growth rates,[50,56,61] as well as alumina layers around a core of non-porous sand. An un-named radioactive waste has been processed with similar results.[41] The evidence for layered or "onion-ring" growth in the work mentioned above depends on the sectioning of individual particles and various tracer techniques. The same conclusions about growth mechanism have been drawn from observations of a rounding-off of initial bed particles to give a spherical product.[62]

Some studies have produced both types of product particle, either co-existent[14,49,62] or at different temperatures.[37] Mortensen and Hovmand[5] have suggested that the growth mechanism depends upon such physical properties as the solubility and stickiness of wet particles or the feed concentration, and have granulated sodium and ferous sulphates by layering and agglomeration mechanisms respectively.

2.5.2 Spouted bed granulation

Granulation and drying of solutions in a spouted bed is probably more widespread than the literature would suggest,[35] although it was first demonstrated in 1961.[63] A spouted bed consists of a conical base with a central gas inlet and a vertical cylindrical section containing the bed particles. Solids are entrained in the central high velocity gas stream and, after forming a fountain or spout, fall back onto an annulus of particles which move slowly downwards. Particle motion which is regular and ordered (far more so than in a fluidised bed), large particles and high gas velocities are all characteristic of a spouted bed. Mathur and Epstein[35] point out the advantages of this type of equipment: it is suitable for continuous operation, gives a product of near uniform size and allows particles to grow much larger than in a fluidised bed granulator. The high voidage, high temperature zone near the gas inlet allows very rapid evaporation of solvent and, together with the cyclic particle motion, results in very low rates of agglomeration.

Little fundamental study has been reported, although two papers are concerned with the mechanisms affecting particle growth and both report on experiments in batch granulators. Uemaki and Mathur[64] granulated ammonium sulphate and recorded growth over periods of up to nine hours, with granules between $1.0 \times 10^{-3}$ and $4.0 \times 10^{-3}$ m in diameter being produced. In similar apparatus[65] sodium chloride granules up to $7.0 \times 10^{-3}$ m in diameter were produced from a 23% feed solution. Both sets of workers conclude that the dominant mechanism is growth by

continuous deposition and layering of solute on the seed particles, although the evidence presented for the relative significance of competing mechanisms, and for size dependency of growth, is contradictory. Uemaki and Mathur also interpret their data in terms of a simple model, since modified,[66] which is based on a mass and number balance.

2.5.3 Other types of granulation

Considerable attention has been given to the growth mechanisms which exist in rotary drums and tumblers and the literature contains reviews of the techniques and basic principles of this type of size enlargement.[67,68] Experimental studies, in general, have employed ideal systems and simple materials such as sand, with water as the binding agent. This approach is of wider interest than would be the study of a particular process and allows closer comparison of reports in the literature.

Newitt and Conway-Jones[69] published the first attempt at an understanding of basic mechanisms. They postulated that water was held initially in discrete lens-shaped rings between individual particles in what they called a pendular state. Funicular and capillary states followed with increasing liquid content of the system in which a continuous liquid network between particles, but interspersed with air, becomes a granule with all of its void spaces filled with liquid. On collision, two such aggregates are kneaded together by the tumbling action of the drum and, because of their surface plasticity, form an approximately spherical granule. Capes and Danckwerts[70] suggested that this sequence of events, forming a nucleation stage, continued until the granules were sufficiently large that the torque tending to separate them was too great to allow a permanent bond. Subsequent growth occurred by a "crushing and layering" mechanism in which the smallest and weakest granules are crushed by larger ones and the material redistributed around the surface of the large granule in a

uniform layer. A distinction must be drawn here between the layering of smaller particles around a larger granule and the layering or onion-ring type deposition of solute on a core particle in fluidised bed granulation.

In contrast it has been claimed that coalescence is mainly responsible for growth,[71] although Linkson et al.[72] show that this is due to the use of a wide size distribution of particles which form strong granules, resistant to crushing, and then grow by coalescence until a terminal size is reached. Some of this work[69,70] showed that the amount of liquid required for granulation was equal to the saturation content of the voids and therefore a function of the packing density of the original particles. Sherrington[73] found that only one half of this amount was required and subsequently developed a model to relate liquid phase content and average granule size. This is discussed with other modelling work in Section 2.7.2.

## 2.6 EFFECT OF OPERATING PARAMETERS ON GROWTH

### 2.6.1 Rate and volume of feed

The growth rates of particles in a fluidised bed granulator increase when increasing quantities of solute or binder are introduced into the bed, either by increasing the feed rate of solution or the concentration of dissolved solids,[14] and as might be expected in a batch operation, the mean particle diameter increases with the volume of liquid introduced.[19,53] The growth data of Rankell et al.[17] pass through a maximum, suggesting that a spray rate exists at which the agglomeration of bed particles is balanced by attrition and break-down, a tendency noted in another agglomerating system.[19] Most of the information on particle growth as a function of the rate, volume and concentration of feed liquid is to be found in the published work on pharmaceutical granulation, in which agglomeration is the dominant growth mode. Similar detailed information is not available for layering systems, except where experimental data have been fitted to growth models. These are discussed in Section 2.7.1.

Several authors[19,27,53,74] have found that the rate of spraying a fixed amount of feed into the bed affects particle growth. Generally, increased addition rates (i.e. shorter total spraying times) have produced larger mean particle diameters and Davies and Gloor[27] attribute this, as well as a slight increase in granule porosity (or lower packing density), to greater penetration of the bed by the liquid feed. However, the results described by Ormos et al.[19,20] are not in agreement and show a slight decrease in mean diameter at higher rates, although no change was observed in the spread of the particle size distribution. This work also indicates that shorter spraying times, for a fixed feed volume, are responsible for less uniform distribution of binder between different particle size fractions, something which is important in assessing the quality of drug granules.[53]

2.6.2 Nozzle position and atomising air rate

In addition to its effect on bed quenching, the position of the atomising nozzle appears to have some consequences for particle growth, particularly when "top spraying" of the feed is employed and spray drying occurs in the freeboard.[39] Smaller mean particle diameters, due to an increased spray drying effect, are reported when the nozzle is placed at increasing distances from the bed surface;[27] maximum growth occurring when the nozzle is actually below the bed surface.[5,17] The findings of Ormos et al.[21] do not agree here; they report no change in particle size with nozzle position and claim that spray drying is a stronger function of air temperature and liquid droplet size. An equation is presented which predicts the optimum nozzle height by avoiding overspray onto the bed walls. Increasing the air to liquid ratio (normalised air ratio, or NAR) through the nozzle gives a smaller particle size which has been attributed to both attrition[24,50] and to the production of finer liquid droplets.[27]

2.6.3 Bed temperature

It has been verified experimentally[17] that allowable liquid flowrates are directly proportional to the air inlet temperature; however the true effect of bed temperature is unclear. Granulation of pharmaceutical powders with aqueous binding solutions,[27,53] below 100°C, has shown that mean particle size decreases with increasing bed temperature. Davies and Gloor[27] increased the air inlet temperature to the bed over the range 25° C to 55° C (giving a higher bed temperature for the same liquid flowrate) and claim this to be responsible for decreased penetration and wetting of the fluidised solids, and consequently the observed decrease in mean particle diameter from 311 μm to 235 μm. Conversely, three sets of workers investigating the calcination of uranyl nitrate at high temperatures have found particle size to increase with temperature. Various explanations have been offered to account for this. Bjorklund and Offutt[30] have controlled the mean particle dia-

meter, in the range 150 to 400 μm, by alternating the bed temperature between 300°C and 400°C although they give no indication of the mechanism involved. Philoon et al.,[24] working at bed temperatures around 700° C, explain their observations by postulating that bed voidage (at a given gas velocity) increases with temperature and that this results in preferential growth of the fewer particles present in the spray zone. A more plausible theory[14] is that higher temperatures result in a more rapid evaporation of nitrate on the particle surface - before penetration of the intra-particle pores is possible - and therefore fracture of the particle, due to vaporisation within the pores, is avoided. In this way the net growth is greater at higher temperatures. However these same authors report the opposite effect of temperature with aluminium nitrate calcination, i.e. lower bed temperatures promoting particle agglomeration.

2.6.4 Fluidising gas velocity

For a given fluidised bed geometry and particle size, the superficial gas velocity through the bed is the most important and fundamental parameter - affecting bed expansion, the extent of bubbling and particle mixing, in other words the degree or quality of fluidisation. For this reason it is very surprising that the effect of velocity on the granulation process, and particularly on particle size, remains largely uninvestigated. Almost no quantitative information is available and the majority of experimental studies have been carried out at a constant gas velocity chosen, for example, to give the least elutriation and maximum cylone efficiency[17] or perhaps the lowest possible velocity consistent with adequate fluidisation.[30] Qualitative observations have suggested that an increase in gas velocity leads to less agglomeration[5] due to the higher degree of particle-particle impact and attrition, and that a more uniform particle size distribution is produced with higher fluidising air rates.[45] Data has been presented[21]

which shows that an increase in bed expansion produces a linear decrease in mean particle diameter, because of increased abrasion, although the corresponding gas velocities are not given.

2.6.5 Particle size

Size dependent growth of particles has been reported in a few cases.[41,44,53,56] Grimmett[56] suggests that larger particles remain for longer in the spray zone because the atomising air forms a barrier through which large particles selectively penetrate.

2.6.6 Binder properties

The effect of different binders and solutes, and their physical properties, on the granulation process and on the nature of the product granules can be judged only from the literature on pharmaceutical granulation. Higher concentrations of feed solution (at a given solution flowrate) obviously increase the amount of solid material available to produce growth of bed particles, but it has been also clearly demonstrated that different binders (at the same concentration) have very different growth characteristics.[75] Water alone was a very poor granulating agent,[17,76] while diluted syrup gave granules which were too small for tabletting and only an aqueous gelatin solution produced a satisfactory granulation.[17] The literature does not contain any data on the physical properties of binder solutions and therefore conclusions must be drawn solely from qualitative observations and remarks. For example, Davies and Gloor[75] have linked the effectiveness of binders with their adhesiveness or tackiness and have found that more viscous binder solutions increase the size of granules and reduce the bulk density. Hydroxypropylcellulose (HPC) - with which atomising difficulties were encountered because of its viscosity - was responsible for the largest increase in mean particle size over the concentration range 2·0 to 4·25 % w/w formula weight. This was closely followed, in its effect on particle growth, by aqueous gelatin solutions, the vis-

cosity of which are known to increase exponentially with concentration. HPC solutions increased mean particle diameters to 257 μm at 2% w/w and 406 μm at 4·25% w/w, whilst solutions of povidone produced granules with mean diameters of only 200 μm and 250 μm respectively. This growth effect is reflected in the granule friability data which showed that gelatin and HPC solutions produced significantly stronger granules than other binders. Gelatin has also been used to granulate quartz sand to produce particles of high wear resistance.[19]

Crooks and Schade[53] successfully granulated lactose particles with aqueous solutions of polyvinylpyrolidone (PVP), however, attempts to repeat the experiments with solutions of PVP in absolute alcohol failed because of the relative insolubility of lactose in the solvent. Wurster[57,58] reports using a variety of binders in preparing coated drug particles. Solutions of carbowax (polyethylene glycol), "simple syrup", starch and combinations of these in both water and methyl alcohol have been used, but no information is supplied about their relative performance.

## 2.7 GROWTH MODELS

### 2.7.1 Fluidised bed granulation

A number of mathematical models have been developed to describe layered, or onion-ring, growth in continuous systems, which involve the application of the population balance concept.[77] The far more complicated case of agglomeration[78] has however been ignored from a fluidised granulation point of view. Markvart et al.[37] devised an equation to indicate the type of growth taking place and whether significant particle break-down existed. If no agglomeration or break-down is present, then:

$$\log \frac{dp}{(d_p)_{t=o}} = \frac{1}{6{\cdot}91} \frac{(P)}{(Z)} t \qquad (2.4)$$

where $d_p$ is the particle size at time t, P is the product discharge rate and Z is the bed hold-up. A plot of log dp / $(dp)_{t=o}$ against Pt / Z should result in a straight line of slope 1 / 6·91. Deviations from this indicate that onion-ring growth is not the only mechanism operating, for example a slope much greater than 1 / 6·91 suggests that agglomeration is taking place.

Most models[41,44,56] assume that bed particles pass regularly through a well-defined spray zone, and that growth can be described by Equs. 2.5 and 2.6, in which $R^1$ is a constant.

$$dp = (d_p)_{t=o} + R^1 t \qquad (2.5)$$

$$\frac{d\,(dp)}{dt} = R^1 \qquad (2.6)$$

Grimmett[56] has found growth to be size dependent and thus suggests Equ.2.7.

$$\frac{d\,(dp)}{dt} = R^1 + R^{11}.dp \qquad (2.7)$$

Dunlop et al.,[23] Lee et al.,[44] Fukomoto et al.[41] and Shakhova et al.[78] have all assumed the bed to be perfectly mixed, that the product removal steam has a representative particle size distribution and that their models are equivalent to a mixed suspension, mixed product removal

crystalliser.[31] More complex mathematical descriptions can include functions to represent attrition,[43] or to predict particle size distributions rather than mean particle diameters.[79]

Whilst these models may predict particle growth in a fluidised bed granulator quite well under certain conditions, they do not give any indications of precise growth mechanisms.

2.7.2 Steady-state agglomeration models

Sherrington,[73] in experiments conducted in a paddle mixer, found that the liquid phase requirement for sand granulation was considerably less than previous work[69,70] had suggested. This observation was explained by the development of a dry granule surface model, which related the liquid to solid ratio in the granulator to the final granule size. It was found that, at residence times greater than four minutes, the mean product size was independent of residence time and therefore this may be regarded as a steady-state model. A similar theory was proposed independently by Butensky and Hyman.[80] The details of the model, which has been used with agglomeration data acquired in the present study, are set out in Section 3.3.2.

Recently Capes et al.[81] have suggested the use of Equ. 2.8 to predict binding liquid requirements for agglomeration by tumbling.

$$F = \frac{1}{1 + K\frac{\rho_S}{\rho_L}} \qquad (2.8)$$

Here, F is the weight fraction of liquid in the agglomerate, $\rho_S$ and $\rho_L$ are the solid and liquid densities respectively and K is a parameter theoretically equal to $(1 - \varepsilon) / \varepsilon\rho_L$, where $\varepsilon$ is the agglomerate void fraction. The authors have fitted data from over forty published papers to Equ. 2.8 and recommend volumes for K of 1·85 for particles smaller than 30 μm and 2·17 for particles larger than 30 μm.

## 2.8 GRANULE STRENGTH

### 2.8.1 Theory

Whilst the theoretical treatment of the strength of moist agglomerates and particles bound by liquid is quite extensive,[82] solid bridges between particles "do not lend themselves readily to theoretical treatment".[68] The strength of crystalline bridges depends not only on the amount of material present, but also upon its structure.[83] A finer crystal structure results in stronger bonds and there is some correlation between bond strength and higher drying temperatures. The complex interaction of drying behaviour and the tensile strength of agglomerates is detailed by Pietsch and Rumpf.[84] Pietsch,[85] by assuming that all the material available for forming solid bridges is distributed uniformly over all points of contact between constituent particles in the granule and that the material has a constant tensile strength, has defined the strength of an agglomerate ($\Psi$) by Equ.2.9:

$$\Psi = \varepsilon \, \theta \, f \qquad (2.9)$$

in which $\varepsilon$ is the voidage in the granule, f is the fraction of the void volume filled with binder and $\theta$ is the intrinsic tensile strength of the bridge.

Little more can be said from a theoretical point of view. For a given concentration of binder, particle size and granule size, granule strength is clearly a function of the structure and physical properties of the binder used. Further information can only be obtained by experiment.

### 2.8.2 Measurement of granule strength

Although the literature contains references to standard methods for determining the strength of, for example, pharmaceutical tablets,[86,87] there does not appear to be a definitive test for granules.[18] Several workers, however, report on methods of varying sophistication.

Ganderton and Selkirk[88] simply crushed granules with a spatula and

observed that strength was a function of the amount of granulating liquid present. Harwood and Pilpel[89] placed a single 0·0028 m diameter granule on a horizontal plate so that it was just in contact with the underside of one of two balance pans which were in equilibrium. Lead shot was then poured into the pan until the granule disintegrated and the resulting mass of shot was taken as the granule strength. In a similar way Newitt and Conway-Jones[69] used two flat plates, one of which was the pan of a spring-balance, to load granules. A more elaborate technique is described by Gold et al.[90] who employed a mechanical linkage to apply compressive loads to single granules at a uniform rate. A Strain-gauge instrumental cantilever beam converted the load into a millivolt response which then drove a chart recorder. A further method described by at least four sets of workers,[18,91,92,93] depends upon subjecting closely sieved granules to attrition and abrasion for a given period and then measuring the percentage of material retained on a certain screen, upon which 100% of the original material was retained. Thus Fonner et al.[91] produced a hardness index, equal to the fraction of -850 + 600 μm granules retained upon a 600 μm screen after being shaken for five minutes in a closed box.

# CHAPTER THREE

# THEORETICAL CONSIDERATIONS

## 3.1 PRINCIPLES OF FLUIDISED BED GRANULATION

### 3.1.1 The balance between granulation and fluidisation

The successful operation of a fluidised bed granulator depends upon the balance between two, essentially opposing, factors. Firstly the binding mechanism which results in particles joining together to form larger ones because of the presence of liquid in the fluidised layer and, secondly, the abrasive action of, and solids circulation within, the fluidised bed - which tends to break down, or prevent the formation of, agglomerated particles. The magnitude and relative importance of these effects will depend upon, on the one hand, the quantity and physical properties of the liquid feed and, on the other, upon the characteristics of the fluidised bed such as the size and nature of the bed particles and the fluidising gas velocity.

When a liquid, in any quantity, is introduced into a fluidised bed, liquid bands will be formed between individual bed particles, unless the particles are porous and capable of absorbing liquid. The formation of these bonds, which involve considerably stronger forces than either Van der Waal or electrostatic effects, is inevitable - whether the required particle growth is to be by agglomeration or by layering - because contact between two wet particles cannot be avoided in the dense phase. The extent and strength of these bonds will depend upon the amount of liquid available and its adhesiveness with the solid surface and the strength of the resultant solid bridges will be a function of the amount of deposited material and its intrinsic strength.

In conventional granulators the mechanical action of the system, such as the tumbling or rolling of a drum, helps in the binding process by kneading the materials together. In contrast, the particle motion in a fluidised bed acts against the binding mechanism and tends to control agglomeration and bond formation and consequently the particle size. The initial stages of agglomeration and bed quenching are identi-

cal and, for a given liquid feed, the fluidised bed parameters determine whether controlled particle growth takes place or whether the bed defluidises. At one extreme it may be imagined that liquid sprayed into a packed bed, or a bed at the minimum fluidising velocity, will result in a large, agglomerated mass of wet particles, whilst at the other, in a dilute phase system, fewer particles will contact the liquid and those that do are much less likely to come together and form permanent bonds.

Although it is not suggested that the two elements which have been outlined above act consecutively to produce a granular material - the physical picture is obviously far more complex - it is important to realise that the existence of the "binding element" and the "fluidisation element" differentiates fluidised bed granulation from other rival processes such as rotary drum granulation and, more particularly, spray drying.

### 3.1.2 Factors leading to bed quenching

The heat and mass balances over a fluidised bed granulator must be satisfied if it is to operate successfully without wet quenching. Sufficient heat must be supplied to the bed, either through the bed walls or in the fluidising gas, to provide the latent heat of vaporisation of the solvent, and the quantity of solvent evaporated must not exceed that which will saturate the off-gases at the operating temperature. Failure to meet either of these requirements will result in excess liquid in the fluidised layer and therefore wet quenching. Clearly there must be a limit to the amount of liquid that can be tolerated in the bed and beyond which operation becomes impossible. This excess need not be over the whole bed, but may occur in a localised region, for example close to the nozzle or "feed zone". Localised wet quenching in this manner will give large clumps or agglomerates which then segregate at the bottom of the bed. Once this has happened, and

the bed is partly defluidised, loss of important fluidised bed characteristics (such as particle mixing and good heat transfer) quickly follow leading to further agglomeration and complete failure of the process. This will certainly be the case if the bed is not sufficiently well fluidised to break-up agglomerates as they form. Whether wet or dry quenching occurs depends on the rate of drying of the feed liquid and therefore its concentration and the bed temperature.

Other than gas velocity and the physical properties of the feed, particle size is a parameter which will have a significant effect. Smaller bed particles are more likely to form permanent bonds, and to quench, because of their smaller inertia. The force tending to pull apart two particles is equal to the product of the particle mass and the distance between the two centres of mass. For the case of two spherical particles joined together at their surfaces, this force will be proportional to the particle diameter raised to the fourth power. Other cases will approximate to this relationship.

## 3.2 DISCUSSION OF PARTICLE GROWTH MECHANISMS

### 3.2.1 Criticism of existing growth mechanisms

The mechanisms proposed to account for layered growth rely on the existence of a region of high voidage, a "spray zone", through which bed particles pass in a regular and ordered manner. It is far from certain that such regimes can exist within a fluidised bed; a spray zone, with a submerged nozzle, would require a jet to be blown in the dense phase by the atomising air and recent work by Rowe et al.[94] has shown that this does not occur. Plainly, atomisation of a liquid beneath the fluidised surface cannot be the same as atomisation into free air, and in the absence of a permanent high voidage zone the often quoted physical picture of small liquid droplets adhering to, and coating, single bed particles seems unrealistic. Bubbles, formed from either the fluidising or atomising gas, may approximate to the required void zone but they will be periodic and the same arguments can be used against the theory when bubbles are not present. Further, should such a zone exist the circulation of particles (although not entirely random because it is caused by relatively regular bubble motion) is far from ordered and the coating procedure which may take place in a spouted bed cannot occur. However, granules have been produced which consist of a core particle surrounded by deposited feed material. The subsequent mathematical models in the literature have described the product particles but have made no attempt to explain the precise mechanism by which such granules are produced.

### 3.2.2 Consideration of the fluidising gas velocity and of particle mixing

There is some evidence in the literature (see Section 2.6.4) to suggest that the fluidising gas velocity affects the extent of agglomeration and that its magnitude is an important factor in determining whether or not a bed will quench. The two-phase theory of fluidisation states that an increase in the superficial gas velocity through the bed,

over and above the minimum fluidising velocity, will increase the volumetric bubble flow through the bed. Bubbles are the only cause of particle motion in a gas-solid system and thus particle circulation will be proportional to the excess gas velocity.[95] Bed quenching is less likely if the solids circulation rate increases relative to the liquid feedrate. Better particle mixing will mean improved liquid distribution and a reduced possibility of localised quenching. However, should quenching occur and substantial inter-particle bonds or bridges form, higher gas velocities than for normal operation will be required to prevent segregation[96] and ensure that clumps of material do not build-up at the bottom of the bed.

It is also more probable, at higher velocities, that increased inter-particle impacts, and impacts between particles and submerged surfaces, will result in greater abrasion and break-down of agglomerates. Some slight improvement in heat and mass transfer between moist particles and the fluidising gas can also be expected.

### 3.2.3 Binder properties

The nature of the feed liquid and its physical properties will affect liquid distribution within the bed and thus the distribution of binder after solvent has evaporated. The viscosity of the feed liquid will affect its atomisation characteristics and, for the same atomising air flow, more viscous liquids will give a larger droplet size.[97] Solutions which become increasingly viscous as solvent evaporates may also have different distribution characteristics from those whose viscosity remains more or less constant. The distribution of binder is important in determining the type of granule produced; particles whose surfaces become entirely covered with liquid have a greater chance of drying before impacting with other particles and thus giving layered growth. Perhaps more probable, and more importantly, their contacts with similarly coated particles are less likely to result in permanent

bonds because less binder will be concentrated into the small area of contact.

## 3.3 PROPOSED GROWTH MODELS

### 3.3.1 Layered growth

When layered, or onion-ring, growth takes place in a batch granulator a simple expression for the increase in mean particle diameter with time can be obtained by assuming uniform distribution of binder around an idealised core particle - a physical picture which is illustrated in Fig. 3.1.

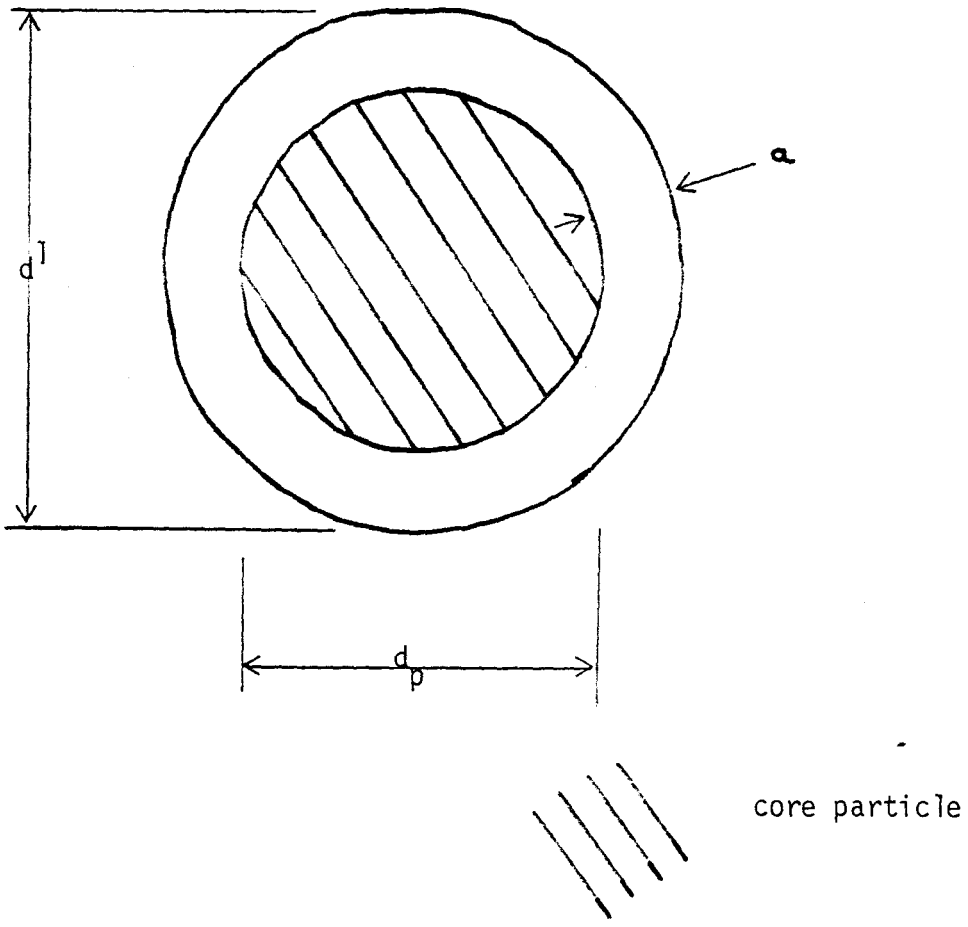


Fig. 3.1 Layered growth model

Suppose the fluidised bed contains n particles, all of which are spherical and have a diameter $d_p$. If all of the binder, or solute, which is introduced into the bed is distributed evenly so that each particle is coated with a layer of thickness a, then the mean bed particle diameter for a given mass of distributed binder, $d^1$, is given by Equ. 3.1:

$$d^1 = d_p + 2a \tag{3.1}$$

The volume of binder adhering to each core particle is equal to the difference in volume between a sphere of diameter $d_p$ and a sphere of diameter $d^1$, thus:

$$\Delta V = V_{d^1} - V_{d_p} \tag{3.2}$$

$$\text{and: } \Delta V = \frac{\Pi}{6} (d_p + 2a)^3 - \frac{\Pi}{6} dp^3 \tag{3.3}$$

which becomes:

$$\Delta V = \frac{\Pi}{6} (8a^3 + 12a^2 d_p + 6d^2{}_p a) \tag{3.4}$$

The mass of a single core particle, m, is given by:

$$m = \frac{\Pi}{6} d^3{}_p \, \rho_s \tag{3.5}$$

and, if M is the total mass of bed particles, then:

$$n = \frac{M}{m} \tag{3.6}$$

and the total number of particles in the bed is:

$$n = \frac{6M}{\rho_s \, \pi \, d^3{}_p} \tag{3.7}$$

The volume of binder associated with each particle, $V_b$, is:

$$V_b = \frac{M_b}{\rho_b \, n} \tag{3.8}$$

where $M_b$ is the mass of binder introduced into the bed. Substituting from Equ. 3.7 gives:

$$\frac{V_b = M_b \, \Pi \, d^3{}_p \, \rho_s}{6M \, \rho_b} \tag{3.9}$$

Equating $V_b$ with $\Delta V$ and combining Equs. 3.4 and 3.9 gives:

$$\frac{M_b \pi d_p^3 \rho_s}{6 M \rho_b} = \frac{\pi}{6} (8a^3 + 12a^2 d_p + 6d_p^2 a) \qquad (3.10)$$

and therefore:

$$4a^3 + 6a^2 d_p + 3 d_p^2 a = \frac{M_b \rho_s d_p^3}{2 \rho_b M} \qquad (3.11)$$

Equ. 3.11 can be solved for a, the growth layer thickness, in terms of the total mass, density and mean diameter of the initial bed particles, the binder density and the mass of binder added to the bed. If values of $M_b$ at different times are known, then a, and consequently $d^1$ from Equ. 3.1, can be calculated as a function of time. This allows comparison of a calculated mean particle diameter with experimentally determined values, at various times from the start of granulation. The simple model detailed above is not intended to demonstrate that particles grow by successive deposition of uniform layers of binder, but is to be used as a test to show that product particles can be approximated to initial bed particles with the addition of binder around the particle surface. This enables such granules to be distinguished from doublets, triplets or larger agglomerates, whatever the actual mechanism of particle growth.

The details of how the model has been applied to experimental data, and the results obtained, are given in Chapter Six.

### 3.3.2 Agglomeration

The agglomeration model derived here from simple geometrical considerations, is essentially that due to Sherrington[73] and was originally applied to moist agglomerates. It has been adapted to describe agglomerates of non-porous particles bound together by solid bridges of material, deposited from a drying solution. The basis of Sherrington's work is that liquid fills the voids in a close packed mass of particles, but is withdrawn by a distance sr (where r is the initial particle radius and s is an arbitrary parameter) into the interstices of the particles which lie at the granule surface. The granule surface is

thus dry (see Fig. 3.2). Here it is assumed that solid binder fills the void spaces between particles and that it is withdrawn at the surface in the same way - in other words it is assumed that a straight substitution of binder for water is valid.

The particles, from which an agglomerate is built, are all assumed to be spherical and of uniform radius r. In an infinite well-packed mass of particles the void volume fraction is $\lambda$ and the solid volume fraction is $\sigma$. By definition therefore:

$$\lambda + \sigma = 1 \tag{3.12}$$

Let also the ratio of voids to solids be defined by:

$$k = \frac{\lambda}{\sigma} \tag{3.13}$$

The product granules are also assumed to be spherical and of uniform radius gr; the envelope volume, $V_g$, and external surface area, $S_g$, of a single granule are thus given by Equs. 3.14 and 3.15 respectively.

$$V_g = \frac{4 \pi r^3 g^3}{3} \tag{3.14}$$

$$S_g = 4 \pi r^2 g^2 \tag{3.15}$$

The ratio of total binder volume to total particle volume in the bed is denoted by y. If all granules are equal this quantity must equal the binder volume to particle volume ratio for each individual granule. The volume of particles per granule is $\sigma V_g$ and the volume of binder per granule is $\lambda V_g$ less the deficiency of binder at the granule surface, which is $\lambda S_g sr$. Therefore y must be given by:

$$y = \frac{\lambda V_g - \lambda S_g sr}{\sigma V_g} \tag{3.16}$$

Rearrangement, using Equs. 3.13, 3.14 and 3.15, gives:

$$y = k(1 - S_g sr / V_g) \tag{3.17}$$

and:

$$y = k(1 - 3s / g) \tag{3.18}$$

If $\beta$ ( = 1 / g), the ratio of initial particle diameter to granule dia-

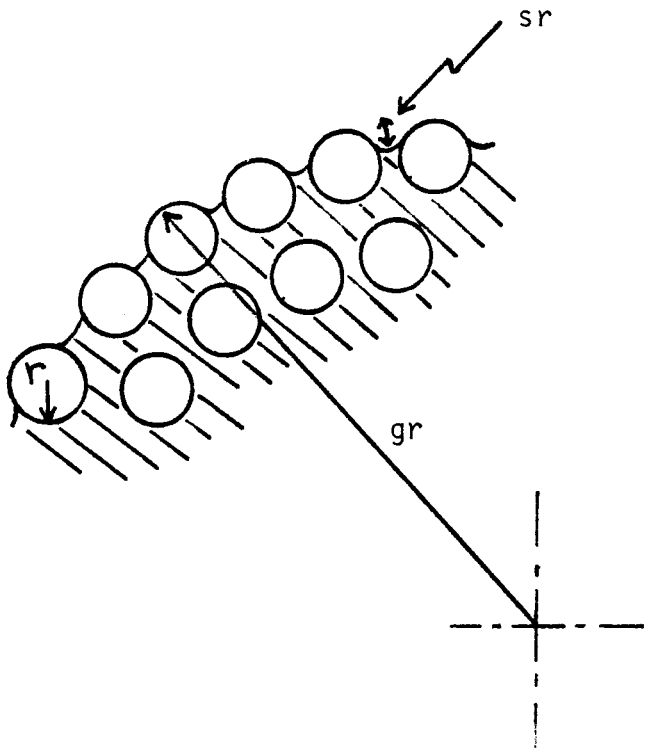


Fig. 3.2 Agglomeration model - a view of the granule surface

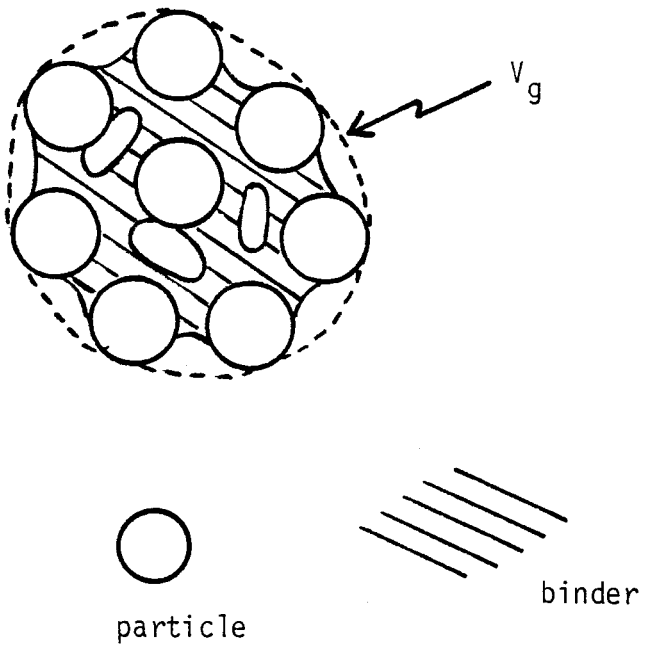


Fig. 3.3 Diagrammatic representation of a granule containing entrapped air

meter, is introduced, Equ. 3.18 becomes:

$$y = k(1 - 3s\beta) \tag{3.19}$$

This equation defines the relationship between the quantity of binder fed into the fluidised bed and the mean diameter of the product granules. A plot of y against β should give a straight line of slope -3ks and an intercept, on the β = o axis, equal to k. It has been pointed out[73] that the value of k obtained should not conflict with those from other sources and that the parameter s should be a plausible fractional number.

The original equation to account for entrapped air within the granule[73] is unsatisfactory because f, the fraction of the granule voids filled with binder, is introduced into the term $\lambda S_g sr$ where, in fact, it has a value of zero. An alternative relationship (Equ. 3.22) has been derived. If the granule contains air, Equ. 3.16 becomes:

$$y = \frac{\lambda f V_g - \lambda S_g sr}{\sigma V_g} \tag{3.20}$$

and

$$y = kf - 3ks\beta \tag{3.21}$$

therefore:

$$y = k(f - 3s\beta) \tag{3.22}$$

The gradient, in a plot of y against β , is unchanged from Equ.3.19, although the intercept now becomes kf. Values of the parameter s obtained from Equ. 3.22 are dependent upon k, which appears in the product kf. One of the quantities k or f must be chosen in order to proceed further and determine s. The value of f can be ascertained by simple experiment and further geometrical considerations.

Consider a granule of diameter $D_g$, mass G, of envelope volume $V_g$ and density $\rho_g$. The components of the granule and their respective volume fractions are listed in Table 3.1, whilst Fig. 3.3 is a diagrammatic representation of the granule.

Table 3.1 Components of a granule

| component | volume fraction | mass |
|---|---|---|
| Particles | $\sigma$ | p |
| Binder | $\lambda f$ | b |
| Air | $\lambda(f - 1)$ | - |

Equating the binder to initial particle volume ratio, y, with the binder to particle mass ratio in a single granule gives:

$$\frac{y\,\rho_b}{\rho_p} = \frac{b}{p} \tag{3.23}$$

where $\rho_b$ and $\rho_p$ are the binder and particle densities respectively. Let

$$\frac{\rho_b}{\rho_p} = q \tag{3.24}$$

then:

$$yq = \frac{b}{p} \tag{3.25}$$

By definition:

$$G = p + b \tag{3.26}$$

and this with Equ.3.25 gives:

$$p = \frac{G}{(yq + 1)} \tag{3.27}$$

$$b = \frac{Gyq}{(yq + 1)} \tag{3.28}$$

again by definition, f is equal to the binder volume in a granule divided by the sum of this and the volume of entrapped air, $V_a$:

$$f = \frac{b / \rho_b}{(b / \rho_b) + V_a} \tag{3.29}$$

The volume of a single granule, $V_g$, is the sum of the volumes of binder, particles and air. Thus:

$$V_g = \frac{p}{\rho_p} + \frac{b}{\rho_b} + V_a \tag{3.30}$$

and

$$V_a = V_g - \frac{p}{\rho_p} - \frac{b}{\rho_b} \tag{3.31}$$

Substitution of Equ.3.31 into Equ.3.29 gives:

$$f = \frac{b}{\rho_b \, (V_g - p \, / \, \rho_p)} \tag{3.32}$$

and further substitution from Equas. 3.24, 3.27 and 3.28 results in:

$$f = \frac{Gy}{V_g \, (y \, \frac{\rho_b}{\rho_p} + 1) \, \rho_p - G} \tag{3.33}$$

The granule volume may be substituted for in two ways:

$$\text{(i)} \quad V_g = \frac{G}{\rho_g} \tag{3.34}$$

where G is the mass of a single granule and $\rho_g$ is the envelope density. Combining Equs. 3.33 and 3.34 gives the result:

$$f = \frac{y\rho_g}{y\rho_b + \rho_p - \rho_g} \tag{3.35}$$

in which f, the fraction of the void spaces in an agglomerate which are filled with binder, is a function of y, the binder to particle volume ratio, the densities of the binder and the initial bed particles, and the granule density - which may be determined by specific gravity bottle measurements using a liquid which does not dissolve the binder.

$$\text{(ii)} \quad V_g = f_v \, D_g^3 \tag{3.36}$$

where $f_v$ is the volume shape factor. Substitution in Equ. 3.33 gives:

$$f = \frac{Gy}{f_v \, D_g^3 \, (y\rho_b + \rho_p) - G} \tag{3.37}$$

In order to use Equ. 3.37 the mass of a single granule of diameter $D_g$ must be known. This can be determined by weighing a known number of closely-sieved granules, and taking $D_g$ as the arithmetic mean of the two sieve apertures which pass and retain respectively, all of the

weighed material.

The values of f calculated from Equs. 3.35 and 3.37 are discussed, and compared with those obtained from the agglomeration model, in Section 6.3.3.

## 3.4 PARTICLE SIZE

### 3.4.1 Introduction

Of the quantities which characterise a granular material, particle size is particularly important. It affects the physical properties of powders such as their tendency to flow, the rate of dissolution of soluble materials, the taste of food products and the release and absorbtion of drugs in pharmaceutical granulations. This work is concerned with the granulation of particles, which may be defined as a process in which a mass of small particles is changed into a mass of larger particles, or perhaps as a process in which the majority of particles undergo a change in size. Throughout the work, samples have been taken from the fluidised bed and subjected to particle size analysis (see Section 5.4) and the major experimental observation was the change in particle size of the bed material with time. For particles other than mono-sized spheres, more than a single number or measurement is needed to characterise the particle size, and the following sections are concerned with how the data from particle size analysis can be expressed in terms of mean sizes and size distributions.

### 3.4.2 Mean particle diameters

The purpose of an average particle size is to represent a distribution of sizes by a single quantity; the average should reflect the bulk of a group of particles, not the extreme values of the distribution.[98] Fig. 3.4 is a representation of a distribution of particle sizes.

The most commonly occurring particle size is the mode value, the value at which the frequency distribution curve peaks. The median value is that which divides the area under the curve into two, one half of the particles have sizes larger than the median and one half of the particles are smaller. The mean particle size may be calculated in a number of different ways; suppose the diameters of a group of poly-

disperse particles are known, this distribution may now be represented by a group of monodisperse particles retaining two (but no more than two) of the characteristics of the first group, such as the total number of particles, total length, surface area or volume. Further, the diameter of the monodisperse group is the mean particle diameter of the original distribution with respect to the two retained characteristics. Thus the length-surface mean diameter of a distribution is the diameter of a uniformly sized system of particles having the same total length and the same total surface area as the distribution of interest. The number of particles and their total volume will be different, however.

Two mean diameters which have been used extensively in this work are the surface-volume mean and the weight-moment mean, which are defined by Equs. 3.38 and 3.39 respectively.

$$d_p(sv) = \frac{\sum d^3\, dN}{\sum d^2\, dN} \tag{3.38}$$

$$d_p(wm) = \frac{\sum d^4\, dN}{\sum d^3\, dN} \tag{3.39}$$

where d is the assumed diameter of particles in a small size interval $\delta$ d containing dN particles. The mean diameter is found by summation over the whole system and by assuming that all particles have the same shape. In practice, size analysis data has been obtained from sieving and the interval $\delta$ d becomes the difference between successive sieve apertures, and d is then their arithmetic average. For a given particle size distribution the values of $d_p(sv)$ and $d_p(wm)$ will usually be very different and therefore they can be used to demonstrate different characteristics of the distribution. For example, Table 3.2 contains the distributions of two samples of granules, removed from a fluidised bed at different times, together with the calculated mean particle diameters. An increase in particle size is evident between sample A and sample B and this is reflected in the mean diameters.

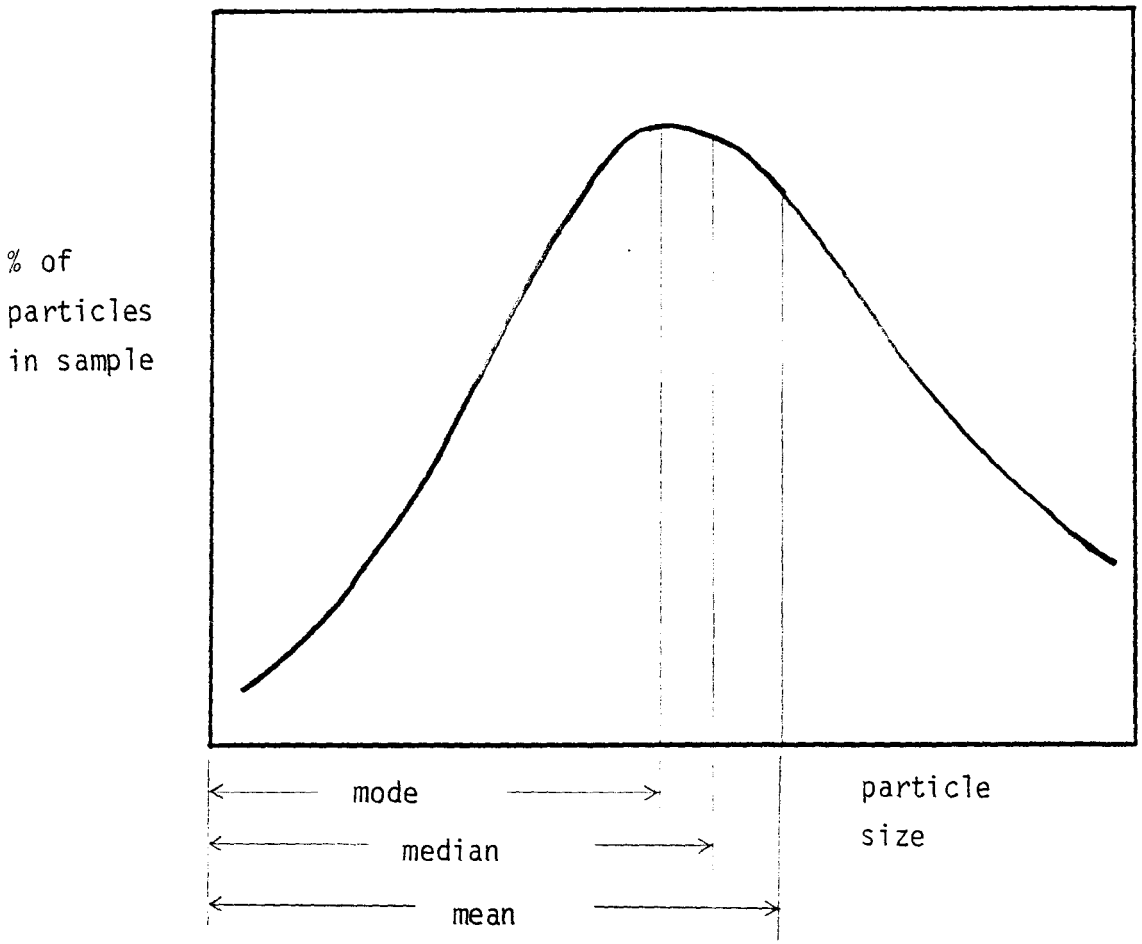


Fig. 3.4 Percentage frequency distribution curve

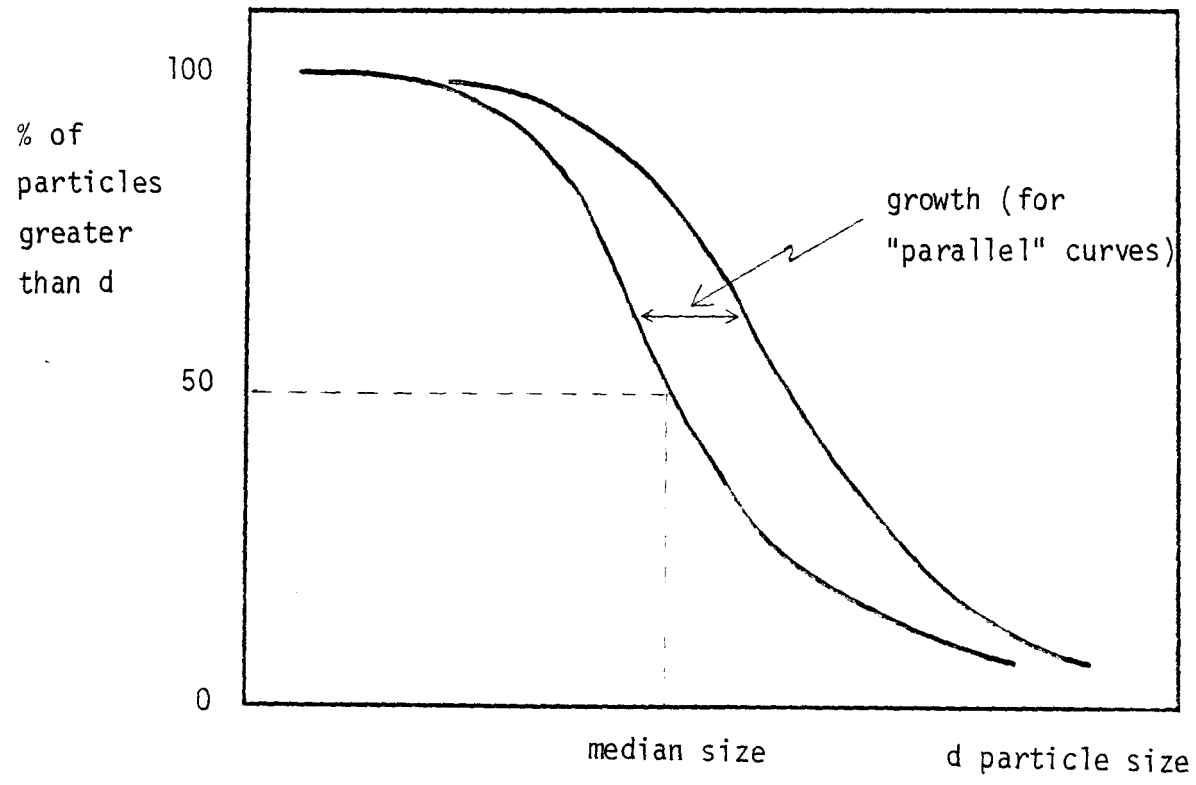


Fig. 3.5 Cumulative oversize curve

Table 3.2 Typical particle size distributions chosen to illustrate the differences between $d_p$(sv) and $d_p$(wm)

| d (μm) | A (wt. %) | B (wt. %) |
|---|---|---|
| 1850 | | 0.05 |
| 1550 | | 0.11 |
| 1290 | | 0.05 |
| 1090 | | 0.05 |
| 925 | | 0.05 |
| 780 | | 0.05 |
| 655 | | 0.05 |
| 550 | | 0.32 |
| 462.5 | 0.55 | 2.29 |
| 390 | 4.41 | 14.52 |
| 327.5 | 19.49 | 32.29 |
| 275 | 17.98 | 19.47 |
| 231 | 26.17 | 16.91 |
| 196 | 21.01 | 8.78 |
| 165 | 9.50 | 4.63 |
| 137.5 | 0.90 | 0.37 |
| $d_p$(sv) : | 237.0 | 276.8 |
| $d_p$(wm) : | 298.4 | 640.4 |

However the weight-moment diameter has increased, proportionately, far more than the surface-volume mean. There has been an increase in size of the bulk of the particles (the mode value has increased from about 230 μm in sample A to about 300 μm in sample B) and a corresponding increase in $d_p$(sv) of 40 μm. The change in weight-moment mean diameter however is much more dramatic; the size increase of 440 μm is due to the very few large particles at the top end of the distribution.

It is clear that plotting different mean diameters against time will give different information on how the particle size distribution is changing throughout a granulation run. In the quoted example, it can be deduced from the value of $d_p$ (wm) that sample B contains some agglomerated particles. For such an increase to occur by layering would require the deposition of a very large amount of material on the particle surface and consequently agglomeration must be responsible. The use of the different mean diameters lies in the ability to convey information about a distribution with a single number, although this is not a substitute for plotting the complete distribution. Methods for doing that are discussed in the next section.

### 3.4.3 Methods of presenting a particle size distribution

The frequency distribution curve (Fig. 3.4) is a simple way of representing the distribution of particle sizes in a sample and allows the mode value to be read-off easily. The same data may be plotted on a cumulative basis; particle size against the percentage of particles larger or smaller than that size. Fig. 3.5 shows a cumulative oversize curve, from which the median is readily obtained. Parallel curves allow growth rates to be determined simply by measuring the horizontal deviation between consecutive curves. Another useful method for showing how the particle size changes is to plot the percentage of fines in the sample against time. "Fines" may be defined as particles below any diameter of interest, but this method is particularly useful if the term fines is taken to be the range of sizes in the original distribution.

Representation of a PSD by a straight line is possible if the data fit a standard equation, such as the normal or log normal distribution laws. The latter requires the use of log probability paper. Other methods of graphical representation are available[99] but, in general, are only used for convenience of presentation and not on theoretical grounds.

# CHAPTER FOUR

## PRELIMINARY EXPERIMENTS

## 4.1 INTRODUCTION

This chapter describes experiments which can be grouped together and given the prefix "preliminary" because:

(i) in general, they pre-date the granulation runs in which it was possible to spray feed into the bed for several hours without quenching, and from which growth rate data were obtained;

(ii) the results have influenced the design of apparatus for later experiments, and the way in which those experiments were conducted.

Most of the work reported here was conducted either in a large heated bed (Section 4.2) or at ambient temperature (Section 4.3). However, the observations of spray drying and of the effect of non-atomisation were made during preliminary work with the main granulation rig (described in Section 5.2). The chapter ends with a section in which conclusions are drawn and the thinking behind the nature of the major granulation experiments is outlined.

## 4.2 EXPERIMENTS IN A LARGE HEATED BED

### 4.2.1 Equipment, materials and procedure

Early attempts to granulate in a large square-sectioned heated bed met with only mixed success and consequently small scale equipment (see Section 4.3) was used at an intermediate stage of the work.

The fluidised bed used for the very first experiments was constructed from sheets of stainless steel so as to form an open-topped box, 0·3 m x 0·3 m in cross-section and 0·6 m deep. The bottom of the box-shape was formed by a porous ceramic plate which evenly distributed the fluidising gas. Heat was supplied by two banks of flat electrical heaters rated at 500 W each and evenly distributed around the bottom of the bed (see Fig. 4.1). Power controllers supplied up to 3·5 kW to each bank - a nominal heating rate of 7 kW was possible therefore - and the walls and windbox were thermally insulated with 0·03 m thick mineral wool. Liquid was fed via an atomising nozzle of either commercial design (described in Section 5.25) or a purpose-built device. The latter consisted of two concentric tubes of internal diameter $1.0 \times 10^{-3}$ m and $4.3 \times 10^{-3}$ m respectively and external diameter $2.2 \times 10^{-3}$ m and $6.4 \times 10^{-3}$ m respectively. The inner tube, through which liquid was fed, projected $1.5 \times 10^{-3}$ m beyond the end of the outer tube. Atomising air passed through the annulus. Samples for particle size analysis (Section 4.4.3) were obtained in the same way as is described in the main experimental detail section (Section 5.4) and the analysis was obtained by sieving.

The bed was charged to a depth of 0·3 m with either alumina (aluminium oxide) or sodium chloride. The feed was a 10% (by weight) solution of sodium chloride in distilled water.

### 4.2.2 Operational problems

Spraying liquids onto, or beneath, the surface of fluidised beds presents several severe practical problems, many of which are described

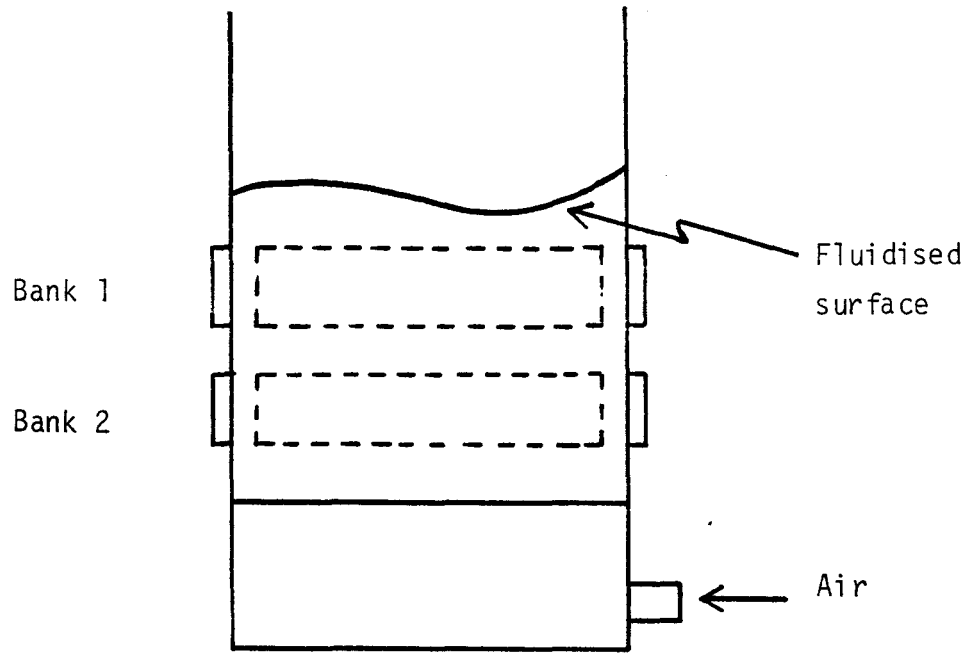


Fig. 4.1 Arrangement of heaters around the square bed

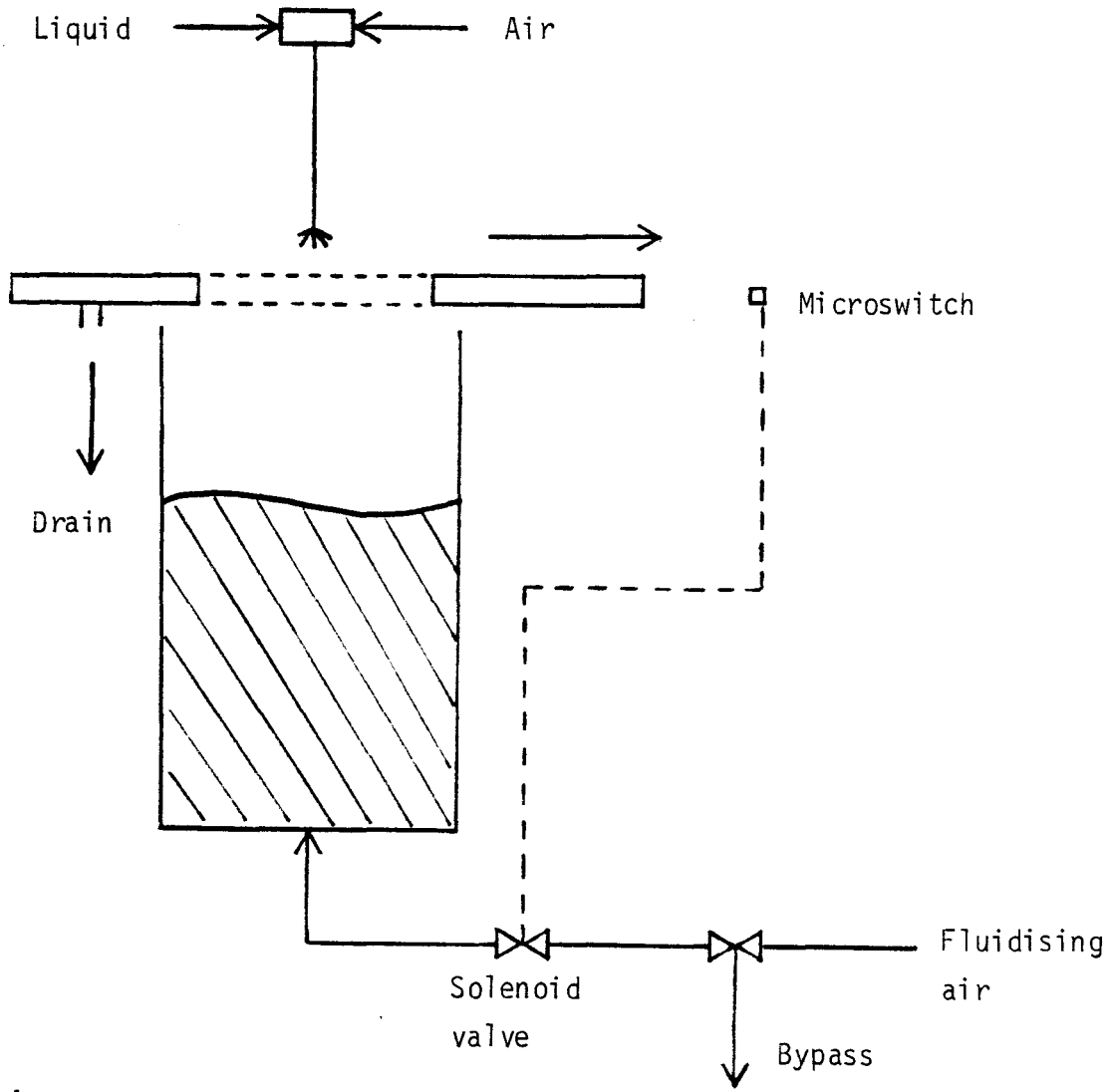


Fig. 4.2 Arrangement of apparatus for short feed-time experiments

in the literature. Positioning the atomising nozzle in the freeboard region often results in the formation of cakes of bed material around the nozzle and leads to blockage and shut-down. Cake formation and nozzle blockage was found to be a great problem with the simple home made device, which gave insufficient liquid atomisation, and therefore a commercial nozzle system has been used for all granulation experiments. Nozzle position has been found to be critical from considerations of spray drying, cake formation and overspraying. The latter was a serious problem when brine was sprayed onto salt particles. With the bed wall at a higher temperature than the bed, liquid is quickly evaporated leaving behind cakes of solid sodium chloride. This experimental arrangement was also generally unsatisfactory because of the large bed volume and attendant solids handling problems.

## 4.3 EXPERIMENTS AT AMBIENT TEMPERATURE

### 4.3.1 Introduction

In these experiments a Perspex fluidised bed at ambient temperature was used in an attempt to obtain a large amount of information quickly before commencing genuine granulation experiments. Liquid was sprayed into the bed for very short time periods, and at high rates, in order to simulate the initiation of agglomeration; the effect of liquid volume, feed rate and fluidising gas velocity on the mass of wet aggregated material formed in the bed was determined. Visual observations of the bed could also be made because of the transparent walls.

### 4.3.2 Equipment, materials and procedure

The fluidised bed consisted of a 0·14 m diameter Perspex tube, 0·25 m long, mounted vertically on top of a 0·10 m deep windbox section. A 0·003 m thick porous bronze distributor plate sat in a recess cut in the top flange of the windbox and was held in place between this and a flange attached to the cylindrical section of the bed. The air for fluidising the particles is metered by a bank of rotameters and enters the windbox horizontally before passing upwards, through the distributor plate. In order to spray onto the bed surface for short periods and to introduce known amounts of liquid with reasonable accuracy, it was necessary to start-up the liquid spray before commencing the experiment and to switch it off only after the spraying period was complete. This was achieved by placing a horizontal tray (Fig. 4.2), between the nozzle and the top of the bed wall, onto which the spray was directed (and from which liquid could drain) before and after the set period. The spray passed through a square hole cut in the tray, which was moved into position by hand along two guide rails. The tip of the nozzle (which was mounted vertically) was 0·3 m above the centre of the distributor plate.

To begin an experiment the bed was charged with particles to a packed

depth of 0·12 m. A solenoid valve in the main air-line was activated, allowing air to pass into the bed and fluidise the particles and the air flow rate was then set to the required value. With the tray covering the bed, liquid was pumped to the atomising nozzle (of the commercial design) and the flowrate, measured with a graduated cylinder, adjusted. After starting the atomising air flow and ensuring that the nozzle was operating satisfactorily, the tray was moved by hand so that the nozzle sprayed liquid through the hole cut in the tray and onto the fluidised surface. A stop watch was started simultaneously with this movement. After spraying for the required length of time, between 10 and 45 seconds, the tray was again moved (in the same direction as before) so that it came to rest between the nozzle and the bed, and liquid could again drain away. At the end of this second traverse the tray activated a microswitch on the frame of the apparatus (Fig.4.2) which closed the solenoid valve and this instantly defluidised the bed. In this way the fluidising gas was prevented from breaking up agglomerates or lumps which may have formed in the bed by the addition of the feed liquid. It was also necessary to open a by-pass valve, upstream of the solenoid valve, to release the air pressure. The liquid feed was then stopped and the nozzle and tray taken away to facilitate removal of agglomerates from the bed. This was done by lifting up through the bed a disc of wire mesh (aperture = 0·0017 m) which normally sat on the distributor plate, by means of vertical wire supports. Wet agglomerated material was retained on the wire mesh whilst unagglomerated particles passed through and remained in the bed. The wire mesh disc was gently tapped to remove any loose dry material and the remainder was quickly weighed. It was found necessary to have a low flowrate of air, equivalent to a superficial velocity of about 0·6 $U_{mf}$, through the bed during this operation. The period from stopping the liquid flow to weighing the agglomerated particles was of the order of one minute and

consequently negligible drying of the powder took place.

The materials used for these experiments are listed in Tables 4.1, 4.2 and 4.3.

Table 4.1 Materials for observation of nozzle cake formation (Section 4.4.1)

BED PARTICLES : ALUMINA

| | |
|---|---|
| Mean particle diameter, dp(sv) | = 614 μm |
| Minimum fluidising velocity | = 0·158 $ms^{-1}$ |
| Bed weight (dry) | = 1·58 kg |
| Bed height (packed) | = 0·14 m |

FEED LIQUID : DISTILLED WATER

Table 4.2 Materials for determining the effect of feedrate, gas velocity and viscosity (sections 4.4.2, 4.4.4 and 4.4.5)

BED PARTICLES : ALUMINA

| | |
|---|---|
| Particle size range | = -250 + 180 μm |
| Minimum fluidising velocity | = 0·044 $ms^{-1}$ |
| Bed weight (dry) | = 1·58 kg |
| Bed height (packed) | = 0·12 m |

FEED LIQUID : AQUEOUS SOLUTIONS OF:

Anhydrous Calcium Chloride

Sucrose

(supplied by BDH Ltd.)

Table 4.3 Materials for determining the effect of particle structure (section 4.4.3)

BED PARTICLES : ALUMINA

| | |
|---|---|
| Mean particle diameter, dp(sv) | = 262 μm |
| Minimum fluidising velocity | = 0·049 $ms^{-1}$ |
| Bed weight (dry) | = 1·34 kg |

Ballotini (glass microspheres)

| | |
|---|---|
| Mean particle diameter, $d_p$(sv) | = 221 μm |
| Minimum fluidising velocity | = 0·046 $ms^{-1}$ |
| Bed weight (dry) | = 2.89 kg |

FEED LIQUID : DISTILLED WATER

NB. Quoted weight percent concentrations are

(weight of solute / weight of solution) x 100.

## 4.4 EXPERIMENTAL RESULTS

### 4.4.1 Feed methods

The formation of nozzle cakes, which cannot be seen in the square-section steel bed, has been observed by spraying water (at a rate of $8{\cdot}3 \times 10^{-8}$ $m^3$ $s^{-1}$) into a bed of alumina particles (Table 4.1) contained in the Perspex bed, (i.e. the ambient temperature tests) and fluidised at a relative gas velocity of $U / U_{mf} = 1{\cdot}3$. Water was sprayed into the bed with the nozzle in three different positions (0·10 m above, 0·05 m above and 0·04 m below the fluidised surface, respectively) and visual observations recorded between five and ten minutes after the commencement of spraying. With the nozzle at a height of 0·10 m above the bed surface, a few particles, carried in the bubble wakes and thrown up into the freeboard, adhered to the nozzle cap - although this was insufficient to form a wet clump or nozzle cake. Moving the nozzle to within 0·05 m of the surface increases the amount of material impinging upon the nozzle, due to the action of the atomising air in further agitating the bed surface. In this position distinct clumps of wet material were formed and periodically broke away and fell into the bed. When the nozzle was placed below the fluidised surface a wet clump was found adhering to the nozzle on removal, but no other large agglomerates were found in the bed. X-ray film taken of a similar system has shown nozzle cake formation and localised wet quenching more clearly and is discussed in Chapter Seven.

Some preliminary tests in the main granulation rig have demonstrated the importance of nozzle position and the need for atomisation of the feed. For example, spray drying of a pure solvent (methanol) occurred with the nozzle located in the freeboard; the measured bed temperature being some $20^{o}$ C higher than would be the case if all evaporation took place in the bed. Predicted bed temperatures were only attained when the nozzle was submerged beneath the surface, although severe abrasion

of the bronze distributor plate resulted (presumably due to a jet grinding effect) when the nozzle was 0·06 m above it. It is clear that atomisation of the feed liquid is necessary for successful operation. Non-atomisation of solution resulted, almost instantly, in a solid lump of aggregated particles below the nozzle and extending over much of the bed depth, even when the heat and mass balances were satisfied, and the home-made feed device proved a failure (see Section 4.2.2). These observations support those of Ormos et al.,[21] although no justification for particular air-to-liquid ratios can be advanced; it appears from these tests that a volumetric flow of air which will finely atomise the liquid in free air is adequate for the purposes of fluidised bed granulation. However the effect of atomising air flowrate on particle size has not been established and experiments to do this would need to be conducted in a continuous system.

4.4.2 Volume of liquid feed and feedrate

The greater the quantity of liquid sprayed into the fluidised bed, the greater is the mass of agglomerated (or quenched) material which is formed in the bed, and subsequently removed by the wire mesh technique. This is clearly illustrated in Fig. 4.3 in which the agglomerated mass of alumina (W) is plotted against the volume of 25% calcium chloride solution sprayed onto the bed surface during a period of ten seconds, with each point representing the arithmetic average of two observations. This is also therefore a plot of W against liquid feedrate, as indeed is Fig. 4.4 - although here the length of the spraying period (t) has been varied for a fixed feed volume of $20 \times 10^{-6}$ $m^3$ of solution. In this case each point is the average of three observations.

These experiments, using the materials of Table 4.2 and a constant relative gas velocity of $U / U_{mf} = 1{\cdot}5$, were performed at room temperature ($20^{o}$ C) with an air inlet temperature of $17{\cdot}5^{o}$ C and therefore there can have been little or no evaporation from the deliquescent

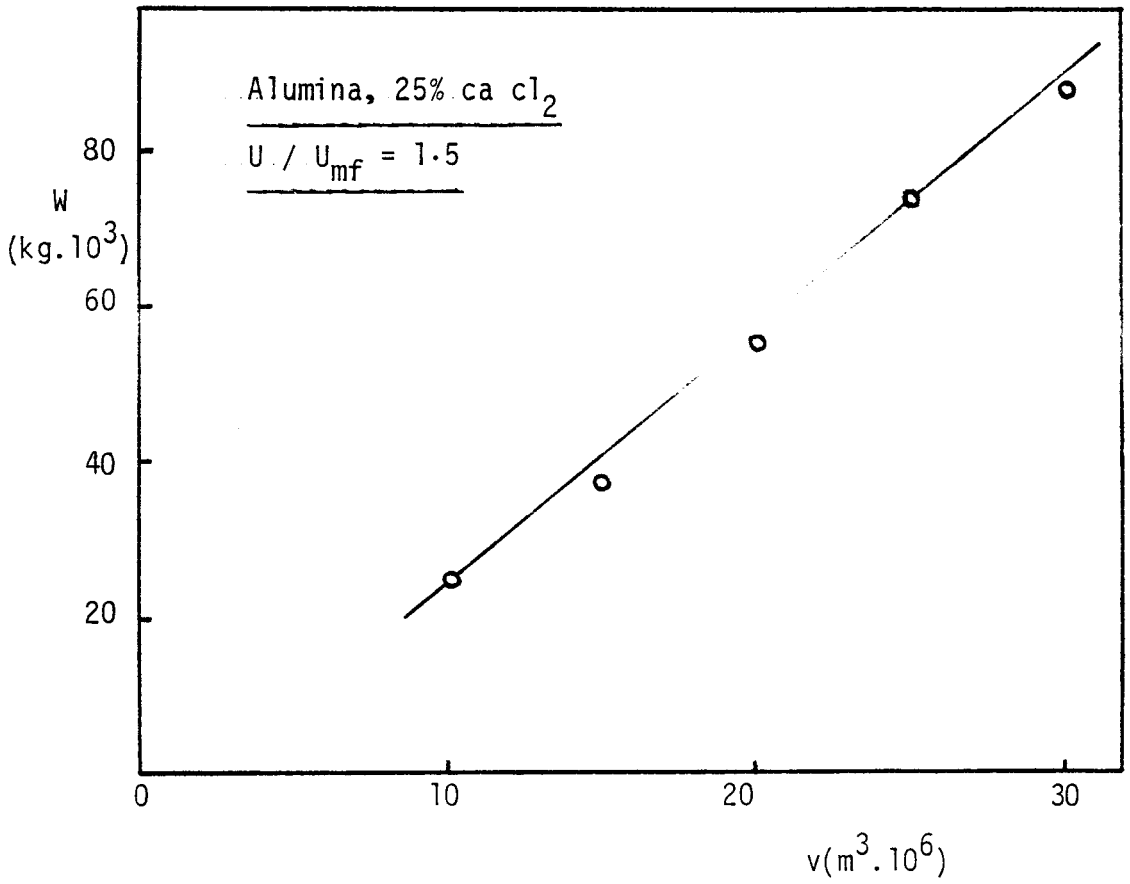


Fig. 4.3 Agglomerated mass (W) against feed volume (v)

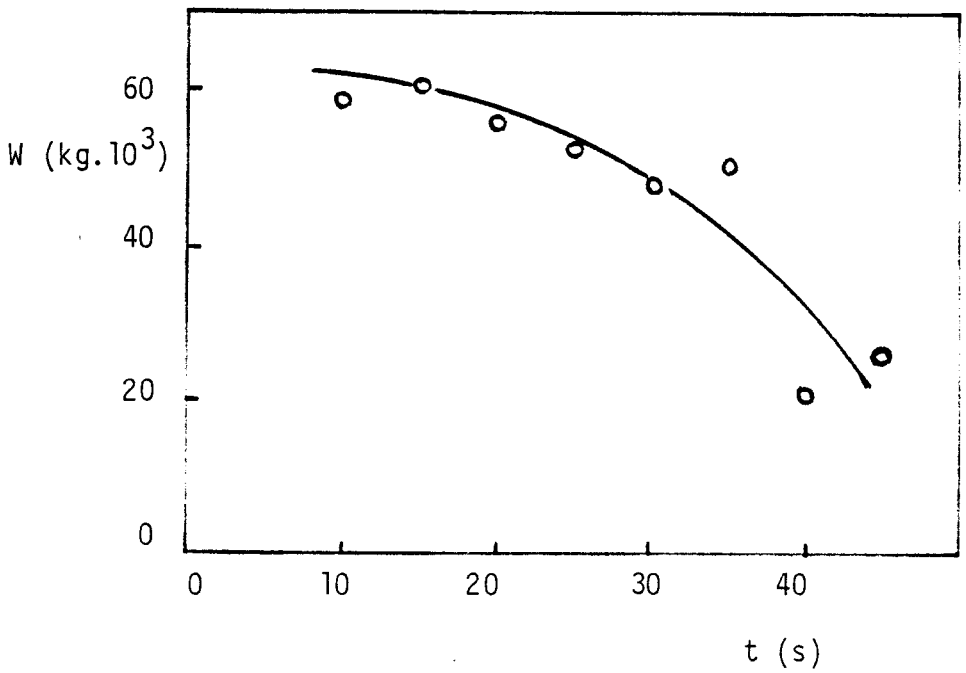


Fig. 4.4 Agglomerated mass (W) against spraying time (t) for a given feed volume

calcium chloride solution. The saturation humidity at this temperature is 0·013 kg of water per kg of dry air, which would be far exceeded if all the water in the feed solution was evaporated into the fluidising air stream. At the lowest feedrate used (corresponding to t = 45 s in Fig. 4.4) only 2·5% by weight of the water sprayed into the bed was required to saturate the air. Clearly, very little drying of the feed can take place, either in the bed or in the freeboard region, and it is inevitable that wet quenching of the bed will occur. Some liquid may penetrate the intra-particle pores of the alumina (see Section 4.4.3) but, nevertheless, Fig. 4.3 shows that the magnitude of the quenching problem increases with an increase in the feedrate of liquid, and confirms an observation made in several previous studies.[14,27,52,53,58] The bulk of the water contained in the sprayed solution remains in the wet clumps, rather than in the well fluidised particles. Drying samples from the agglomerated material in an oven and performing a simple mass balance has shown that, for the case of t = 45 s in Fig. 4.4, the moisture content of this material was 32% by weight (representing 55% of the water feed) compared with 0·4% (45% of the water feed) for the remainder of the bed particles.

The trend in Fig. 4.4 is less well defined than that in Fig. 4.3, although the increase in W with feedrate is still apparent. Each run involved spraying a fixed amount of solution ($20 \times 10^{-6}$ $m^3$), but over different lengths of time, and it might be expected that the mass of agglomerated material would remain constant. However, W is genuinely a function of the rate at which liquid is introduced to the bed, rather than simply of the volume of feed. The shape of Fig. 4.4 is perhaps explained by an increased break-up of agglomerated material with increased time spent in the bed. After 40 or 45 seconds, although agglomerated material is still being formed, some of the liquid bonds which formed at an earlier stage have had sufficient time, and have been sub-

jected to sufficient attrition or abrasion, to be pulled apart.

4.4.3 Particle structure

The effect of particle structure on fluidised bed behaviour when a liquid is introduced into the bed has been demonstrated in two ways. Firstly by an experiment in the large heated bed in which the heat balance was satisfied and water evaporated, and secondly in some short tests in which quenching was simulated as described in the previous section.

With a bed of alumina particles, and the atomising nozzle 0·15 m above the fluidised surface, water was evaporated from a 10% sodium chloride solution at a bed temperature of 110° C. The change in mean particle size with time is given in Table 4.4.

Table 4.4 Effect of particle structure on particle size

| t (hours) | MEAN PARTICLE DIAMETER (μm) | |
|---|---|---|
| | $d_p$ (sv) | $d_p$ (wm) |
| 0 | 114 | 125 |
| 21¾ | 114 | 129 |
| 37¾ | 112 | 128 |
| 67¼ | 116 | 134 |
| 139¼ | 126 | 172 |

almost no particle growth occurs over the first 67 hours of operation, although beyond this point the change in weight - moment mean diameter suggests that agglomeration has taken place; after 140 hours both $d_p$ (sv) and $d_p$ (wm) showed an increase. The suggestion here is that the intra-particle porosity of the alumina allowed solute (in this case sodium chloride) to be deposited within the particles, rather than on the surface which would inevitably have caused particle growth. This evidence, particularly without a mass balance, is inconclusive. However, direct comparison between alumina and a non-porous material (ballotini) was provided by the second experiment, in which distilled water was

sprayed into the bed over a range of feedrates and with different gas velocities. Details of the bed particles used are given in Table 4.3 and the masses of agglomerated particles obtained under the various conditions are shown in Table 4.5.

Table 4.5 Effect of particle structure on the mass of agglomerated material

(i) Alumina

| $V\ (m^3.\ 10^6)$ | $t\ (s)$ | $U - U_{mf} (ms^{-1}.\ 10^2)$ | $W\ (kg)$ |
|---|---|---|---|
| 10 | 20 | 1·5 | 0 |
| 20 | 15 | 2·9 | 0 |
| 30 | 15 | 2·9 | 0 |
| 30 | 10 | 1·5 | 0 |

(ii) Ballotini

| $V\ (m^3.\ 10^6)$ | $t\ (s)$ | $U - U_{mf} (ms^{-1}.\ 10^2)$ | $W\ (kg)$ |
|---|---|---|---|
| 10 | 20 | 1·5 | 222 |
| 20 | 15 | 2·9 | 416 |
| 30 | 15 | 2·9 | 423 |
| 30 | 10 | 1·5 | 264 |

In each of four separate runs using alumina no agglomerated particles were produced that could be removed from the bed. The same four runs repeated with ballotini in place of alumina, resulted in substantial quenching of the bed and between 7% and 15% (by weight) of the bed material could be removed as a wet agglomerated mass. The major difference between the two sets of particles, in terms of physical properties, is intra-particle porosity (shape and density are also different) and it seems likely that this is the cause of their very different behaviour. This explanation is in keeping with the findings of Meissner and Mickley,[46] McCarthy et al.[47] and D'Amore et al.[48]

4.4.4 Fluidising gas velocity

The same experimental system and the materials of Table 4.2 have been used to bring about bed quenching and to determine the effect of gas velocity. The results are listed in Table 4.6.

Table 4.6 Effect of fluidising gas velocity

(i) 25% calcium chloride solution : V = 20 ($m^3$. $10^6$), t = 20 s.

| $U - U_{mf}$ ($ms^{-1}$. $10^2$) | $U / U_{mf}$ | W (kg. $10^3$) |
|---|---|---|
| 2·2 | 1·5 | 56·0 |
| 4·4 | 2·0 | 18·0 |
| 8·8 | 3·0 | 1·0 |
| 13·2 | 4·0 | 0 |

(ii) 30% sucrose solution: V = 30 ($m^3$. $10^6$), t = 10 s.

| $U - U_{mf}$ ($ms^{-1}$. $10^2$) | $U / U_{mf}$ | W (kg. $10^3$) |
|---|---|---|
| 3·2 | 1·7 | 27·0 |
| 3·7 | 1·8 | 24·0 |
| 4·6 | 2·0 | 17·0 |
| 5·6 | 2·2 | 14·0 |

Increasing the superficial gas velocity through the fluidised bed (expressed here both as relative and excess gas velocity) markedly decreases the amount of agglomerated material. The increase in volumetric air flow does not bring the theoretical moisture content of the exhaust gas below saturation level and therefore a genuine velocity effect has been observed, which lends considerable support to the ideas (outlined in Chapter Three) of an increase in gas velocity being responsible for better liquid distribution and greater break-down of particle - particle bonds.

4.4.5 Viscosity of liquid feed

Solutions of sucrose have been used in various concentrations to determine the effect of liquid feed viscosity on particle agglomeration

in beds of alumina (Table 4.2). The normalised air to liquid ratio (NAR) was kept constant and therefore the effect of viscosity on the quality of atomisation was not eliminated, although this is not a large effect, mean droplet size being a function of viscosity raised to a power in the range 0·30 to 0·37.[97] The viscosity of aqueous sucrose solution as a function of concentration was obtained from a standard reference work.[100]

Table 4.7 Effect of liquid feed viscosity

$V = 20\ (m^3.\ 10^6)$, $t = 15$ s, $U - U_{mf} = 1{\cdot}5\ (ms^{-1}\ 10^2)$

| concentration (wt. %) | viscosity (Pa S), 20°C | viscosity (cP), 20° C | W (kg. $10^3$) |
|---|---|---|---|
| 34·0 | $4{\cdot}0 \times 10^{-3}$ | 4·0 | 14·0 |
| 39·6 | $6{\cdot}0 \times 10^{-3}$ | 6·0 | 34·5 |
| 43·2 | $8{\cdot}0 \times 10^{-3}$ | 8·0 | 68·5 |
| 45·6 | $10{\cdot}0 \times 10^{-3}$ | 10·0 | 87·0 |

The data of Table 4.7 (where each value of W is the average of two observations) strongly indicate that an increased resistance to flow into the intra-particle pores (due to increased viscosity) is responsible for larger amounts of quenched bed material with higher liquid feed concentrations. This information supports the observation, made in work on pharmaceutical granulation,[75] that increased feed viscosity results in dramatically increased particle growth.

## 4.5 CONCLUSIONS

### 4.5.1 General conclusions

The results described in the preceding sections demonstrate the effect of various parameters on bed quenching. However they are also valid as an indication of the effect of the same parameters on particle growth, because both undesirable quenching and desirable particle growth by agglomeration are initiated in exactly the same way. The evidence presented is not conclusive and several further experiments suggest themselves, but from this preliminary work indications and pointers to the type of more rigorous experimental work required have been obtained. These results show that gas velocity, particle structure, the type of binder or solute used and the rate of liquid feed are all important parameters, the correct choice of which is essential for the successful operation of a fluidised bed granulator.

### 4.5.2 The type of granulation experiments required

A systematic study of fluidised bed granulation is required in order to determine, first of all, the effect of these parameters on particle growth and operation of the bed and, secondly, to be able to draw conclusions about fundamental growth mechanisms. The experiments which will be described in the following chapters therefore, have been carried out using an "idealised" system. In other words rather than use materials of real interest (such as sodium chloride, sodium sulphate or aluminium nitrate) as have been used in past studies, materials have been chosen which possess specific physical properties and thus can clearly demonstrate the effects of those properties on the granulation process. Batchwise experiments were decided upon because they involve simpler equipment than continuous processes and sufficient fundamental investigation (which is more easily carried out under batch conditions) remains to be done before further continuous granulation studies are undertaken. Although true steady-state cannot be attained in a batch

process, a near approximation is possible, for example by constantly increasing the superficial fluidising velocity to compensate for particle growth and the increase in minimum fluidising velocity of the particles.

The major operating parameters chosen for investigation were:

(i) the structure and size of the bed particles

(ii) fluidising gas velocity

(iii) the rate of feed and solute concentration

(iv) the properties of the binder

4.5.3 Choice of equipment and materials

A relatively small fluidised bed (0·15 m in diameter) was chosen in order to reduce the quantity of bed particles which must be prepared for the granulation experiments. In addition to easing the handling problems of the solids, a smaller bed requires less compressed air for fluidisation. This, combined with the absence of wall heating, allows for greater flexibility and makes control of bed quenching easier. Supplying the heat in the fluidising gas also allows the bed walls to be made of glass, which gives the advantage of being able to record visual observations. This is particularly important in the early stages of the experimental programme. A glass bed requires bed temperatures lower than are permissible with steel and this, together with a desire to minimise the heat load for evaporation, necessitates the use of an organic solvent with a low boiling point, and methanol was chosen for this reason. Two different bed materials were chosen: alumina, which has a high intra-particle porosity, and glass powder which is representative of non-porous particles. Both types of particle are irregularly shaped and batches of similar mean size and particle size distribution were used. Four bed particle / binder combinations have been used for all the granulation experiments. The two binders chosen were benzoic acid and "carbowax", a polyethylene glycol with a molecular weight of about 4000, both of which are readily soluble in methanol. They, and their solutions, have very different physical and chemical properties

and it was expected that their behaviour as binding agents would be very different. Benzoic acid is crystalline and sublimes at 100° C, carbowax is a synthetic wax and melts at about 55° C: when in solution with methanol their viscosities change with concentration in very different ways.

Following the tests discussed in Section 4.4.1 a fixed nozzle position was adopted, with the nozzle entering the bed from above and with the tip coincident with the surface of the packed bed; in practice the nozzle was 0·12 m above the distributor plate. This nozzle position elminated spray drying effects (enabling a mass balance on the binder to be determined) and avoided abrasion of the distributor. The details of the granulation rig, of ancillary equipment and other experimental detail, are given in the next chapter.

# CHAPTER FIVE

## MAIN GRANULATION EXPERIMENTS : EXPERIMENTAL DETAIL

## 5.1 INTRODUCTION

This chapter contains detail of the granulation experiments and of related work. The granulation apparatus is first described, followed by details of the operating techniques. The major observations were changes in mean particle size and particle size distribution with time, obtained by the sieving of particle samples which were withdrawn from the bed during the course of a run. Visual observations of the bed and changes in bed temperature were also recorded. Some physical properties of theproduct granules (e.g. granule strength) and of the binder solutions (e.g. viscosity and surface tension) were determined and details of their measurement are included. The granulation experiments were followed by experiments designed to discover whether different zones existed within the fluidised bed. Two techniques were used: the measurement of temperature profiles with closely spaced thermocouples and X-ray photography.

## 5.2 GRANULATION APPARATUS

### 5.2.1 General description

A schematic diagram of the granulation apparatus is shown in Fig. 5.1 and the rig is illustrated in Fig. 5.2. Metered air passes through an electrical preheater, enters the windbox and passes up through the distributor plate to fluidise the particles. The liquid feed is pumped from a reservoir to the spray nozzle where it is atomised by being mixed with an auxiliary air stream. The exhaust gases comprising the fluidising gas, atomising air and the evaporated solvent vapour pass upwards via an extraction hood into the fume cupboard ventilation system, the draught being increased by enclosing the bed on three sides with polythene sheeting. Temperatures were measured at the exit to the preheater, in the windbox, in the fluidised bed and in the freeboard.

### 5.2.2 Fluidised bed

The fluidised bed consisted of four main parts. At the bottom was a windbox, a steel chamber in the form of an upright cylinder, closed at the bottom, 0·15 m in diameter and 0·12 m deep, into which fluidising air passed horizontally through a pipe set into the wall. Between this and the vertical open cylinder which contained the particles was a porous sintered bronze plate, 0·0065 m thick, which supported the particles and distributed the air so as to give a uniformly fluidised layer. On top of the glass section was a disengaging zone in the form of a short open cylinder surmounted by an inverted frustrum of half angle $30^{o}$. This device allowed high gas velocities to be used without serious elutriation. A diagram of the fluidised bed appears in Fig. 5.3, together with the principal dimensions.

The distributor plate (grade B porosint, supplied by Sintered Products Ltd.) was clamped between the two flanges of the windbox and sealed by a 0·16 m diameter 'O' ring on the underside and an asbestos paper gasket on the top face. The fluidised bed chamber itself was

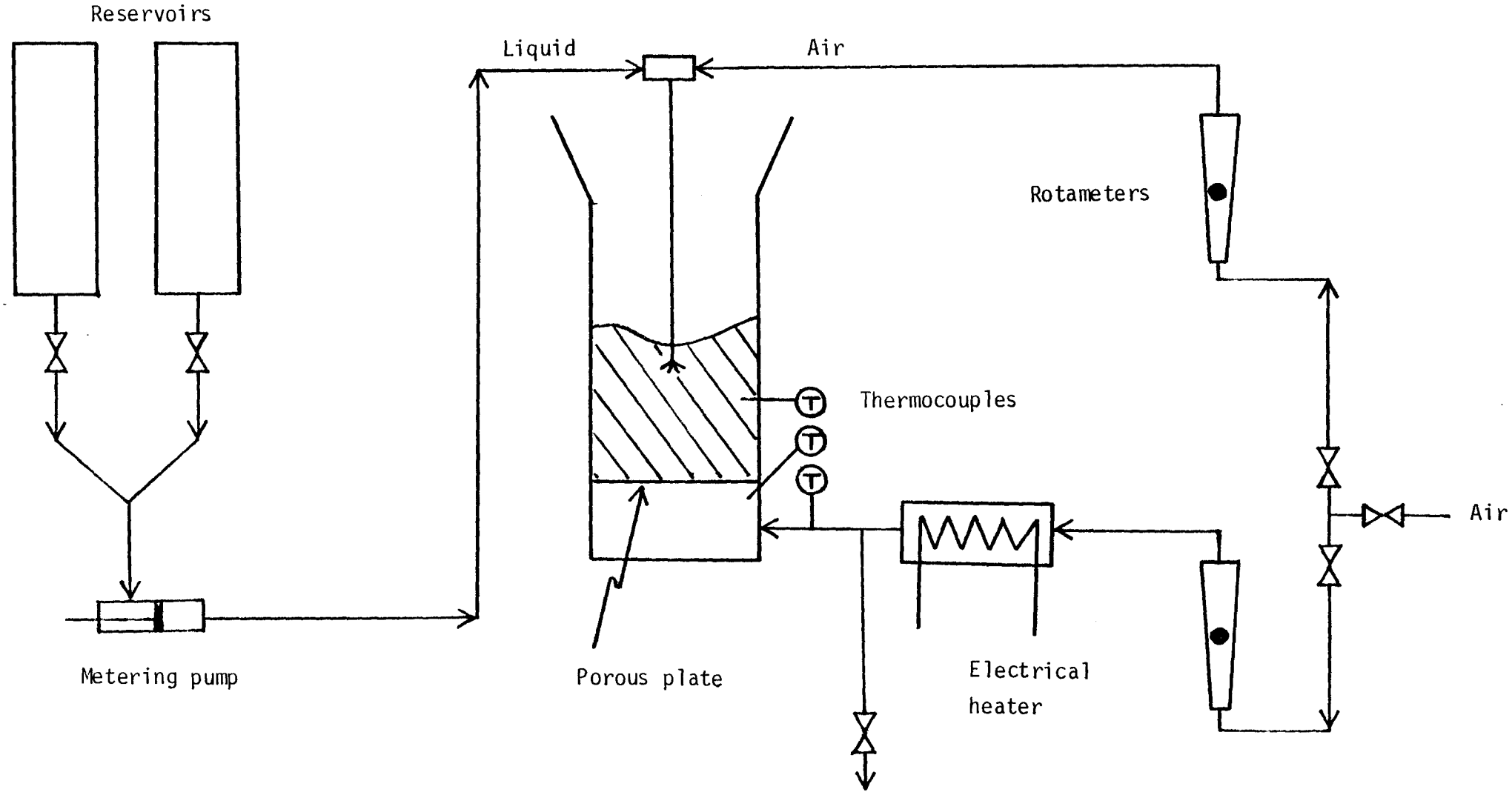


Fig. 5.1 Schematic diagram of granulation apparatus

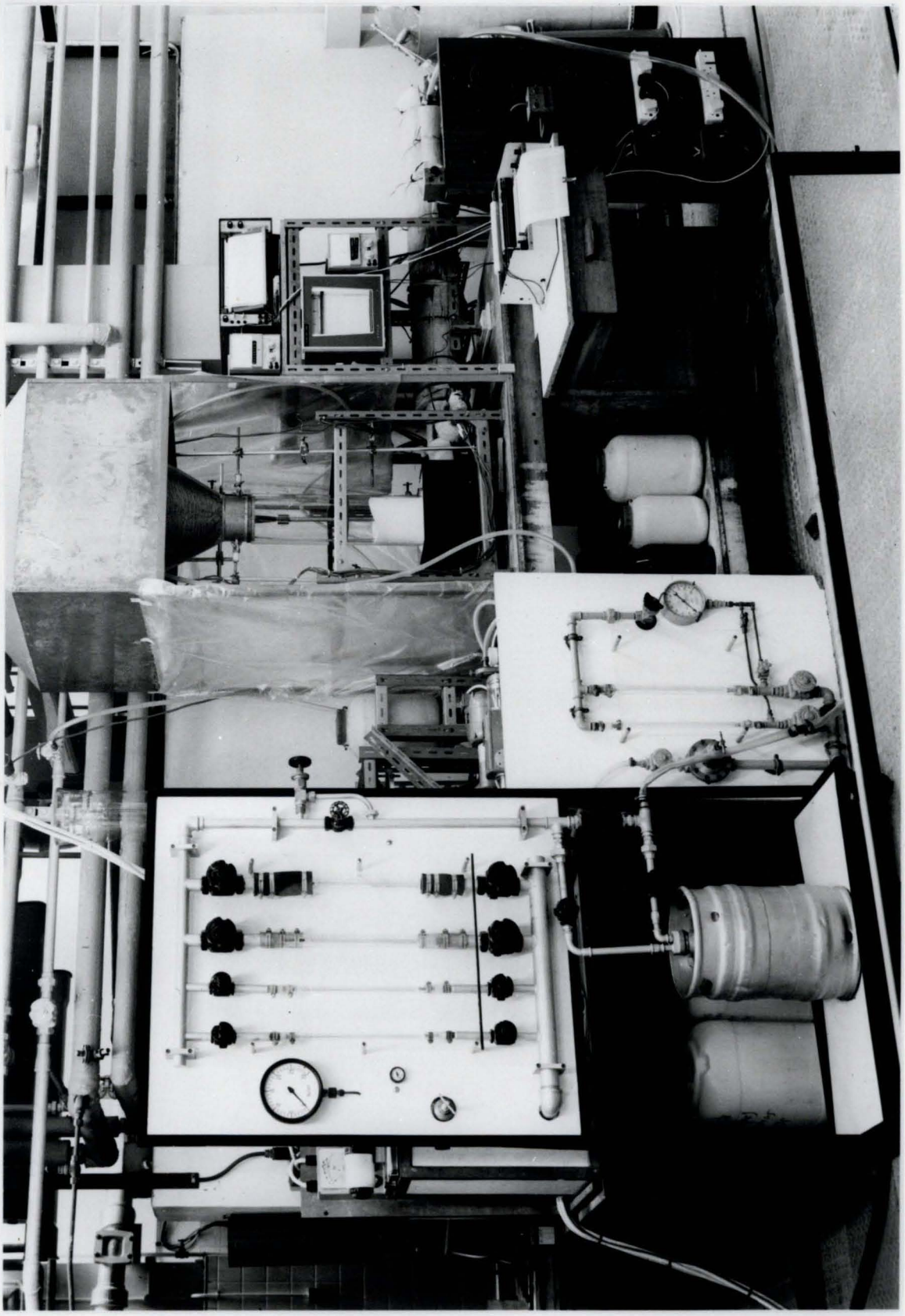

Fig. 5.2 Granulation apparatus

formed from a 0·15 m diameter glass "Quickfit" tube with a wall thickness of 0·007 m, and cut into two sections to facilitate filling and emptying of the bed. The two halves were taped together during a run, with the bottom section held in a recess in the top windbox flange by silicone rubber glue. In order to reduce heat losses from the windbox it was placed in an asbestos lined wooden box, 0·25 m x 0·25 m x 0·15 m deep, packed with coarse alumina particles (to a depth sufficient to cover the top flange) which acted as thermal insulation.

5.2.3 Preheater

The fluidising air is preheated electrically in a 0·10 m internal diameter, flanged tube. Current flows through Nichrome V ribbon wound on the outside of the tube. The preheater is made from 0·0016 m stainless steel with an overall length of 0·78 m and is mounted horizontally. A 0·019 m diameter pipe connects it to the windbox beneath the fluidised bed. Nichrome ribbon (0·0016 m x 1·5 x $10^{-4}$m) sleeved in Refrasil high temperature insulation is wound around the tube (which is first covered in asbestos paper) in four separate sections. Each winding consists of 12·5 m of ribbon, has a resistance of approximately 60 ohms and covers a 0·15 m length of tube. Steel bands hold the ends of the ribbon in place and also serve as terminals. Several layers of asbestos rope and a final layer of 0·05 m thick glass fibre insulation prevent heat losses. Heat transfer to the air stream is improved by 0·01 m ceramic Raschig rings packed inside the tube. The current for each winding is supplied by an 8 amp Variac with a maximum output of 270 volts, although for most runs a voltage of less than 200 v from each of two Variacs was sufficient. The overall theoretical rating of the preheater was approximately 4 kW.

5.2.4 Air supply

Fig. 5.4 shows the air flow system which supplied air both for fluidising the bed and atomising the feed solution. The mains supply

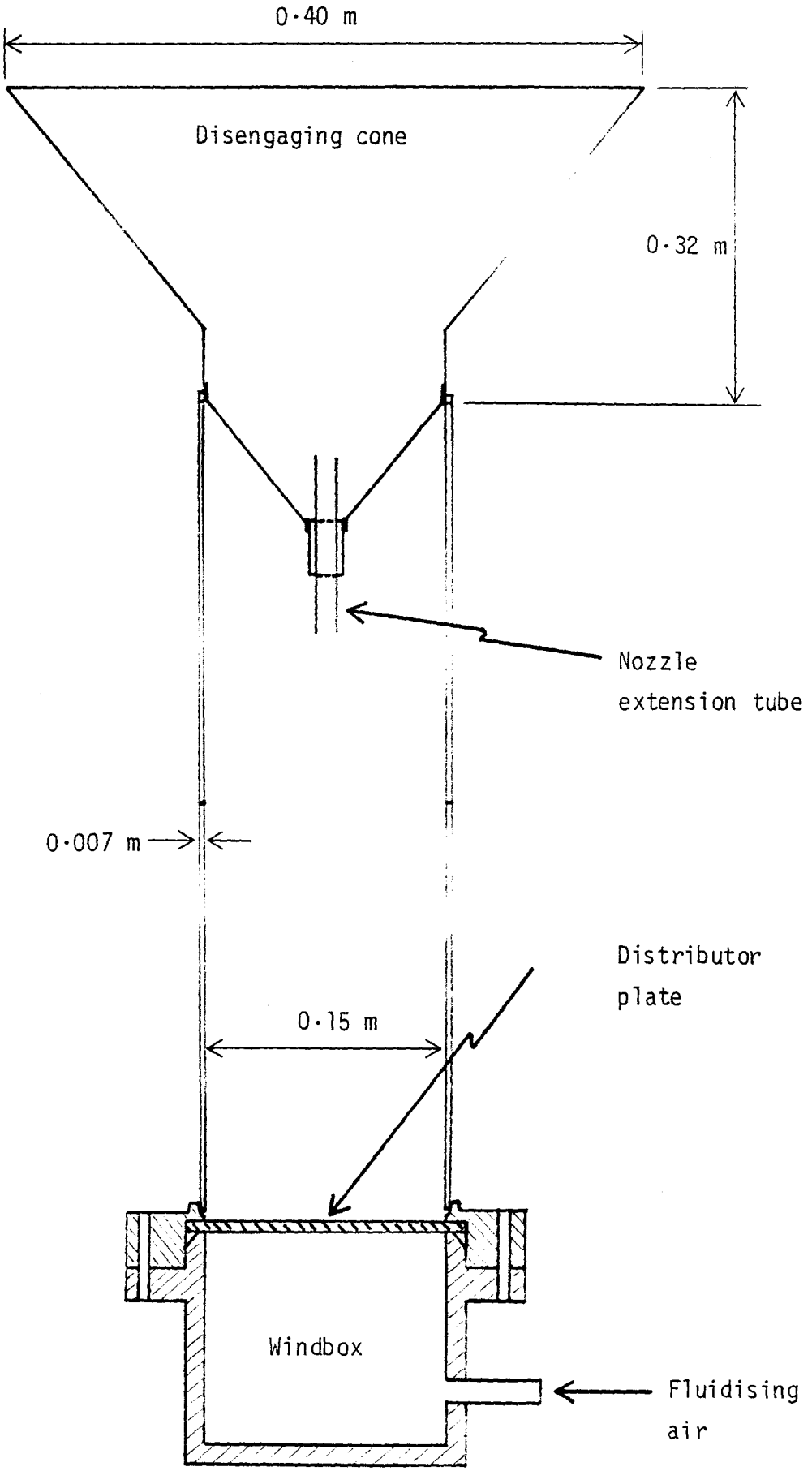


Fig. 5.3 Fluidised bed for granulation experiments

Fig. 5.4 Air flow system

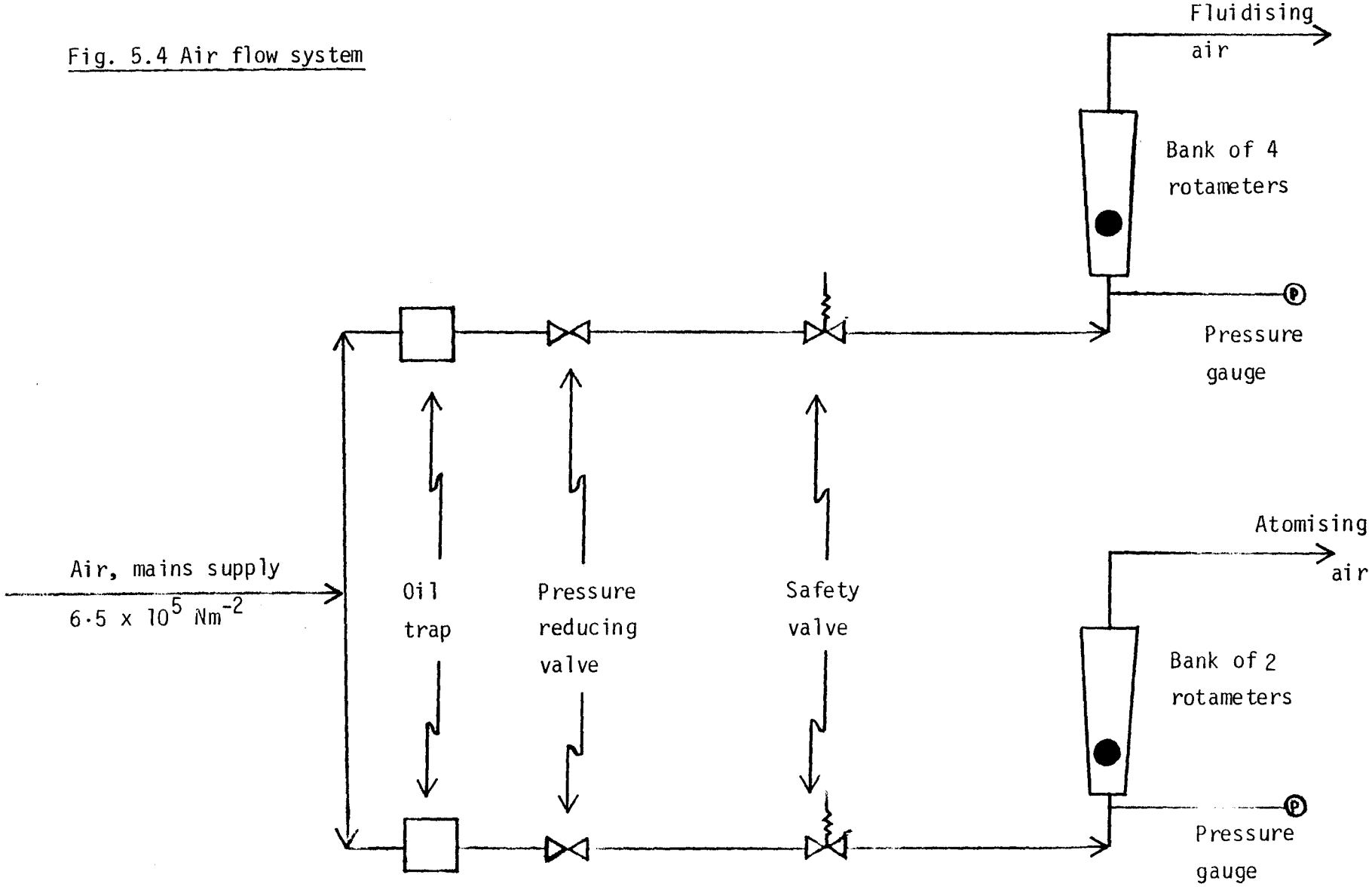

at $6{\cdot}5 \times 10^5$ $Nm^{-2}$ (80 psig) was first filtered and then passed, via a pressure reducing valve, to rotameters calibrated at 10 psig and at 20 psig. Polythene tubing connected the flow rig with the preheater whilst 0·009 m diameter reinforced nylon tubing supplied atomising air to the spray nozzle. The main flow rig contained a bank of four rotameter tubes covering the range $6{\cdot}7 \times 10^{-5}$ $m^3$ $s^{-1}$ to $2{\cdot}0 \times 10^{-2}$ $m^3$ $s^{-1}$ of free air, with the flow controlled by either a 0·02 m ($\frac{3}{4}$") gate valve or a 0·006 m ($\frac{1}{4}$") fine needle valve. The two rotameter tubes for the atomising air covered the range $1{\cdot}0 \times 10^{-4}$ $m^3$ $s^{-1}$ to $2{\cdot}8 \times 10^{-3}$ $m^3$ $s^{-1}$ of free air.

5.2.5 Liquid feed system

The feed liquid was held in a reservoir constructed from a 0·15 m diameter x 1·08 m high glass "Quickfit" tube. At one end an aluminium disc was bolted to a flange arrangement to provide a base for the tank and the liquid flow from the central outlet was controlled by a 0·006 m ($\frac{1}{4}$") Saunders valve. At the top, a Perspex lid prevented evaporation from the solution. The volume of liquid in the reservoir was calculated from the level which was read against a millimetre scale, calibrated to give the reservoir contents to an accuracy of $2{\cdot}0 \times 10^{-5}$ $m^3$. The change in liquid volume with time throughout a run was used to calculate the liquid feedrate and, knowing the solution concentration and density, the mass deposition rate of binder. A second, uncalibrated reservoir was piped in parallel so that, for example, either solution or pure solvent could be fed to the nozzle. The volumetric flow of liquid was controlled by adjusting the stroke of a plunger head metering pump (type "M", supplied by Metering Pumps Ltd.) which had a maximum output of $1{\cdot}03 \times 10^{-5}$ $m^3$ $s^{-1}$ (620 ml $min^{-1}$). A flowrate of $2{\cdot}8 \times 10^{-7}$ $m^3$ $s^{-1}$ (17 ml $min^{-1}$) varied by only 3% over, say, a ten hour period. All the liquid lines between reservoirs, pump and the nozzle head were 0·009 m diameter reinforced nylon tubing.

Liquid was fed into the fluidised bed by means of a pneumatic atomis-

ing nozzle, manufactured by Spraying Systems Co. (USA). Two different sizes of nozzle have been used, depending on the liquid flowrate:

(i) for flowrates less than $1{\cdot}3 \times 10^{-6}$ $m^3$ $s^{-1}$ (80 ml $min^{-1}$), including all the main granulation experiments:

Fluid nozzle 1650 (liquid orifice diameter = $4{\cdot}06 \times 10^{-4}$ m)

Air nozzle 67147

(ii) for flowrates greater than $1{\cdot}3 \times 10^{-6}$ $m^3$ $s^{-1}$, including some preliminary experiments (Chapter Four) and temperature profile experiments:

Fluid nozzle 40100 (liquid orifice diameter = $1{\cdot}02 \times 10^{-3}$ m)

Air nozzle 1401110

The atomising nozzle arrangement is shown in Figs. 5.5 and 5.6 and consisted of three parts:

(i) the nozzle body to which liquid and air were supplied under pressure;

(ii) the fluid nozzle which concentrated the liquid into a narrow stream, and the air into an annulus around it;

(iii) the air nozzle, within which the air and liquid were mixed to produce an atomised spray.

The entire nozzle was made from stainless steel with a PTFE gasket between (i) and (ii). Air was supplied at a metered pressure of $1{\cdot}38 \times 10^5$ N $m^{-2}$ (20 psig) and the normal liquid pressure was $6{\cdot}9 \times 10^4$ $N m^{-2}$ (10 psig). In free air the nozzle produced a finely atomised, round patterned spray with a solid angle of 12 - 15°. The quality of the spray and the droplet size distribution will depend upon the volumetric air to liquid ratio (NAR).[97] In all granulation and temperature profile experiments this ratio was kept constant at a value of 500 (calculated at 273 K).

In order to conveniently position the nozzle below the fluidised bed surface a 0·46 m long extension tube connected the liquid nozzle to the nozzle body. This consisted simply of two concentric tubes, liquid

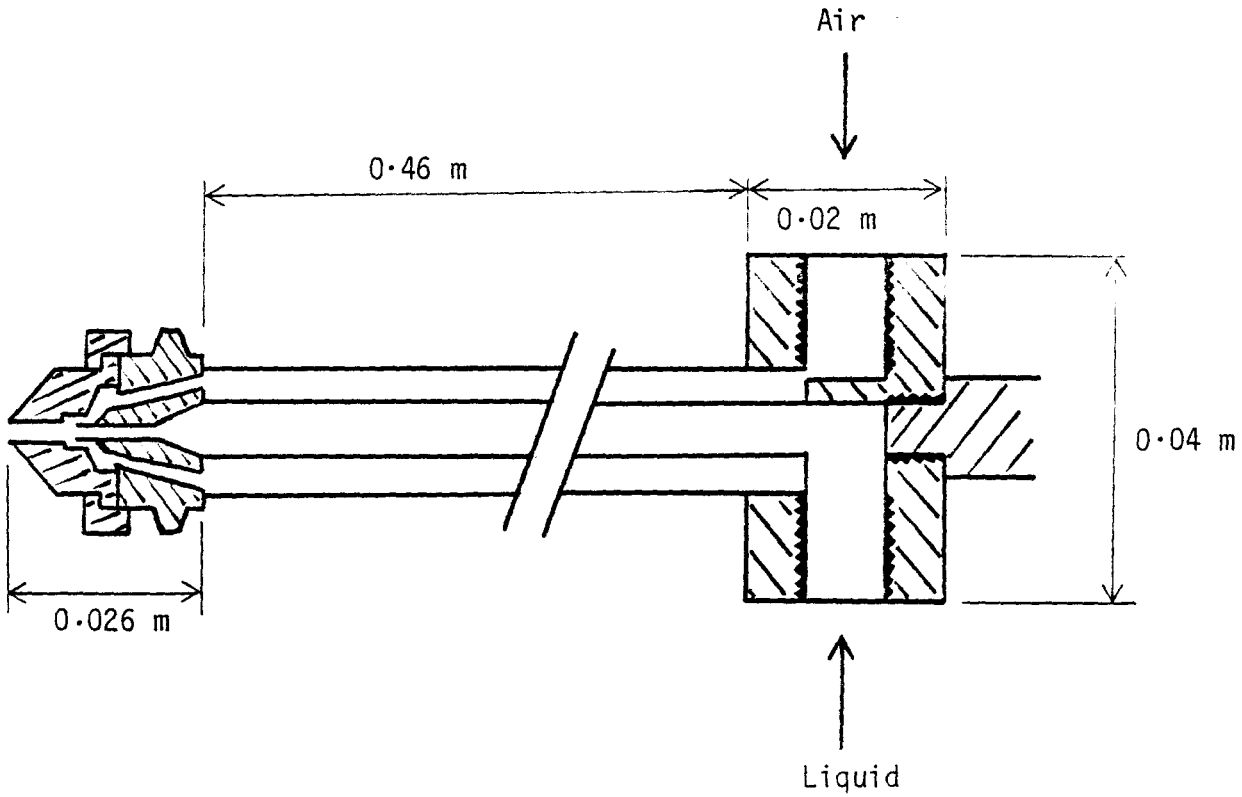


Fig. 5.5 Diagram of atomising nozzle and extension tube

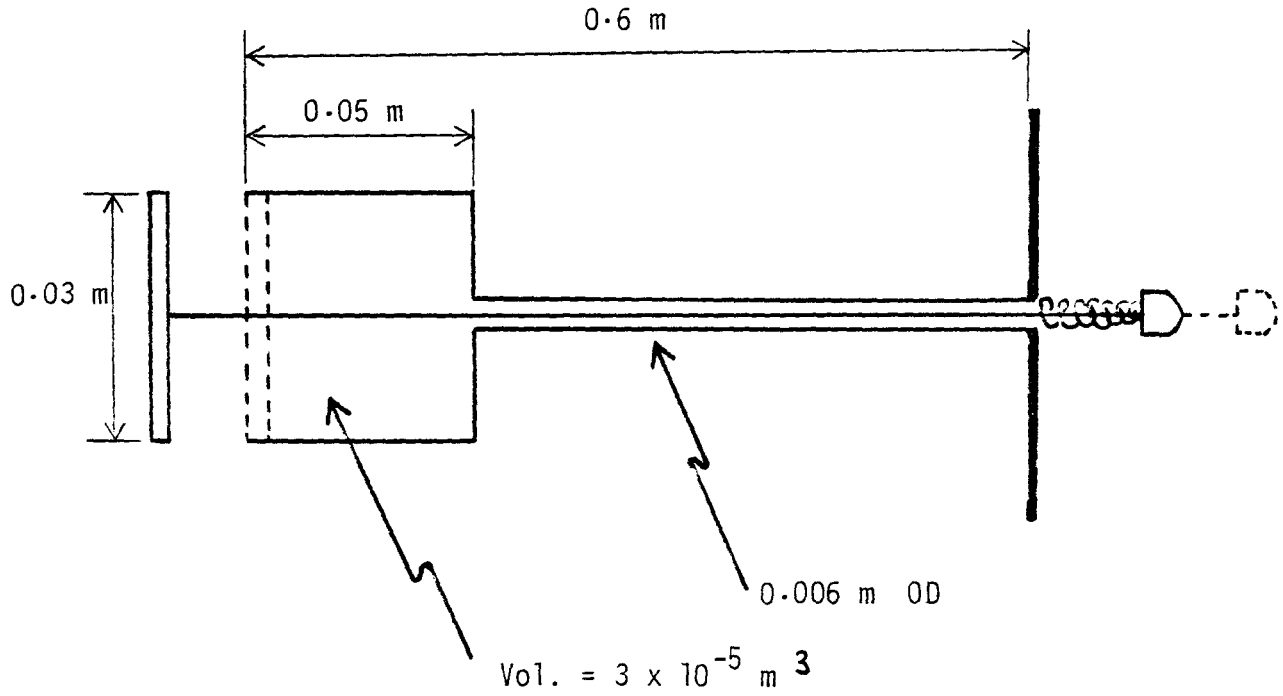


Fig. 5.7 Sampling device

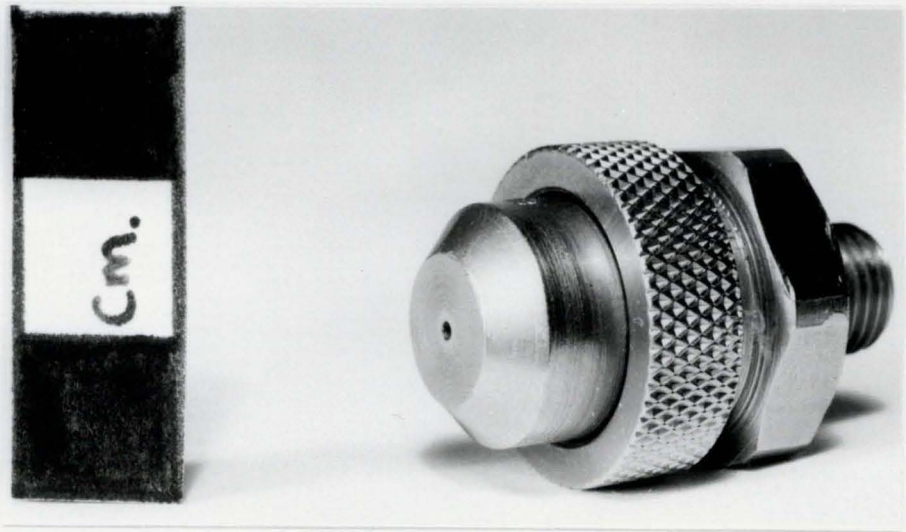


Fig. 5.6 Atomising nozzle

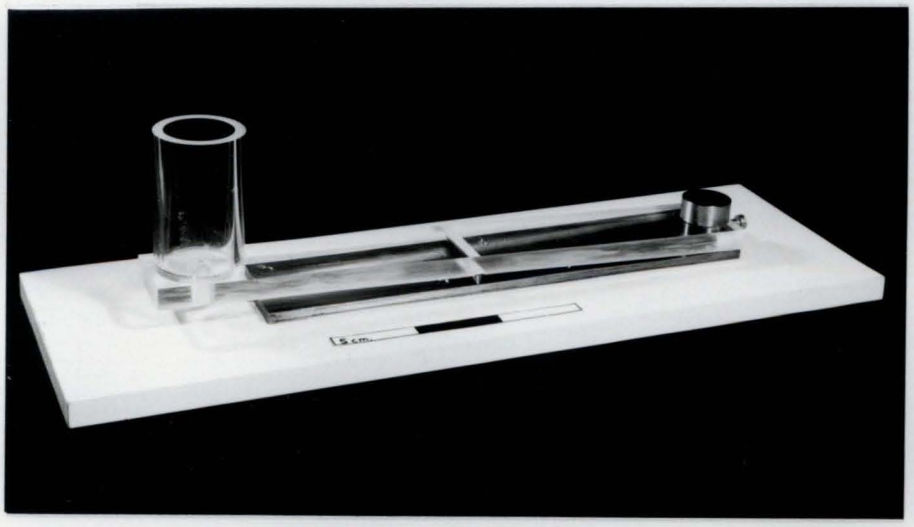


Fig. 5.12 Apparatus for measuring granule strength

passing through the centre and air through the annulus. During experiments the nozzle was held vertically, with the tip at the top of the packed bed (0·12 m above the centre of the distributor plate). The whole assembly was kept in position by a clamp, above the disengaging cone, which held a rod screwed into the nozzle body and by a bush on the barrel of the extension tube which located in a brass collar. The collar was supported centrally 0·10 m below the disengaging cone by two batons attached to its inside surface (see Fig. 5.3) and ensured that the nozzle assembly remained rigid.

5.2.6 Temperature measurement

During the course of an experiment the air temperature in the preheater, in the windbox and in the freeboard and the temperature of the fluidised bed itself were all monitored. The preheater air temperature was measured close to the exit by means of a sheathed chromel / alumel thermocouple; all other temperatures were measured by bare wire thermocouples made from 0·0016 m (1/16") chromel / alumel wire. At one end the two wires were spot welded together and at the other were fixed into a connecting block. Compensating cable led from the block to the measuring or recording device. The windbox thermocouple entered via a 0·0016 m (1/16") coupling welded into the side wall and was directed upwards so as to measure the air temperature just below the distributor plate. The bed temperature was measured in three positions (0·005 m, 0·07 m and 0·12 m above the distributor respectively) and these thermocouples, together with that in the freeboard, were mounted in straight lengths of 0·0032 m (1/8") stainless steel tubing to give them sufficient rigidity to withstand the buffeting action of the bed. They were mounted vertically, in pairs, close to the bed wall and were held in position by clamps protruding through two circular holes (0·04 m in diameter) cut, opposite one another, in the cylindrical part of the disengaging device. The preheater temperature and that 0·07 m above the distributor

plate were displayed on a Comark electronic thermometer and could also be traced by a chart recorder. The remaining temperatures were logged directly on an Ether multi-pen recorder.

## 5.3 GRANULATION MATERIALS

Either alumina or glass powder particles have been used for these experiments; they conveniently represent porous and non-porous solids respectively and both were available in the laboratory in large quantities. They have similar irregular shapes and were closely sieved before use to give approximately the same particle size. The chosen size range was - 355 + 180 μm but, because fresh material was required constantly, new batches were sieved and consequently both $d_p$ and $U_{mf}$ changed slightly from time to time. The mean particle diameter was measured at the start of each run and the minimum fluidising velocity checked periodically.

Solutions of benzoic acid and of "carbowax" (polyethylene glycol 4000) in methanol have been used as granulating liquids. All the chemicals were supplied by BDH Ltd. Solution concentrations are given as weight percent, defined as:

$$\frac{\text{weight of solute}}{\text{weight of solution}} \times 100$$

Details of the granulation materials, their physical properties and the methods used to measure those properties appear in Appendix A.

## 5.4 PROCEDURE FOR GRANULATION EXPERIMENTS

### 5.4.1 Start-up procedure and pseudo steady-state operation

To commence a granulation experiment the bed, with the upper glass and disengaging sections removed, was charged with the required weight of fresh material and the upper sections were placed in position, together with the bed thermocouples. The fluidising air and the Variac voltages were then set to the required levels. The former was chosen to give the desired excess gas velocity at the bed operating temperature, usually $40^{o}$ C, taking into account the expansion of air and the small change in minimum fluidising velocity due to the increase in gas viscosity with temperature. An equation has been derived to give the flowrate of air Q, at room temperature $T_1$, necessary to fluidise the bed with an excess gas velocity $(U - U_{mf})$ at the bed operating temperature $T_B$. Minimum fluidising velocity is inversely proportional to the viscosity of the fluidising gas[1]:

$$U_{mf} \propto \mu^{-1} \tag{5.1}$$

$$\text{but } \mu \propto T^{1.5} \tag{5.2}$$

where T is the absolute temperature.

$$\text{Therefore } U_{mf} \propto T^{-1.5} \tag{5.3}$$

The minimum fluidising velocity at $T_B$, $U_{mf}(T_B)$, is given by:

$$U_{mf}(T_B) = U_{mf}(T_1 / T_B)^{1.5} \tag{5.4}$$

$$\text{therefore } Q_{mf}(T_B) = AU_{mf}(T_1 / T_B)^{1.5} \tag{5.5}$$

$$\text{Now, } Q(T_B) = A\,U(T_B) \tag{5.6}$$

where $Q(T_B)$ and $U(T_B)$ are the volumetric gas flowrate and gas velocity respectively, at the temperature $T_B$. It follows therefore that:

$$Q(T_B) = A\left\{ U(T_B) - U_{mf}(T_B) + U_{mf}(T_1 / T_B)^{1.5} \right\} \tag{5.7}$$

$$\text{and } Q(T_B) = A\left( (U - U_{mf}) + U_{mf}(T_1 / T_B)^{1.5} \right) \tag{5.8}$$

From the ideal gas law:

$$Q = Q(T_B)(T_1 / T_B) \tag{5.9}$$

and therefore:

$$Q = A(T_1 / T_B) \left( (U - U_{mf}) + U_{mf}(T_1 / T_B)^{1.5} \right) \qquad (5.10)$$

With the experience gained after a few runs, the correct heater voltage could be set accurately to give the windbox (air inlet) temperature required to satisfy the heat balance (Equ. 2.2).

When the bed temperature reached steady-state (somewhat above the operating temperature) a stream of pure methanol was fed into the bed at the desired rate until the operating temperature was reached. (As liquid is introduced into a bed the temperature, previously constant, will fall as sensible heat in the incoming gas is used to provide the latent heat of vaporisation of the liquid.) The feed stream was then switched to solution and in this way granulation could be carried out at a constant bed temperature. The exact procedure was as follows: the flowrate of methanol through the nozzle was adjusted and measured with a graduated cylinder. Then, with the liquid stream turned off and a flow of air issuing from the nozzle (which prevented blockage of the liquid orifice), the nozzle assembly was put into position in the bed. Liquid was then pumped to the nozzle and the atomising air adjusted to the correct level. With the bed temperature once again steady, the liquid flow was switched to solution and the flowrate increased slightly to compensate for the lower solvent content of the solution. (If this was not done an increase in bed temperature would result.) Inevitably some slight temperature variation occurred but did not significantly affect the steady-state temperature assumption. The time required for solution to break through was previously determined and the clock started at the appropriate time. During a run there were small fluctuations in solution flowrate, air flowrate and possibly in the heater current, however the bed temperature varied by only one or two $^{o}C$ over periods of up to ten hours.

As the particle size in the bed increases, so the minimum fluidising velocity increases and the "quality" of fluidisation will change. To compensate for this the air flowrate can be periodically increased, thus keeping the excess gas velocity constant. If there is some knowledge of how the particle size will change from time to time, the necessary increase in flowrate can be predicted with reasonable accuracy by using a theoretical or semi-empirical equation which gives the minimum fluidising velocity as a function of particle size. Leva's[101] equation (Equ. 5.11) was used for this purpose:

$$U_{mf} = \frac{1.28 \times 10^{-13} \, d_p^{1.8} \left[ \rho_f \left( \rho_p - \rho_f \right) \right]^{0.94}}{\rho_f \, \mu_f^{0.88}} \qquad (5.11)$$

where $U_{mf}$ is the minimum fluidising velocity ($ms^{-1}$), $d_p$ ($\mu m$) is the mean particle diameter, $\rho_f$ and $\rho_p$ the fluid and particle densities respectively ($kg\ m^{-3}$) and $\mu_f$ is the fluid viscosity (Pa s).

5.4.2 Sampling

A simple "thief" sampling device, shown in Fig. 5.7, was used to remove samples of bed particles for analysis. It consisted of a small cylindrical steel vessel with one end sealed and attached to a tubular handle. The other end was closed by a disc attached to a central shaft which moved inside the handle. A spring normally kept the sampler closed, but when the shaft was depressed against the spring the disc was displaced and the sampler was opened. To take a sample the device was lowered into the fluidised bed and then opened so as to fill, or partly fill, the vessel with particles. It was then closed, removed from the bed, and the particles tipped into a sealed container. In order to acquire the desired amount of material, it was sometimes necessary to remove two samples in quick succession. However, the whole procedure took less than one minute.

The sampler was positioned at a point half way between the central

axis and the bed wall and, in general, at the centre of the fluidised layer. In some early experiments samples were also taken from the top of the bed (just below the fluidised surface) and from the bottom - with the disc of the open sampler touching the distributor plate. With such a large sampling volume it is clearly impossible to specify a precise sampling point. The sample was assumed to be representative at the high excess gas velocities used.[96]

5.4.3 Sieving and establishing a mass balance

The samples removed from the bed were sieved in a nest of 20 0·10 m diameter British Standard sieves, supplied by Endecotts Ltd. Each sample was shaken for a period of ten minutes on a mechanical sieve shaker before the contents of each sieve were brushed out and weighed. A proportion of each sample was retained in order to establish a mass balance; i.e., compare the mass of binder adhering to the bed particles with the mass input of binder up to the time of the sample and thus determine that all the binder was available for particle growth. A sample was divided into four arbitrary sieve fractions and a known mass of granules taken from each (or as many as were present in a particular sample) and placed in a $5{\cdot}0 \times 10^{-5}$ $m^3$ (50 ml) flask. Binder was then removed from the particles by washing and shaking with methanol and then decanting the liquid, leaving binder-free particles in the flask. This process was repeated until the sample reached a constant weight on drying. The chosen sieve fractions were :

(i) - 250 μm

(ii) - 500 + 250 μm

(iii) - 1400 + 500 μm

(iv) + 1400 μm

This procedure gives a mass ratio of binder to initial bed particles E for each of i arbitrary sieve fractions. If the combined mass fractions are $\varphi_i$ (i = 1, 2, 3, 4) and the initial bed mass is M, then the

total mass of binder adhering to the bed particles, $M_b$, (assuming the samples to be representative of the bed) will be given by:

$$M_b = M \sum_{i=1}^{i=4} \varphi_i E_i \qquad (5.12)$$

where $$\sum \varphi_i = 1 \qquad (5.13)$$

$M_b$ can be compared with the mass input of binder calculated from the volumetric flowrate of solution R, which was measured by observing the change in level of solution in the calibrated reservoir. Knowing the solution density $\rho$, and concentration $x_s$, the mass input at any time t is given by:

$$M_b = Rtx_s \rho \qquad (5.14)$$

This method of establishing a mass balance was possible only with glass powder particles. With a simple washing technique it was not possible to remove binder entirely from within the pores of the alumina particles, nor to remove it selectively from the external surface. Therefore it was assumed that if a mass balance could be established for glass powder particles then, under otherwise identical conditions, it also held for alumina.

## 5.5 MEASUREMENT OF TEMPERATURE PROFILES

### 5.5.1 Introduction

The measurement of temperature profiles within the bed and the subsequent construction of isotherms is one method of determining whether particular zones exist in the fluidised layer. These zones, for example, may indicate where drying or evaporation takes place.

### 5.5.2 Apparatus

A stainless steel bed was chosen for this work, firstly because it allowed thermocouples to enter through the wall and to be traversed radially, and secondly because air inlet and bed temperatures higher than those in the glass bed were permissible. The bed, made from 0·003 m thick stainless steel tube, was in three flanged sections. The 0·003 m thick porous stainless steel distributor plate (grade 10 PORAL, supplied by Ugine Kuhlmann Ltd.) sat in a recess cut in the windbox flange and was held in position by the lower bed section, which contained eleven thermocouple wells. A further section was placed on top of this and was surmounted by the disengaging cone previously described. The principal dimensions of the apparatus are given in Fig. 5.8.

Each thermocouple well consisted of a hole 0·0032 m in diameter drilled radially through the bed wall and a 0·01 m length of tube, of the same diameter, welded over it so that a probe could be pushed through into the bed and, supported by the tubular section, make a radial traverse of the bed. A PTFE sleeve was fitted tightly into each well so that gas or particles could not escape. The first well was placed at a height of 0·02 m above the distributor plate and thereafter at 0·01 m intervals up to a level of 0·12 m, but in different vertical planes to facilitate construction. Fig. 5.9 gives a plan view of the thermocouple well positions. Bed temperatures were measured with bare wire chromel / alumel thermocouples supported, as before, in 0·0032 m diameter tubing. Rigidity was particularly important because temperatures

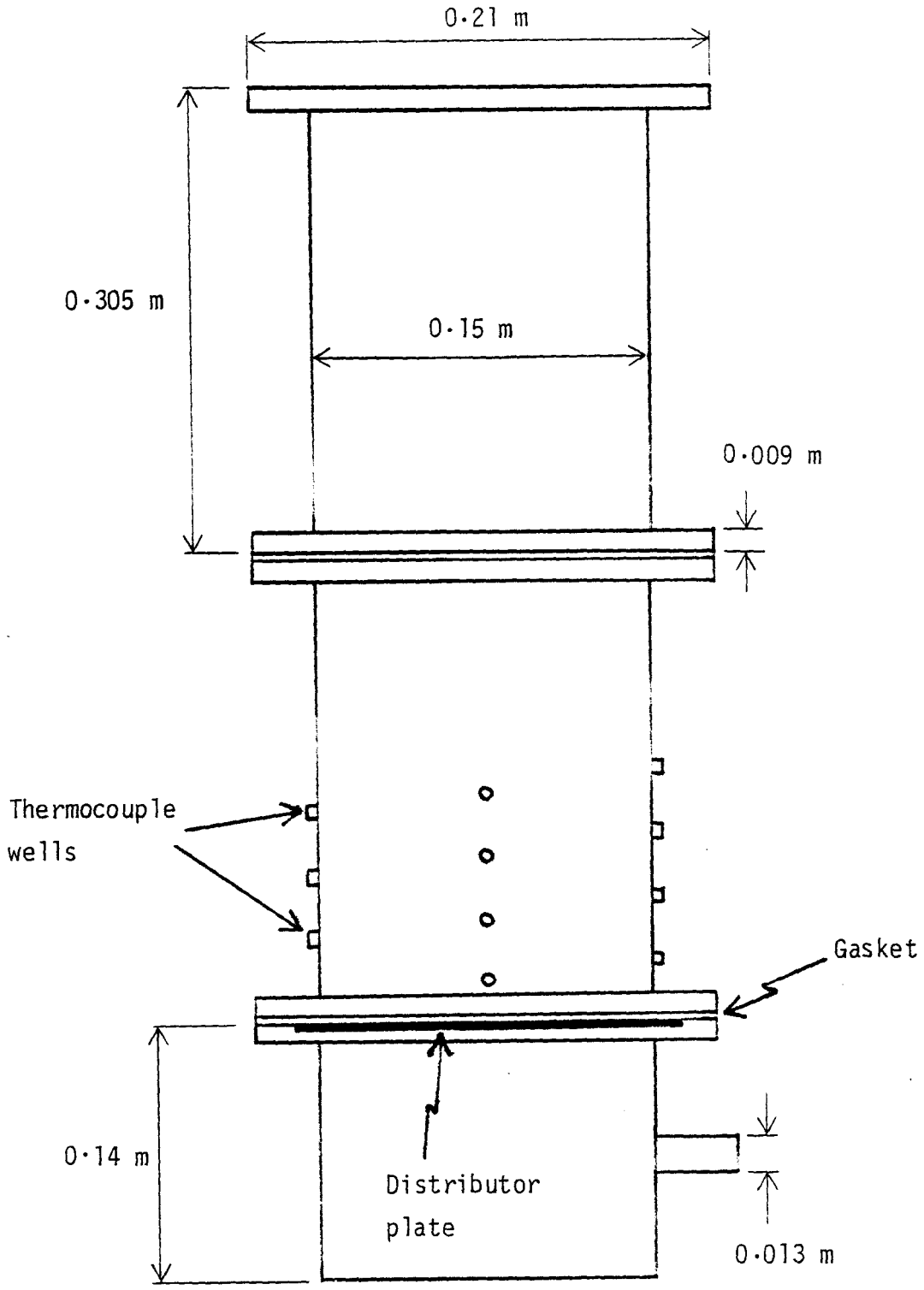


Fig. 5.8 Stainless steel fluidised bed for temperature profile measurements

were being measured at precise points. Temperatures were displayed on a Comark electronic thermometer and, where necessary because of severe fluctuations, traced by a chart recorder.

The nozzle arrangement and the air and liquid feed supplies were as described previously. Experiments have been carried out with both alumina and glass powder as bed material, and methanol as the feed liquid.

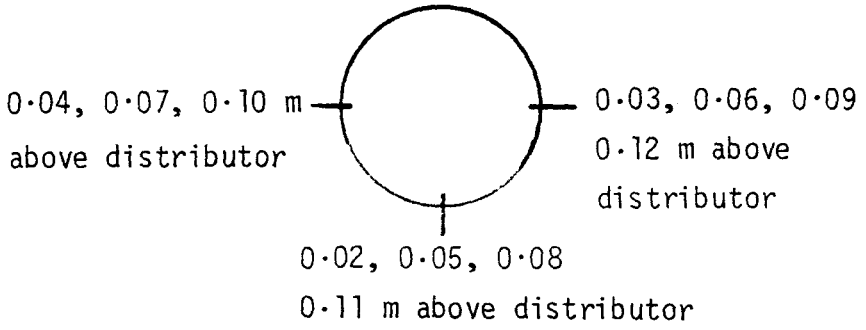


Fig. 5.9 Position of thermocouple wells - plan view

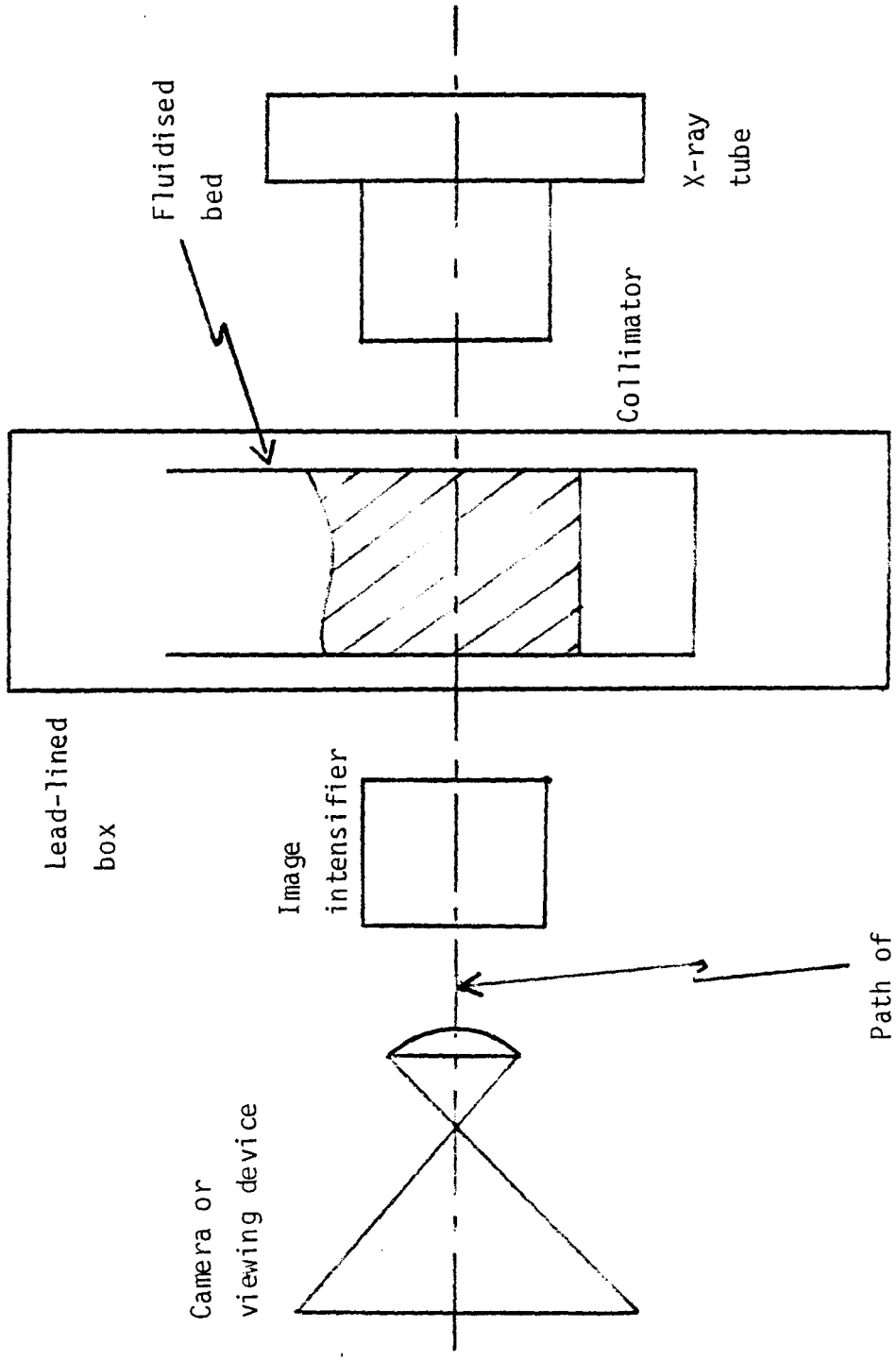


Fig. 5.10 Schematic diagram of X-ray apparatus

## 5.6 X-RAY PHOTOGRAPHY OF GRANULATION

### 5.6.1 Introduction and arrangement of apparatus

A powerful and well-tried technique for studying the behaviour of fluidised beds is to place the bed in an X-ray beam which then passes to a camera and exposes photographic film.[102] It was used here in conjunction with radiopaque solutions which were sprayed into the bed in the normal way, with the intention of discovering whether or not a spray zone or feed zone existed close to the nozzle, or whether any other type of zone could be identified in the bed. Two separate X-ray sets have been used, with two different experimental arrangements. Fig. 5.10 is a general diagrammatic representation.

(i) The granulation rig was re-assembled inside a lead-lined box (2·0 m x 1·20 m x 2·30 m) with the extraction hood in place of a section of the roof panelling, enabling methanol to be evaporated and a normal granulation run to be filmed by X-rays. All the equipment, except air flow rigs and temperature displays, was placed inside the box.

(ii) A more powerful X-ray set, but with a smaller and unenclosed lead-lined cabinet in place of the box, was used to film experiments in the Perspex bed at room temperature and with water as the liquid. The spray nozzle was clamped in position 0·12 m above the distributor and air and liquid supplied in the usual way. An extra cylindrical section, 0·43 m high, was added to prevent elutriation.

Details of the X-ray equipment and of the film analysis techniques are given in Appendix B.

### 5.6.2 Limitations of the technique

It proved impossible to penetrate a bed of glass powder with the X-ray beam and be able to make useful observations. Accordingly, only beds of alumina particles have been filmed. For the granulation runs, an extra 10% (by weight) of barium bromide was added to the methanol based solutions so that the feed liquid and the deposited solute became

radiopaque. A solution of 25% barium chloride in water was used for the experiments at ambient temperature. On negative film the solutions appear white and are sufficiently different in intensity to be distinguished from the dense phase of the fluidised bed.

## 5.7 MEASUREMENT OF GRANULE STRENGTH

### 5.7.1 Introduction

The relative strengths of product granules were measured in order to determine the relative strengths of particle - particle bonds formed from different binders. In turn, this information allowed conclusions to be drawn about the mechanism of particle growth in fluidised bed granulation.

### 5.7.2 Apparatus

The apparatus used for obtaining a measure of the compressive strength of a granule is shown in Figs. 5.11 and 5.12 and consisted of a Perspex beam (0·05 m wide and 0·013 m thick) fixed to the underside of which, and running perpendicular to the length, was a steel knife edge. The knife edge sat in a 0·001 m deep V-shaped groove cut at right angles across a horizontal steel plate. At one end of the beam was a cylindrical Perspex container (internal volume = $1.0 \times 10^{-4}$ $m^3$), with its weight exactly balanced by a brass weight (approximately 0·1 kg) at the opposite end of the beam. The container overhung the plate by 0·06 m and, when balanced, there was a gap between beam and plate of about 0·003 m.

### 5.7.3 Procedure

A single granule was placed, centrally and close to the edge, at the container end of the plate, and the beam carefully balanced so that it just touched the granule. A constant flow of water ($3.3 \times 10^{-7}$ $m^3$ $s^{-1}$) from a peristaltic pump was then started and pumped to a beaker close to the apparatus. To start the test the water outlet was positioned directly over the container and a stop watch started simultaneously. Thus the container slowly filled with water and applied a load to the granule, which was crushed between the nearly parallel surfaces of the beam and the plate. The destruction of the granule was viewed through the transparent beam and the time taken for it to be crushed was recor-

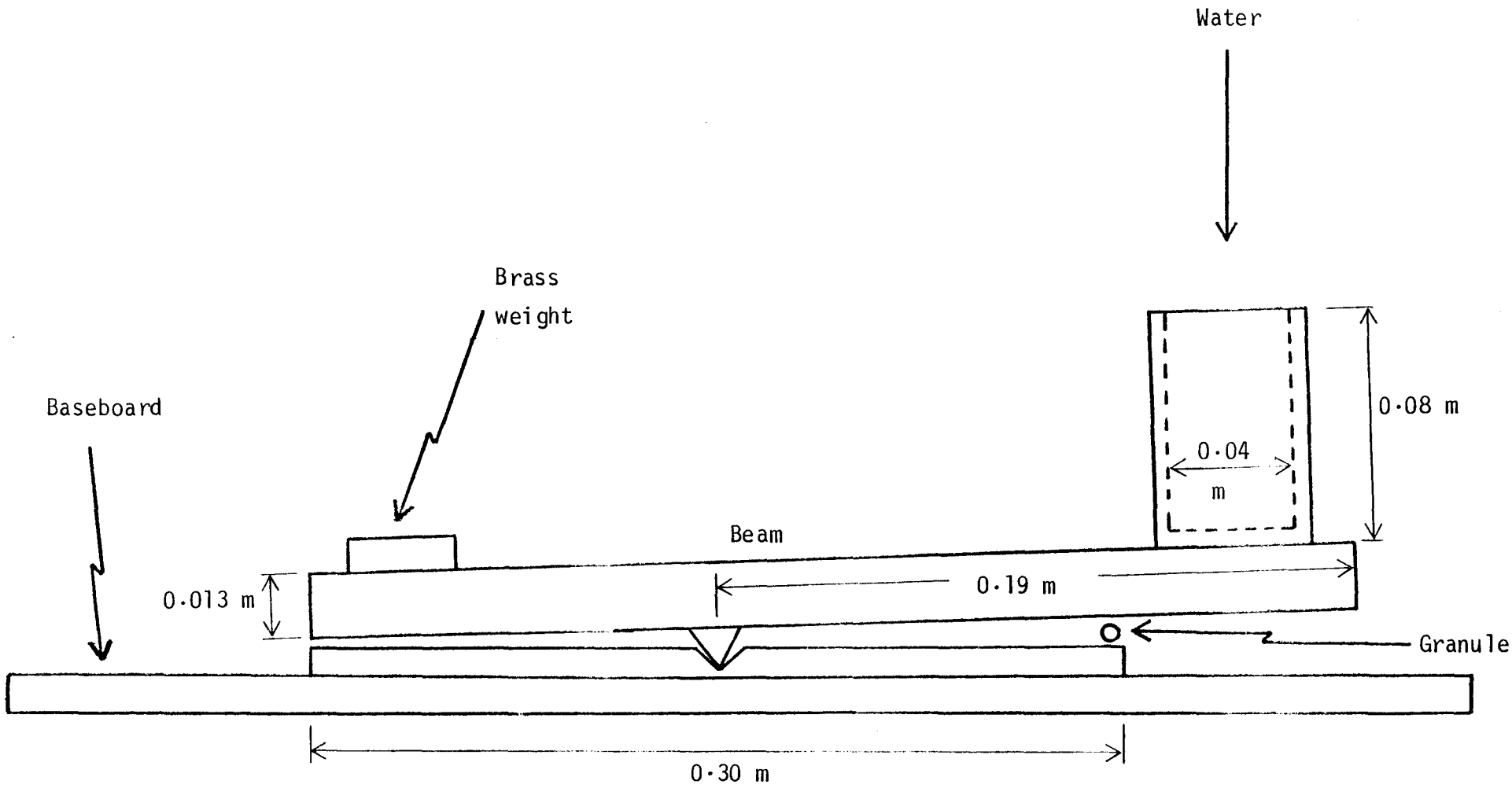


Fig. 5.11 Apparatus for measuring granule strength

ded. This period is then a measure of compressive strength for similarly sized granules.

Agglomerates in the sieve range - 2360 + 2000 μm were chosen for these tests. The granules were selected to be as near spherical as possible; irregular shaped ones were rejected. Tests were discounted when a granule broke as the beam was being balanced and when a granule did not disintegrate instantaneously, i.e. when individual constituent particles were shed as the load was increased.

# CHAPTER SIX

# GRANULATION RESULTS

## 6.1 INTRODUCTION

This chapter presents the results of experiments in which particles in a fluidised bed have been caused to increase in size by the deposition of solute on the particle surfaces. In all the experiments sufficient heat was supplied in the fluidising gas to evaporate the solvent contained in the feed solution, thus satisfying the heat balance (Equ. 2.2). Consequently, the reported instances of bed quenching were not due to saturation of the exhaust gases, although localised moisture imbalances may still have occurred. The same volumetric feedrate of solution was used for all the experiments ($2{\cdot}8 \pm 0{\cdot}1 \times 10^{-7}$ m$^3$ s$^{-1}$; $16{\cdot}8 \pm 0{\cdot}6$ ml min$^{-1}$) but with different concentrations of solute. Therefore, as the solution feedrate (and thus the head load) was kept constant, the mass feedrate of binder changed with solution concentration. Tables 6.1 and 6.2 give the solvent and solute mass feedrates for a solution flowrate of $2{\cdot}8 \times 10^{-7}$ m$^3$ s$^{-1}$. Equal concentration solutions of carbowax and benzoic acid have the same density (see Appendix A).

Table 6.1 Solvent evaporation rates; 10% solution

| | | |
|---|---|---|
| volumetric feedrate (solution) | : | $2{\cdot}80 \times 10^{-7}$ m$^3$ s$^{-1}$ |
| mass feedrate (solution) | : | $2{\cdot}29 \times 10^{-4}$ kg s$^{-1}$ |
| solvent evaporation rate | : | $2{\cdot}07 \times 10^{-4}$ kg s$^{-1}$ |
| evaporation rate / bed x-section | : | $1{\cdot}17 \times 10^{-2}$ kg s$^{-1}$ m$^{-2}$ |
| evaporation rate /bed volume | : | $7{\cdot}79 \times 10^{-2}$ kg s$^{-1}$ m$^{-3}$ |

Table 6.2 Binder mass flowrates as a function of solution concentration

Solution feedrate = $2{\cdot}80 \times 10^{-7}$ $m^3$ $s^{-1}$

| Concentration (wt. %) | Binder mass flowrate ($kg\ s^{-1}$) |
|---|---|
| 1·0 | $2{\cdot}24 \times 10^{-6}$ |
| 5·0 | $1{\cdot}13 \times 10^{-5}$ |
| 10·0 | $2{\cdot}29 \times 10^{-5}$ |
| 20·0 | $4{\cdot}75 \times 10^{-5}$ |

With the exception of those experiments where temperature variation was an experimental observation, the nominal bed operating temperature was always $40^{o}$ C.

Using a non-porous substrate, two types of product granule have been observed: layered or onion-ring particles and agglomerates. After an initial period during which no growth took place, porous alumina particles grew in similar modes. The evidence for each type of growth has been set out and the effects of a series of operating parameters on the mode and extent of growth have been described. With a knowledge of the physical properties of the product granules and of the binder solutions, a mechanism of particle growth has been proposed (see Chapter Eight) which accounts for the experimental observations.

## 6.2 LAYERED GROWTH

### 6.2.1 Visual observations

Layered, or onion-ring, granules have been produced by granulating particles of glass powder with a 10% benzoic acid solution, at an excess gas velocity towards the high end of the studied range. The structure of the granules can be seen clearly when viewed with an optical microscope; photographs taken through the microscope are reproduced in Figs. 6.1 and 6.2 and show the original, ungranulated material and the layered granules respectively.

A mass balance on the system was established (see Section 5.4.3) and confirmed that the binder which was introduced in the feed solution remained in the bed, adhering to the surface of the bed particles. The masses of binder calculated firstly from the product of flowrate and feed concentration, and secondly from the washing of particle samples, have been compared and agree to within 3%. Although some agglomerated particles were produced in this experiment (as will be seen from the particle size data in Section 6.2.2) the granules in Fig. 6.2 are representative of the vast majority of the product. They are less translucent than the initial particles, because of binder adhering to the surface, but of a similar size and are clearly formed from single particles, rather than from doublets or triplets. Particle shape is also similar except for a slight rounding of corners, making the granules less angular in appearance. However, they are not at all comparable to the particles built up from clearly identifiable growth rings which have been reported in the literature,[23,44,56] save for the absence of agglomerates. The granules in Fig. 6.2 have not assumed a spherical shape and, on close inspection, the binder can be seen to be unevenly distributed over the particle surface, often in small lumps, as in Fig. 6.3.

Scale ; 1000 μm

Fig. 6.1 Initial glass powder particles

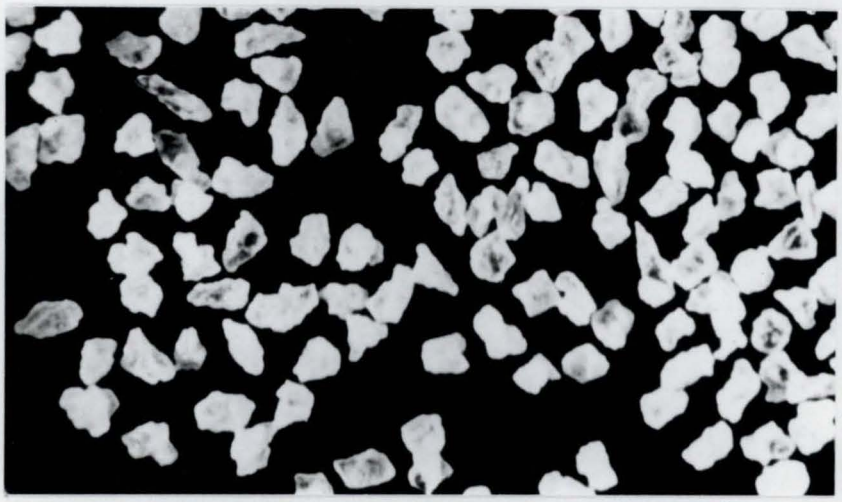

Fig. 6.2 Layered glass powder granules

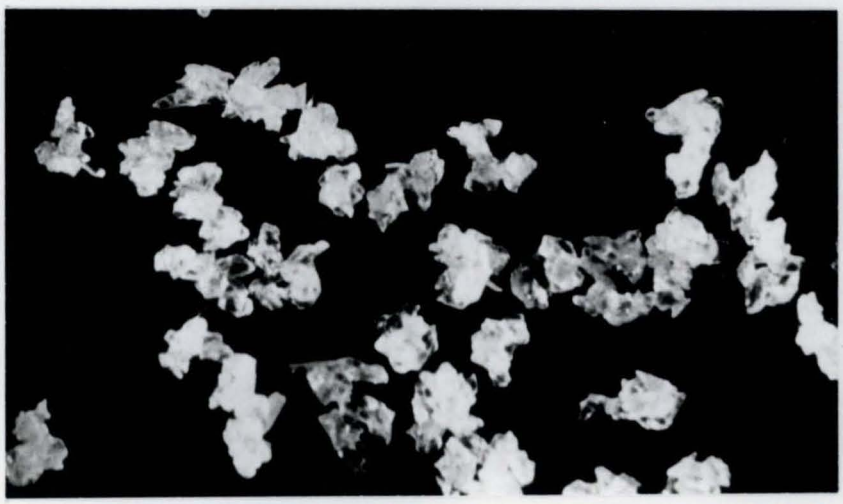

Fig. 6.8 Agglomerated glass powder

Fig. 6.3 Appearance of binder on the surface of a layered granule

6.2.2 Growth curves and particle size distribution

A total of 0·85 kg of benzoic acid was sprayed into a bed of glass powder, fluidised at an excess gas velocity of 0·525 $ms^{-1}$, over a period of ten hours. Unless this material forms nuclei or new bed particles (elutriation has been discounted because a binder mass balance has been established), the existing bed particles will inevitably increase in size; this is demonstrated by the change in mean particle diameter with time, shown in Fig. 6.4. Particle growth begins as soon as binder is introduced into the bed and takes place continuously there-

after, as is shown by the gradual increase in surface - volume mean diameter over the length of the run. It will be demonstrated in the next section that this is the expected increase in particle size for layered growth. In contrast, the weight - moment mean diameter fluctuates wildly before increasing relatively steadily towards the end of the experiment. A few large agglomerates are responsible for the initially high value of $d_p$ (wm). After sixty minutes of operation 0·41% of the sample was retained on a 1400 μm sieve, but by 240 minutes this had been reduced to 0·18% and after 600 minutes, at the end of the experiment, the size of the largest mesh on which granules were retained was 850 μm. Thus, after an initial period, the small percentage of large agglomerates in the bed are broken down while the bulk of the bed material continues to grow, producing layered granules and an increase in $d_p$ (sv). At later stages, between t = 360 minutes and 480 minutes and again between t = 540 minutes and 600 minutes, there was an increase in the weight - moment mean diameter after a sharp decrease, suggesting that an equilibrium is being established between the tendency to form agglomerates and the inertial forces pulling them apart. Obviously $d_p$ (wm) will continue to increase if any particle growth is taking place, but the significant point about the plot of the weight - moment diameter in Fig. 6.4 is that the rate of change of $d_p$ (wm) decreases dramatically as the run proceeds, indicating a decrease in the importance of agglomeration and a domination of particle growth by the layering mechanism and by inertial forces.

The change in particle size distribution with time is shown in Figs. 6.5 and 6.6. The initial narrow distribution becomes flatter and broader as granulation proceeds and the cumulative oversize curves move towards the larger particle sizes but paralleling each other, confirming that continuous particle growth is taking place. Both the mode and median sizes increase, the latter (the 50% point on the cumulative plot)

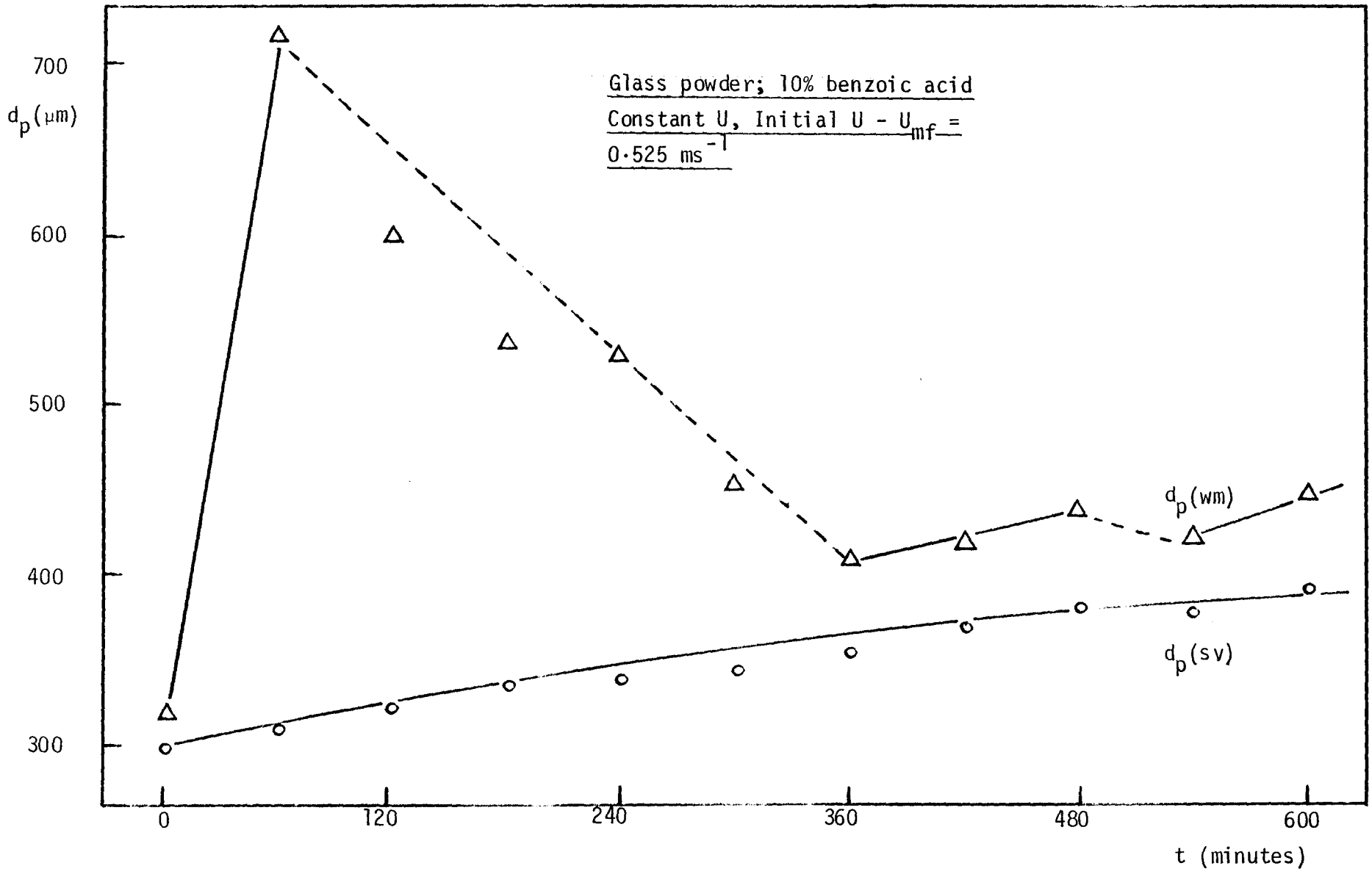


Fig. 6.4 Change in mean particle size with time for layered growth

increasing from 315 μm to 400 μm over the whole run.

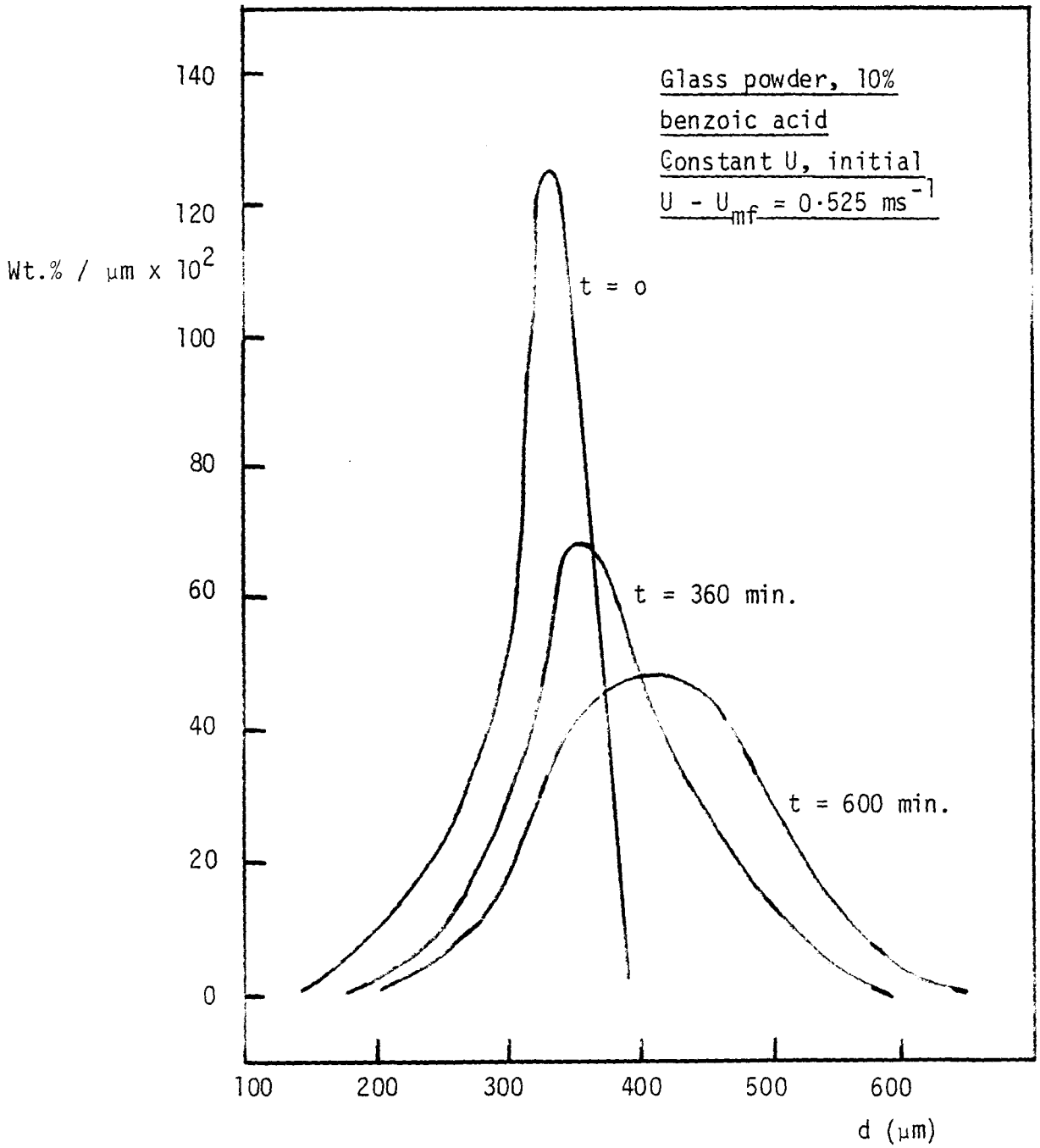


Fig. 6.5 Change in PSD with time for layered growth: frequency distribution curve

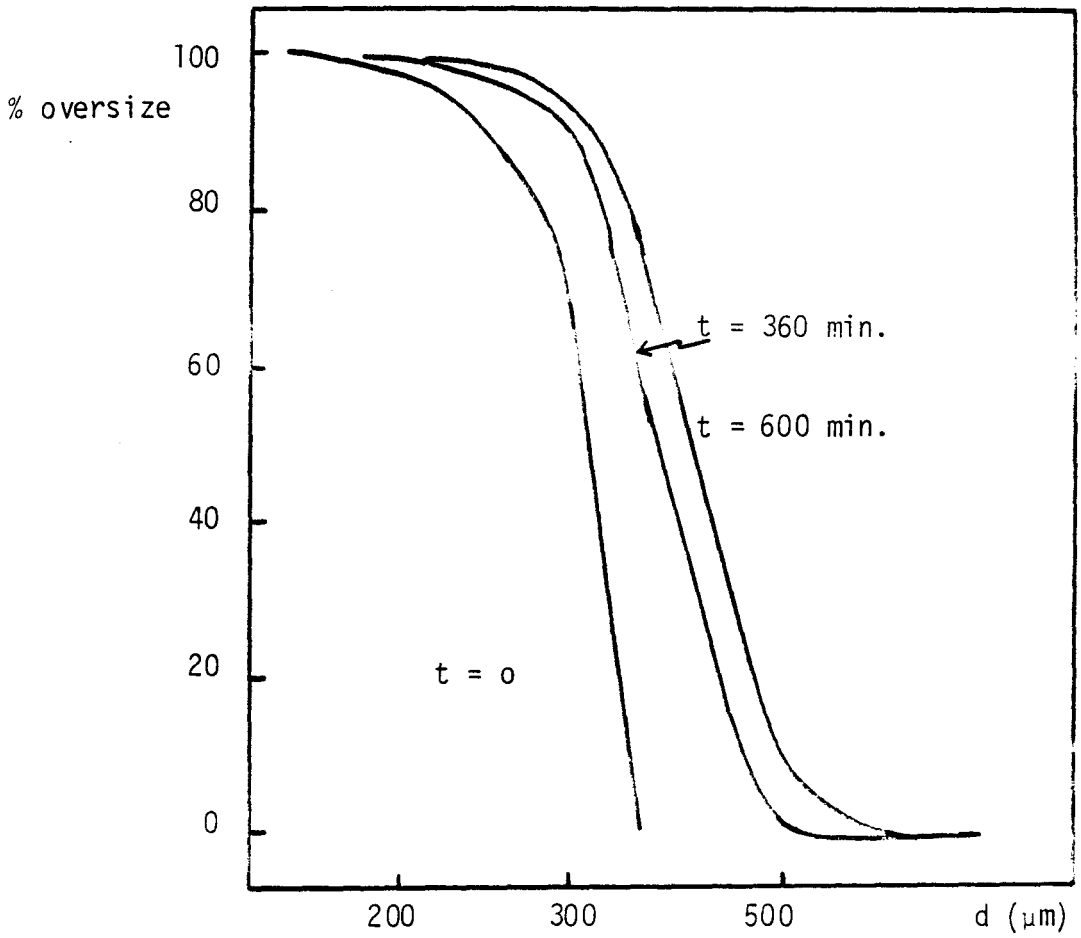


Fig. 6.6 Change in PSD with time for layered growth: cumulative oversize curve

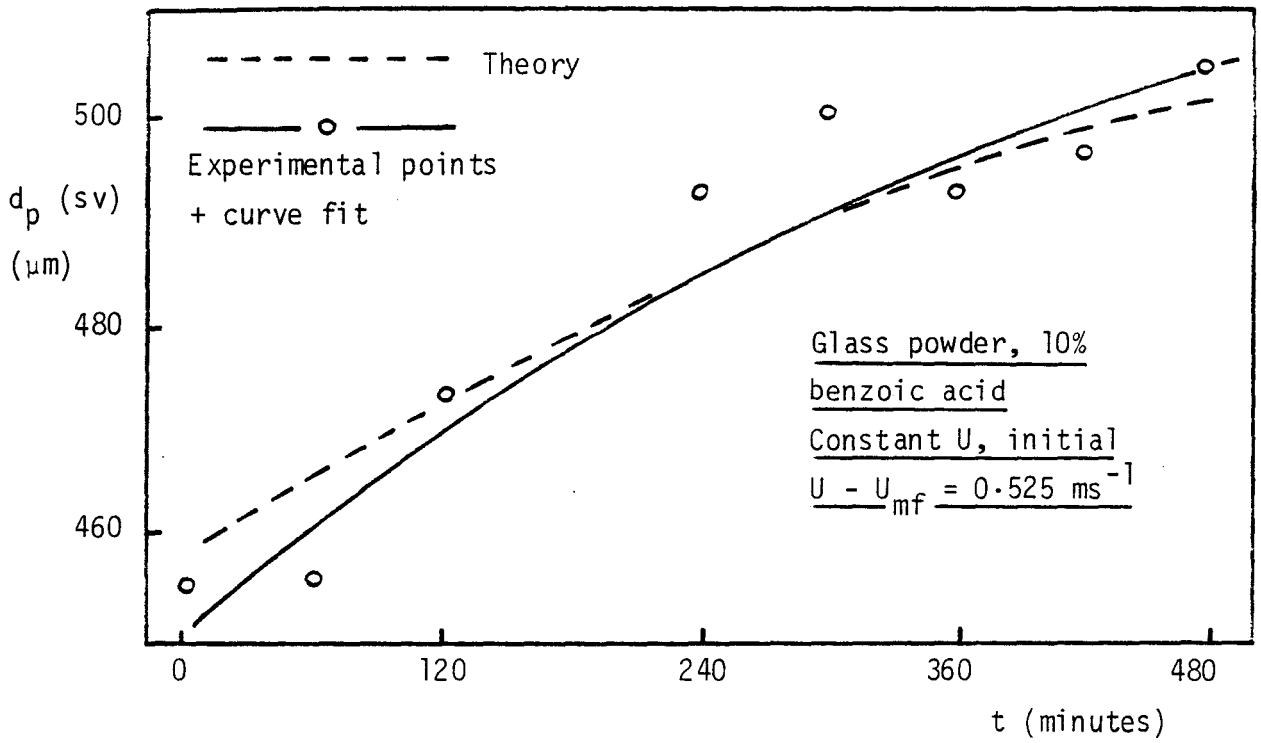


Fig. 6.7 Comparison of experimental data with layered growth model

6.2.3 Layered growth model

Particle size data for large glass powder (nominal size 437 μm, see Appendix A) granulated with 10% benzoic acid at $U - U_{mf} = 0{\cdot}525\ ms^{-1}$, a run which produced granules similar to those in Fig. 6.2, has been fitted to the simple layered growth model which was derived in Chapter Three. The thickness, a, of the hypothetical growth layer was calculated from Equ. 3.11 by substituting for the densities of the bed particles and binder, the initial volume of $d_p$ (sv) and for $M_b$ as a function of time, calculated from the solution flowrate (Equ. 5.14). The theoretical granule diameter calculated from Equ. 3.1 was then plotted against time. Theory and experiment are compared in Fig. 6.7. The theoretical curve (a cubic equation) agrees very well with the quadratic regression curve fitted to the experimental points.

It must be strongly emphasised that the use of this model is in helping to describe the experimental data and is another way of demonstrating (in addition to photographic evidence and graphs of particle size) that the granules produced are not agglomerates of several particles but consist of single particles with binder adhering to the surface. However it does not necessarily imply that growth actually occurs by the deposition of uniformly thick layers. The appearance of the granules does not lend any support to truly layered growth and it will be proposed later that the actual mechanism of growth is very different.

## 6.3 AGGLOMERATION

### 6.3.1 Visual observations

Glass powder has been granulated to produce agglomerates, by the addition of a 5% carbowax solution to a bed fluidised at an excess gas velocity of 0·525 $ms^{-1}$. The product granules (Fig. 6.8), typical of a sample, are very different in structure from those described in Section 6.2. They are composed of several particles bound together by solid bridges of carbowax and can be easily broken down into their constituent particles by applying gentle pressure.

### 6.3.2 Growth curves and particle size distribution

Fig. 6.9 shows the change in mean particle diameter with time for the experiment which produced agglomerates. There are some similarities with the growth curves for the layered growth system; continuous particle growth is demonstrated by the consistent increase in $d_p$ (sv) as well as the more dramatic increase in $d_p$ (wm). However, growth rates for the agglomerating system are much higher. Starting with $d_p$ (sv) = 245 μm, the surface - volume mean diameter reaches a value of 611 μm after 240 minutes' granulation, whilst over the same period Fig. 6.4 (for layered growth) showed an increase from 298 μm to only 340 μm. The mean linear growth rates for agglomeration and layered growth, based on the surface - volume diameter over the initial 240 minute period, are $2.54 \times 10^{-8}$ $ms^{-1}$ (91·5 μm $hour^{-1}$) and $2.92 \times 10^{-9}$ $ms^{-1}$ (10·5 μm $hour^{-1}$) respectively, almost an order of magnitude different. Thus, for similar binder mass inputs, an agglomerating system produces a much greater growth rate than one in which a layering mechanism is dominant. Far less material is required to provide solid bridges, at a relatively small number of contact points between adjacent particles in the agglomerate, than is required to layer or to coat the entire surface of a particle - for which the amount of binder needed is proportional to the cube of the particle diameter.

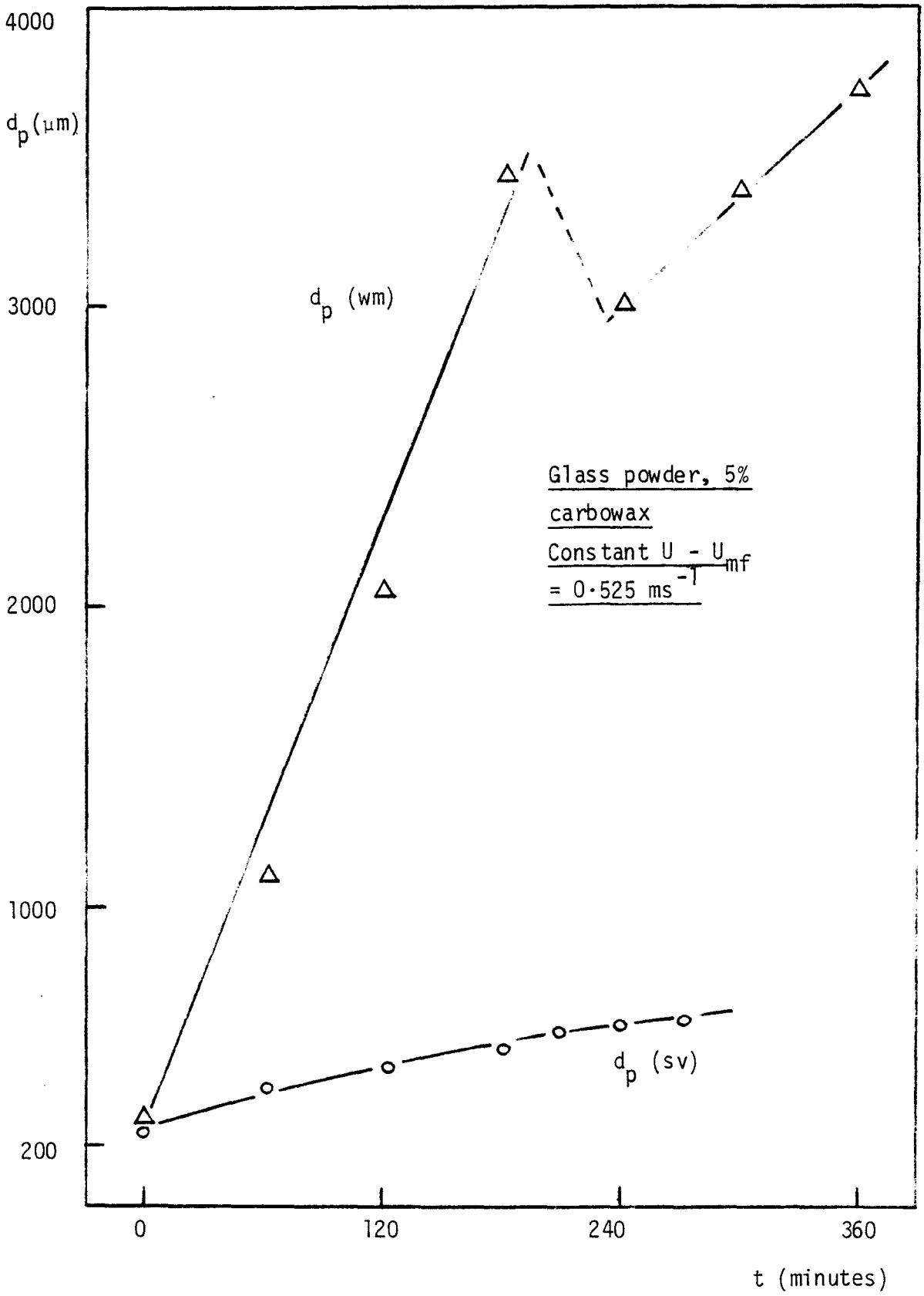


Fig. 6.9 Change in mean particle size for agglomeration

The increase in weight - moment mean diameter is much greater than the increase in surface - volume mean diameter for an agglomerating system, as well as for a layering system. Again, a sharp decrease in $d_p$ (wm) occurs, followed by a further increase. Over the first sixty minutes of granulation the agglomerating bed showed an increase of 821 μm ($2{\cdot}28 \times 10^{-7}$ $ms^{-1}$) in $d_p$ (wm) compared to 403 μm ($1{\cdot}12 \times 10^{-7}$ $ms^{-1}$) for the layering case, and the total increase was much greater (3400 μm compared to 720 μm); a strong indication of substantial agglomeration throughout the entire distribution of particle sizes. Once again there is some evidence of break-down, in this case after a period of about 180 minutes, but it is less indicative of a tendency to reach equilibrium, which suggests that agglomeration is very dominant. A further comparison of the growth rates of the agglomerating and layering systems is made in Fig. 6.10 which shows the decrease with time in the weight percentage of bed particles remaining in the original size range (- 355 μm). Agglomeration reduces this size fraction much more quickly than layering.

The particle size distribution is illustrated graphically in Figs. 6.11 to 6.13. The frequency distribution curve demonstrates greater particle growth than for layering and a decrease in growth rate with time. The latter may be explained thus: large agglomerates are far less likely to combine with each other than are smaller ones, because the inertial forces tending to pull them apart are proportional to particle (or granule) diameter to the power of four (see Section 3.12). Large "twin" or dumb-bell shaped agglomerates have never been observed and, as the number of smaller particles (with which large agglomerates could combine) decreases rapidly, growth rates must decrease. A further significant feature of Fig. 6.11, in comparison with Fig. 6.5, is the much broader distribution of sizes obtained when agglomeration occurs. The log probability plot (Fig. 6.13) shows that, although the initial particle size distribution may be described by a log normal relationship,

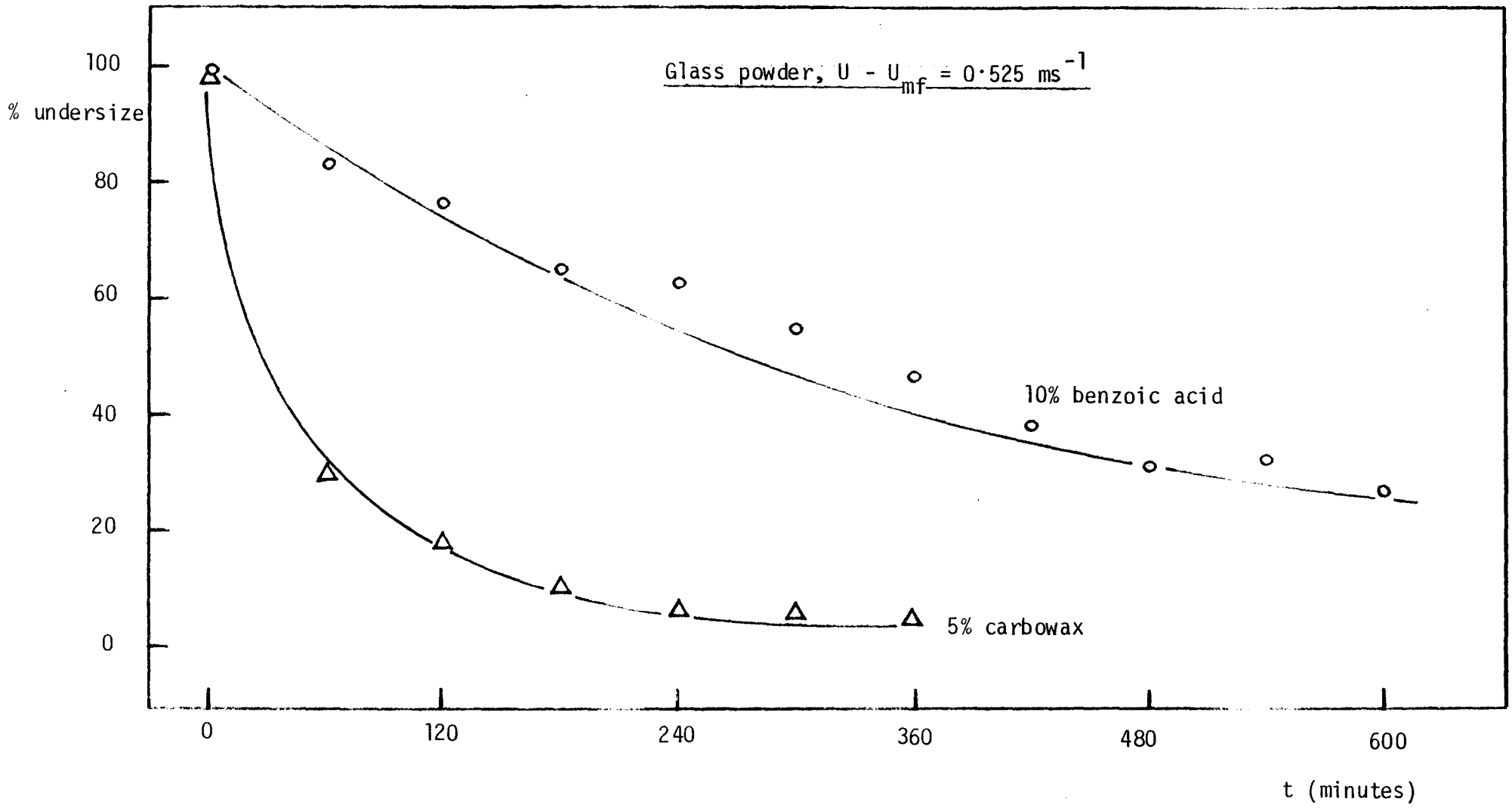


Fig. 6.10 Comparison of change in PSD of aggomerating and layered systems: % of particles still in original size range

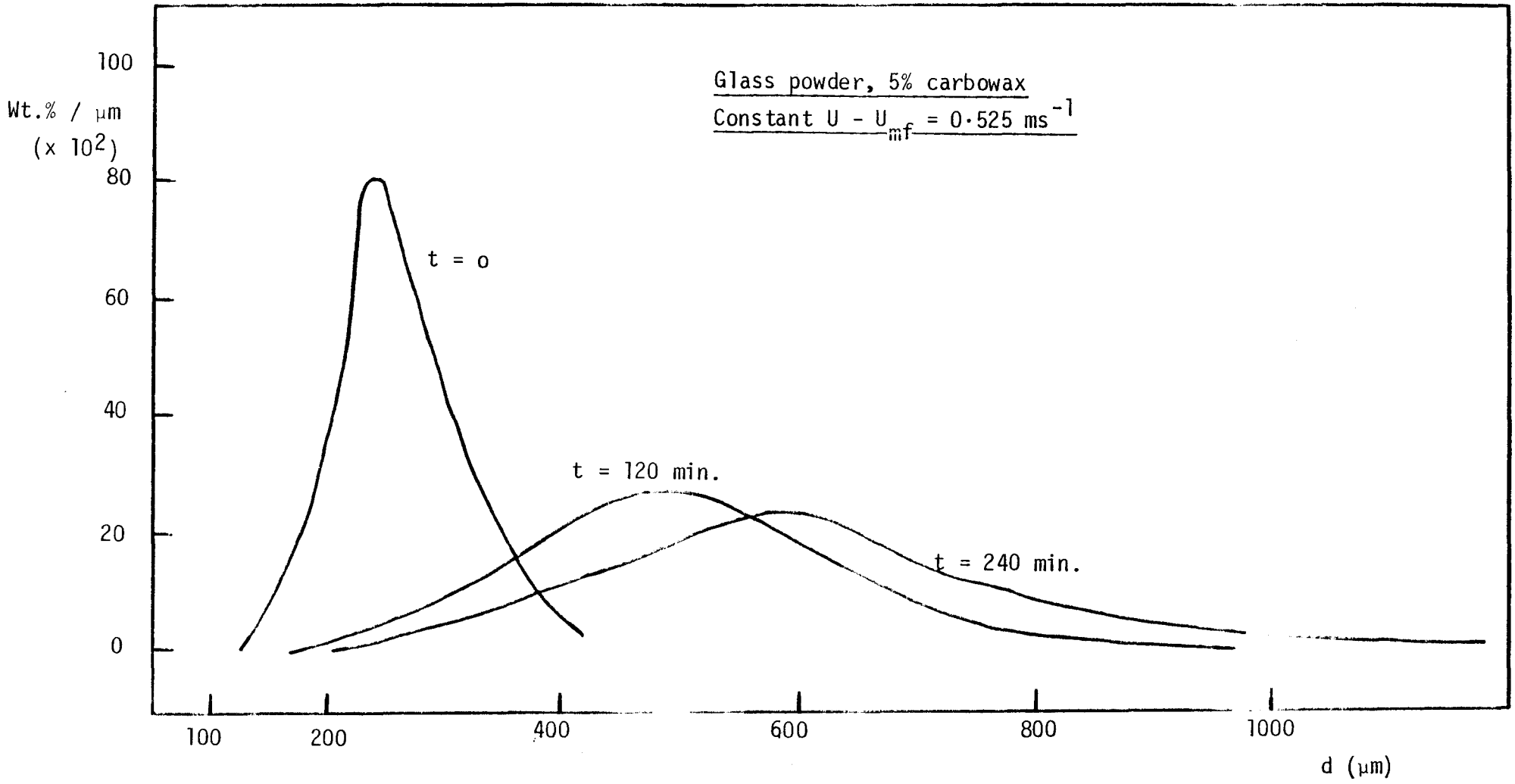


Fig. 6.11 Change in PSD with time for agglomeration: cumulative oversize curve

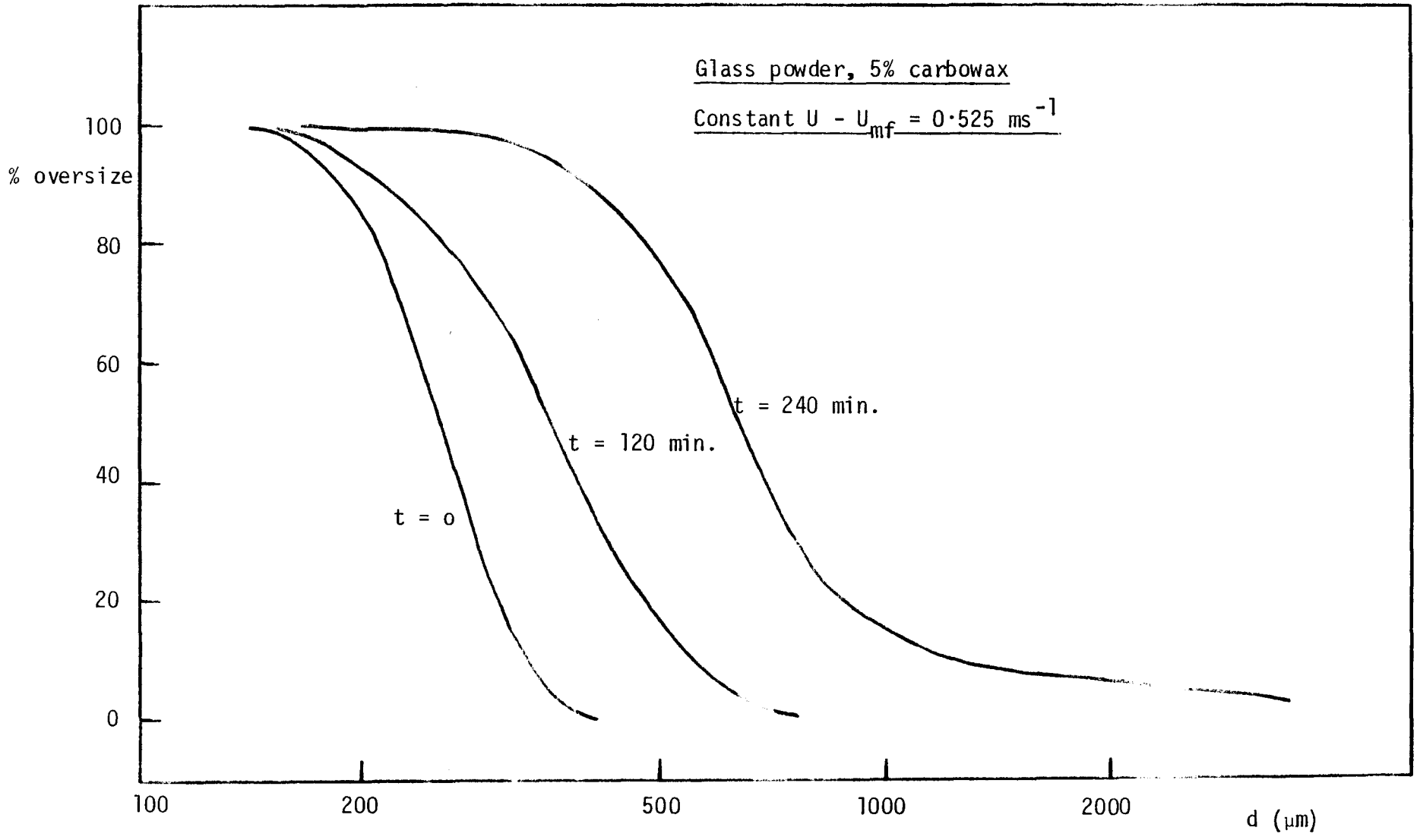


Fig. 6.12 Change in PSD with time for agglomeration: cumulative oversize curve

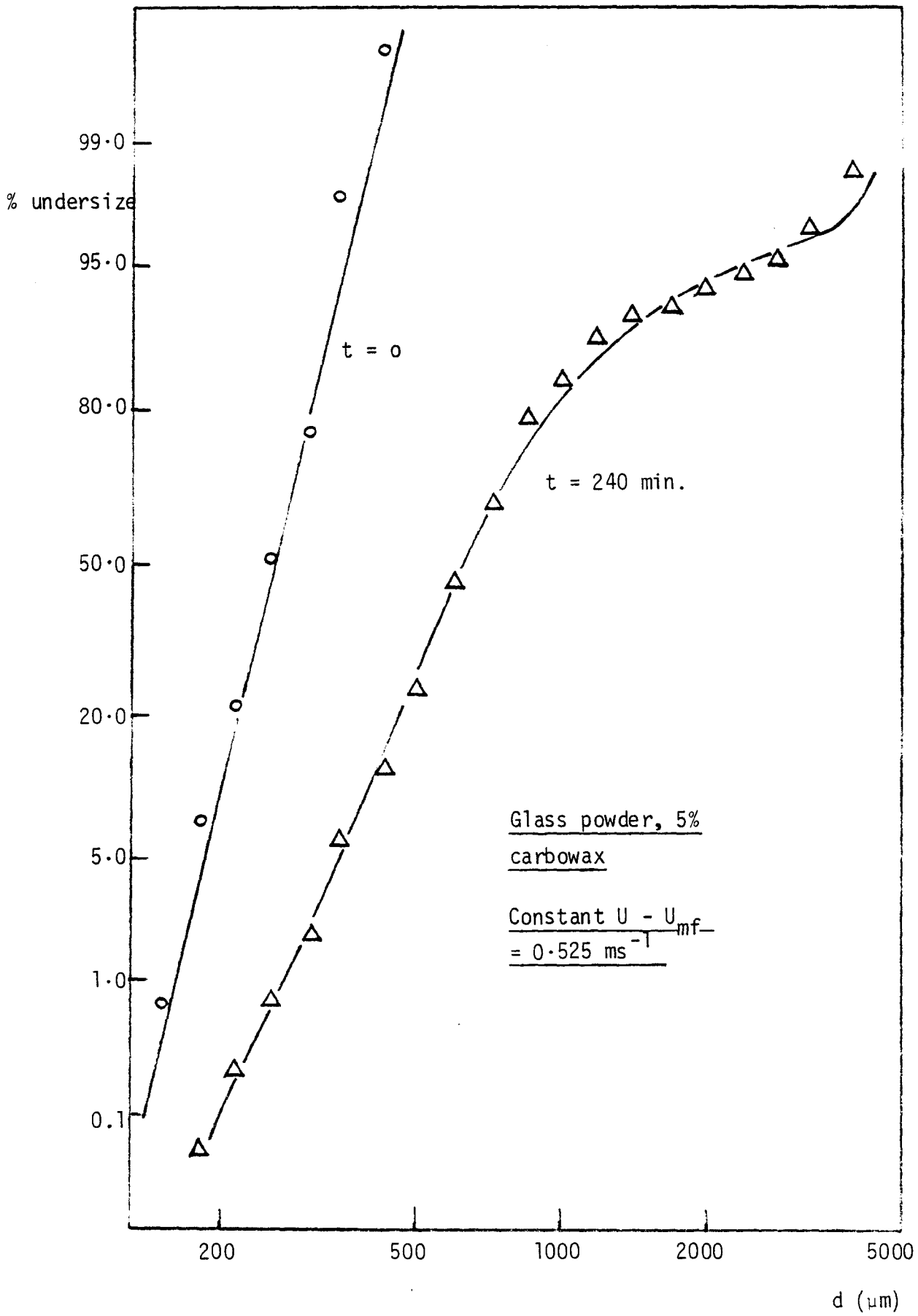


Fig. 6.13 Comparison of agglomeration data with the log normal law

this does not hold for the product size distribution data, unlike those of Ormos et al.[19]

6.3.3 Agglomeration model

Growth and granule binder content data for glass powder /carbowax granules have been fitted to the "steady-state" agglomeration model which was derived in Chapter Three. The model is not concerned with the kinetics of agglomeration, but with the relationship between granule size and binder content. Its use is firstly in demonstrating that the product granules bear some resemblance to the physical picture of the model, and is thus a test for agglomeration, and secondly in providing information on the structure of the granules, in particular determination of the fraction of the granule voids occupied by binder.

The experimental data have been plotted in Fig. 6.14, according to the equation:

$$y = k\,(f - 3\,s\,\beta) \qquad (6.1)$$

Values of y and $\beta$ were calculated from the mass balance and sieve data respectively. Thus, time is implicit in both y and $\beta$ axes, as both the binder content of the bed and the granule size increase with time. It is not strictly therefore a steady-state plot,because each point in Fig. 6.14 represents a different time from the start of granulation. However the model is applied here to show that, for a given binder feedrate, the size of product granules is dependent upon the total quantity of binder supplied to the fluidised bed. The quantity y, the volume ratio of binder to initial particles in the total mass of material present in the bed, is calculated from the mass ratio of binder to particles (determined by the method of Section 5.4.3) and the densities of glass powder and carbowax. The dimensionless granule diameter,$\beta$ (the ratio of initial particle diameter to granule diameter), may be calculated in several ways depending upon the choice of mean particle diameter. Fig. 6.14 presents the data for the 5% carbowax / glass powder system, fluidised

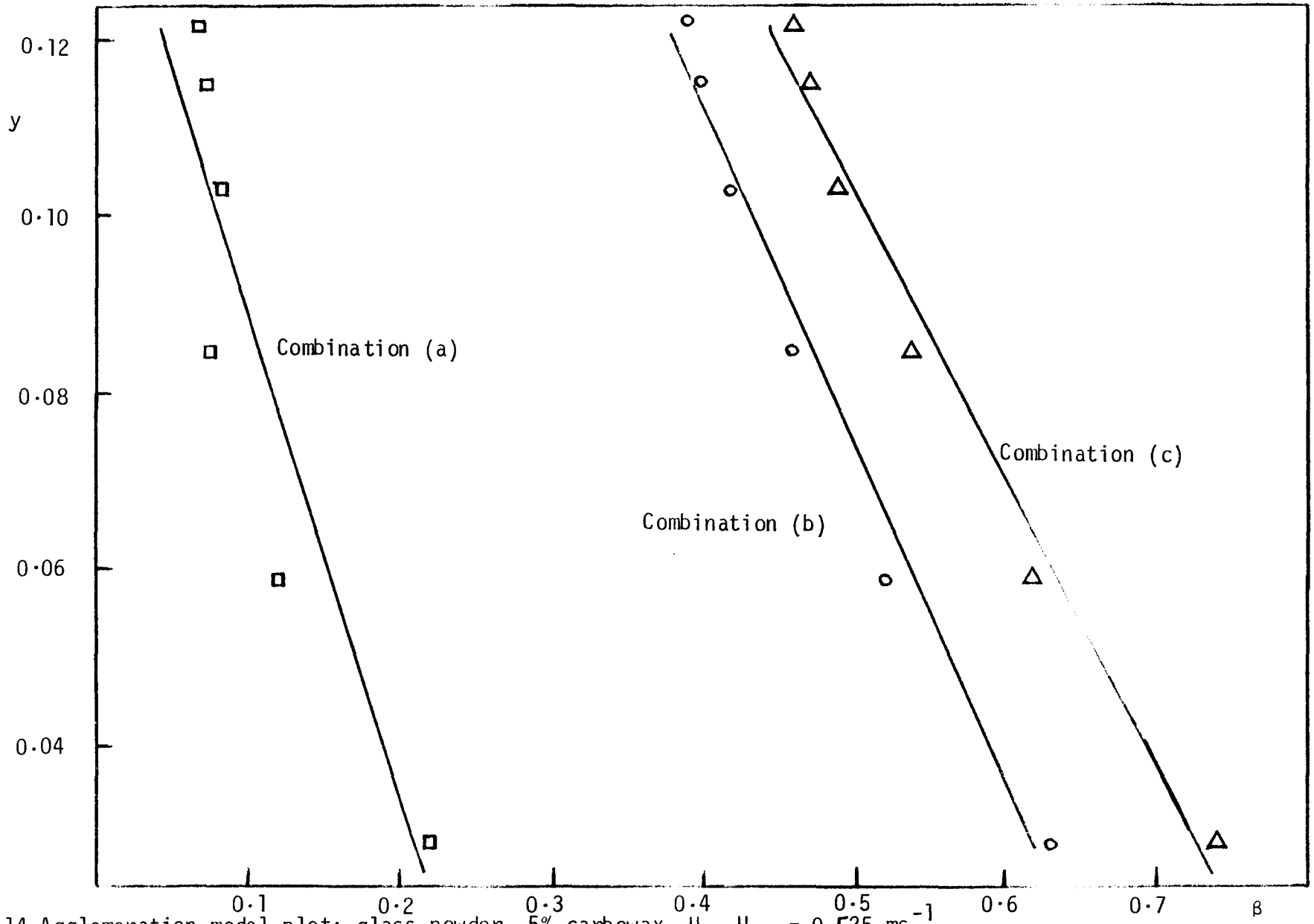


Fig. 6.14 Agglomeration model plot: glass powder, 5% carbowax, $U - U_{mf} = 0{\cdot}525$ ms$^{-1}$

at an excess gas velocity of 0·525 $ms^{-1}$, and with $\beta$ calculated in the three ways listed in Table 6.3.

Table 6.3 Different methods of calculating the value of $\beta$

| | Mean particle diameter | |
|---|---|---|
| | Initial particles | Granules |
| (a) | $d_p$ (sv) | $d_p$ (wm) |
| (b) | $d_p$ (sv) | $d_p$ (sv) |
| (c) | $d_p$ (wm) | $d_p$ (sv) |

A least squares straight line has been fitted to the data in Fig. 6.14, and in further examples which are given in Appendix C. The fraction of granule void space filled with binder, f, can be calculated from the value of the intercept at $\beta$ = o (= kf), by assuming a value for k. This can be done by using the relationship:

$$k = \frac{\varepsilon}{(1 - \varepsilon)} \qquad (6.2)$$

where $\varepsilon$ is the inter-particle voidage of the initial bed material, having a value of 0·42 for glass powder of nominal size 270 μm (see Appendix A). The resultant value of f can then be compared with that from independent calculation and measurement, and division of the gradient of the line by - 3k gives the parameter s. These results are listed in Table 6.4.

Table 6.4 Results from the agglomeration model; glass powder / 5% carbowax, $U - U_{mf} = 0{\cdot}525\ ms^{-1}$

| Definition of β | ε | k | f | s |
|---|---|---|---|---|
| (a) | 0·42 | 0·72 | 0·24 | 0·30 |
| kf = 0·170, gradient = - 0·648 | | | | |
| (b) | 0·42 | 0·72 | 0·44 | 0·21 |
| kf = 0·316, gradient = - 0·456 | | | | |
| (c) | 0·42 | 0·72 | 0·44 | 0·18 |
| kf = 0·315, gradient = - 0·385 | | | | |

Of the three methods for calculating β, combination (a) gives a value of f which is lower and less plausible than those from either (b) or (c), which are similar. Sherrington[73] recommends the use of the surface-volume mean for granules and the weight-mean diameter for the initial particles.

Combination (b) has been used to treat subsequent data because $d_p$ (sv) better represents the bulk of the distribution, and is less affected by the presence of a few unrepresentative large particles. Table 6.5 lists the values of the parameters f and s obtained from experiments with different binder concentrations.

Table 6.5 Values of f and s as a function of carbowax concentration; $\varepsilon = 0{\cdot}42$, $k = 0{\cdot}72$

| Carbowax concentration | Intercept (kf) | Gradient (- 3ks) | f | s |
|---|---|---|---|---|
| 5% (1.) | 0·316 | - 0·456 | 0·44 | 0·21 |
| 5% (2.) | 0·416 | - 0·538 | 0·58 | 0·25 |
| 1% (3.) | 0·108 | - 0·120 | 0·15 | 0·06 |
| 1% (1.) | 0·096 | - 0·099 | 0·13 | 0·05 |

1. $U - U_{mf} = 0{\cdot}525\ ms^{-1}$
2. $U - U_{mf} = 0{\cdot}65\ ms^{-1}$
3. $U - U_{mf} = 0{\cdot}40\ ms^{-1}$

The values of s, the dimensionless measure of the withdrawal of binder from the granule surface, fulfil the criterion of being fractional numbers. Those values for the cases where a 5% solution was used are perhaps more realistic than those for the cases where a 1% solution was used. The equation proposed in the original version of the model (Equ. 3.19) gives values (independent of k and f) of s of 0·48 and 0·43 respectively for the 5% solution and 0·37 and 0·34 respectively for the 1% solution (see Table 6.5). Similarly, f is also a plausible fractional number. A higher concentration of binder in the feed solution results in larger fractions of the granule void space being filled with binder. On average, f is 3·6 times greater for a 5% than a 1% solution. If one considers a given mass of particles at a given voidage, a simple explanation for these values of f can be offered. If the spray solution is distributed evenly throughout the void spaces of the mass of particles, and then dries, it will leave behind the binder similarly distributed. A more concentrated solution will deposit a greater volume of binder and thus f will be correspondingly higher (Fig. 6.15). This is obviously an unrealistically simple picture, but it serves to illustrate the point.

An independent check on the value of f can be made by using either Equ. 3.35 or Equ. 3.37. The former requires a measurement to be made of the granule density as defined by:

$$\rho_g = \frac{G}{V_g} \qquad (6.3)$$

A value of $\rho_g$ was obtained, for granules produced with a 5% carbowax solution, close to that for glass powder itself ($2{\cdot}023 \times 10^3$ kg $m^{-3}$ compared with $2{\cdot}20 \times 10^3$ kg $m^{-3}$, see Appendix A), and on substitution into Equ. 3.35 gave the result f = 0·933. This is unrealistically high and is much greater than the values obtained from the model, because some granule voids are connected to the surface. In order to calculate f from Equ. 3.37, a value of the volume shape factor ($f_v$), as defined by Equ. 6.4, is required.

$$V_g = f_v D_g^3 \qquad (6.4)$$

The necessary value of $f_v$ (see Table 6.6) to give the desired value of f (i.e. about 0·44 of the voids filled with binder) is closely approximated by experimental measurement of the volume shape factor, details of which are given in Appendix A.

Table 6.6 Calculated value of $f_v$

| | | |
|---|---|---|
| Granule diameter, $D_g$ | = | $3{\cdot}675 \times 10^{-3}$ m |
| Granule mass, G | = | $3{\cdot}65 \times 10^{-5}$ kg |
| Binder/particle vol. ratio, y | = | 0·06 |
| Desired value of f | = | 0·44 |
| Calculated value of shape factor, $f_v$ | = | 0·37 |

Experimental measurement of $f_v$ gives an average value of 0·41 from eight determinations, demonstrating that the required value of $f_v$ in Table 6.6 is quite realistic (particularly as Equ. 3.37 is very sensitive to the value of $f_v$, see Fig. 6.16). Hence, the fraction of granule voids filled with binder calculated the agglomeration model can be justified

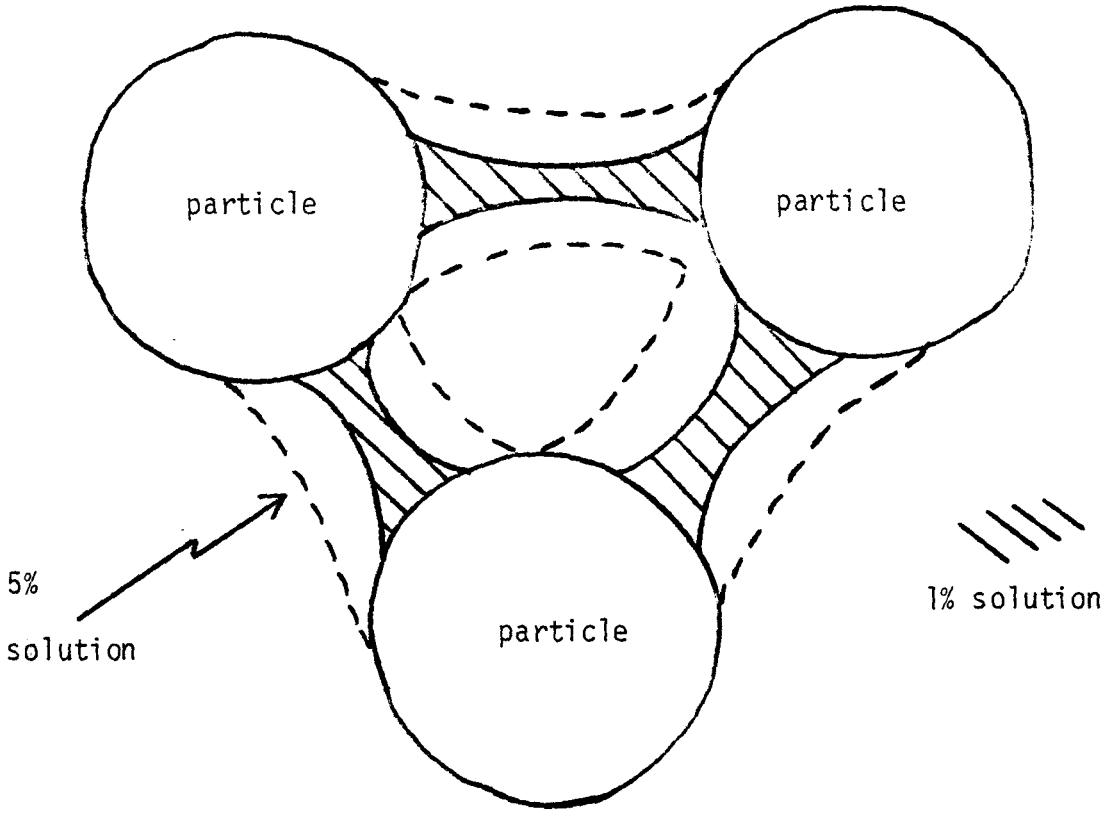


Fig. 6.15 Effect of binder concentration on f

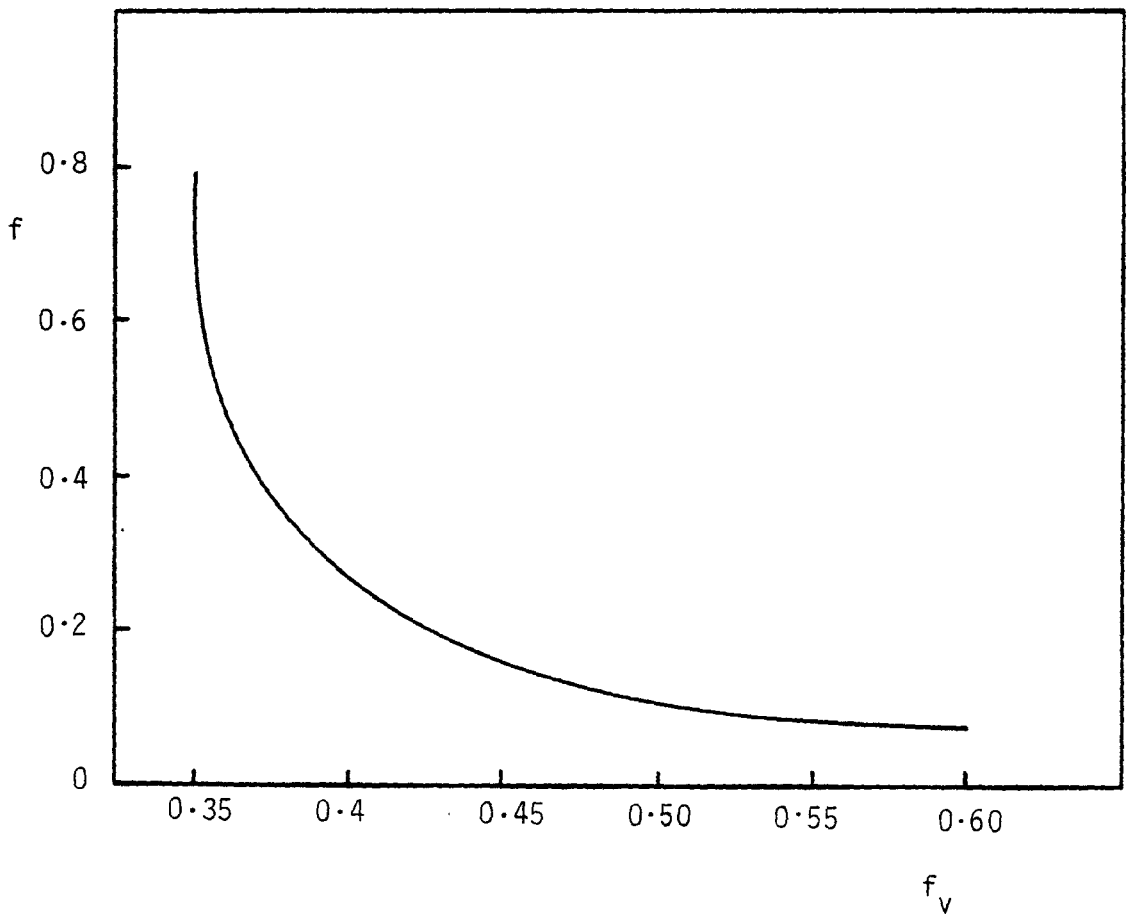


Fig. 6.16 The parameter f as a function of volume shape factor

independently.

## 6.4 EFFECT OF BINDER AND BINDER CONCENTRATION

### 6.4.1 Comparison of carbowax and benzoic acid

When they are dissolved in methanol and used as granulating solutions, carbowax and benzoic acid behave very differently. For example, using a 10% solution of each binder sprayed at the same mass flowrate into a bed of glass powder particles (nominal $d_p$ (sv) = 270 μm), fluidised with an initial excess gas velocity of 0·525 $ms^{-1}$, benzoic acid produced layered granules whereas carbowax precipitated bed quenching.

The growth curves generated when benzoic acid was sprayed into the bed are those reproduced in Figs. 6.4 to 6.6 and show that controlled particle growth, without bed quenching, can be achieved over a period of 600 minutes. On the other hand, carbowax solution was responsible for complete defluidisation of the bed within 50 minutes. The first visual indication of quenching is the appearance of large agglomerated particles, about 0·005 m in diameter, at the bottom of the bed and around the perimeter, where they can be seen through the glass wall. It is presumed that there is no radial variation in this phenomenon, although this cannot be confirmed visually. The agglomerates segregate at the bottom of the bed because they are too large to be fluidised at the set superficial gas velocity. However they are buffeted in the gas stream and occasionally appear to loose particles from their surface. Coincident with, or perhaps a few minutes before, the appearance of the segregated granules, there is a rise in temperature at the bottom of the bed, detected by a thermocouple placed 0·005 m above the distributor plate. Loss of fluidisation in this region reduces particle motion and results in a decrease in heat transfer, within this localised zone, between the incoming hot gas and the fluidised bed. Consequently the temperature just above the distributor increases and approaches the windbox temperature. In this case, within four or five minutes, the temperature was 67° C compared with 70° C in the windbox and 40° C in

the well-fluidised bulk of the bed. This is not wet quenching but an example of dry quenching due to the build-up of material which has dried before it reaches the distributor plate (see Section 3.1.2). Wet quenching, with the presence of free liquid in the defluidised layer, would produce a drop in temperature at the bottom of the bed.

The number of large agglomerates gradually increased to form a defluidised layer, through which air passed in discrete channels, and above which was a well-fluidised zone. As spraying of the feed solution continued, the defluidised layer grew in size to between half and three-quarters of the bed depth and became a solid agglomerated mass. Air continued to pass through in channels causing loose material to spout high into the freeboard. Particles at the surface of the bed became defluidised because the air distribution was uneven. A sample of this material taken 50 minutes after the start of granulation gave a value of $d_p$ (sv) of 621 μm, but this has little meaning, other than to show that it consisted of agglomerated particles rather than ungranulated ones.

Thus, under otherwise identical conditions, a fluidised bed granulator may be operated to give desirable particle growth, or perhaps become unstable and quench, depending upon the choice of binder. The following sections describe the effect on granulation of the concentration of binder solution used.

### 6.4.2 Effect of binder concentration on an agglomeration system; glass powder and carbowax

The concentration of binder in the feed liquid may be as important as the nature of the binder itself in determining how the fluidised bed operates. Increasing the concentration results in greater particle growth and, if increased sufficiently, brings about bed quenching. This is demonstrated by the results of three separate experiments in which carbowax solution was sprayed into beds of glass powder (nominal size 270 μm). The volumetric air flowrate through the bed was set, at the

beginning of each run, to give the required superficial velocity of 0·60 $ms^{-1}$ (initially equivalent to $U - U_{mf}$ = 0·525 $ms^{-1}$) and was kept constant despite the increase in particle size and the resulting increase in minimum fluidising velocity.

The result of using a 10% solution was described in detail in the previous section. Briefly, agglomeration was very rapid and produced a defluidised layer of agglomerated particles at the bottom of the bed, leading quickly to bed quenching. An indication of this behaviour was given by an increase in bed temperature just above the distributor plate, after a period of 32 minutes.

Granulation could be continued for longer periods by reducing the feed concentration. With a 5% solution, no temperature increase was recorded until 73 minutes had elapsed from the start of granulation, but this was quickly followed by the appearance of large granules on the distributor, as before. The temperature again approached that of the inlet air, rising to 66$^{o}$ C. After 90 minutes of operation it was found to be impossible to continue granulation without increasing the volumetric air flow, so as to prevent quenching. After 60 minutes of stable operation the surface - volume mean diameter had increased to 424 μm.

When a 1% solution of carbowax was used, a slower initial growth rate was recorded and, as illustrated by Fig. 6.17, stable operation was maintained for 240 minutes during which agglomerated granules were produced. No variation in the temperature trace was detected. Therefore, although not carried out at steady-state with respect to excess gas velocity, these experiments have shown the importance of binder feedrate. Whilst a batchwise fluidised bed granulator can be operated stably for a considerable period with a relatively low binder feedrate, increasing it brings about more rapid agglomeration, to be followed possibly by partial defluidisation and ultimately bed quenching.

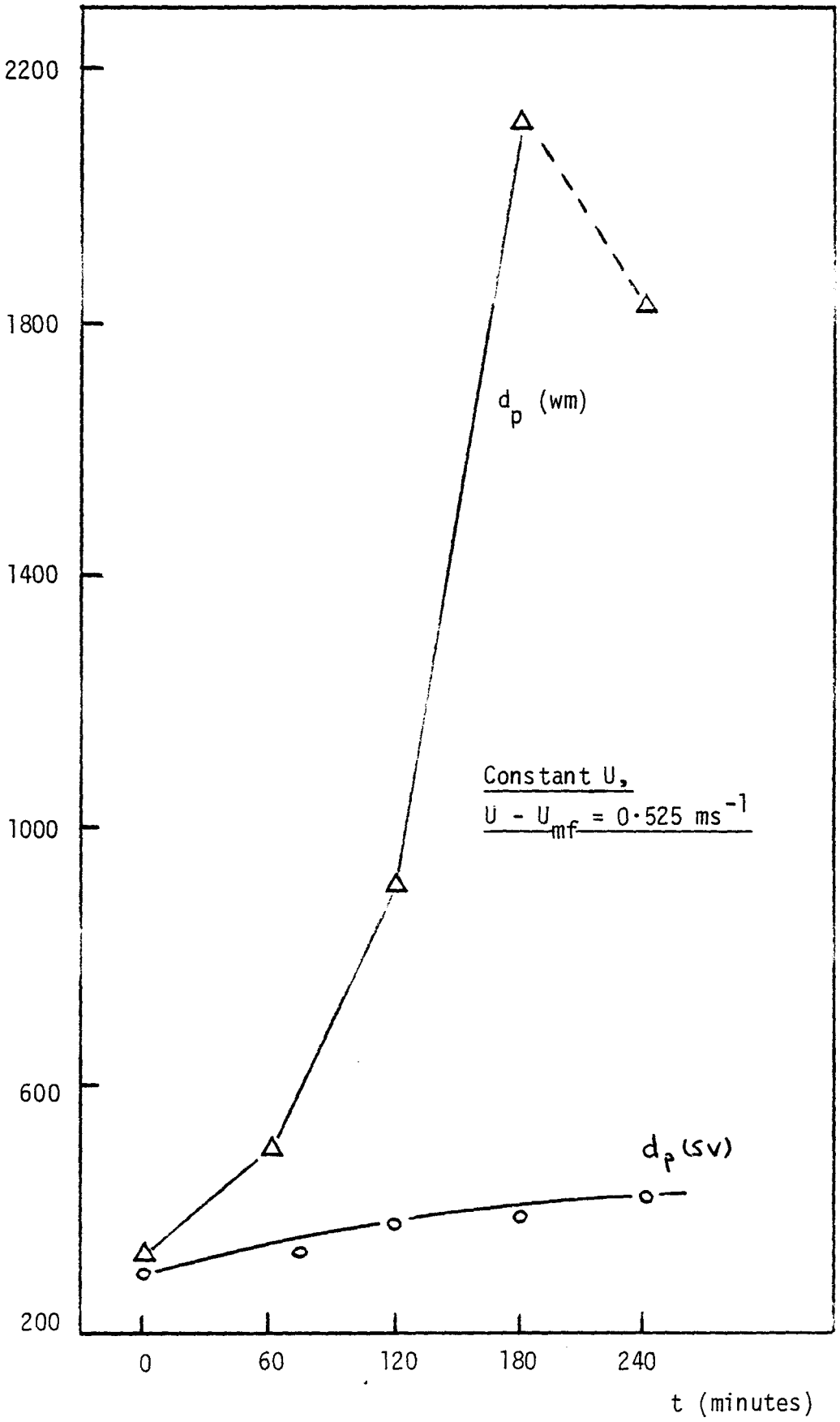


Fig. 6.17 Growth curves obtained with glass powder and 1% carbowax solution

### 6.4.3 Effect of binder concentration on a layering system; glass powder and benzoic acid

An increase in the concentration of benzoic acid solution did not bring about any change in the type of granule produced. No variation in bed temperature (which would indicate the onset of quenching) was recorded and the bed particles increased in size because of binder deposition around the particle surface. The product granules resembled those of Fig. 6.2. However the increase in binder mass input, although it precipitates neither a change in growth mechanism nor bed quenching (as is the case with carbowax), does lead to greater particle growth. In Fig. 6.18 the dimensionless surface - volume mean diameter (defined as $d_p$ (sv) / $d_p$ (sv) at t = o) is plotted against time for both 10% and 20% solutions. A dimensionless particle diameter has been used because the bed particles used for each experiment were at the extremes of the size range for the smaller glass powder (see Appendix A).

A two-fold increase in the mass of binder available for particle growth will not, of course, result in a doubling of the growth layer thickness because binder is deposited over an ever increasing surface area (see Equ. 3.11). This is reflected in Fig. 6.18 which shows that as particle size increases the ratio of diameter increase at 20% concentration to diameter increase at 10% concentration becomes progressively smaller.

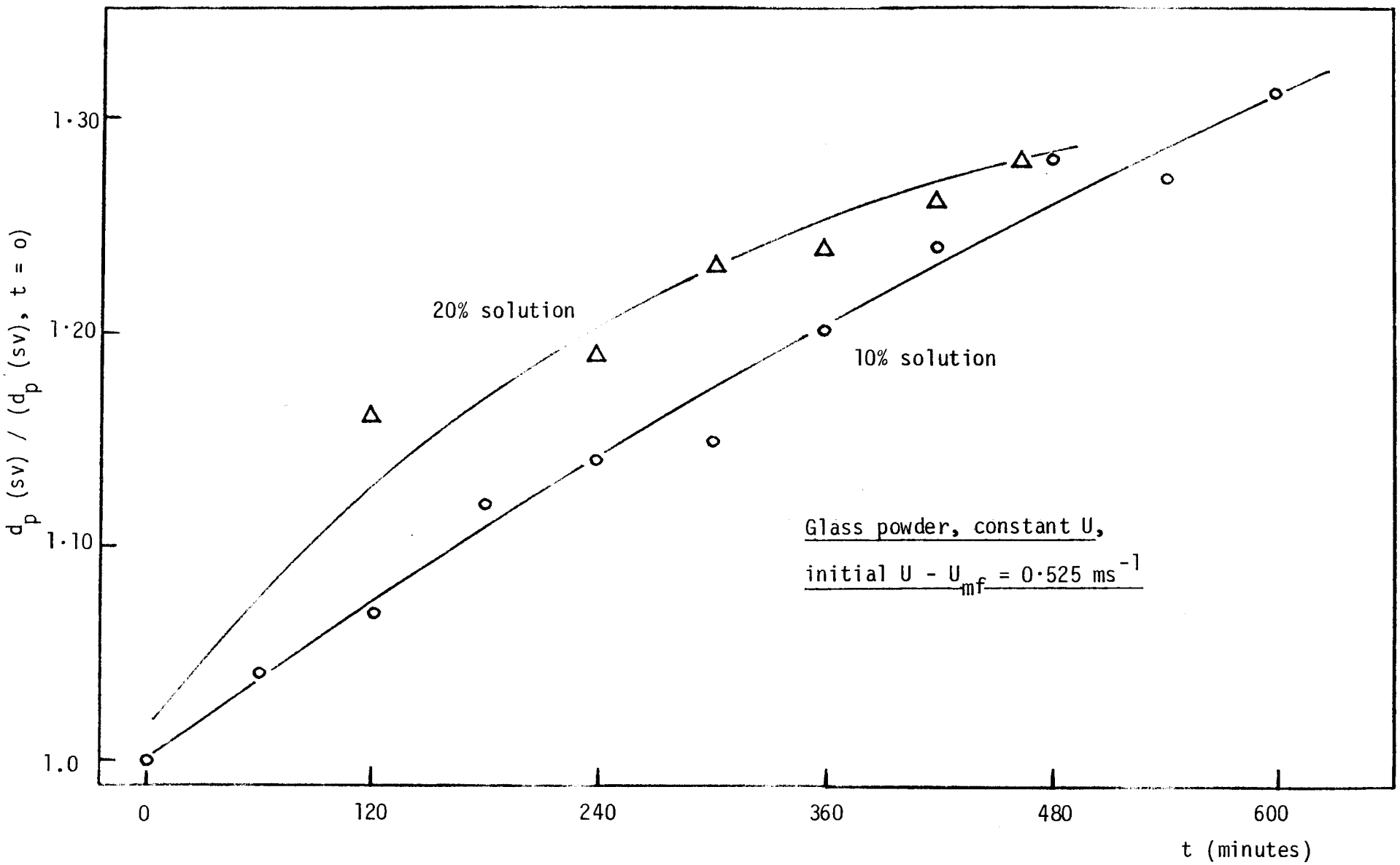


Fig. 6.18 Effect of benzoic acid concentration on particle growth

## 6.5 EFFECT OF FLUIDISING GAS VELOCITY

### 6.5.1 Effect of gas velocity on bed quenching; glass powder and benzoic acid

Superficial fluidising gas velocity is a quantitative measure of the "fluidisation element" in the balance between fluidisation and granulation which it is postulated governs the operation of a fluidised bed granulator (see Section 3.1.1). A series of experiments conducted at different fluidising velocities has demonstrated that the choice of gas velocity can determine whether a bed quenches or whether stable operation can be maintained. A 10% solution of benzoic acid was sprayed into beds of glass powder (nominal size 270 μm) at five excess gas velocities: 0·15, 0·275, 0·40, 0·525 and 0·65 $ms^{-1}$. The required air rate was set at the beginning of the experiment and kept constant throughout, i.e. U remained constant but $U - U_{mf}$ decreased.

At an excess gas velocity of 0·15 $ms^{-1}$ the fluidised bed quickly quenched. Only five minutes after the introduction of benzoic acid, the temperature at the bottom of the bed began to increase and after 40 minutes a considerable fraction of the bed was defluidised; samples from the top and bottom halves of the bed gave the weight - moment mean diameter as 893 μm and 1230 μm respectively. With the bed fluidised at $U - U_{mf}$ = 0·275 $ms^{-1}$ operation could be continued for longer. No temperature rise was recorded until 35 minutes from the start of granulation, and not until t = 106 minutes did the bed temperature approach that of the inlet gas. A defluidised layer 0·04 m to 0·05 m deep was present at t = 120 minutes and the bed was totally quenched after 170 minutes.

The onset of bed quenching in both of these experiments was very similar to that described earlier for the glass powder and carbowax system: large, dry agglomerates segregate and form a defluidised layer leading to poor heat transfer, temperature fluctuations and eventually

total defluidisation with channeling and spouting of the fluidising gas stream. However, these effects were absent at higher excess gas velocities; 0·40 $ms^{-1}$ (an experiment which was continued for only 120 minutes) and 0·525 and 0·65 $ms^{-1}$, at both of which granulation was continued satisfactorily for a period of 600 minutes. At $U - U_{mf} = 0·15$ $ms^{-1}$, operation could not be continued long enough for a granule sample to be removed at t = 60 minutes. However, in each of the other experiments particle size was determined both at t = 60 minutes and at t = 120 minutes, and this information is presented in Fig. 6.19 (in which each pair of points, at a particular value of $U - U_{mf}$, represents a separate experiment). Two curves have been constructed showing the surface - volume mean diameter, after 60 minutes and 120 minutes respectively, as a function of excess gas velocity. The surface - volume mean diameter decreases with increasing gas velocity and its value levels out at the high end of the studied velocity range. Samples removed from the bed with $U - U_{mf} = 0·15$ or 0·275 $ms^{-1}$ were composed of agglomerates, although a few layered granules may have been present, but at high velocities (0·525 and 0·65 $ms^{-1}$) growth by layering is the dominant mechanism (see Section 6.2). This is reflected by Fig. 6.19 which shows that, for a given mass feed of binder, particle growth is greatest at low velocities. Similarly, Fig. 6.20 indicates a change in particle growth mode as $U - U_{mf}$ is increased; the positive rate of change of weight - moment mean diameter decreases markedly with $U - U_{mf}$ ($d_p$ (wm) is very sensitive to a few large, and therefore agglomerated, particles). The shape of Fig. 6.19 is to be expected if a layering mechanism becomes dominant at high excess gas velocity. In such a regime growth is dependent only on the quantity of material which is available for deposition on the particle surface. The levelling out of $d_p$ (sv) with velocity, as opposed to a continual decrease, suggests that this is the case.

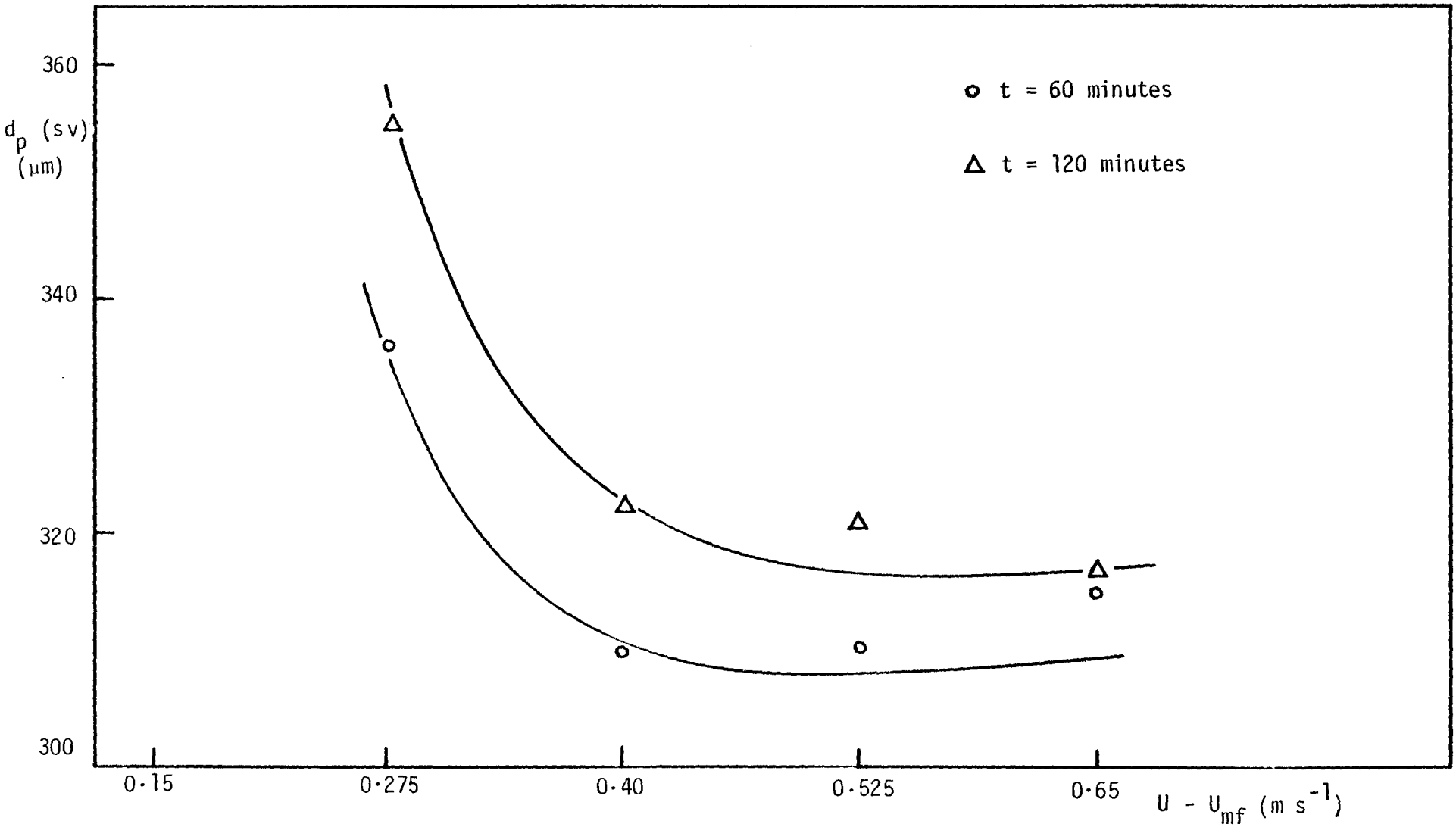


Fig. 6.19 Effect of fluidising gas velocity on mean particle size: glass powder, 10% benzoic acid

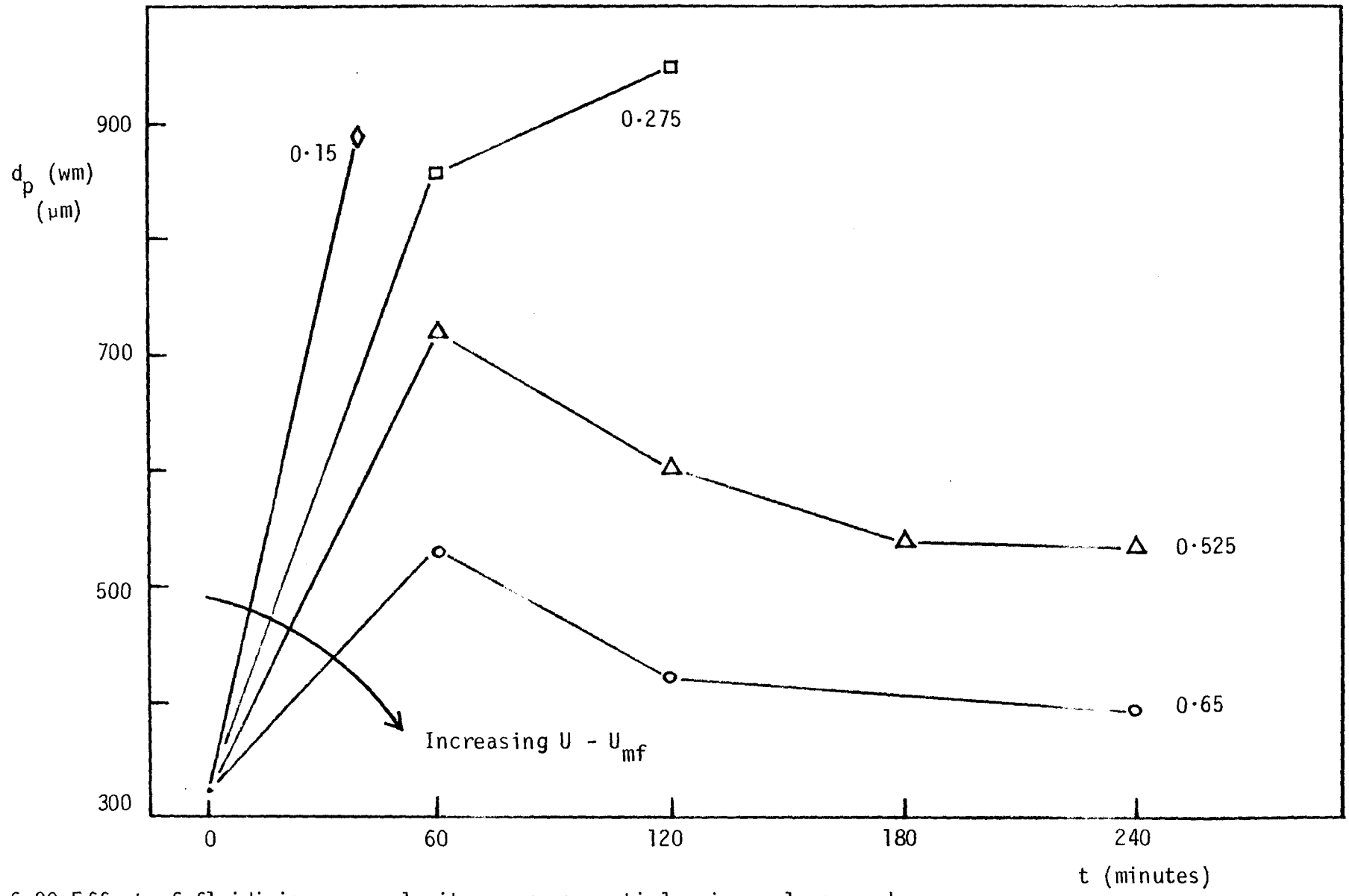


Fig. 6.20 Effect of fluidising gas velocity on mean particle size: glass powder, 10% benzoic acid

Nienow and Rowe[4] have presented a table of superficial gas velocities reported in the literature and, where possible, have calculated values of the relative gas velocity ($U / U_{mf}$), from the equation of Leva.[101] This has been reordered and, together with calculated values of the excess gas velocity, is reproduced in Table 6.7.

Table 6.7 Correlation of reported fluidising velocities with the mode of particle growth

| | Reference | From Nienow & Rowe[4] $U$ ($ms^{-1}$) | From Nienow & Rowe[4] $U / U_{mf}$ | Calculated* $U - U_{mf}$ ($ms^{-1}$) |
|---|---|---|---|---|
| (a) | Fukumoto et al. (41) | 0·4 - 0·9 | 3 - 8 | 0·27 - 0·79 |
| | Lee et al. (44) | 0·4 - 0·6 | 4 | 0·30 - 0·45 |
| | Grimmett (56) | 0.4 | 9 | 0·35 |
| | Buckham et al. (61) | 0·3 | 4 | 0·23 |
| | Otero, Garcia (42) | 0·15 - 0·47 | 5 - 15 | 0·12 - 0·44 |
| (b) | Jonke et al. (14) | 0·4 - 0·6 | 4 - 6 | 0·30 - 0·50 |
| | Bakshi, Nihilani (62) | 0·15 | 10 - 17 | 0·13 |
| (c) | Bjorklund, Offutt (30) | 0·10 - 0·15 | 2·5 | 0·06 - 0·09 |
| | Frantz (16) | 0·13 - 0·27 | 2 - 4 | 0·06 - 0·20 |
| | Bakshi, Chai (45) | 0·1 - 0·2 | 7 - 12 | 0·09 - 0·18 |

* $(U - U_{mf}) = U - \dfrac{U}{(U / U_{mf})}$

Section (a) in the table contains those papers in which growth by layering is reported, section (c) those in which agglomeration is the dominant or only type of growth, and section (b) contains papers in which both types of particle growth are reported as being co-existent. Although there are exceptions, a strong trend is discernible; the excess gas velocities in (a) are generally higher than those in (b), and the excess gas velocities in (b) are higher than those in section (c). This trend is consistent with the observations recorded above, that increasing the gas velocity for a particular system results in less agglomera-

tion and eventually a dominance by layered growth.

6.5.2 Constant excess gas velocity

As fluidised bed particles grow, the minimum fluidising velocity (a function of particle diameter) increases. Therefore, if the volumetric flowrate of gas through the bed is kept constant, the superficial fluidising velocity will decrease relative to $U_{mf}$ and the "fluidisation element" in the granulation balance will also decrease.

In Section 6.4.2 the effect of granulating glass powder with a 5% carbowax solution was described. Within 90 minutes the bed was partially defluidised, however it was possible to prevent bed quenching and to prolong the experiment by means of periodic increases in the superficial gas velocity thereafter. Increasing the gas rate always improved the uniformity of fluidisation by reducing or removing completely the defluidised layer at the bottom of the bed. Changes in bed temperature profile and in particle size were also brought about. When a segregated layer is present the temperature just above the distributor plate is higher than in the bulk of the bed, but is almost instantly reduced to the nominal level by an increase in gas rate.* Changes of $15^{o}$ C have been registered.

At t = 245 minutes, i.e. after a further 100 minutes of relatively stable operation with no visible defluidised layer, a temperature rise of $7^{o}$ C at the bottom of the bed, over a period of five minutes, was taken as an indication of possible bed quenching. Accordingly the gas rate was further increased enabling granulation to continue for another 180 minutes, with a temperature difference of only 3 or $4^{o}$ C between the bottom and the bulk of the bed.

---

* Although increases in gas rate bring about increases in the bed temperature, because of improved heat transfer in the preheater, these are usually small (about 2 or $3^{o}$ C). In addition, with substantial increases in air flowrate this effect was balanced by a drop in the total heat load per unit mass of air. In general, control of the bed temperature when the gas velocity was changed was not a problem.

The above experiment is illustrated in Fig. 6.21. This is a graph of surface - volume mean diameter as a function of time. It shows how the particle size responds to changes in fluidising gas flowrate, together with the values of superficial gas velocity at different stages of the experiment. Two samples were removed from the bed at t = 110 minutes which reveal that the mean particle size in the top, well-fluidised half of the bed is smaller than that in the segregated layer at the bottom of the bed. Increases in gas velocity are responsible for sudden decreases in particle size, followed by further growth requiring yet higher gas rates. This process prolongs granulation under conditions which would otherwise produce bed quenching, although the excess gas velocity in this case was not kept constant; after 305 minutes' granulation, calculation showed $U - U_{mf}$ to be 0·813 $ms^{-1}$. However, this knowledge of particle growth has enabled the experiment to be repeated with precise and programmed increases in gas rate, in order to maintain the excess gas velocity at a pre-determined level. This is important in an agglomerating system where particle growth is rapid, but less so where layered growth takes place.

Using the method outlined in Section 5.4.1 and Equs. 5.10 and 5.11, the required air flowrates were calculated and glass powder was again granulated with a 5% carbowax solution. Gas rate was increased every 30 minutes until t = 180 minutes, after which ad hoc increases were made at irregular intervals of between 8 and 20 minutes. Actual values of the mean particle diameter, or interpolated values from a least squares fit to the $d_p$ (sv) versus time curve, were used to calculate minimum fluidising velocities (from Equ. 5.11), and thus $U - U_{mf}$, throughout the experiment. Table 6.8 presents the calculated values of $U - U_{mf}$, together with the percentage error from the nominal value. The particle size plot for this experiment is illustrated in Fig. 6.22.

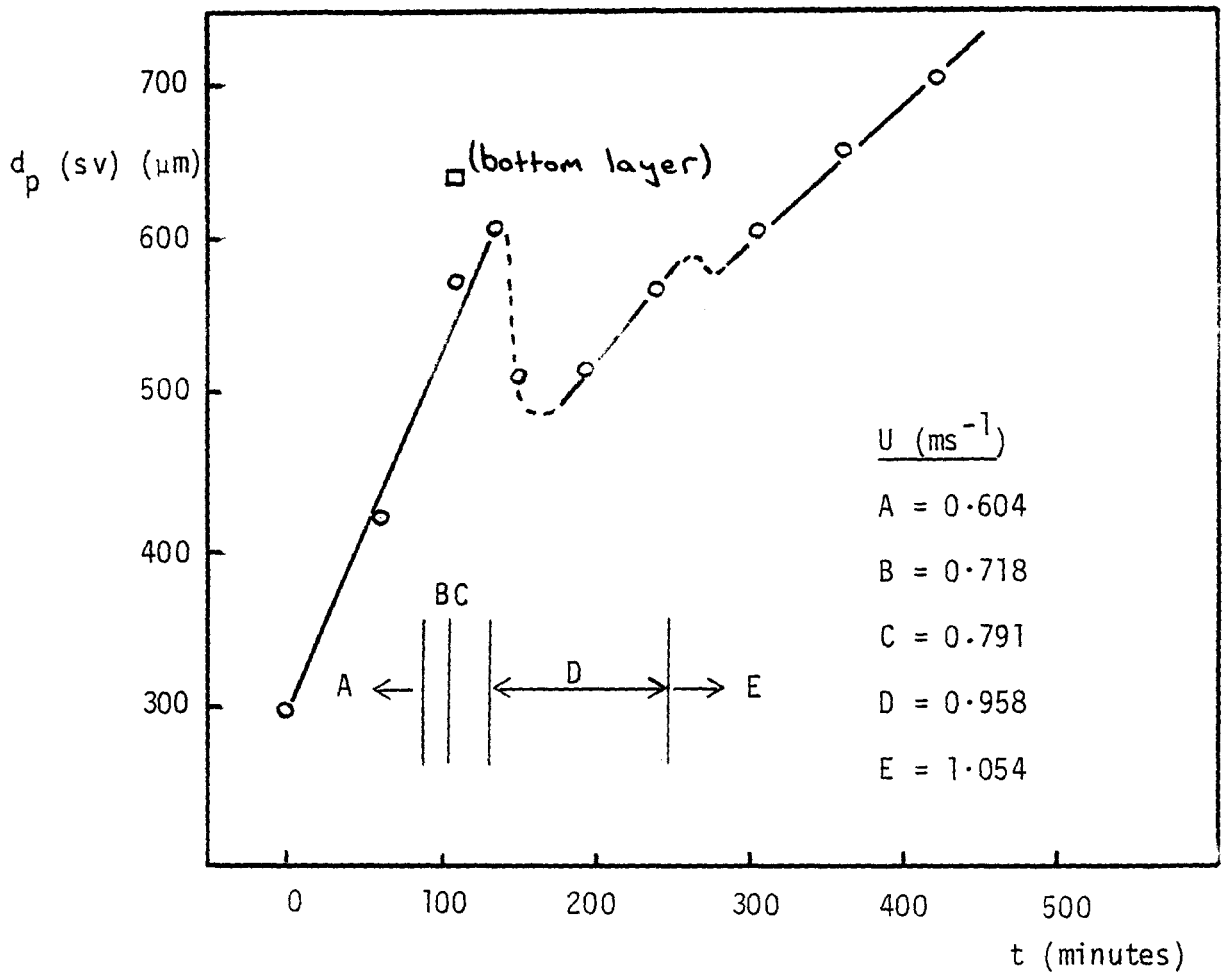


Fig. 6.21 Effect of increased gas rate on a quenching bed

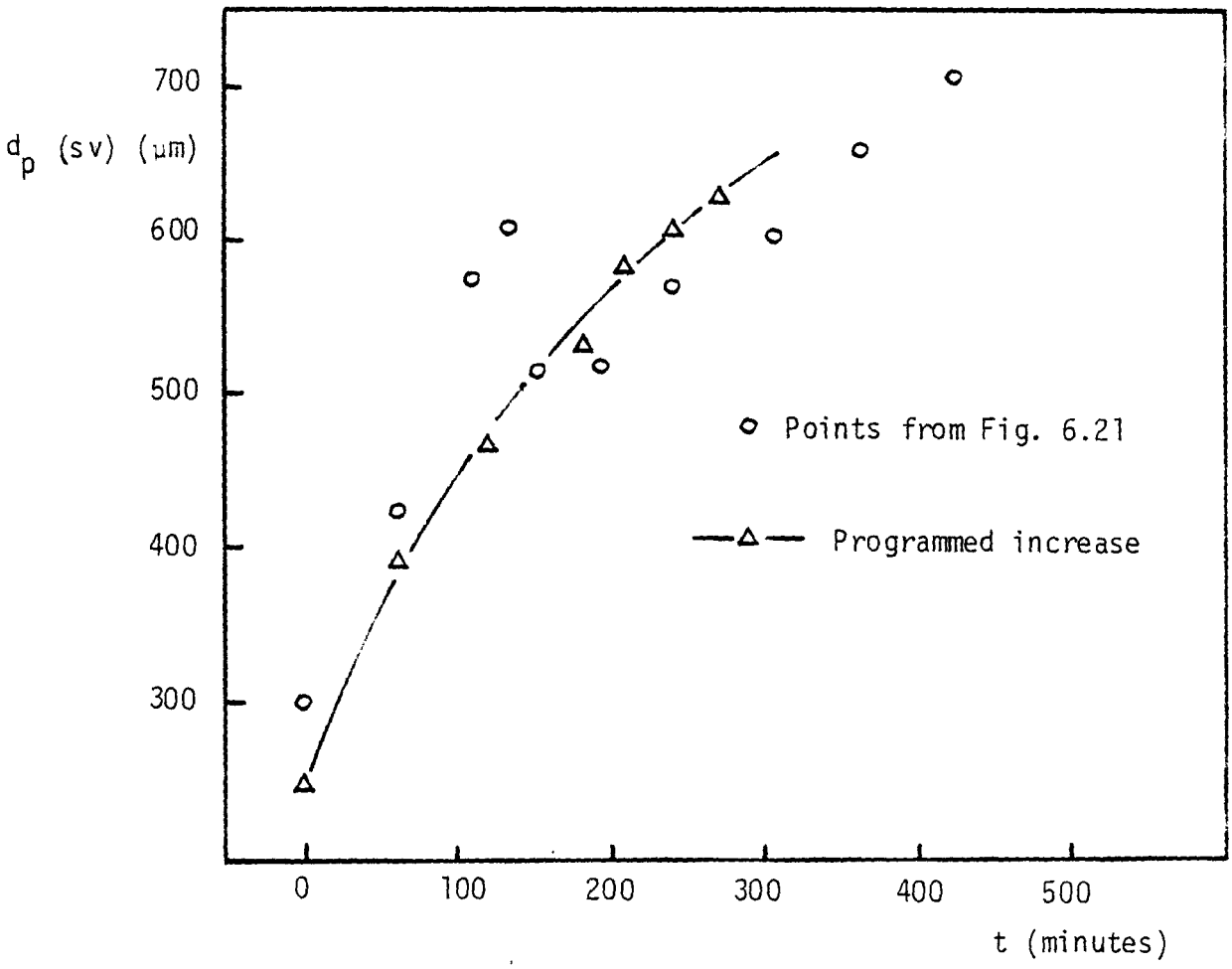


Fig. 6.22 Programmed gas rate increase to give constant
" " glass powder, 5% carbowax

Table 6.8 Excess gas velocity as a function of time; glass powder, 5% carbowax, nominal $U - U_{mf} = 0{\cdot}525\ ms^{-1}$

| Time (minutes) | $U - U_{mf}$ ($ms^{-1}$) | % error from nominal value |
|---|---|---|
| 0 | 0·525 | - |
| 65 | 0·527 | + 0·4 |
| 90 | 0·524 | - 0·2 |
| 120 | 0·513 | - 2·2 |
| 150 | 0·504 | - 4·0 |
| 175 | 0·509 | - 3·0 |
| 183 | 0·527 | + 0·4 |
| 202 | 0·533 | + 1·5 |
| 217 | 0·541 | + 3·0 |
| 235 | 0·546 | + 4·0 |
| 275 | 0·557 | + 5·5 |

Table 6.9 gives the same information for glass powder and 1% carbowax, nominally at $0{\cdot}40\ ms^{-1}$. Gas velocity adjustments for this experiment were based on the change of particle size when using a 1% carbowax solution at $U - U_{mf} = 0{\cdot}525\ ms^{-1}$ (Fig. 6.17).

Table 6.9 Excess gas velocity as a function of time; glass powder, 1% carbowax, nominal $U - U_{mf} = 0{\cdot}40\ ms^{-1}$

| Time (minutes) | $U - U_{mf}$ ($ms^{-1}$) | % error |
|---|---|---|
| 0 | 0·40 | - |
| 90 | 0·406 | + 1·5 |
| 120 | 0·401 | + 0·25 |
| 180 | 0·404 | + 1·0 |
| 210 | 0·404 | + 1·0 |
| 240 | 0·407 | + 1·8 |
| 300 | 0·412 | + 3·0 |
| 360 | 0·406 | + 1·5 |

It is possible to obtain reasonably accurate estimates of $U_{mf}$ during the course of granulation so that adjustments can be made to the gas rate. An in situ measurement of the minimum fluidising velocity of glass powder / carbowax granules was made (at a point corresponding to t = 425 minutes in Fig. 6.21) by simply reducing the air flow and recording the rotameter reading when the bed appeared to be at the point of minimum fluidisation. A value of $U_{mf}$ of 0·42 $ms^{-1}$ resulted. The bed material was then removed and a conventional velocity / pressure drop curve obtained, giving $U_{mf}$ to be 0·48 $ms^{-1}$.

### 6.5.3 Effect of gas velocity on agglomeration; the genuine velocity effect

Having established that it was possible to keep $U - U_{mf}$ constant by periodic increase of the fluidising air flowrate, the "genuine" effect of excess gas velocity on an agglomerating system was investigated using glass powder (nominal size 270 μm and 5% carbowax solution). The growth curves obtained at an excess velocity of 0·525 $ms^{-1}$ are those which were discussed in detail in Section 6.3.2. The curve showing the increase in surface - volume mean diameter is reproduced in Fig. 6.23, together with that for $U - U_{mf}$ = 0·65 $ms^{-1}$. Growth is significantly less at the higher velocity. After 240 minutes, $d_p$ (sv) reached 611 μm at 0·525 $ms^{-1}$ compared with 501 μm at 0·65 $ms^{-1}$, the ratio of diameter increase being 1·54. This result is consistent with the effect of fluidising velocity on particle growth which was described in Section 6.5.1.

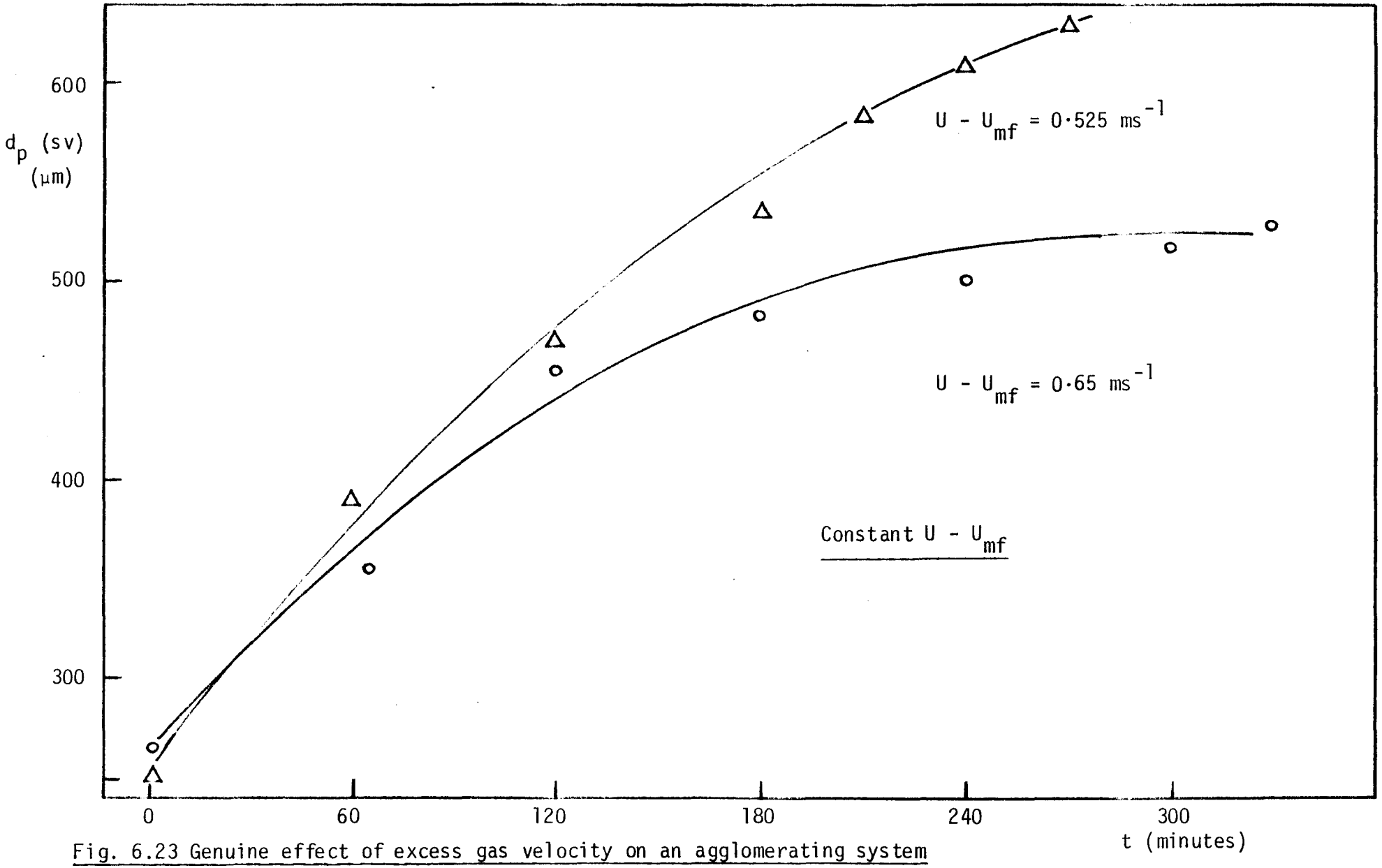


Fig. 6.23 Genuine effect of excess gas velocity on an agglomerating system

## 6.6 EFFECT OF PARTICLE SIZE

### 6.6.1 Introduction

Increasing the starting size of ungranulated particles in the fluidised bed produces similar effects to those observed when higher gas velocities are used, because larger inertial forces (which tend to pull apart bound particles) are associated with larger particles (see Section 3.1.2). Stable operation has resulted under conditions which have led to bed quenching with smaller particles, closer agreement with the layered growth model has been achieved and agglomeration growth rates have been reduced. Two separate, differently-sized charges of glass powder have been used in these experiments (see Appendix A). The ratio of the initial surface - volume mean diameters was 1·60.

### 6.6.2 A weakly agglomerating system

Whereas spraying a 10% benzoic acid solution into a bed of glass powder of nominal size 270 μm, fluidised initially at an excess gas velocity of 0·275 $ms^{-1}$, caused quenching within 170 minutes, the use of larger particles (nominal size 437 μm) allowed an experiment at the same gas velocity to run for a period of 480 minutes. In the second case the product granules grew by layering, rather than by agglomeration as previously.

Fig. 6.24 clearly demonstrates that particle growth, relative to the initial particle size, is significantly less for larger particles than for the smaller particles before bed quenching. The fluctuations in weight - moment mean diameter during the early stages of the experiment (Fig. 6.25) disappear and a gradual increase in $d_p$ (wm) ensues. There is a similarity here with Fig. 6.4 and the way in which an equilibrium in $d_p$ (wm) is established. The small increase in weight - moment diameter over the run as a whole is a further indication of growth by layering. The two experiments which are compared in Figs. 6.24 and 6.25 were carried out under identical conditions, save for the size of

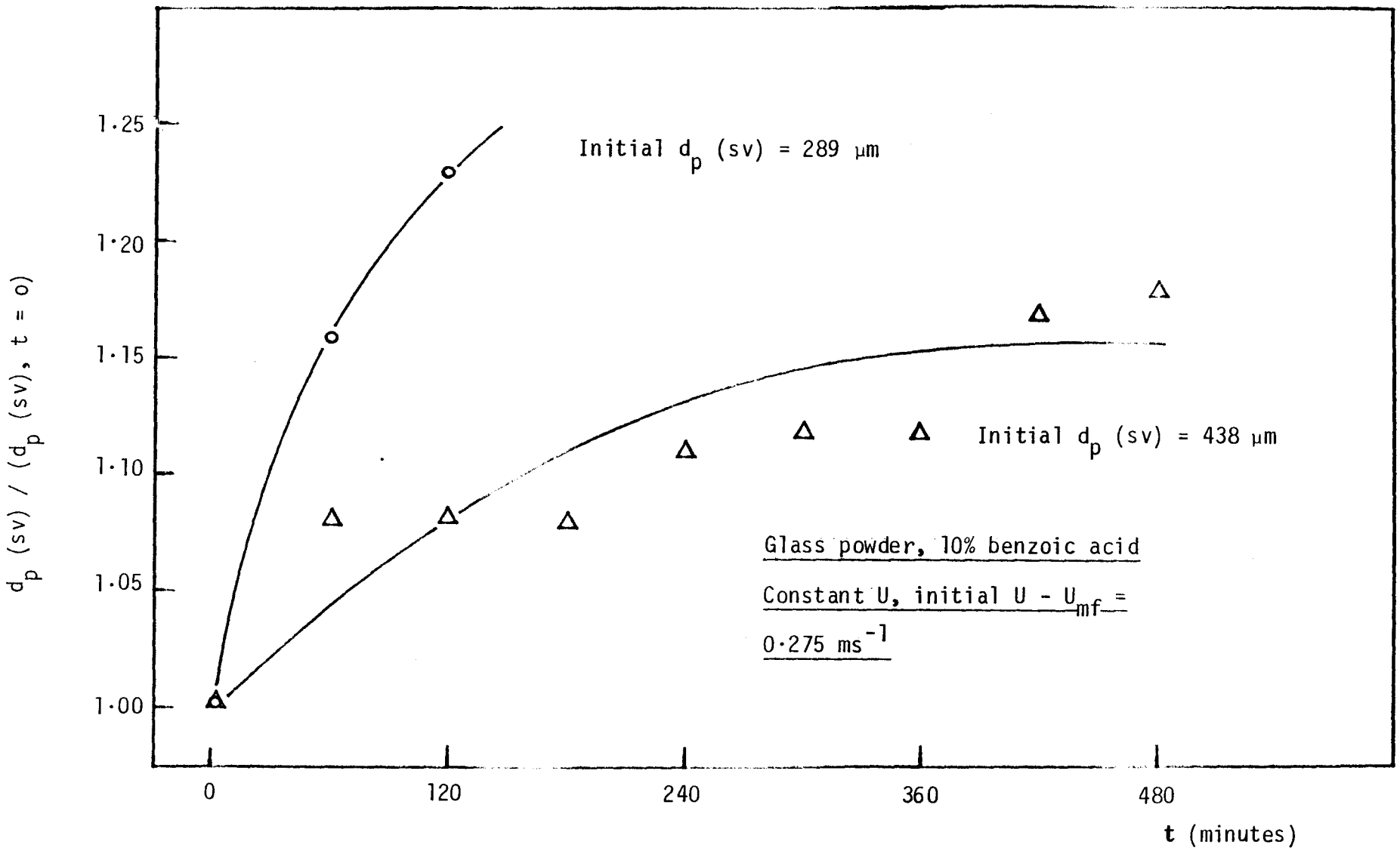


Fig. 6.24 Effect of particle size on a weakly agglomerating system

the initial particles. The same feed solution was used and the particles were fluidised at the same excess gas velocity, although the superficial velocity (kept constant throughout) was greater for the larger particles to take account of the higher minimum fluidising velocity. Thus, what has been shown is that larger particles, because of their greater inertia, are able more easily to overcome the forces which tend to bind them together and lead to agglomeration and bed quenching.

A similar effect was observed at $U - U_{mf} = 0{\cdot}525\ ms^{-1}$ (Fig. 6.26) where larger particles were responsible for a smaller growth rate and the elimination of the small amount of agglomeration which was recorded with the smaller initial particles (see Section 6.2.1). This has resulted in much closer agreement for the larger particles, between the experimental data and the layered growth model. The graphs of measured and predicted granule diameter against time for the 270 μm particles and the 437 μm particles are given in Figs. 6.27 (a poor fit) and 6.7 (a good fit) respectively.

6.6.3 A strongly agglomerating system

Fig. 6.28 shows the effect of initial particle size on a strongly agglomerating system, at a constant excess gas velocity of $0{\cdot}525\ ms^{-1}$. The smaller initial particles produced larger agglomerates, relative to starting size, than did the larger particles. After 180 minutes of granulation the mean granule diameter (surface - volume) had increased by a factor of 2·2 for an initial size of 245 μm (nominally 270 μm, see Appendix A) and by only 1.6 times for an initial size of 420 μm (nominally 437μm).

However, by using a combination of large particles and a very low concentration of binder (0·1%), layered growth has been produced even with this strongly agglomerating system of glass powder and carbowax. No agglomeration was observed in the product granules and this, together with the low binder input ($2{\cdot}2 \times 10^{-7}\ kg\ s^{-1}$) and the small amount of

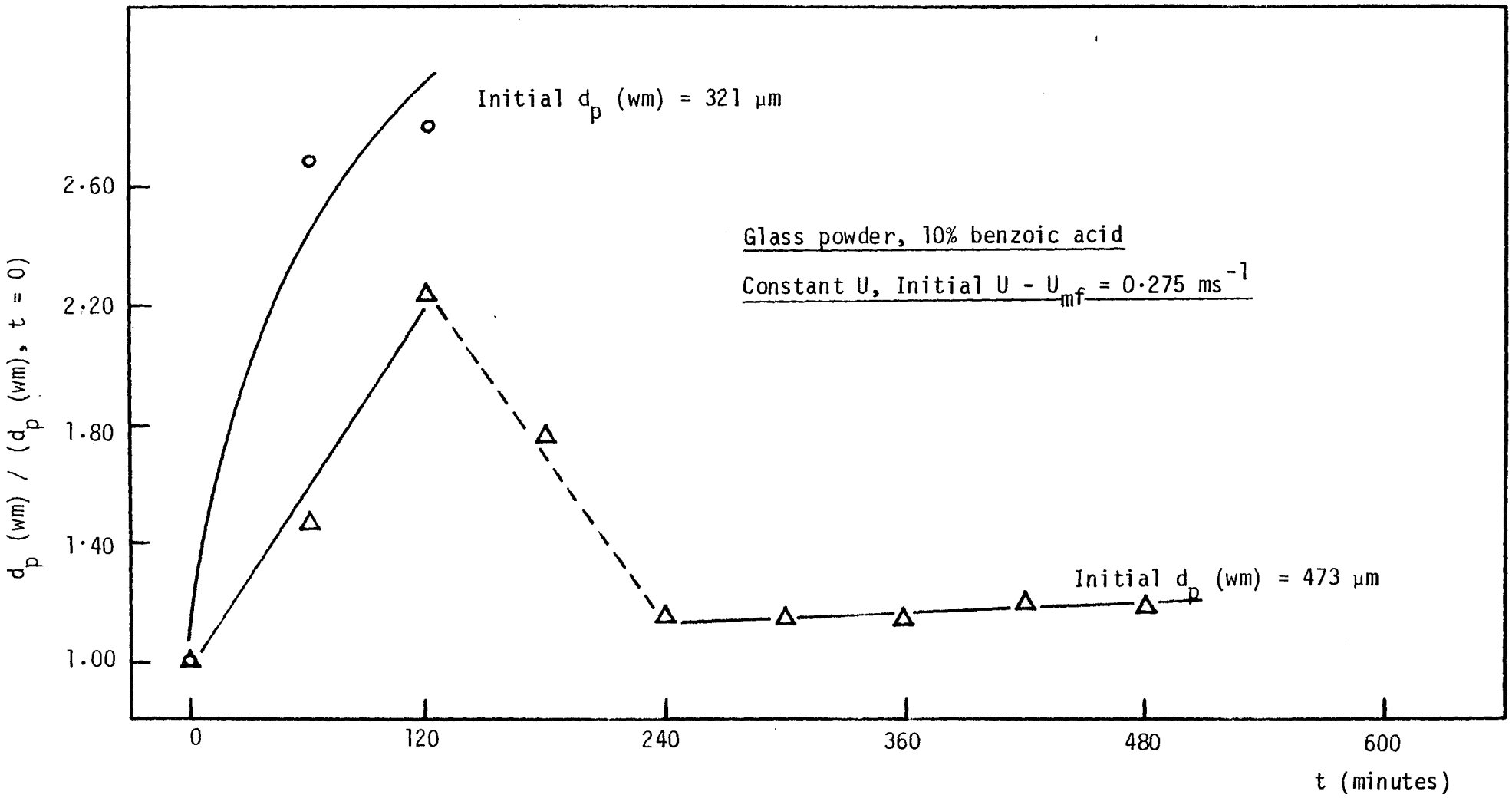


Fig. 6.25 Effect of particle size on a weakly agglomerating system

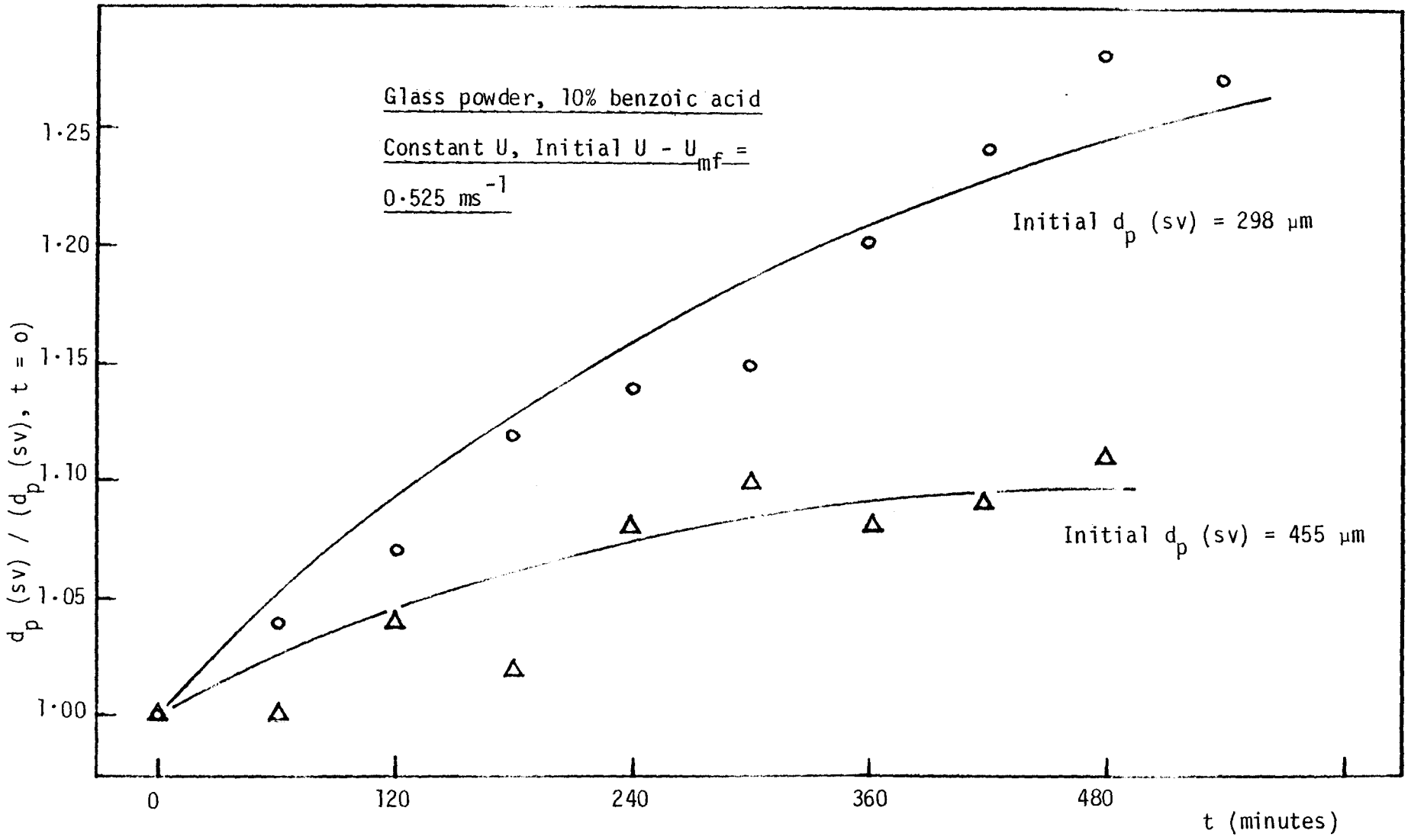


Fig. 6.26 Effect of particle size on a weakly agglomerating system

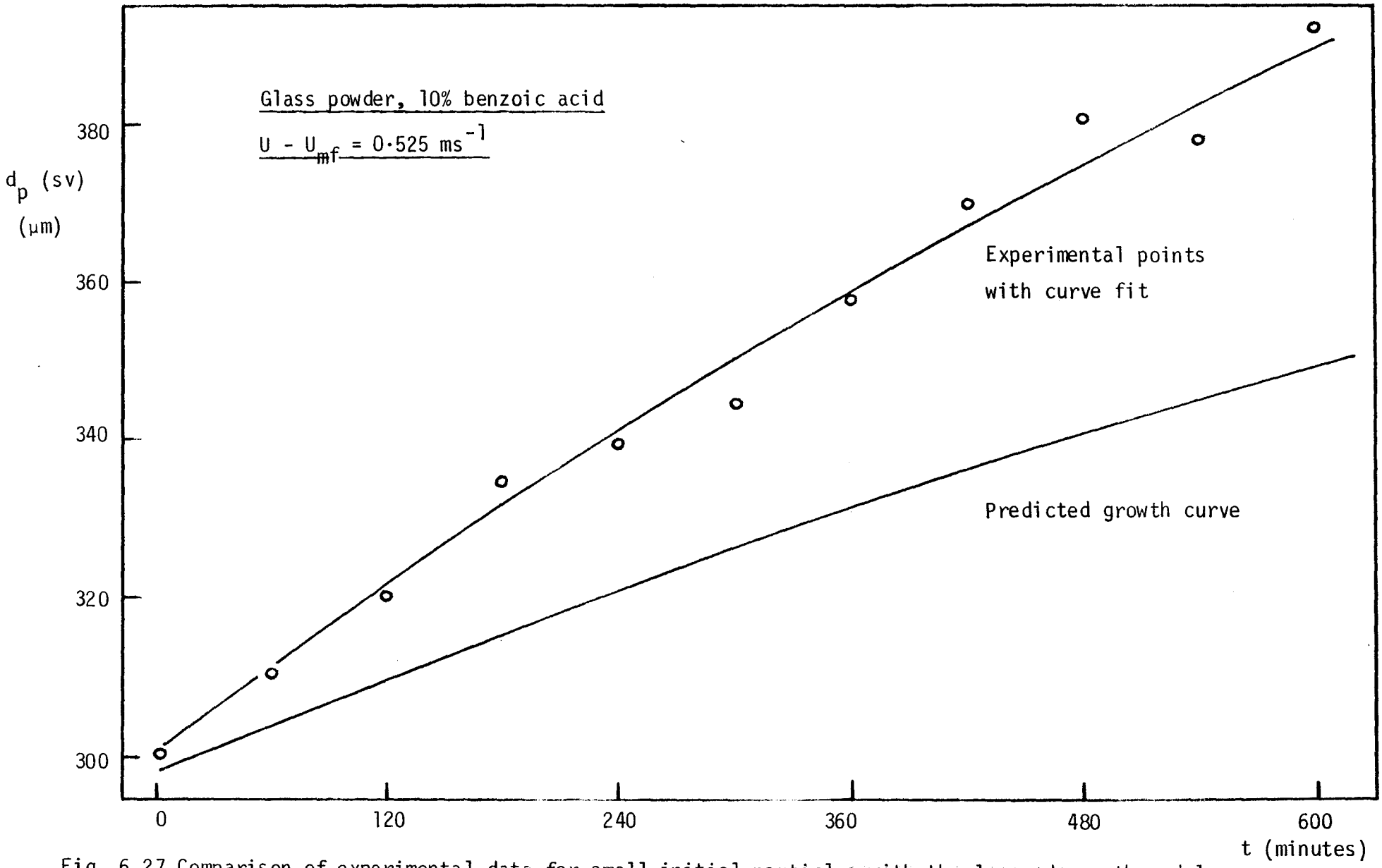


Fig. 6.27 Comparison of experimental data for small initial particles with the layered growth model

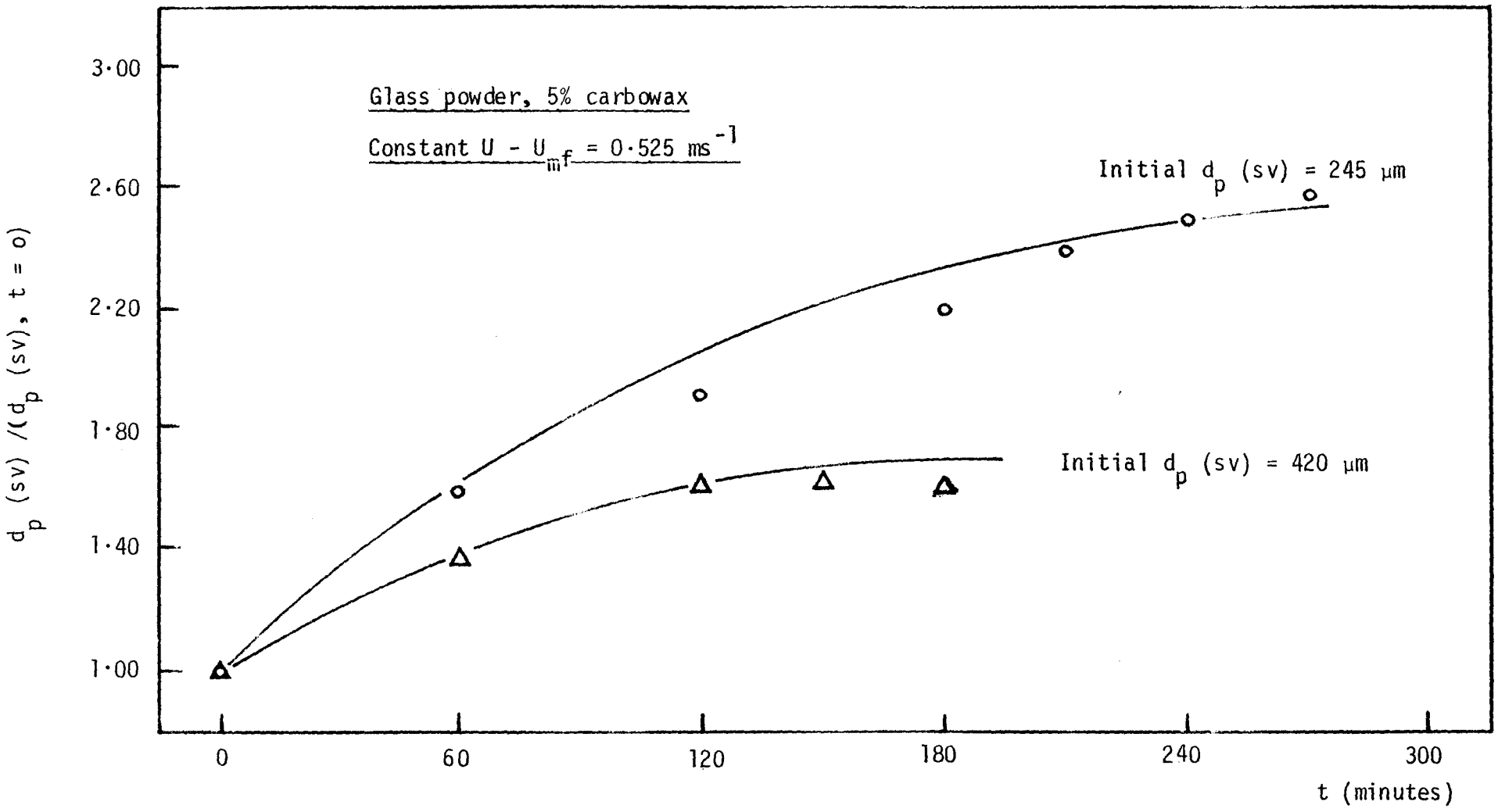


Fig. 6.28 Effect of particle size on a strongly agglomerating system

particle growth (Table 6.10), confirms that growth was by a layering process.

Table 6.10 Change in particle size for layered growth with glass powder / 0·1% carbowax system; $U - U_{mf} = 0{\cdot}525\ ms^{-1}$

| Time (minutes) | mean particle diameter (μm) $d_p$ (sv) | $d_p$ (wm) |
|---|---|---|
| 0 | 425·5 | 457·6 |
| 480 | 430·9 | 467·9 |
| 720 | 427·6 | 476·3 |

## 6.7 EFFECT OF PARTICLE STRUCTURE; GRANULATION EXPERIMENTS WITH ALUMINA

### 6.7.1 No-growth period

Beds of glass powder and of alumina particles behave very differently when feed solutions are introduced into them. Initially, at least, no particle growth takes place with alumina, whereas with glass powder growth occurs from the start of spraying. The results which will be presented in this section confirm those in Chapter Four concerning bed particle structure.

Fig. 6.29 shows that when a 10% benzoic acid solution was sprayed into a bed of alumina particles, fluidised at an excess gas velocity of 0·15 $ms^{-1}$, no significant change in particle size was measured for a considerable period. Beyond a certain point particle growth began to occur, and it will be demonstrated that this is very similar to particle growth with glass powder. The period between the start of an experiment and the beginning of growth has been termed the "no-growth period", and the point at which growth is first observed or indicated, the "transition point". The transition point may be defined by a sudden, large increase in weight - moment mean diameter (due to agglomeration), by a rise in temperature at the bottom of the bed (indicating segregation) or by visual observation of large agglomerates forming on the distributor plate.

Glass powder particles under identical conditions quickly quenched, whereas the no-growth period for alumina in Fig. 6.29 lasted for 280 minutes, defined by the temperature trace. Appendix C contains evidence that the absence of quenching and particle growth is not a function of either bed temperature or of fluidising gas velocity. However, the length of the no-growth period is a function of binder concentration and therefore of the binder mass input; Table 6.11 gives the total mass of benzoic acid sprayed before particle growth occurred.

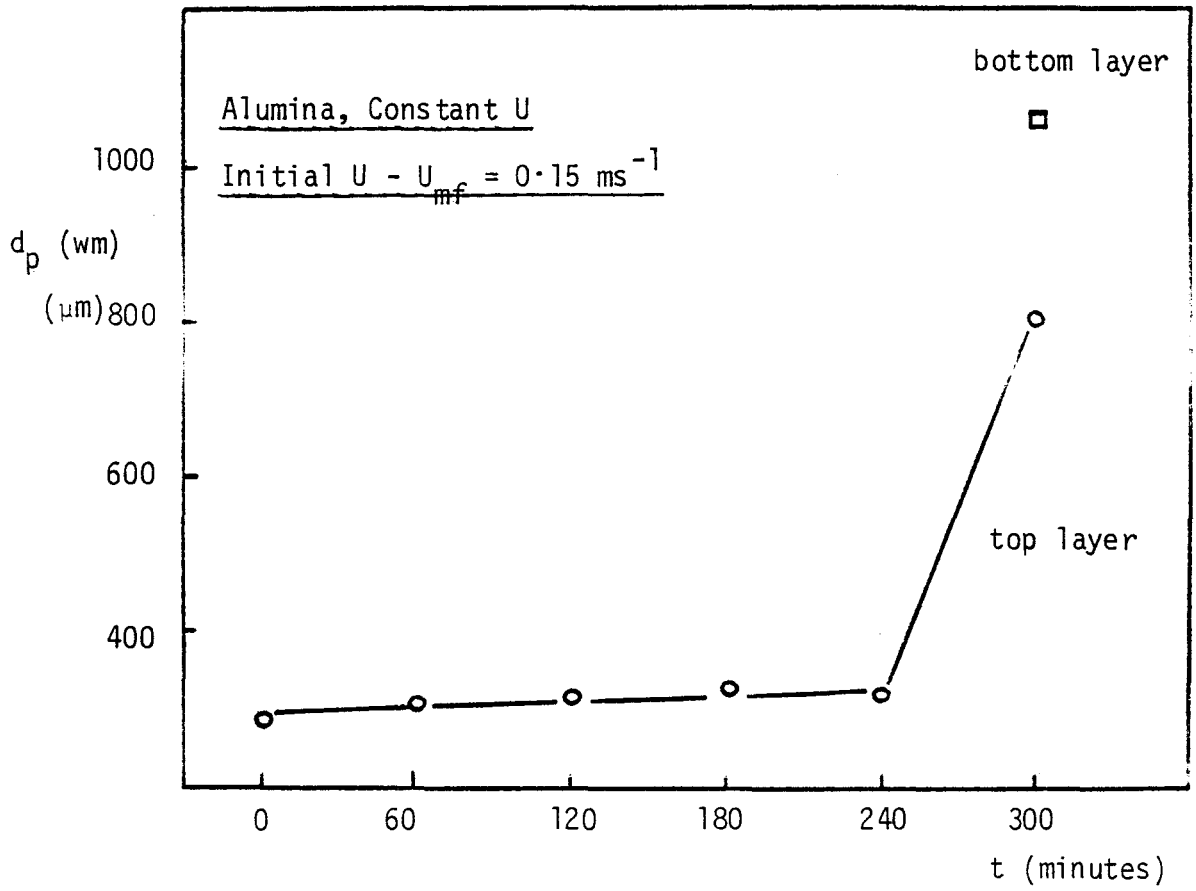


Fig. 6.29 No-growth period: 10% benzoic acid solution

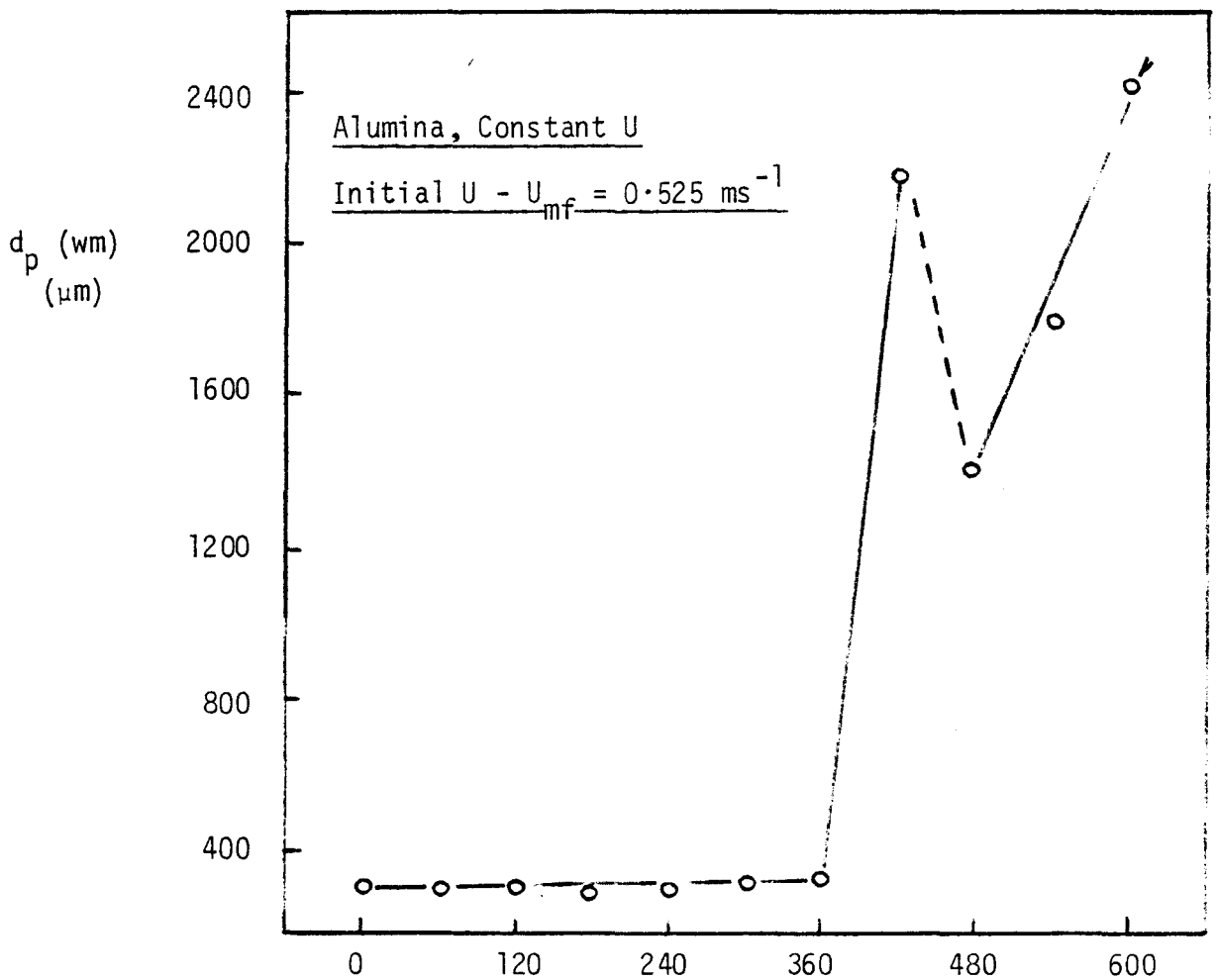


Fig. 6.30 No-growth period: 5% carbowax solution

Table 6.11 Variation of the no-growth period with binder concentration; $U - U_{mf} = 0{\cdot}15\ ms^{-1}$

| Benzoic acid concentration | Binder feedrate ($kg\ s^{-1}$) | Length of no-growth period (minutes)* | Total mass of binder sprayed (kg) |
|---|---|---|---|
| 10% | $2{\cdot}32 \times 10^{-5}$ | 280·0 | 0·389 |
| 20% | $5{\cdot}12 \times 10^{-5}$ | 126·5 | 0·388 |

* by temperature rise.

The same phenomenon occurred when carbowax was sprayed in place of benzoic acid and this is illustrated in Fig. 6.30. However an increase in carbowax concentration from 5% to 10% reduces the length of the period from 360 minutes to only 28 minutes. As will be proposed in Chapter Eight, this behaviour is explained by the different viscosities of benzoic acid and carbowax solutions.

The major difference in physical properties between glass powder and alumina, and one which may account for the observed differences in behaviour, is particle structure: alumina has considerable intra-particle porosity, glass powder is non-porous. An explanation of the no-growth period phenomenon is as follows. The pores of the alumina particles allow liquid to be absorbed and thus to be removed from the external particle surface. Liquid bonds cannot then form between adjacent bed particles, preventing both particle growth and wet quenching but allowing moisture to be evaporated at rates, and at fluidising gas velocities, which would precipitate quenching with glass powder. Because evaporation takes place from within the particle, any solute will be deposited in the pores, thus removing the possibility of forming solid bridges between particles and also preventing growth by deposition on the exterior surface of the particle. As "granulation" continues more and more binder is deposited within the pores until, at the transition point, further binder cannot be accommodated. Binder then forms on the exterior surface and particle growth ensues.

A simple calculation has shown that, in the examples of Table 6.11, insufficient binder was supplied to fill the entire intra-particle porosity of the bed. The porosity of alumina was measured to be 0·708 of the particle volume and consequently only 40·8% of the pore volume could be occupied by the binder sprayed into the bed (see Appendix A for details of the calculation). Therefore it is not suggested that the pores are completely filled but perhaps blocked in some way so as to prevent further liquid entering and further binder deposition. In this way, beyond the transition point, alumina behaves effectively like a non-porous solid. Nitrogen adsorption measurements of the internal surface area have been made on alumina samples removedfrom the bed during the no-growth period when a 5% carbowax solution was sprayed. Table 6.12 lists the results.

Table 6.12 Change in internal surface area during the no-growth period; 5% carbowax, $U - U_{mf} = 0{\cdot}525\ ms^{-1}$

| Time (minutes) | $A_s$ ($m^2\ kg^{-1}$) | $d_p$ (wm) (μm) |
|---|---|---|
| 0 | $1.86 \times 10^5$ | 307·7 |
| 120 | $1.26 \times 10^5$ | 307·5 |
| 360 | $5.90 \times 10^4$ | 324·7 |
| ——— | transition point ——— | ——— |
| 435 | $5.80 \times 10^4$ | 2180·2 |

It is not possible to easily measure the pore volume when material has been deposited within the pores. However the fact that pore surface area decreases as spraying proceeds, indicates that an effective reduction in pore volume is taking place. A surface area at the transition point greater than zero suggests that some pores are still open to the exterior surface and are blocked, or partially blocked, rather than filled. This would still allow adsorption of nitrogen but not the entry of large carbowax molecules.

6.7.2 Comparison of alumina and glass powder

Beyond the transition point, alumina particles behave in a similar manner to glass powder particles. Particle growth takes place and, at low velocities, rapid agglomeration again results in the formation of a segregated layer, causing a rise in temperature and ultimately bed quenching. The transition point has only been detected by temperature rise in experiments at $U - U_{mf} = 0.15$ ms$^{-1}$. At the highest excess gas velocity (0·525 ms$^{-1}$) which was used in experiments with alumina, the bed remained well-fluidised throughout and an increase in particle size was the only indication that the no-growth period had ended. By plotting particle size against time on a scale incorporating a false zero (i.e. equating the transition point with t = o), direct comparison of the particle growth rates of alumina and glass powder can be made. For example, in Fig. 6.31, the time axis for alumina has been shifted so that t = 280 minutes (the transition point) coincides with t = o for glass powder (with which growth takes place as soon as binder is introduced.)

In this experiment, samples were taken from both the well-fluidised bulk of the bed and from the shallow segregated layer at the bottom of the bed. Initial particle growth rates are very similar for alumina and glass powder. At this low gas velocity rapid agglomeration takes place and, as with glass powder and benzoic acid at $U - U_{mf} = 0.15$ ms$^{-1}$, it was found necessary to increase the gas rate in order to prevent quenching and to maintain fluidisation of the alumina. The effect of fluidising gas velocity is the same as with glass powder. With benzoic acid as the binder, bed quenching did not occur at the higher excess gas velocities and, as is demonstrated by Fig. 6.32, particle growth was less.

There are other similarities between post-transition alumina and glass powder; at a given excess gas velocity (0.525 ms$^{-1}$) carbowax pro-

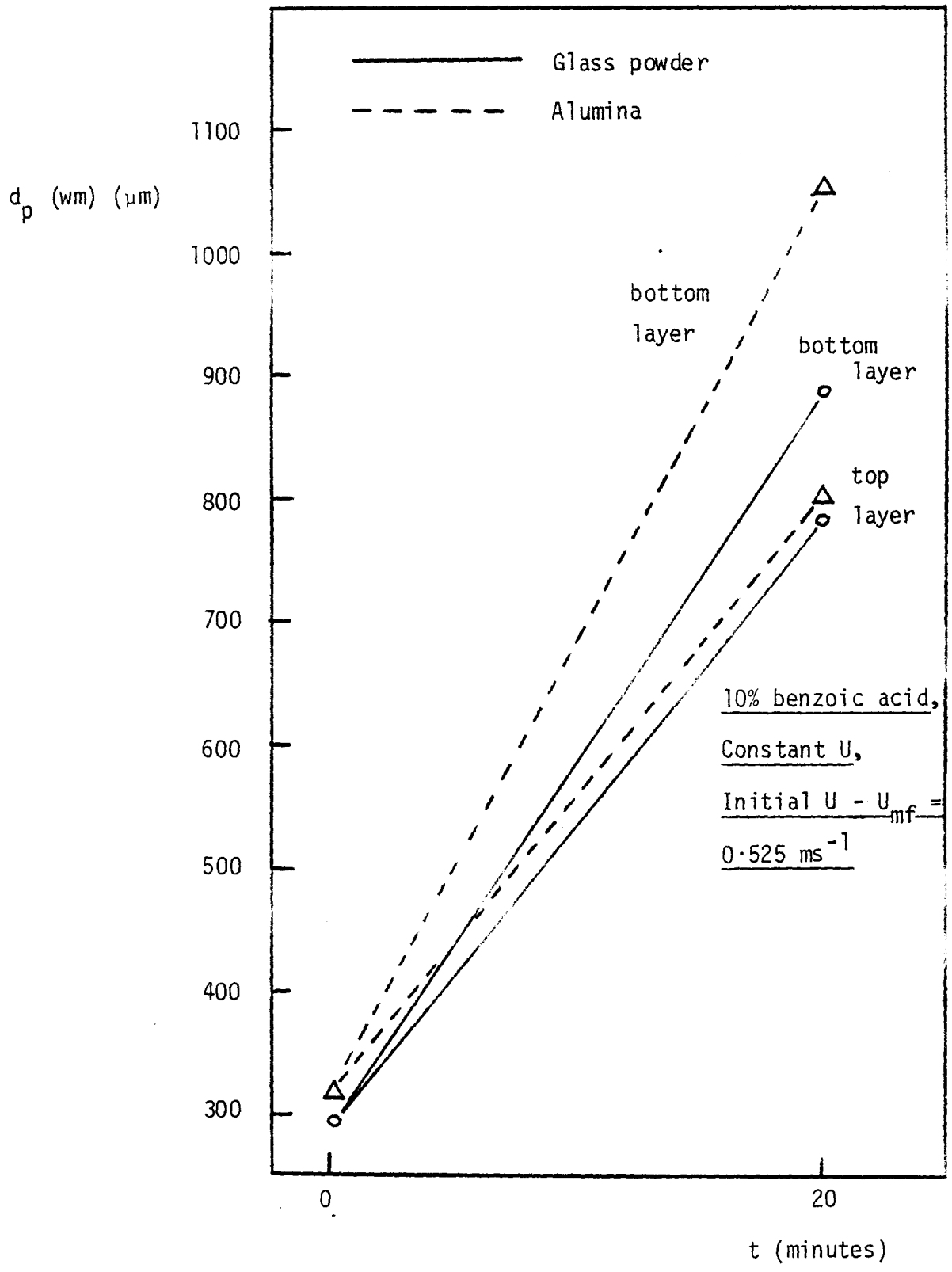


(Time scale includes false zero)

Fig. 6.31 Comparison of initial growth rates: alumina and glass powder

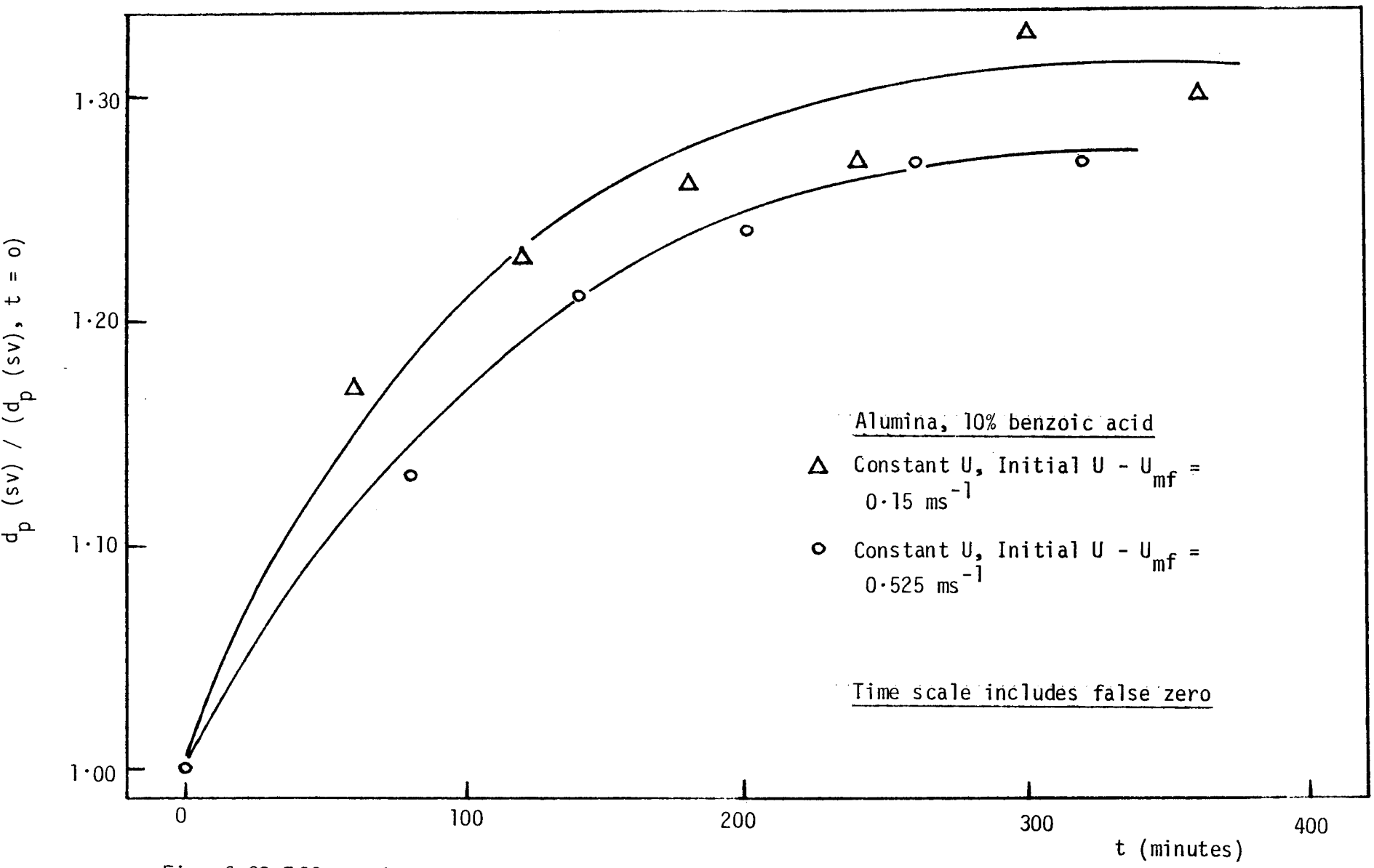


Fig. 6.32 Effect of gas velocity on the growth of alumina

duced agglomerated granules and consequently higher growth rates than with benzoic acid, which granulated predominantly in the layered growth mode (Figs. 6.33 and 6.34). However, with carbowax as binder, growth rates are greatest with non-porous glass powder (Fig. 6.35), although (as Fig. 6.37 shows) substantial agglomeration does take place with the alumina / carbowax system. Although benzoic acid and alumina produce mostly layered granules, the extent of agglomeration in this system is slightly more than with glass powder under comparable conditions (Fig. 6.38). Again this is an inertial effect. The inertial forces tending to pull apart inter-particle bonds are proportional, for particles of the same size, to particle mass and hence proportional to effective particle density.

The series of photographs in Fig. 6.36 illustrate the difficulty in identifying binder distributed around the surface of alumina particles. Little difference in appearance can be detected between ungranulated alumina and particles which have increased in size, but not by agglomeration. The appearance of agglomerated alumina is similar to that of agglomerated glass powder (Fig. 6.8).

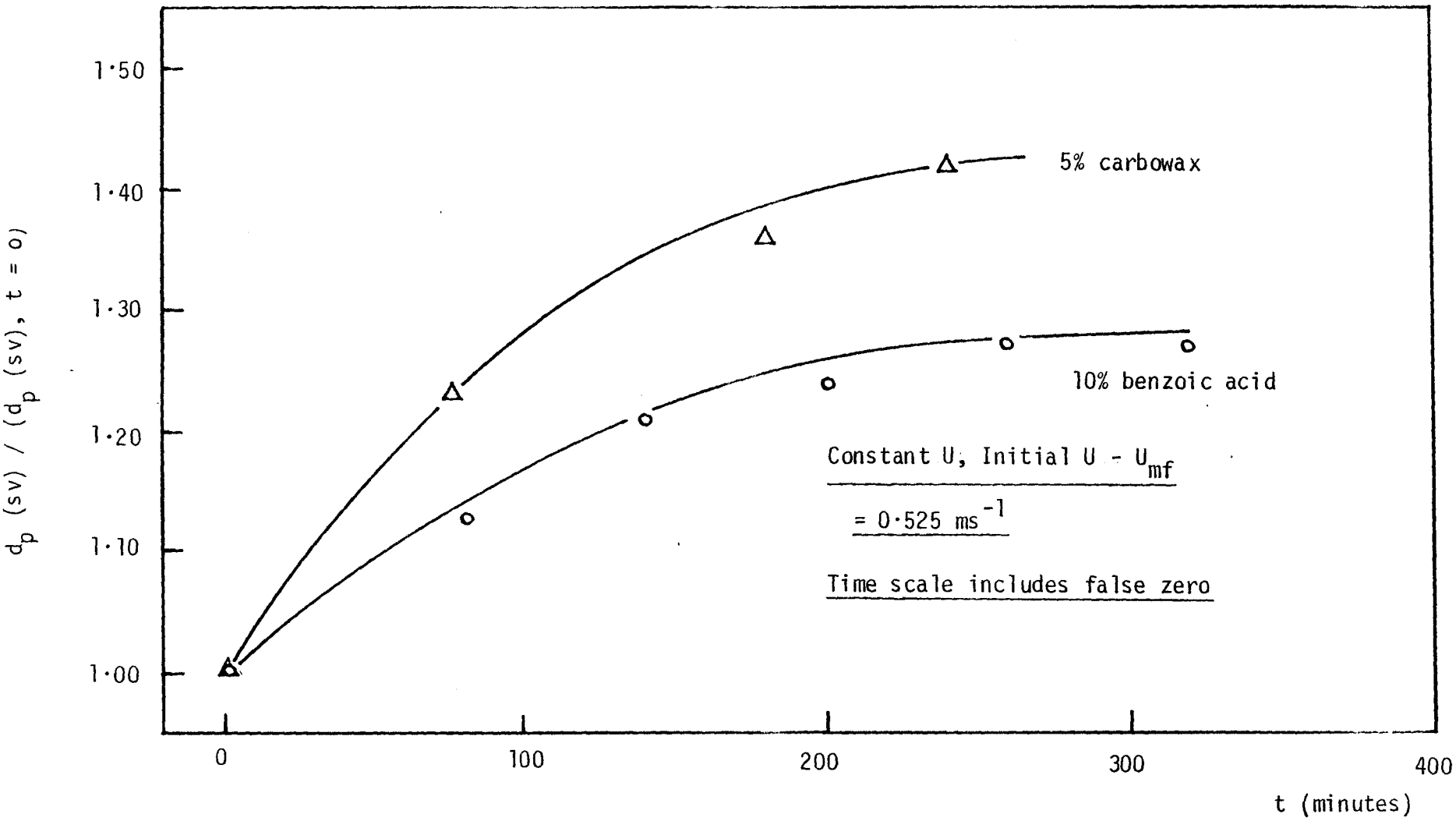


Fig. 6.33 Comparison of benzoic acid with carbowax: change in $d_p$ (sv) of alumina

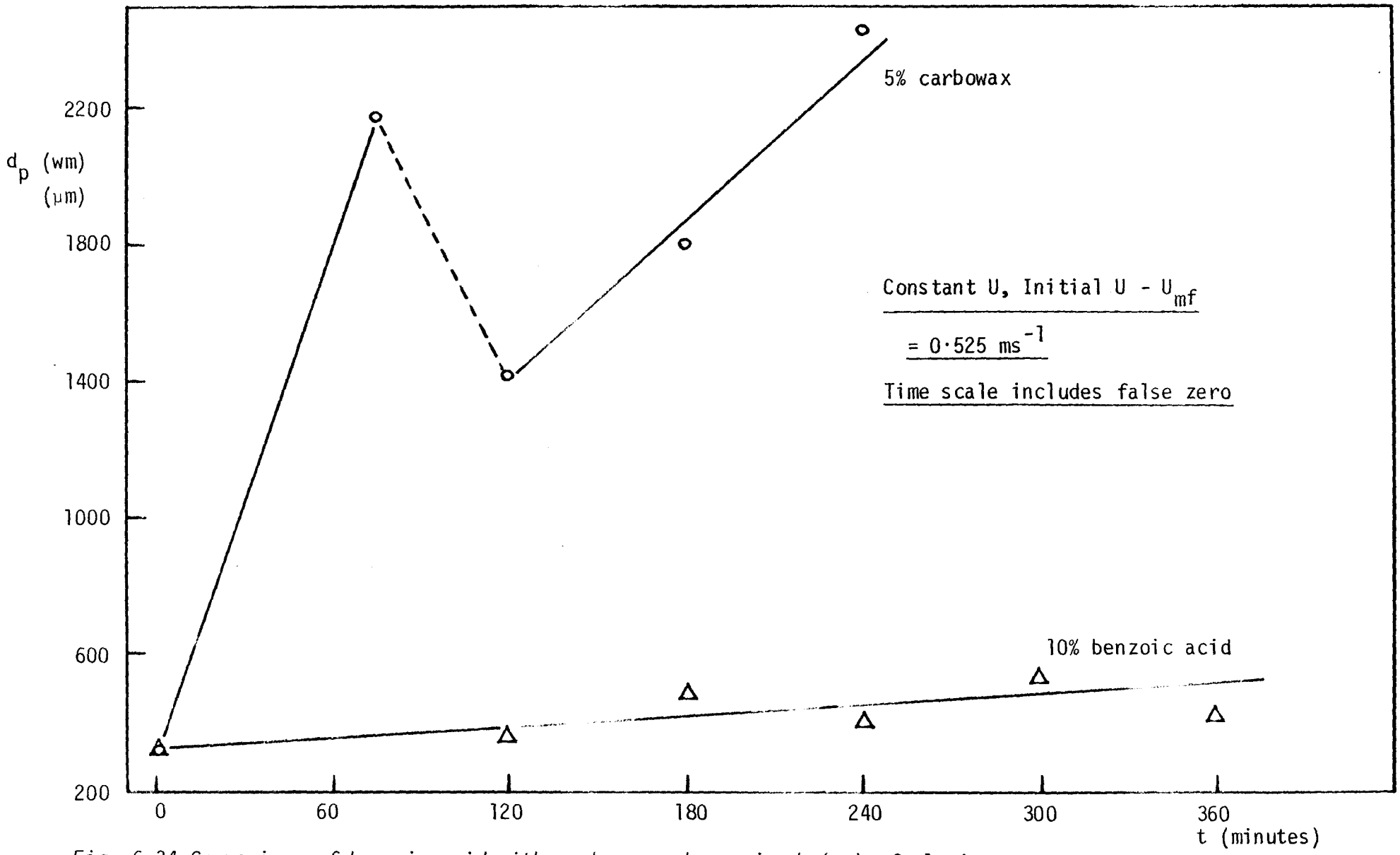


Fig. 6.34 Comparison of benzoic acid with carbowax: change in $d_p$ (wm) of alumina

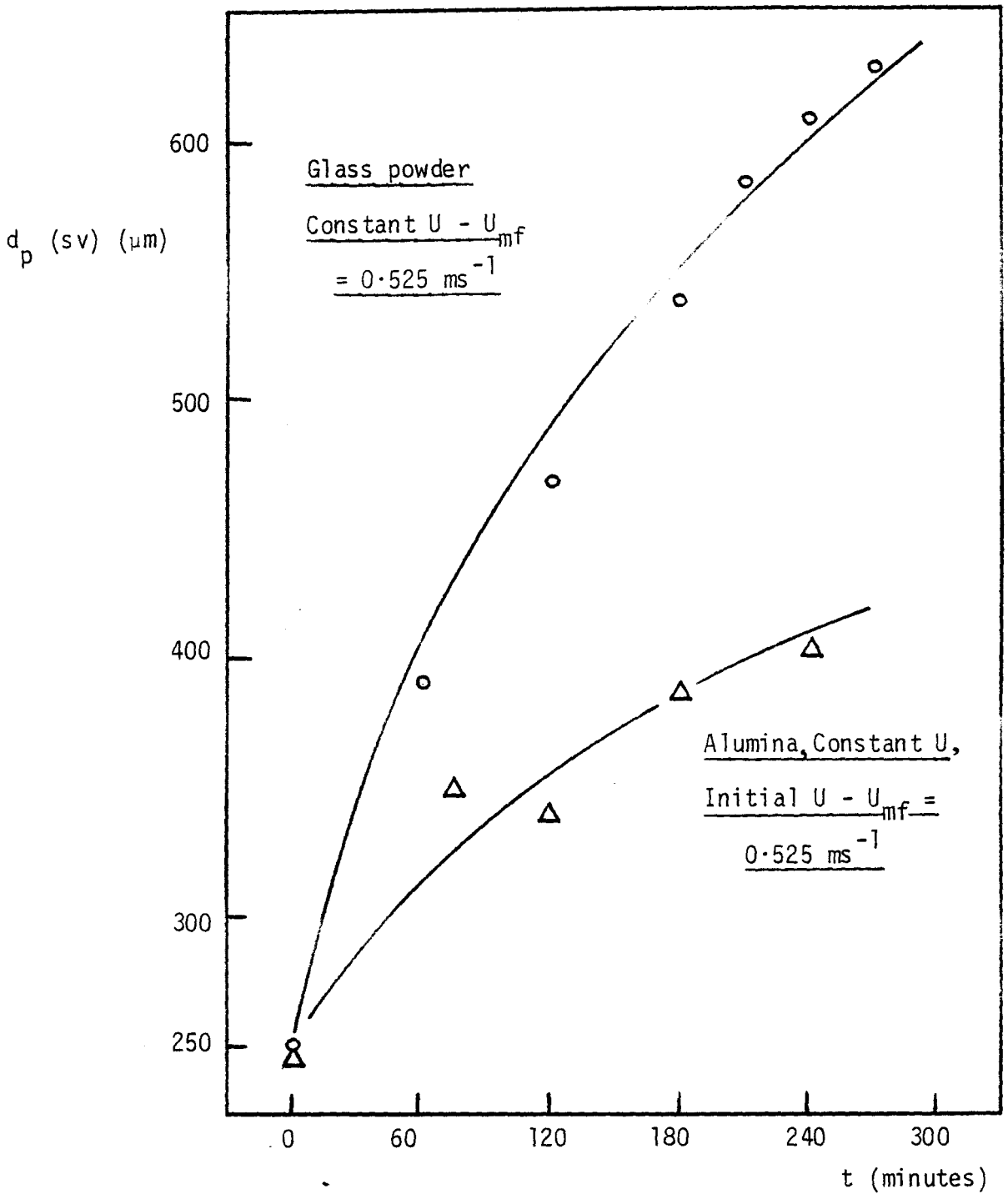


(Time scale includes false zero for alumina)

Fig. 6.35 Comparison of the growth of alumina with the growth of glass powder: 5% carbowax

Scale ; 1000$\mu$m

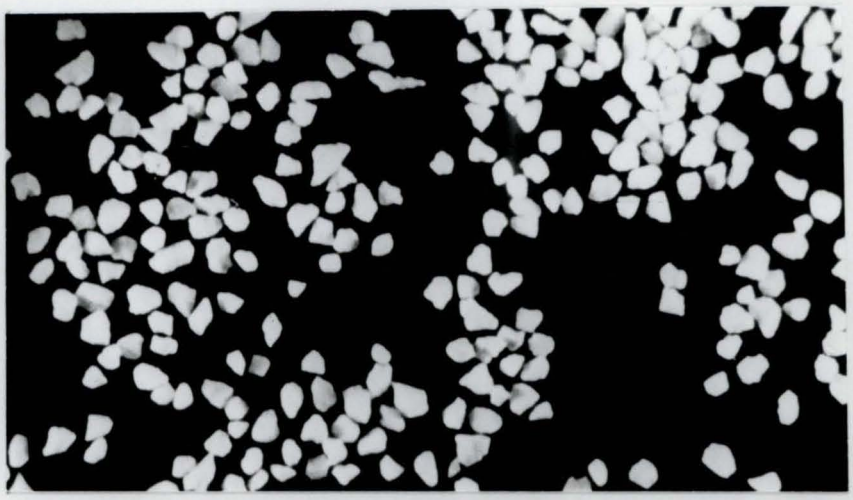

Fig. 6.36(a) Initial alumina particles

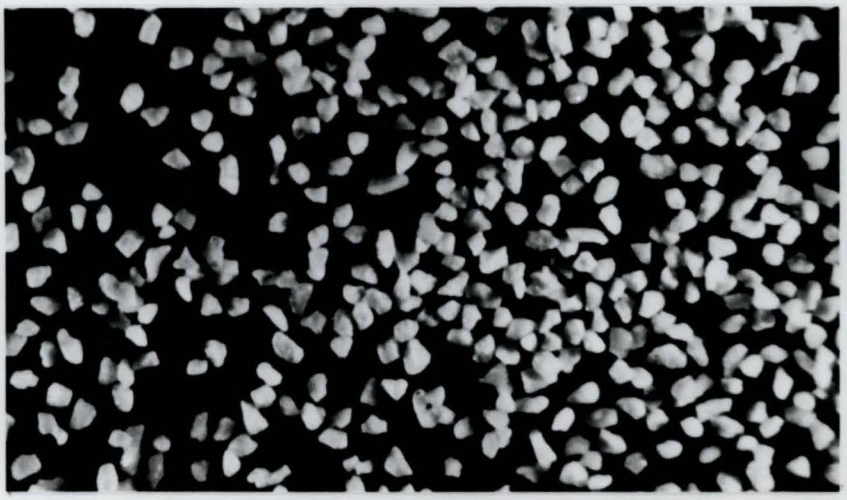

Fig. 6.36(b) Unagglomerated alumina: post no-growth period

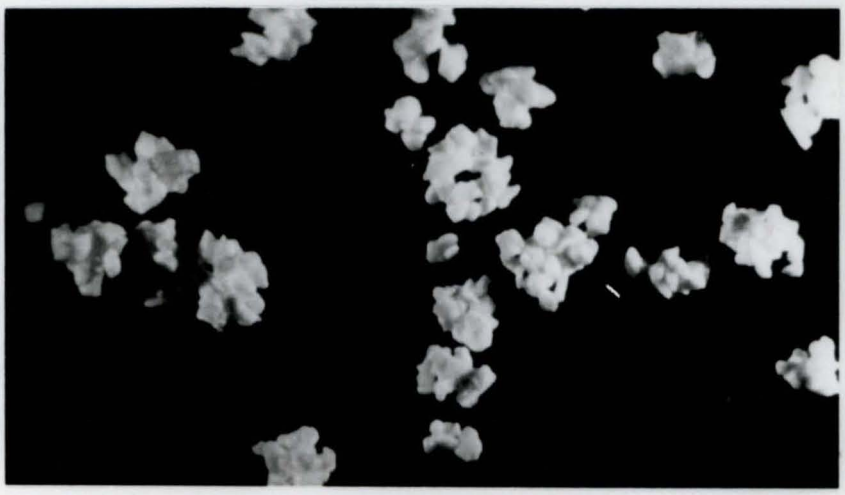

Fig. 6.36(c) Agglomerated alumina

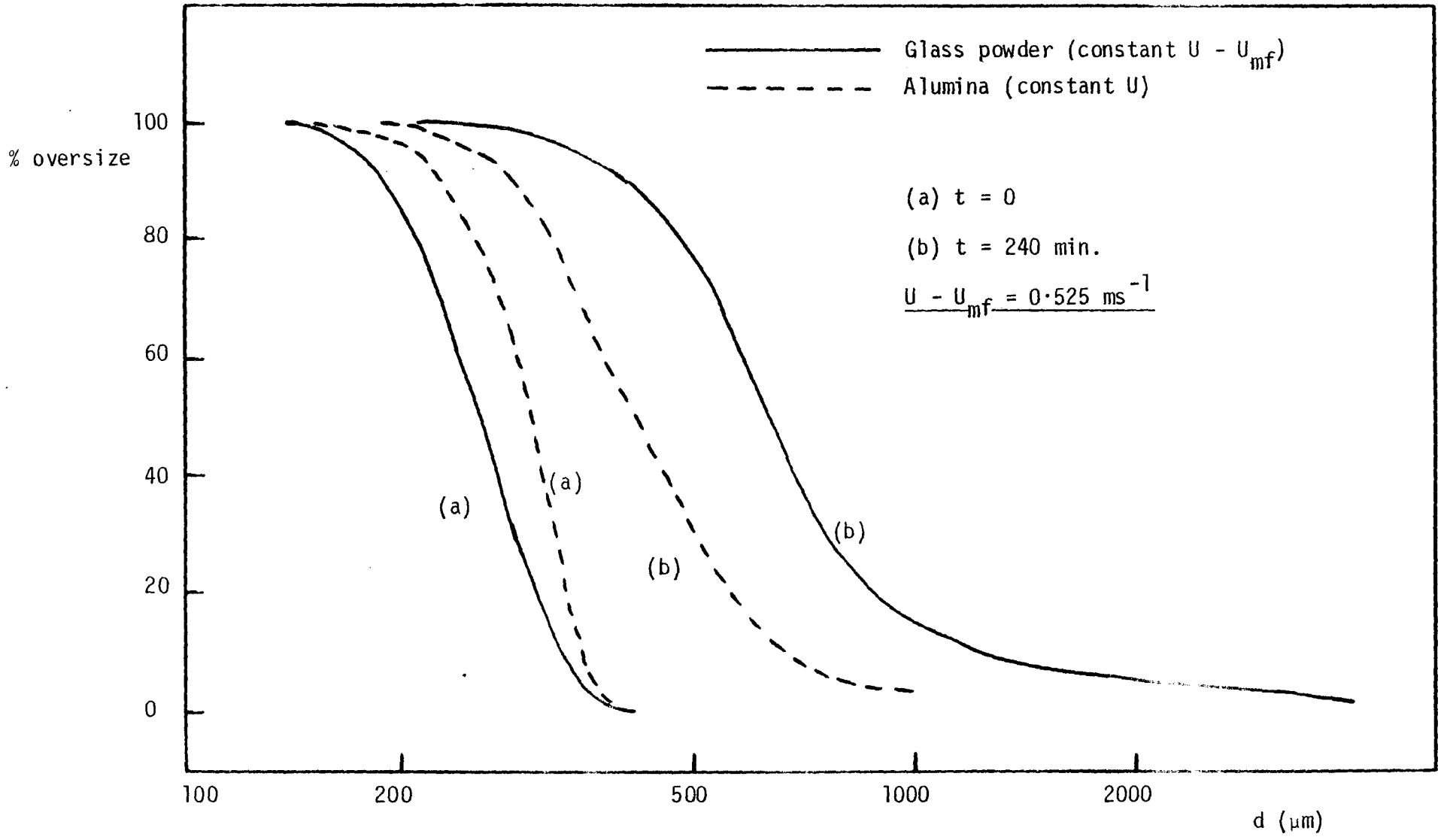


Fig. 6.37 Comparison of the PSD of alumina with the PSD of glass powder: 5% carbowax

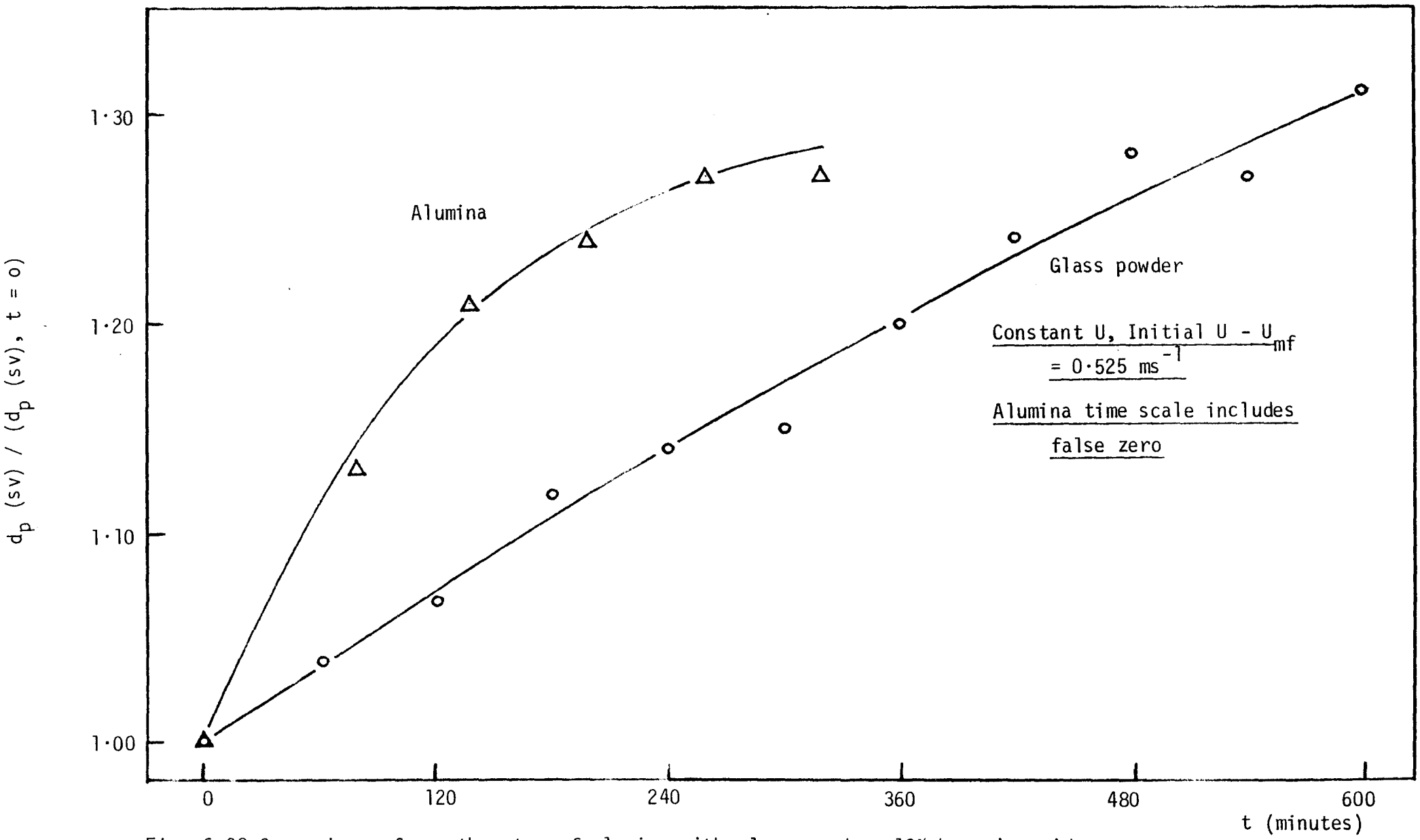


Fig. 6.38 Comparison of growth rates of alumina with glass powder: 10% benzoic acid

## 6.8 CORRELATION OF GRANULATION RESULTS WITH GRANULE AND BINDER PHYSICAL PROPERTIES

### 6.8.1 Granule properties

Measurements have been made of the compressive strengths of equal-sized granules produced by each of the four bed particle / binder systems which have been used in this study. Table 6.13 lists, for each type of granule, the time taken for disintegration and the mass of water (at a constant flowrate) which the average time represents (for experimental details see Section 5.7). The results include a large amount of scatter, reflecting the difficulty inherent in this type of measurement, and there is inevitably some doubt as to precisely what is being measured. However, by selecting equally-sized agglomerates of the same shape, the values in Table 6.13 clearly represent in some way the intrinsic strengths of the bonds in question.

Table 6.13 The compressive strengths of granules

| System | Number of observations | For complete, instantaneous disintegration of granule: Time (s) | Mass of water ($kg.10^3$) | Constituent particle density $\rho_e$ ($kgm^{-3}$) |
|---|---|---|---|---|
| Glass powder / carbowax | 40 | $172.4 \pm 48.0$ | 57·6 | $2.20 \times 10^3$ |
| Alumina / carbowax | 45 | $16.0 \pm 5.2$ | 5·3 | $1.49 \times 10^3$ |
| Alumina / benzoic acid | 25 | $14.4 \pm 5.8$ | 4·8 | $1.49 \times 10^3$ |
| Glass powder / benzoic acid | 36 | $9.1 \pm 8.5$ | 3·0 | $2.20 \times 10^3$ |

The bonds which form between particles in a glass powder / carbowax granule are far stronger than those in any of the other three types of granule. However, although the strengths of the other bonds are of the same order of magnitude, carbowax tends to form stronger bonds than benzoic acid. A strong correlation exists between the type of granule

produced, over a wide range of conditions, and the strength of the bond formed between individual particles in the granule. For example, at a given binder concentration and at fixed fluidising conditions, glass powder tends to form agglomerates (or to quench) when carbowax is used as a binder, whereas with benzoic acid layered granules are produced and bed quenching is less of a problem; carbowax bonds between glass powder particles are stronger than those formed with benzoic acid and glass powder. Similarly, when alumina is used as the bed material, carbowax results in agglomerative growth, and higher growth rates are obtained than with benzoic acid which gives rise to layering. Carbowax / alumina bonds are stronger than benzoic acid / alumina bonds, although the difference between the two binders, both in terms of growth and bond strength, is less than in the case of glass powder.

For a specific binder, the highest growth rates correlate with the strongest bonds. Thus benzoic acid / alumina bonds are slightly stronger than those which benzoic acid forms between glass powder particles; growth with alumina, although giving the same type of granule, is slightly more rapid than with glass powder.

6.8.2 Binder solution properties

Carbowax solution has a slightly higher viscosity than benzoic acid solution at the feed concentrations used in the granulation experiments, but more importantly the viscosity increases rapidly with concentration, whereas benzoic acid solution does not. This has consequences for particle gorwth (carbowax more readily precipitates bed quenching and gives rise to agglomeration) and also for the behaviour of alumina particles; an increase in carbowax concentration reduces the no-growth period disproportionately more than does an increase in benzoic acid concentration. Details of the solution viscosities are given in Appendix A.

# CHAPTER SEVEN

# STUDIES OF BED STRUCTURE

## 7.1 X-RAY PHOTOGRAPHY OF GRANULATION

### 7.1.1 Normal granulation conditions

X-ray photography has been used to observe a fluidised bed in which granulation was taking place. The purpose was two-fold; to ascertain whether or not a spray zone (such as has been proposed in the literature[43,44,56]) could be seen, and secondly to confirm visually the difference in behaviour between carbowax and benzoic acid. Therefore, two experiments were conducted under conditions which were known to give very different results.

Figs. 7.1 and 7.2 show two series of photographs, taken at comparable times after the beginning of granulation, of experiments with 10% carbowax and 10% benzoic acid respectively. In each case the bed consisted of alumina particles fluidised at an excess gas velocity of $0{\cdot}525\ ms^{-1}$, and the solution feedrate was as in previous granulation experiments. Neither in these photographs, nor in several metres of film taken at various stages of each experiment, can a jet of atomising air be seen issuing from the spray nozzle. No visual evidence has been seen of any kind of feed zone in the bed, or of any distinct region associated with the liquid feed stream. However, by assuming that the binder and the barium bromide tracer are distributed similarly, with no preferential deposition, comparison of the two sets of photographs does yield information on the relative distributions of carbowax and benzoic acid.

As time progresses and the total amount of binder which has been sprayed into the bed increases, the photographs in Figs. 7.1 and 7.2 become darker because the bed becomes more opaque to X-rays. Although there is obviously a difference between the photographs for benzoic acid and for carbowax, for example at $t = 53$ minutes, indicating a difference in binder distribution, it is indistinct because of the difficulty in choosing a suitable common exposure. Consequently, optical densitometry

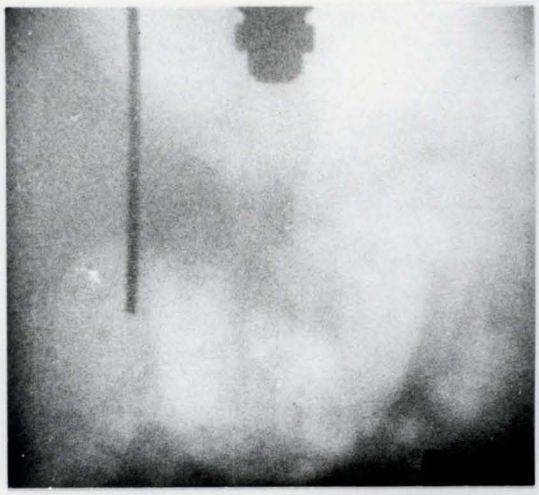

(a) t=0

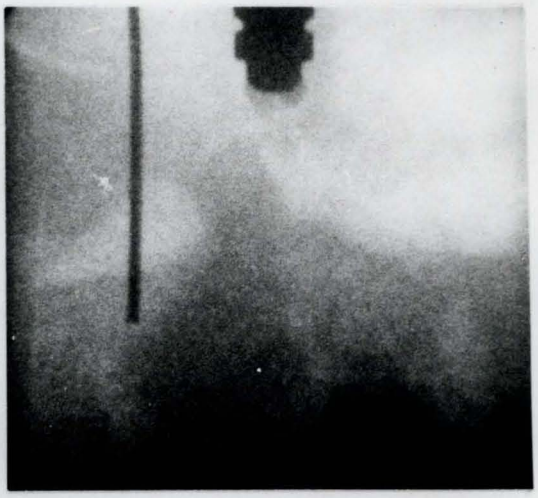

(b) t=28 min.

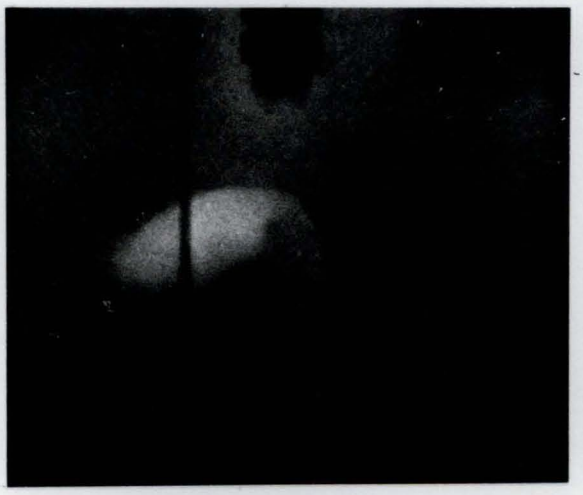

(c) t=53 min.

Scale : 5cm.

Fig. 7.1 Feed liquid : 10 % carbowax solution

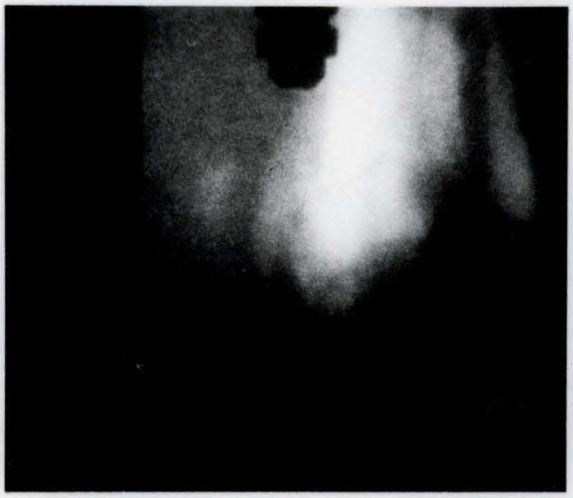

(a) t=31 min.

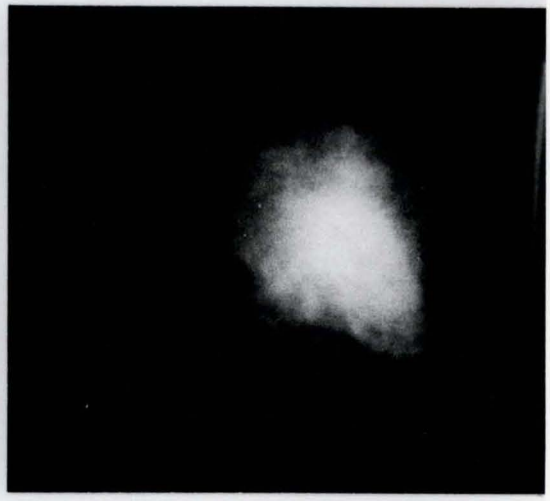

(b) t=53 min.

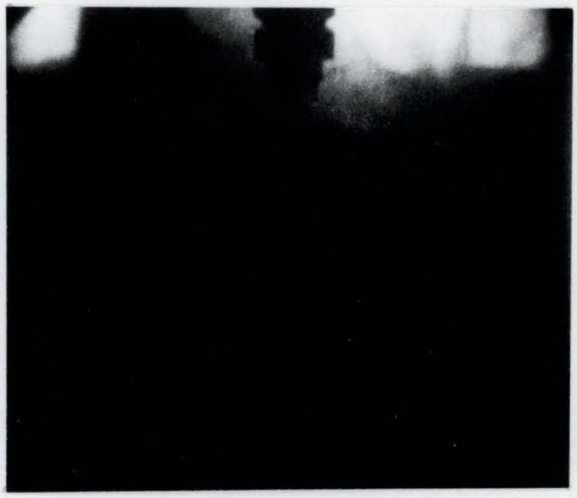

(c) t=120 min.

Scale : 5 cm.

Fig. 7.2 Feed liquid ; 10% benzoic acid solution

was used to analyse the original negatives.

Fig. 7.3 shows a trace of the optical density of the negative (inversely proportional to binder concentration) against bed height for both the alumina / carbowax and alumina / benzoic acid systems after 53 minutes of spraying; the optical density and bed height scales are in arbitrary units. The area under each curve is proportional to the total amount of binder present in the bed, and is therefore a function of time, whereas the shape of the trace is a function of binder distribution. The respective areas (averaged from six or seven frames) for carbowax and benzoic acid are 5·2 and 5·0 at t = 53 minutes (again in arbitrary units, with a value of 9·6 at t = o), thus confirming that the bed contains equal amounts of carbowax or benzoic acid. A uniform binder distribution throughout the bed should result in a constant optical density, and the trace for alumina / benzoic acid is closest to this ideal. Carbowax results in a blocking of the alumina pores and segregation of agglomerated particles, but with benzoic acid as binder the bed remains well-fluidised at t = 53 minutes and beyond. Fig. 7.3 shows that, although the binder concentration at the bottom of the bed appears to be similar in both cases, the carbowax concentration becomes steadily less towards the top of the bed and the concentration of benzoic acid quickly levels out.

7.1.2 X-ray photography at room temperature

Cine film taken of a bed of alumina at room temperature has revealed the mode of entry of atomising air into the fluidised layer and the effect of increased gas velocity on the break-down of agglomerated particles. For the former, the bed was photographed with an atomising air flowrate of $1{\cdot}52 \times 10^{-4}$ $m^3$ $s^{-1}$ (the rate used in all granulation experiments), but with no liquid flow. At the fluidising velocities used for granulation, the pictures were confused because of the high volumetric bubble flow and it was found instructive to study film taken

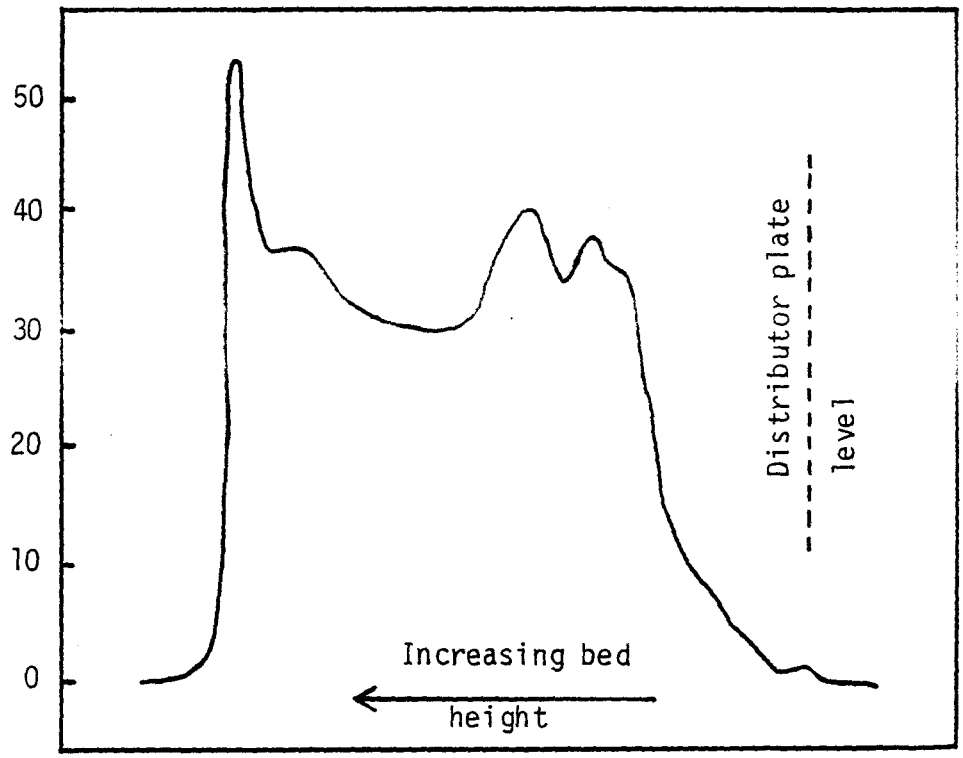


(a) 10% benzoic acid

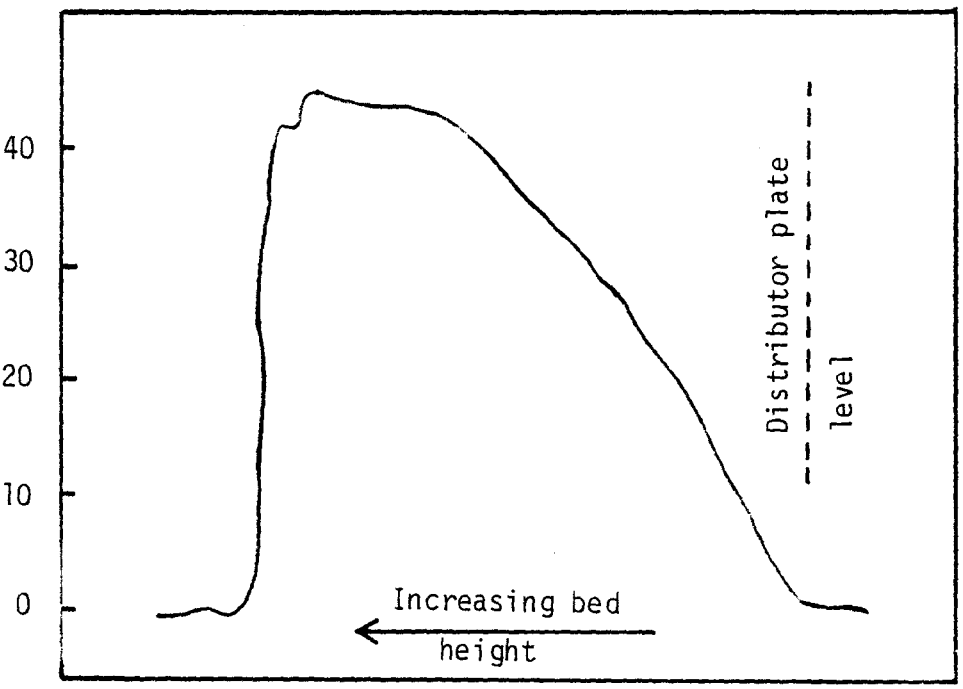


(b) 10% carbowax

Increasing optical density (arbitrary units) - inversely proportional to binder concentration

Fig. 7.3 Change in optical density of X-ray exposed negative film with bed height

with excess velocities below 0·15 $ms^{-1}$. The sequence of photographs in Fig. 7.4 was taken from consecutive frames of 35 mm cine film, with the bed fluidised at a superficial gas velocity of 0·04 $ms^{-1}$ (equivalent to $U / U_{mf} = 0·81$).

It is clear that the atomising air penetrates into the bed and continuously forms discrete bubbles of a classified shape which then rise to the bed surface. Over a length of film, penetration appears to be to a constant depth of about 0·04 m below the nozzle tip. It is difficult to distinguish this periodic bubbling sequence at excess gas velocities greater than 0·07 $ms^{-1}$ by studying 35 mm film frame by frame. However, by projecting 16 mm film at 2 frames per second it becomes discernible occasionally at $U - U_{mf} = 0·15$ $ms^{-1}$. The sequence is only visible for short periods, when bubbles rising from the distributor plate are not present in the region immediately below the nozzle. These conditions are obtained only on very few frames. At higher velocities it was not possible to differentiate between atomising air and fluidising air. The atomising air flowrate employed in these experiments was similar to those used in studies where the existence of a permanent high voidage spray zone was proposed; for example, Lee et al.[44] used a flow of $3·0 \times 10^{-4}$ $m^3$ $s^{-1}$. These observations, that is the lack of a permanent jet, are similar to those of Rowe et al.[94] who reported periodic bubbling from a submerged orifice over a wide range of conditions.

The effect of spraying $3·0 \times 10^{-7}$ $m^3$ $s^{-1}$ (18 ml $min^{-1}$) of 25% barium chloride solution into a fluidised bed at room temperature has been photographed, with an excess gas velocity of 0·15 $ms^{-1}$. At this gas velocity and temperature the exhaust gases are saturated, very little evaporation can take place (see Section 4.4.2) and consequently the bed quenches. The photographs in Fig. 7.5, taken 3 minutes after the start of spraying, show the formation of a clump of wet material on the nozzle tip, which increases in size by the addition of feed liquid and bed

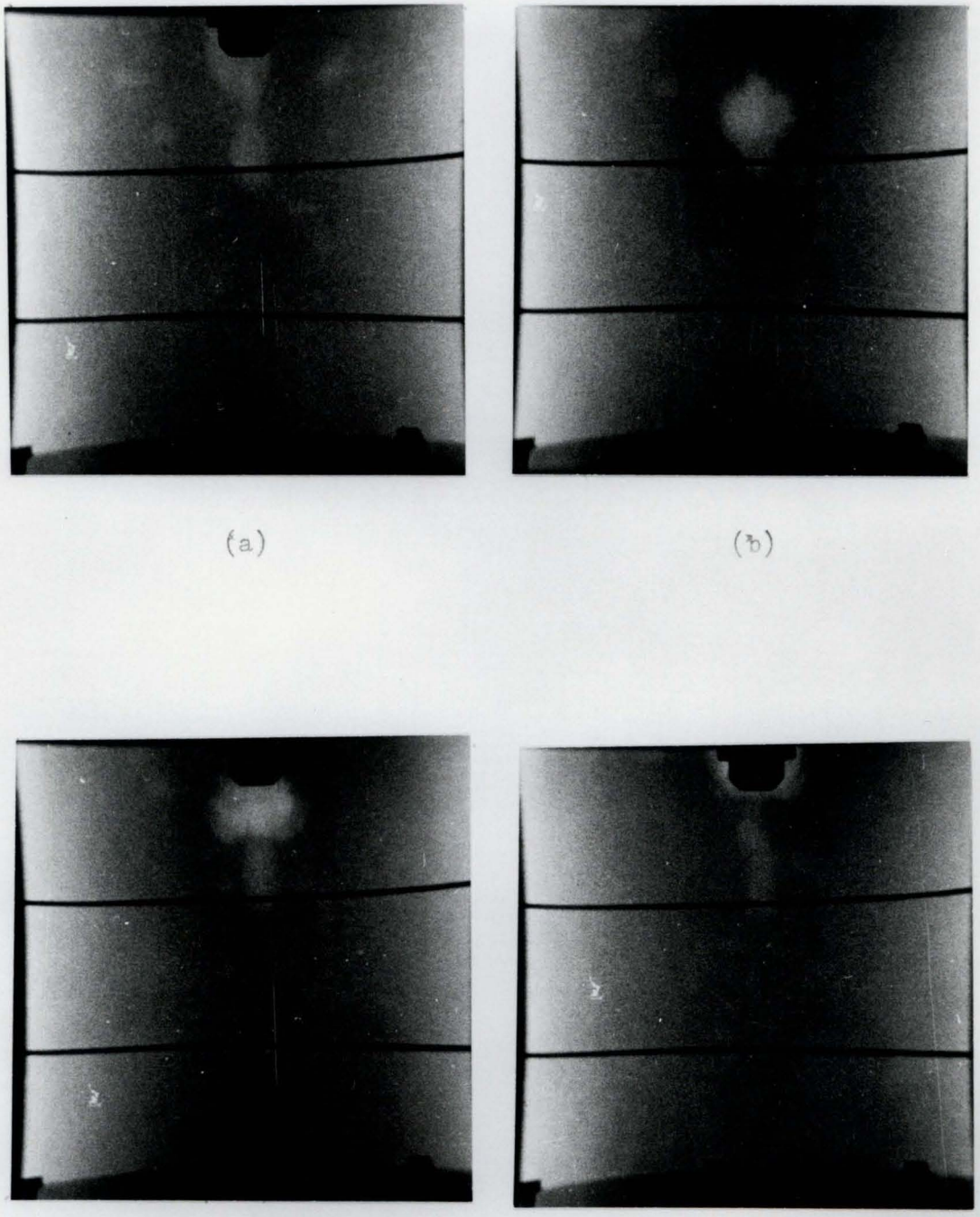

(a) (b)

(c) (d)

Scale : The guide wires are 5 cm. apart

Fig. 7.4 Mode of entry of atomising air

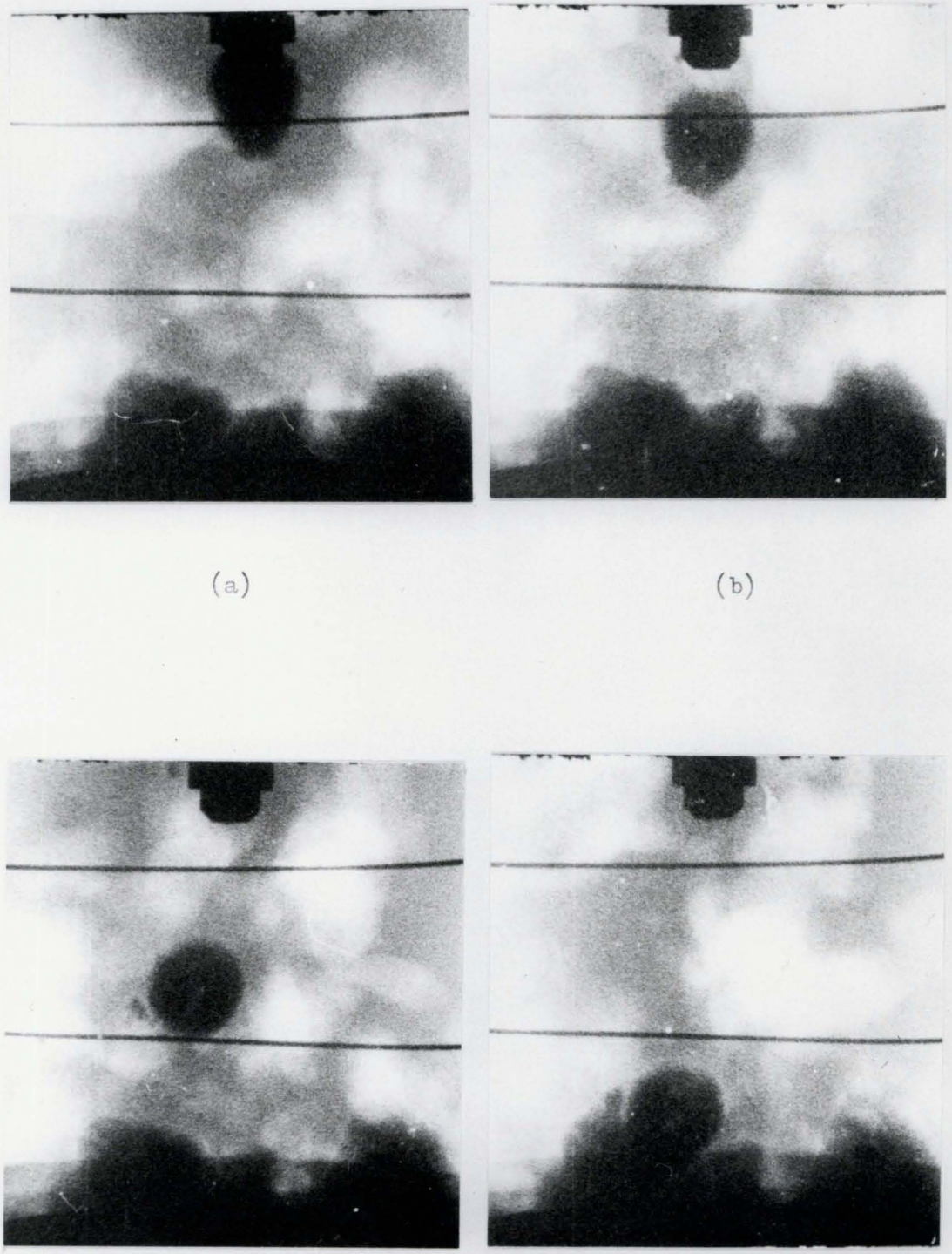

(a) (b)

(c) (d)

Scale : The guide wires are 5 cm. apart

Fig. 7.5 Formation of nozzle cake and segregation of agglomerated bed material

particles until it is detached and falls to the bottom of the bed. Thus, segregation takes place leading to the formation of a defluidised layer and bed quenching. The layer of segregated agglomerates is clearly visible and appears as a dark region at the bottom of the bed in Fig. 7.5. In this case wet quenching has been induced because little or no evaporation is able to take place, although the effect would be similar if suitable conditions (such as binder concentration and gas velocity) were chosen in a bed for which the heat and mass balances (see Section 2.2) were satisfied. The initial particle - particle agglomeration, which precedes bed quenching, takes place in the region immediately below the spray nozzle but the resultant agglomerated mass need not form around the nozzle, although small clumps can be seen attached to the nozzle in bona fide granulation experiments (Fig. 7.1).

An increase in excess gas velocity to 0·04 $ms^{-1}$, after a total of 7 minutes spraying, instantly resulted in the break-up of the clumps of material sitting on the distributor plate as they become subjected to increased buffeting and abrasion. In Fig. 7.6 (photographs taken at t = 7·5 minutes), smaller lumps of material can be seen to break away and to circulate within the bed. Cine film (from which these prints were taken) clearly shows this effect, and also the increase in dense phase opacity due to the more even distribution of the feed, which is in turn brought about by the increase in $U - U_{mf}$. Because of the short time interval over which these observations were made, the contribution of the greater quantity of barium chloride present in the bed at t = 7·5 minutes to the radiopacity of the bulk of the bed is small.

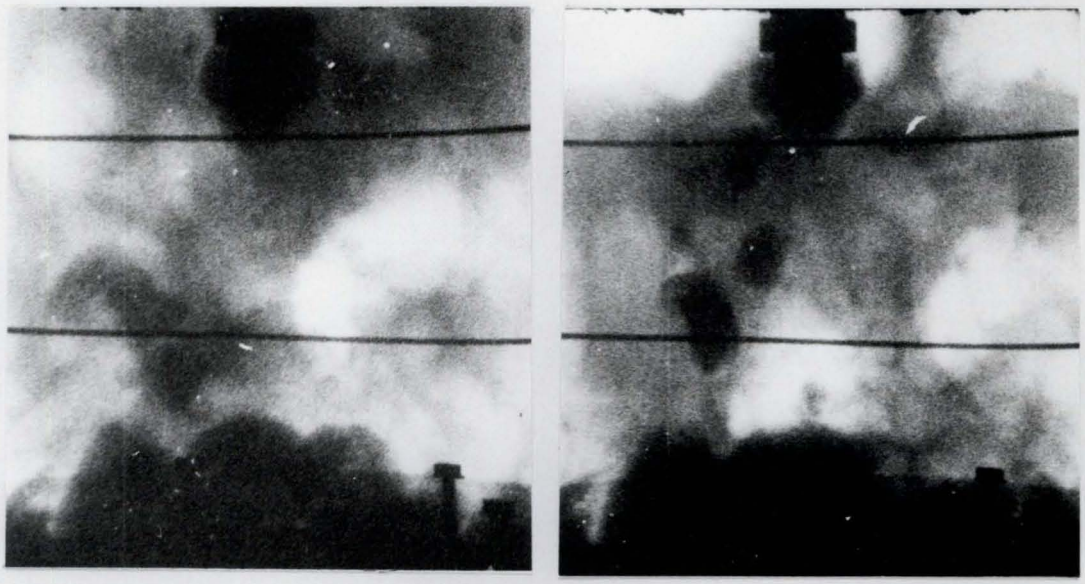

(a) (b)

(c)

Scale : The guide wires are 5 cm. apart

Fig. 7.6 The break-up of agglomerated material at high gas velocity

## 7.2 TEMPERATURE PROFILES

### 7.2.1 Introduction

A fluidised bed is normally characterised by the absence of temperature gradients, because of the inherent rate of particle mixing.[2] However, in this work temperature gradients have been recorded when segregation takes place (resulting in a loss of particle mixing and therefore a decrease in the rate of heat transfer, see Section 6.4.1) and also in a stable granulating bed, in the region immediately below the spray nozzle. The literature contains two reports of temperature measurement in the spray region, both of which propose the existence of a particle-free gas jet in which the feed liquid is atomised.

Sokolovskii et al.[103] concluded that liquid, injected into a fluidised bed from below, was non-uniformly distributed on atomisation and that the maximum density offeed was in an annulus between 0·01 m and 0·02 m from the jet axis (c.f. temperature profile diagrams, Section 7.2.2). A rapid decrease in jet temperature, away from the nozzle, was noted. Shakhova and Minaev,[104] employing side spraying, have measured temperatures in the jet lower than those in the bulk of the bed and which are constant with time. They found that the temperature, measured with a bare wire thermocouple, dropped rapidly along the jet axis away from the nozzle, to a minimum, and then increased assymptotically to the bed temperature. There was also a radial temperature increase across the jet. They surmised that the most intense evaporation of liquid occurred close to the nozzle, due to the sudden reduction in pressure.

In this work, from the steady-state temperature measurements, isotherms have been constructed to give a picture of temperature variation throughout the plane of a bed diameter. The data have been presented as lines of equal temperature difference from a nominal bed temperature. This was necessary for comparative purposes because it was not found

possible to keep the nominal bed temperature exactly the same for experiments with different liquid feedrates. In Section 6.4.2 the effects of increasing binder feedrate (precipitating essentially dry quenching) were described, whereas the experiments here mainly investigate the effect of increased feedrates of binder-free solvent. The results confirm qualitatively the work previously reported, and also relate directly to the granulation experiments of Chapter Six. The fluidised bed temperature profiles constitute evidence for the existence of a region in which evaporation takes place and where, when a binder is dissolved in the feed liquid, agglomeration of the bed particles occurs. The effects of the main fluidised bed granulation parameters on the evaporative pattern have been investigated.

7.2.2 Description of temperature profiles

Fig. 7.7 shows the isotherms obtained when pure methanol was fed at $2{\cdot}10 \times 10^{-4}$ kg $s^{-1}$ (16 ml $min^{-1}$) into a bed of glass powder, fluidised at an excess velocity of $0{\cdot}525$ $ms^{-1}$. This was the usual feedrate employed in granulation experiments and one of the higher gas rates. The two-dimensional shapes are assumed to be bodies of revolution about the bed axis and therefore to represent three-dimensional zones in the bed; a reasonable assumption since temperatures were measured in two separate planes (see Section 5.5.2). Thus, an irregularly shaped low temperature zone, about 0·01 m in diameter and some $15^{o}$ C below the nominal bed temperature ($T_B$), exists in the centre of the bed and extends from close to the nozzle to about 0·07 m above the distributor plate. The temperature rises steeply away from this zone (of the order of $24^{o}$ C in 0·01 m) with the shape of the isotherm remaining constant, i.e. the different temperature zones are concentric. A large, almost disc-shaped region, $2^{o}$ C below the nominal temperature, exists at the bottom of the bed and extends over most of the bed diameter. However, vertical variations in temperature close to the bed wall are not very great, and this explains why large temperature gradients were not recorded during

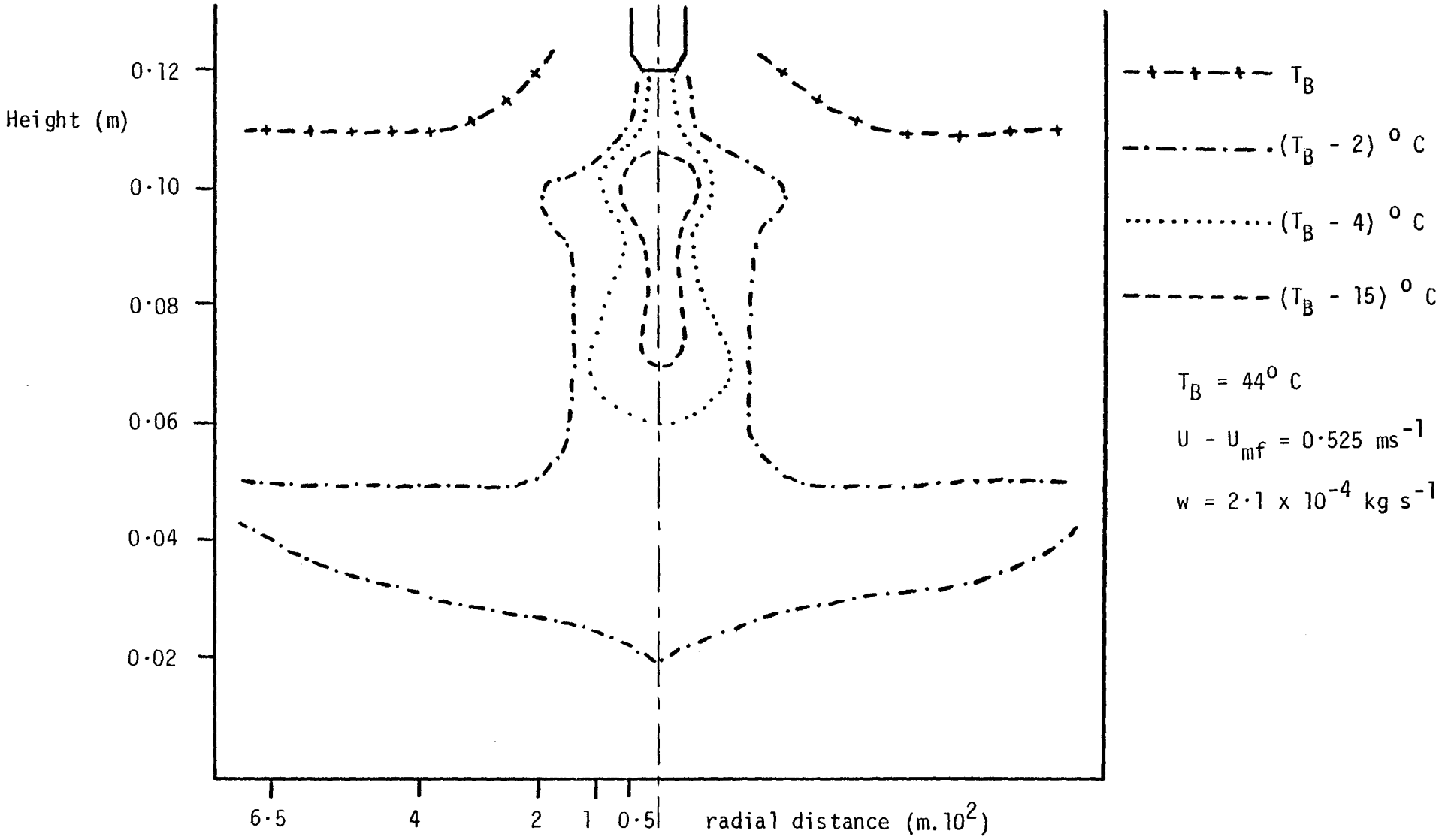


Fig. 7.7 Temperature profile in a diametrical plane of a bed of fluidised glass powder particles

the stable granulation experiments (Chapter Six) in which bed temperature was always measured close to the wall. The data of Fig. 7.7 have been re-plotted in Figs. 7.8 and 7.9, from which it can be seen that temperature decreases quickly to a minimum a short distance away from the nozzle and radially towards the centre of the bed. These latter findings give qualitative support to the literature.[103,104]

Experiments in which carbowax solutions, 1% and 10% respectively, were sprayed into beds of glass powder fluidised at $U - U_{mf} = 0{\cdot}525\ ms^{-1}$, were repeated in this equipment in order to measure a few selected temperatures on the bed axis. Using a 1% solution (with which the bed can be operated under stable agglomerating conditions, see Section 6.4.2) the temperature profile remained as in Fig. 7.7, throughout the 260 minutes of the experiment. Using a 10% solution, bed quenching occurred and the temperature at points 0.02 m and 0.03 m above the distributor increased and approached that of the inlet air, as before. However, from temperature measurements across the bed diameter (at a height of 0·07 m above the distributor plate), it was found that the low temperature zone also remained. Thus, liquid was still evaporated in the zone defined by Fig. 7.7 and dry agglomerates and clumps segregated, causing dry quenching rather than wet quenching.

The low temperature region was found to increase in size with liquid feedrate; the volumes of the zones enclosed by the $(T_B - 2)\ ^{o}C$ and $(T_B - 4)\ ^{o}C$ isotherms were larger and, although the $(T_B - 15)\ ^{o}C$ isotherm varied in shape and size, the extent of temperatures (say) $10^{o}$ C below the nominal bed temperature was increased at higher feedrates (Figs. 7.10 and 7.11). At a feedrate of $6{\cdot}38 \times 10^{-4}\ kg\ s^{-1}$ ($48{\cdot}5\ ml\ min^{-1}$), the highest investigated at this fluidising velocity, the $(T_B - 4)\ ^{o}C$ isotherm extends to the bottom of the bed and a temperature difference of about $5^{o}$ C exists over the bed depth, from the nozzle to the distributor plate (Fig. 7.11). These temperatures were steady over a 60

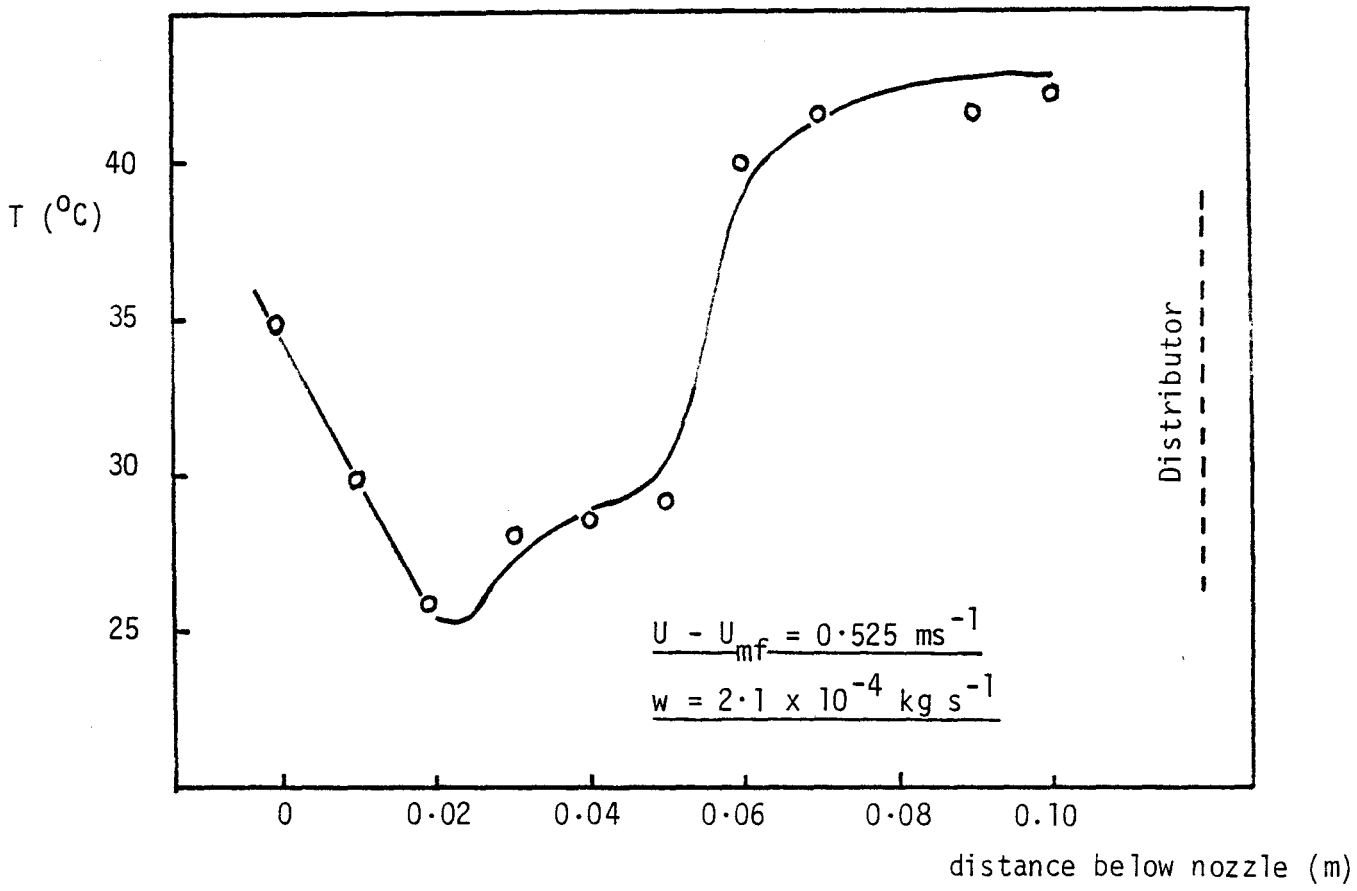


Fig. 7.8 Variation of bed temperature along the bed axis

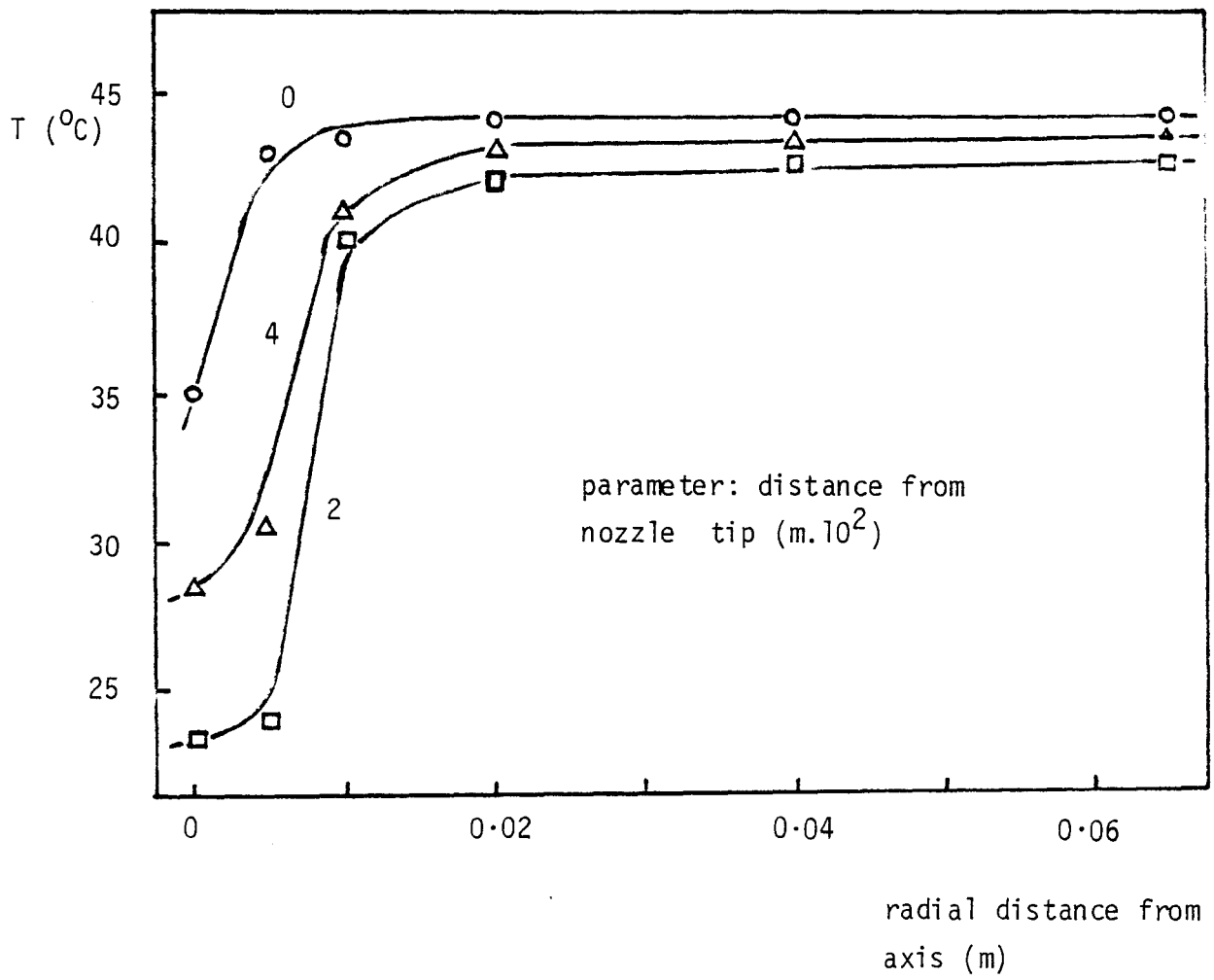


Fig. 7.9 Radial variation of bed temperature

minute period and suggest the presence of free liquid towards the bottom of the bed and therefore that some form of wet quenching has taken place.

A similar pattern of volume increase of the low temperature zones with methanol feedrate was observed at a lower excess gas velocity of 0·15 $ms^{-1}$; the zones also tended to be larger, for a given feedrate, at this velocity (Figs. 7.12 to 7.14). Again, nozzle-to-distributor temperature gradients increased with feedrate.

When alumina is used as the bed material, the wide variations in bed temperature observed with glass powder are absent (Fig. 7.15). A much smaller low-temperature region exists, again along the bed axis and of a similar shape. The size of the zone increases with feedrate (Fig. 7.16), but the bed temperature is still more uniform than with glass powder (c.f. Fig. 7.11). Intra-particle porosity is again responsible for the differences in behaviour between alumina and glass powder; the pores allow liquid to be distributed more evenly around the bed and therefore evaporation is able to occur over a wider area.

### 7.2.3 Heat and mass transfer coefficients

The size of the zone in which the evaporation of solvent takes place can be assumed from the temperature profiles illustrated in the previous section. This, in turn, allows an estimate to be made of the area over which heat and mass transfer occurs, and thus the transfer coefficients can be calculated. The zone may be approximated by a cylinder, the dimensions of which are chosen to include the major part of the bed volume which is at a temperature of $(T_B - 2)\ ^{o}C$. The number of particles within this zone is assumed to be in proportion to the volume of the zone. Table 7.1 gives the zone size (for glass powder) and the total particle surface area available for heat or mass transfer. Details of these and all other calculations are given in Appendix D.

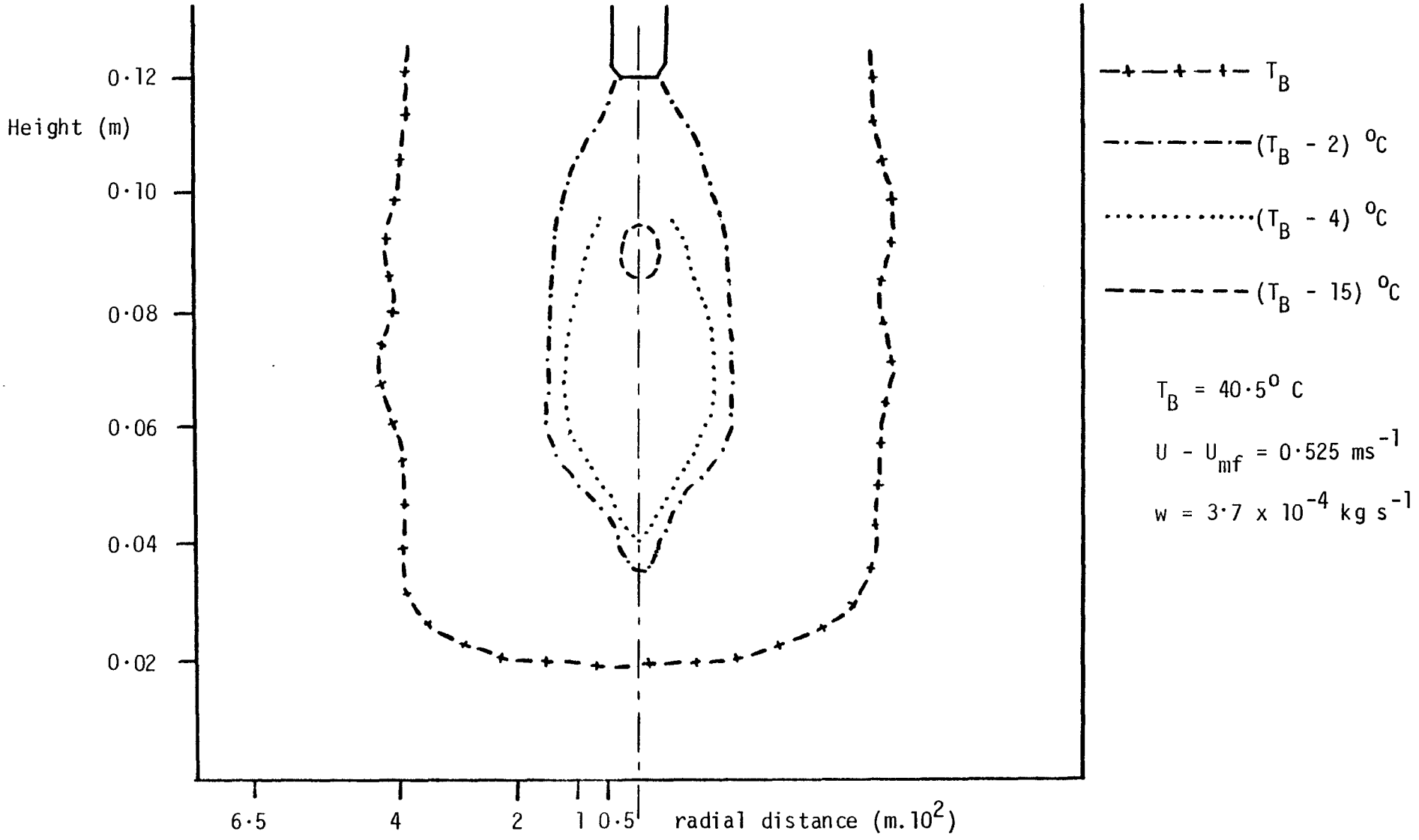


Fig. 7.10 Temperature profile in a diametrical plane of a bed of fluidised glass powder particles

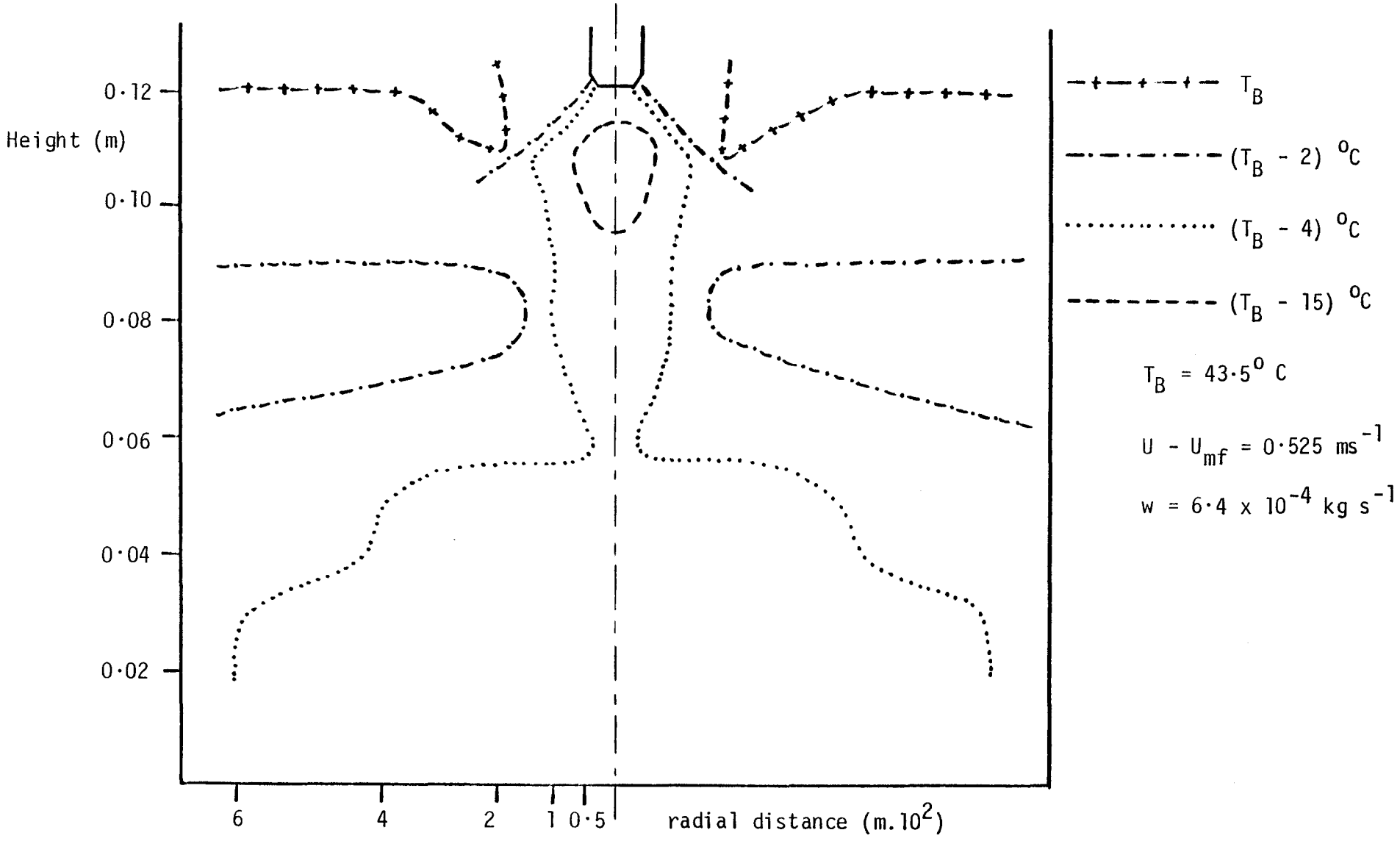


Fig. 7.11 Temperature profile in a diametrical plane of a bed of fluidised glass powder particles

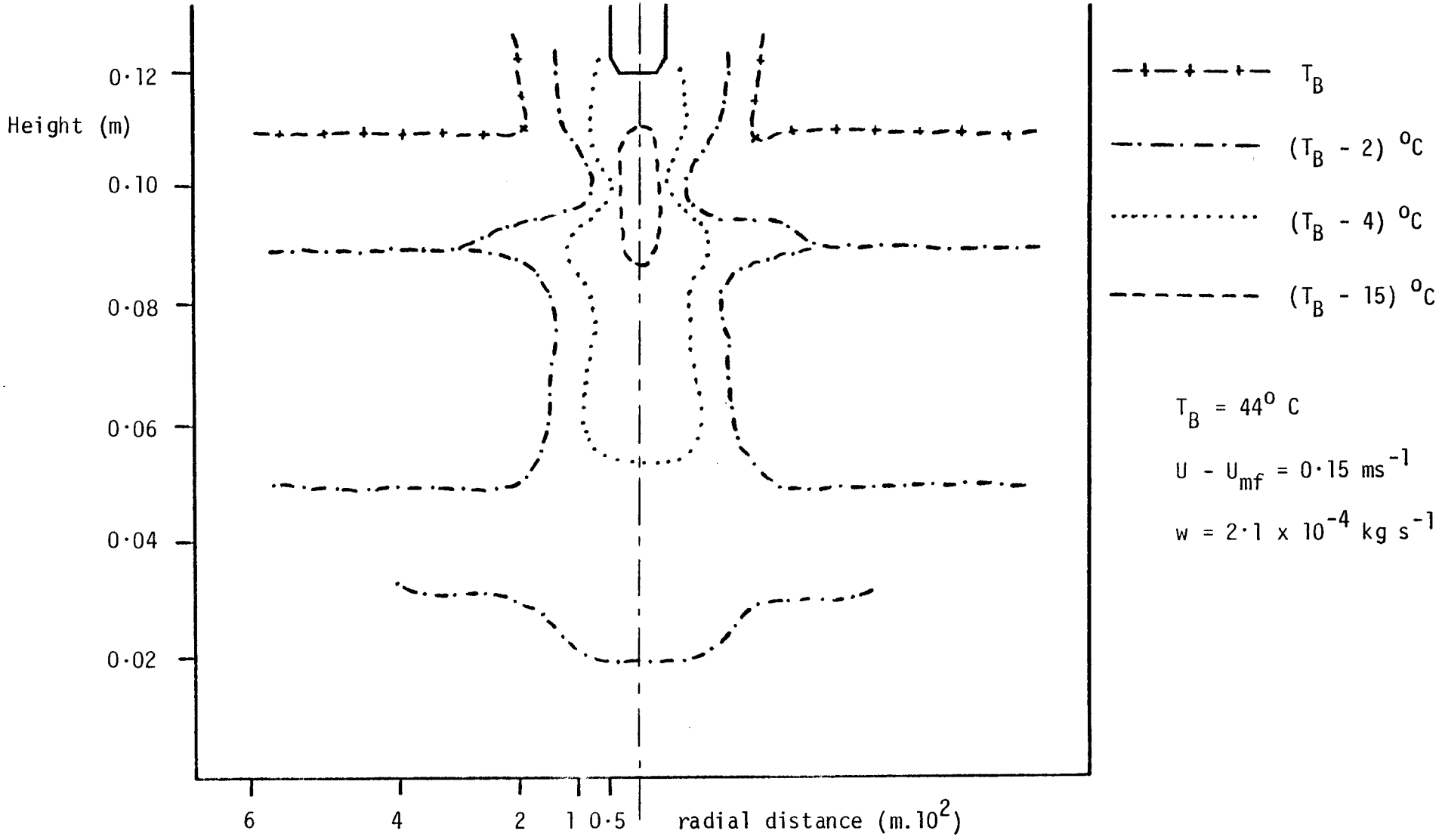


Fig. 7.12 Temperature profile in a diametrical plane of a bed of fluidised glass powder particles

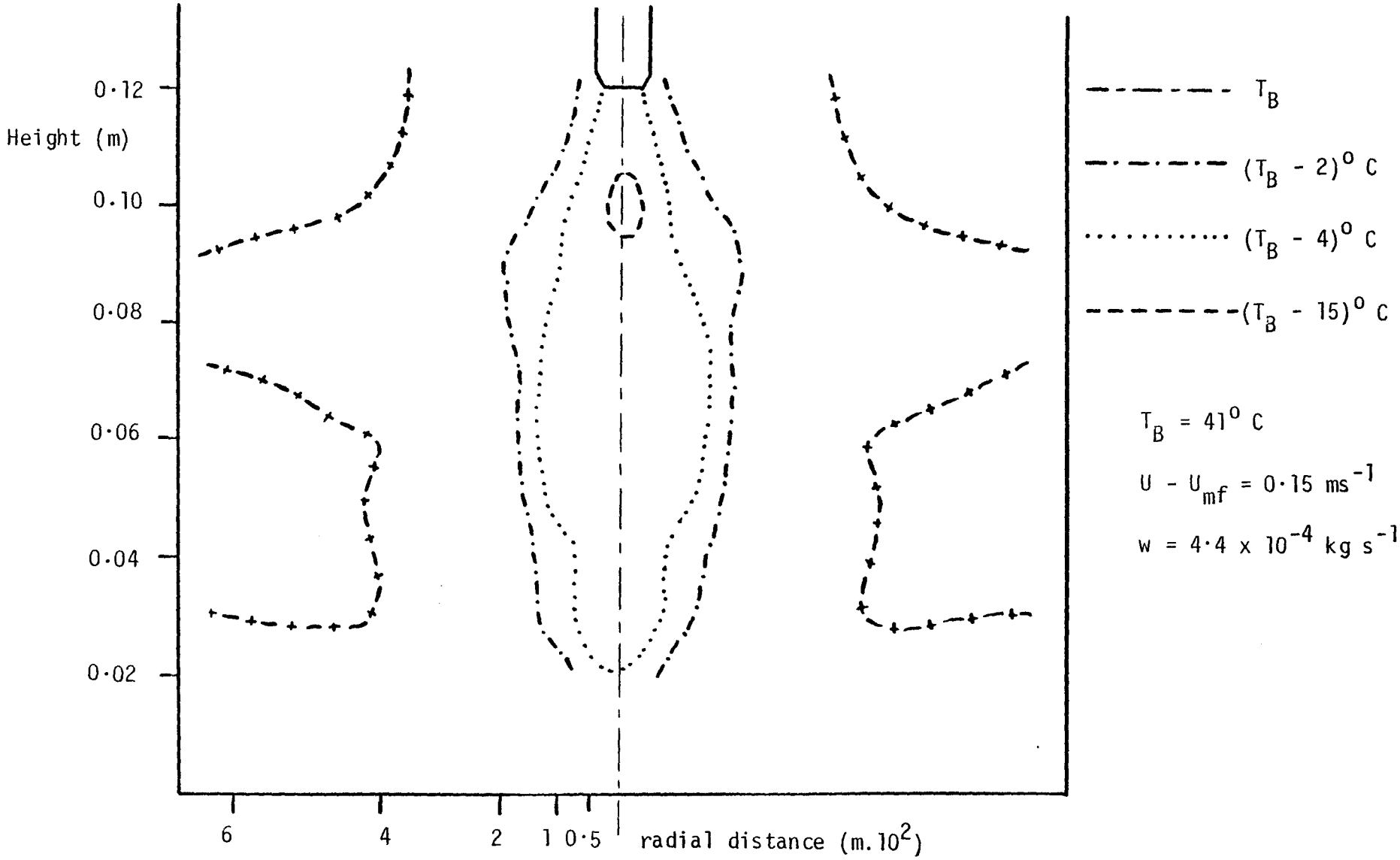


Fig. 7.13 Temperature profile in a diametrical plane of a bed of fluidised glass powder particles

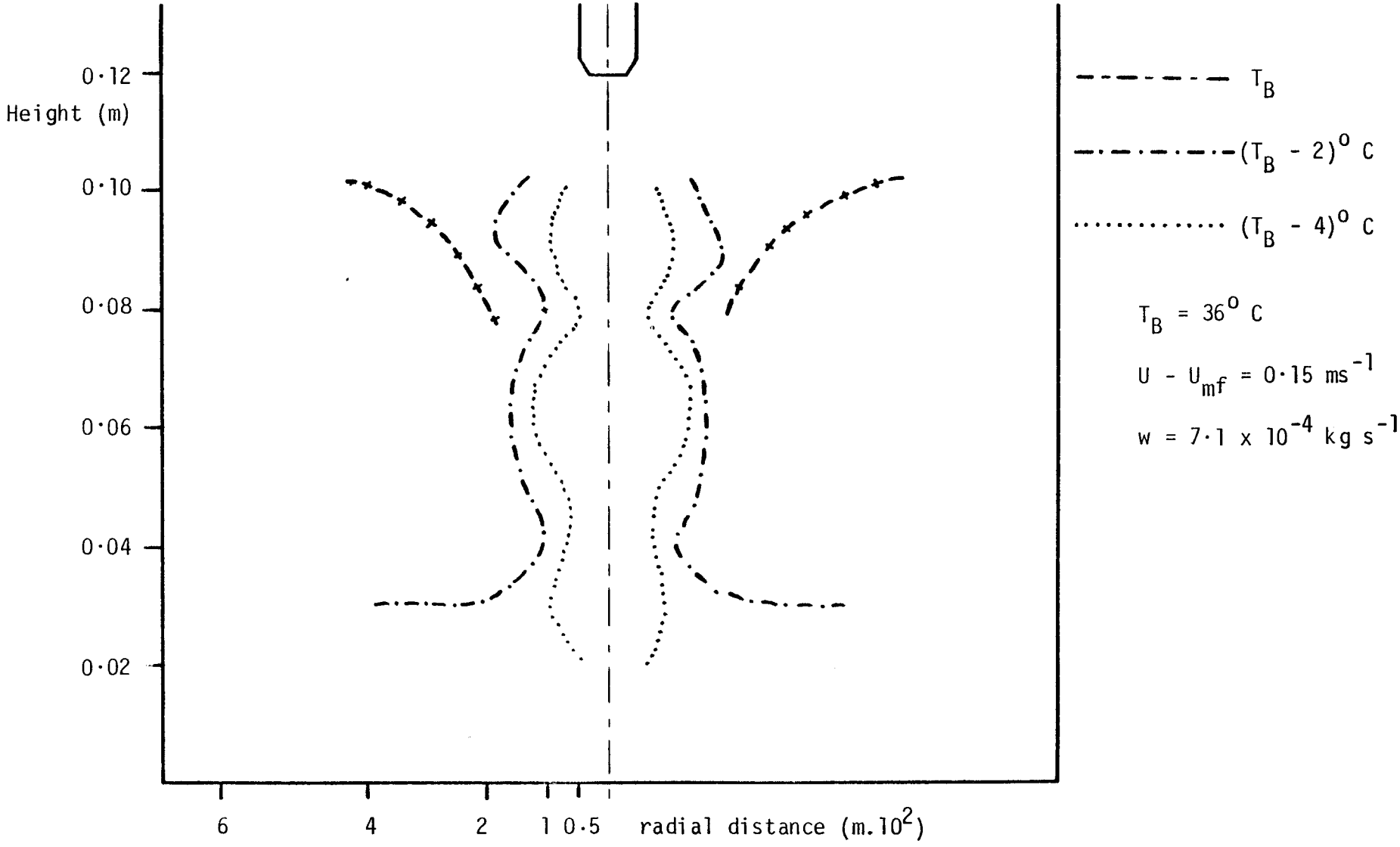


Fig. 7.14 Temperature profile in a diametrical plane of a bed of fluidised glass powder particles

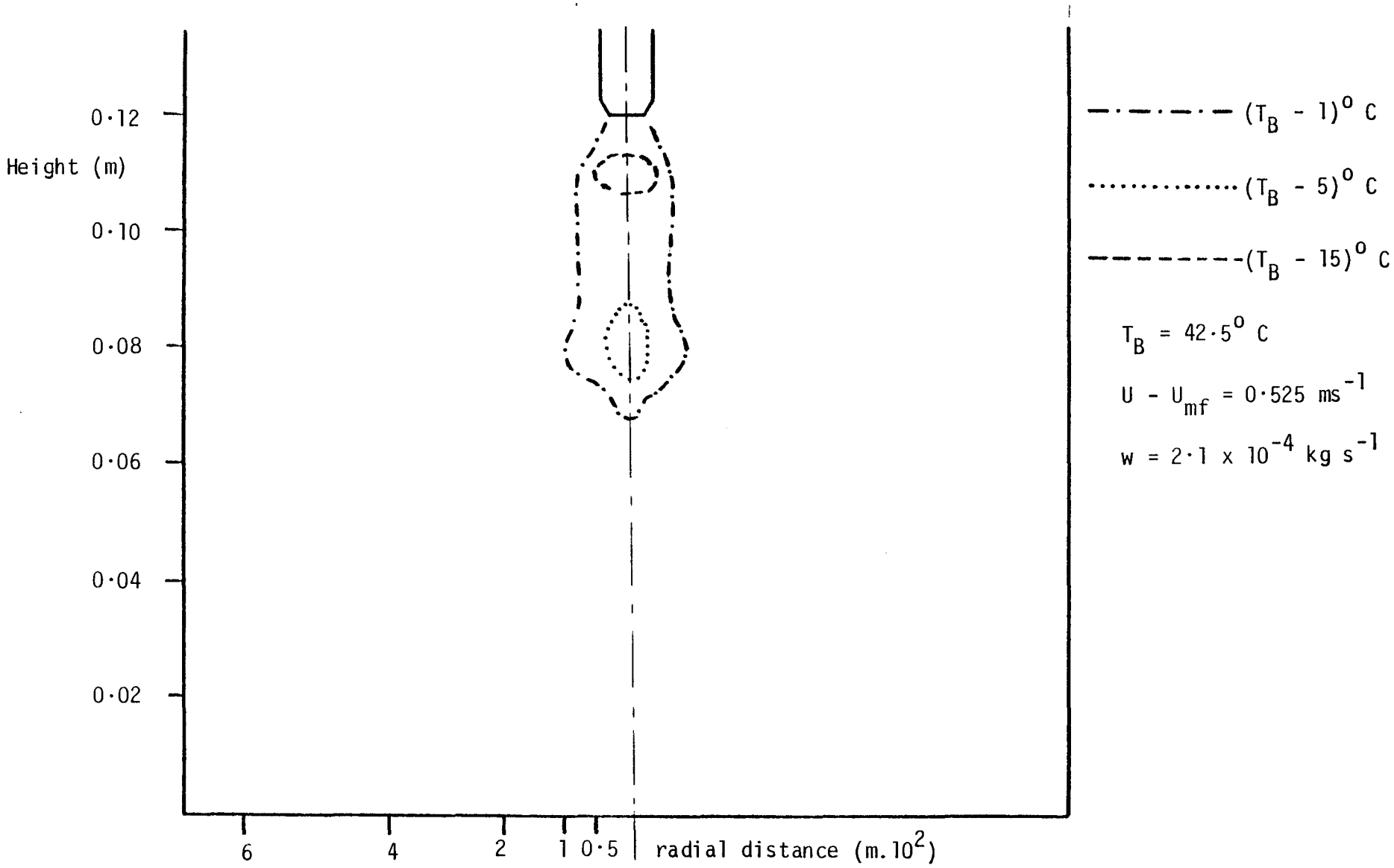


Fig. 7.15 Temperature profile in a diametrical plane of a bed of fluidised alumina particles

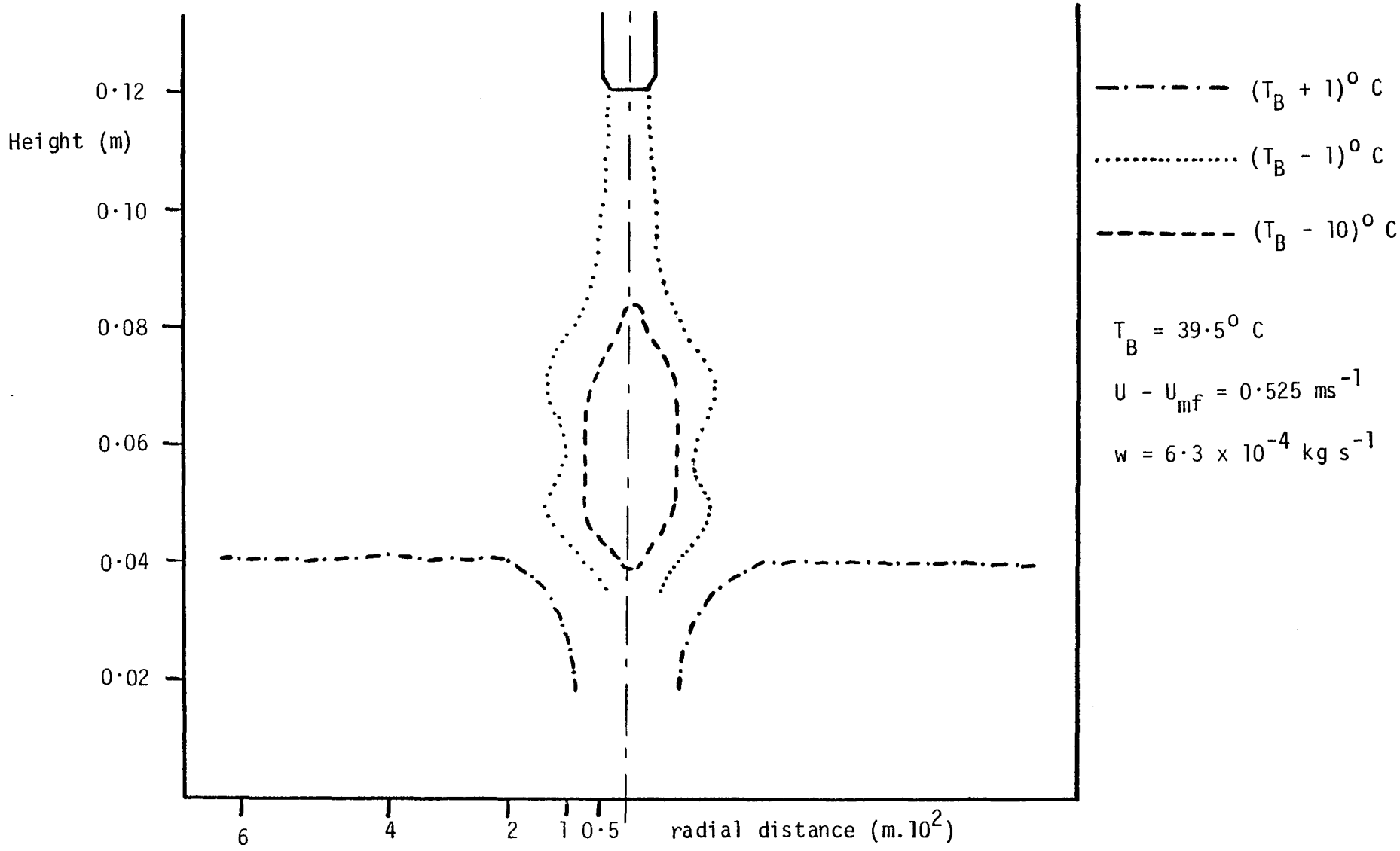


Fig. 7.16 Temperature profile in a diametrical plane of a bed of fluidised alumina particles

Table 7.1 Zone dimensions and particle surface area available for heat or mass transfer

| methanol feedrate (kg $s^{-1}$) | $U - U_{mf}$ ($ms^{-1}$) | height of zone, $H_z$ (m) | diameter of zone, $D_z$ (m) | surface area, $A_z$ ($m^2$) | Ref |
|---|---|---|---|---|---|
| $2{\cdot}1 \times 10^{-4}$ | 0·525 | 0·060 | 0·030 | 0·464 | Fig. 7.7 |
| $6{\cdot}4 \times 10^{-4}$ | 0·525 | 0·060 | 0·030 | 0·464 | Fig. 7.11 |
| $2{\cdot}1 \times 10^{-4}$ | 0·15 | 0·065 | 0·030 | 0·502 | Fig. 7.12 |
| $7{\cdot}1 \times 10^{-4}$ | 0·15 | 0·150 | 0·030 | 1·160 | Fig. 7.14 |

The heat transfer coefficient for heat transfer between particles and fluid, h, is given by:

$$q = h A_z \Delta T \qquad (7.1)$$

where q, the rate of heat transfer, is given by the product of the evaporation rate and the latent heat of vaporisation of methanol at $T_B$. The driving force for heat transfer, $\Delta T$, is provided by the difference in temperature between bed particles ($T_B$), which for the purposes of the calculation are assumed to circulate through the zone, and the average zone temperature, $T_z$. Table 7.2 lists the resultant coefficients, together with those quoted by Richardson and Ayers[105] for similar sized particles.

Table 7.2 Heat transfer coefficients

| methanol feedrate (kg $s^{-1}$) | $U - U_{mf}$ ($ms^{-1}$) | h ($Wm^{-2} K^{-1}$) experiment | h ($Wm^{-2} K^{-1}$) correlation[105] |
|---|---|---|---|
| $2{\cdot}1 \times 10^{-4}$ | 0·525 | 64·5 | 90·0 |
| $6{\cdot}4 \times 10^{-4}$ | 0·525 | 216·9 | 90·0 |
| $2{\cdot}1 \times 10^{-4}$ | 0·15 | 56·8 | 28·0 |
| $7{\cdot}1 \times 10^{-4}$ | 0·15 | 134·2 | 28·0 |

Similarly, a particle to fluid mass transfer coefficient, k, may be defined:

$$w_m = k A_z \Delta c \qquad (7.2)$$

$w_m$, the rate of mass transfer, is equal to the volumetric evaporation rate of methanol vapour. The driving force ($\Delta c$) is the difference between the mole fraction of methanol in the air / methanol mixture at the liquid interface and in the zone as a whole. Plug flow is assumed and the log mean concentration difference is used.

Table 7.3 Mass transfer coefficients

| methanol feedrate ($kg\ s^{-1}$) | $U - U_{mf}$ ($ms^{-1}$) | $k$ ($ms^{-1}$) experiment | $k$ ($ms^{-1}$) correlation[106] |
|---|---|---|---|
| $2{\cdot}1 \times 10^{-4}$ | 0·525 | $1{\cdot}39 \times 10^{-3}$ | $1{\cdot}35 \times 10^{-4}$ |
| $6{\cdot}4 \times 10^{-4}$ | 0·525 | $9{\cdot}26 \times 10^{-3}$ | $1{\cdot}35 \times 10^{-4}$ |
| $2{\cdot}1 \times 10^{-4}$ | 0·15 | $2{\cdot}35 \times 10^{-3}$ | $8{\cdot}1 \times 10^{-3}$ |
| $7{\cdot}1 \times 10^{-4}$ | 0·15 | * | $8{\cdot}1 \times 10^{-3}$ |

* Calculated $\Delta c$ is negative, i.e. possible wet quenching.

These calculations, despite the simple assumptions, offer an explanation as to why the apparent size of the evaporative zone should vary wtih the fluidised bed granulation parameters. For the case of low methanol feedrate and high excess fluidising velocity ($2{\cdot}1 \times 10^{-4}$ kg $s^{-1}$, $U - U_{mf} = 0{\cdot}525$ $ms^{-1}$) the calculated heat transfer coefficient is close to that proposed by Richardson and Ayers,[105] which is typical of the values quoted in the literature.[107] An increase in the feedrate to $6{\cdot}4 \times 10^{-4}$ kg $s^{-1}$ requires a coefficient which is considerably greater. In other words, the assumed heat transfer area is too small and evaporation must take place outside the zone defined in Table 7.1. Thus, as is clear in Fig. 7.11, the low-temperature region extends beyond the vicinity of the spray nozzle, as far as the distributor. A similar conclusion may be drawn from the calculated coefficients at $U - U_{mf} = 0{\cdot}15$ $ms^{-1}$.

The experimentally determined mass transfer coefficients are always less than the values from the correlation of Kettenring et al.[106]

(again typical literature values[107]), suggesting that mass transfer takes place well within the defined zone. However, at high feedrate and low excess gas velocity the calculated concentration driving force is negative and therefore, as for heat transfer, the effective zone must be larger in order to provide sufficient surface area for mass transfer to take place.

# CHAPTER EIGHT

# A PROPOSED PARTICLE GROWTH MECHANISM

The initial stages of agglomeration, which is a desirable growth mechanism, and of bed quenching, which is disastrous for granulation and is to be avoided, are exactly the same. This is well substantiated and supported by evidence in the literature. What will be proposed here is that all modes of growth, and bed quenching, have the same initial stage; i.e. the formulation of liquid bonds between adjacent particles in the fluidised bed. When solvent is evaporated from the feed solution, liquid bonds will give rise to solid bridges between those same adjacent particles, unless there is a redistribution of binder either before or after the solution dries. Whether this redistribution takes place by a breaking of either liquid bonds or solid bridges, will depend on the balance between the two elements of fluidised bed granulation that were identified in Chapter Three.

The distribution of the feed liquid and of binder throughout the bed and on the surface of individual particles will depend upon the structure of the bed particles and the viscosity of the feed solution. The binder solutions used in this study have similar viscosities over the range of feed concentrations, and therefore any effect of viscosity on atomisation of the feed is eliminated. However, carbowax solution increases rapidly in viscosity as methanol is evaporated and the concentration of binder increases. Therefore carbowax is less likely to be able to flow around a bed particle and cover the surface area, consequently layered particle growth, or the formation of "onion-rings", is much less probable. Benzoic acid solution, the viscosity of which remains more or less constant with concentration, is able to spread around a particle far more before the solution dries and forms a solid crust. The intensity of particle - particle contacts makes it extremely unlikely that significant coverage of the surface will occur, but benzoic acid should be more capable than carbowax of forming more of a growth layer.

The existence of intra-particle porosity in the bed allows liquid to be evaporated over a larger proportion of the bed than is possible when

non-porous particles are used. Consequently, temperature gradients are far less pronounced and there is a reduced possibility of wet quenching, with generally more stable operation. The viscosity of the feed solution is an important factor in determining the behaviour of porous bed particles. Liquids have a resistance to flow which is measured by their viscosity and, just as carbowax solution has an increased resistance to flow around a bed particle, so it is less likely than benzoic acid to flow into the intra-particle pores of alumina. A two-fold increase in benzoic acid concentration reduces the no-growth period by half because a given amount of binder (required for pore blockage) is being deposited in the same pore volume, but at twice the rate. However, when the carbowax concentration is doubled the no-growth period is considerably shorter because, with an increased viscosity, the time taken for solution to enter the pores is much greater and it dries before significant penetration is achieved. The pores become blocked more quickly, with a smaller fraction of the pore volume filled, and liquid bonds begin to form on the exterior particle surface far earlier than is the case with benzoic acid. Beyond the transition point alumina behaves very much like glass powder.

When the fluidised bed consists of non-porous particles, solvent in the feed liquid is evaporated in a well-defined zone, close to the spray nozzle, and from the surface of the bed particles with which it inevitably comes into contact. No permanent gas jet or void exists in this region; particle motion is not well-ordered and no regular coating of particles with feed solution takes place. The random and intense contact between particles and liquid results in agglomeration. Even if the mass and heat balances for the bed as a whole have been satisfied, that is if sufficient heat has been supplied to evaporate liquid at the feedrate and the exhaust gases are not saturated, localised wet quenching may still occur in this zone. Localised dry quenching may also occur. In this case, as the agglomerated mass which is produced begins to move away

from the zone where liquid first contacts the bed particles, drying of the solution takes place. If the dry mass is not broken down and reduced to smaller packets of agglomerated particles, it will segregate as an effectively very large particle and sink to the bottom of the bed. Dry quenching rather than wet quenching has been observed in the granulation experiments in this work, evidenced by the rise in temperature at the bottom of the bed when a segregated layer is formed. The deposition of larger amounts of solute from the same volume of feed solution results in a bridge between two particles of greater strength; bond strength being proportional to the product of intrinsic binder strength and the quantity of binder present. Thus, a high mass flowrate of binder (and therefore a high solution concentration) will dominate the fluidisation / granulation balance and intensify the quenching problem, as the aggregated mass is less able to break down.

The extent to which clumps of agglomerated particles remain intact determines the outcome of the fluidised bed granulation process; it governs the type and size of the granular material which is produced. Bed quenching results if insufficient break-down takes place; and break-down into smaller agglomerates, to an equilibrium size, will give a product of agglomerated granules. Further reduction and tearing apart of smaller agglomerates ultimately produces a single bed particle with associated binder, in other words a layered or "onion-ring" granule.

What determines the extent of this process? For a given fluidising gas velocity and a given initial bed particle size, i.e. keeping the fluidisation element constant, the relative dominance of the granulation element over fluidisation will be a function of bond strength, and of intrinsic bond strength if the binder concentration is constant. The stronger the solid matter between particles (either pairs of particles or particles in a large mass) the less will be the break-down of that agglomerate. Therefore, the intrinsic bond strength of carbowax or

benzoic acid is crucial. Carbowax bonds between glass powder particles are far stronger than those composed of benzoic acid and thus using carbowax as binder tends to produce agglomerates, whereas benzoic acid tends to give rise to layered granules. Benzoic acid bonds are weak and therefore are torn apart more easily than carbowax bonds, by fluid drag on the bed particles and by abrasion in the fluidised layer. When such bonds are broken the binder will be either left behind attached to the surface of one or both of the particles which it bound together, or partially or completely removed so as to form new separate particles or nuclei; no evidence to support the latter has been found. As agglomerates break down to single particles, the attached binder causes an increase in size of the initial particles. Constant repetition of this process, the re-agglomeration of particles with fresh feed liquid followed by break-down (before or after complete drying has taken place) produces a growth layer. The absence of any evidence of concentric growth rings, or of spherical product granules, strongly suggests that growth has not occurred by the traditionally proposed mechanism of regular and uniform coating with successive layers of feed material. The appearance of the layered granules (Figs. 6.2 and 6.3), due to the matt, uneven surface of the benzoic acid coating, is consistent with the random deposition of binder which would result from continual formation, breakage and re-formation of liquid bonds and solid bridges, on the particle surface. Subsequent redissolution of binder and particle attrition will produce a less angular product.

The use of carbowax, except under extreme conditions, results in agglomeration or in quenching of the bed, although the particle growth rate varies with the operating parameters. Benzoic acid, which gives layered granules at high gas velocities and with larger initial particles, can also give rise to agglomeration and bed quenching. For a particular binder, the mode of particle growth, and the growth rate, will depend

upon the fluidisation parameters: gas velocity and particle size. The experimentally determined dependence of growth on these two parameters supports the foregoing hypothesis of a particle growth mechanism. Increasing the excess gas velocity causes a reduction in size of granules formed from glass powder and carbowax; the glass powder / benzoic acid system moves from bed quenching through agglomeration to layered growth as gas velocity is increased. The fluidising gas velocity contributes to two effects. Firstly, particle circulation increases at higher excess gas velocity and, as it is increased in relation to the solution feed-rate, the amount of feed associated with each particle decreases. Bed quenching therefore becomes less probable, allowing higher feedrates than at lower gas velocities. Secondly, once inter-particle bonds or bridges have formed they will be broken down more easily at higher velocities, because of increased fluid drag and increased abrasion of granules due to the greater number of particle - particle impacts occurring.

When larger initial particles are used, the mean diameter of glass powder / carbowax granules decreases and with benzoic acid it is possible to achieve layered growth under conditions which would otherwise lead to quenching. The average diameter ratio of the two sizes of glass powder used in these experiments was 1·6, but the particle size effect is proportional to the diameter to the fourth power, thus increasing the inertia of an agglomerate, and the force tending to pull it apart, by a factor of 6·5.

# CHAPTER NINE

## FURTHER RESEARCH POSSIBILITIES

Despite the operating guidelines which can be extracted from this work, the successful design of a fluidised bed granulator requires further information which must be obtained by experimentation. It is envisaged that future research will fall into five major categories:
(1.) The feasibility of supplying all of, or a substantialamount of, the heat for evaporation through the bed wall remains to be demonstrated. Direct wall heating should result in greater heat efficiency and energy savings and, for example, would allow the use of steam heating in external jackets. Initially, direct heating should be attempted under conditions which have been shown to be successful with preheating of the fluidising air. Other methods of bed heating remain unproved; for example, using combustion products as the fluidising gas or the use of in-bed electrical heaters, which could be separated from the feed zone in a multi-compartment bed and therefore avoid caking problems.
(2.) There is a need to develop instrumentation which will detect instabilities in a fluidised bed granulator and which can therefore be used to prevent bed quenching. Changes in bed temperature can be used to predict quenching but are insufficiently sensitive. The measurement of pressure fluctuations has been tried and proved unsuccessful. The most promising technique, and one on which work is in progress at University College London, is the use of thermistors to measure localised heat flux from which heat transfer coefficients can be estimated.
(3.) Knowledge of the physical properties of the materials to be granulated, and one or two trial runs in equipment such as that used in this work would enable the tentative design of a granulator to be executed. However, no scale-up information exists and some fundamental questions are unanswered. For example, should scale-up be based on the bed cross-sectional area or on the bed volume? Experiments must be conducted with different bed geometries (varying the bed depth and bed diameter) in order to determine the effect on quenching and therefore on the maximum permitted feedrates of binder and liquid. Consideration must also be

given to scale-up of feed nozzles; are multiple nozzles necessary in order to increase the capacity of the granulator?

(4.) With the exception of pharmaceutical granulation, which is usually conducted on a relatively small scale, the applications of fluidised bed granulation require continuous operation. Application of the theories and practice of continuous crystallisation should be useful in the design of continuous granulation systems; in particular the concept of the population balance could be used, especially where layered growth occurs. The effect of residence time distribution on the drying of particles and associated feed material (particularly where the particles are porous), and therefore on quenching and particle growth, must be determined. Development work on methods for the production of nuclei and for solids feeding will be required.

(5.) Experimental work is needed with materials of industrial interest, beginning with laboratory scale equipment and moving eventually to pilot plant studies. It would be instructive to granulate materials which have previously been the subject of fluidised bed granulation studies (for example, sodium chloride or sodium sulphate) using the principles elucidated in the current work. Fluidised bed granulation might be used to advantage with hitherto untried materials; food substances that require spray drying followed by agglomeration, for example coffee; or the agglomeration of catalyst powder prior to pelletization (the advantage of a fluidised bed technique lying in the reduction of expensive material losses because of the potentially enclosed system).

REFERENCES


1. Davidson, J.F. and Harrison, D., (Ed.). "Fluidisation", Academic Press, 1971.

2. Botterill, J.S.M., "Fluid-bed heat transfer", Academic Press, 1975.

3. Priestley, R.J., Chem. Eng., 9th July, 1962, 125.

4. Nienow, A.W. and Rowe, P.N., "Fluid bed granulation", Separation Process Services, Harwell, December 1975.

5. Mortensen, S. and Hovmand, S., "Particle formulation and agglomeration in a spray granulator", paper presented to Engng. Found. Conf. on Fluidisation, California, 1975.

6. Pictor, J.W.D., Proc. Eng., June (1974), 66-67.

7. Nielsen, B., "The Anhydro typhoon bed for drying and granulation", paper presented to 6th International Conf. on Powder Techn., Birmingham, 1979.

8. "Niro Spray Fluidizer", Niro Atomiser Ltd., Copenhagen, Denmark.

9. "Calmic Mark II Fluid bed dryer", Calmic Engineering Division, William Boulton Ltd., Burslem, Stoke-on-Trent, England.

10. Pratt, D.C.F. and Jones, E.A., Australian Pat. 219907, (1959).

11. Allied Chemical Corp., British Pat. 1370578, (1974).

12. Foster-Pegg, R.W., British Pat. 1395505, (1975).

13. Legler, B.M., Chem. Eng. Prog.Symp. Series, 66(105), (1970), 167-174.

14. Jonke, A.A., Petkus, E.J., Loeding, J.W. and Lawroski, S., Nucl. Sci. Eng., 2, (1957), 303 - 319.

15. Loeding, J.W. and Jonke, A.A., 2nd U.N. Conf. on Peaceful uses of Atomic Energy, Geneva, 18, (1958), 56.

16. Frantz, J.F., Ph.D. Thesis, Louisiana State University, 1958.

17. Rankell, A.S., Scott, M.W., Lieberman, H.A., Chow, F.S. and Battista, J.V., J. Pharm. Sci., 53, (1964), 320 - 324.

18. Ormos, Z., Hungarian J. Ind. Chem., 1, (1973), 207 - 228.

19. Ormos, Z., Pataki, K. and Csukas, B., Hungarian J. Ind. Chem., 1, (1973), 307 - 328.

20. Ormos, Z., Pataki, K. and Csukas, B., Hungarian J. Ind. Chem., 1, (1973), 463 - 474.

21. Ormos, Z., Pataki, K. and Csukas, B., Hungarian J. Ind. Chem., 1, (1973), 475 - 492.

22. Ormos, Z., Pataki, K. and Csukas, B., "Granulation in a mechanically agitated fluidised bed", paper presented to 5th CHISA Conf., Prague, Czechoslovakia, August 1975.

23. Dunlop, D.D., Griffen, L.I. and Moser, J.F., Chem. Eng. Prog., 54(8), 1958, 39 - 43.

24. Philoon, W.C., Sanders, E.F. and Trask, W.T., Chem. Eng. Prog., 56(4), (1960), 106 - 112.

25. Scott, M.W., Lieberman, H.A., Rankell, A.S. and Battista, J.V., J. Pharm. Sci., 53, (1964), 314 - 319.

26. Vance, S.W. and Lang, R.W., Chem. Eng. Prog., 66(7), (1970), 92 - 93.

27. Davies, W.L. and Gloor, W.T., J. Pharm. Sci., 60, (1971), 1869 - 1874.

28. Metheny, D.E. and Vance, S.W., Chem. Eng. Prog., 58(6), (1962), 45 - 48.

29. Barsukov, E.Y. and Soskind, D.M., Int. Chem. Eng., 13 (1973), 84 - 86.

30. Bjorklund, W.J. and Offutt, G.F., A.I. Ch. E. Symp. Ser., 69(128), (1973), 123 - 129.

31. Garside, J. and Mullin, J.W., "Crystallisation", Separation Process Services, Harwell, April 1974.

32. Gluckman, M.J., Yerushalmi, J. and Squires, A.M., "Defluidisation characteristics of sticky or agglomerating beds", paper presented to Eng. Found. Conf. on Fluidisation, California, 1975.

33. Whalley, B.J.P. and Lau, I., "Instrumental anticipation of defluidisation of heated beds of caking coals", paper presented to 27th Canadian Chem. Eng. Conf., Calgary, Canada, October 1977.

34. Cooke, M.J. and Hodgkinson, N., Inst. of Fuel Symp. Ser., No. 1, (1975), C2-1 to C2-9.

35. Mathur, K.B. and Epstein, N., "Spouted Beds", Academic Press, 1974.

36. Romankov, P.G., in "Fluidisation", Davidson, J.F. and Harrison, D., (Ed.), Academic Press, 1971.

37. Markvart, M., Vanecek, V. and Drbohlav, R., Brit. Chem. Eng., 7, (1962), 503 - 507.

38. Shakhova, N.A., Polyakov, N.N., Mikhailov, V.V. and Tikhonov, I.D., Int. Chem. Eng., 13, (1973), 658 - 661.

39. Legler, B.M., Chem. Eng. Prog., 63(2), (1967), 75 - 82.

40. Hawthorn, E., Shortis, L.P. and Lloyd, J.E., Trans. I. Chem. E., 38, (1960), 197 - 215.

41. Fukomoto, T., Maeda, K. and Matagi, Y., Nucl. Sci. Eng., 7, (1970), 137 - 144.

42. Otero, A.R. and Garcia, V.G., Chem, Eng. Prog. Symp. Ser., 66(105), (1970), 267 - 276.

43. Gonzalez, V. and Otero, A.R., Powd. Tech., 7, (1973), 137 - 143.

44. Lee, B.S., Chu, J.C., Jonke, A.A. and Lawroski, S., A.I. Ch.E. J., 8, (1962), 53 - 58.

45. Bakhshi, N.N. and Chai, C.Y., Ind. Eng. Chem. (Proc. Des. and Dev.), 8, (1969), 275 - 279.

46. Meissner, H.P. and Mickley, H.S., Ind. Eng. Chem., 41, (1949), 1238 - 1242.

47. McCarthy, D., Yankel, A.J., Patterson, R.G. and Jackson, M.L., Ind. Eng. Chem. (Proc. Des. and Dev.), 15, (1976), 266 - 272.

48. D'Amore, M., Donsi, G. and Massimilla, L., Powd. Tech., 23, (1979), 253 - 259.

49. Dell, R.M. and Wheeler, V.J., Trans. Far. Soc., 58, (1962), 1590 - 1607.

50. Buckham, J.A., Lakey, L.T. and McBride, J.A., Chem. Eng. Prog. Symp. Ser., 60(53), (1964), 20 - 31.

51. Parker, H.W. and Stevens, W.F., A. I. Ch. E. J.,5, (1959), 314 - 318.

52. Jackson, J.D., Sorgenti, H.A., Wilcox, G.A. and Brodkey, R.S., Ind. Eng. Chem., 52, (1960), 795 - 798.

53. Crooks, M.J. and Schade, H.W., Powd. Tech., 19, (1978), 103 - 108.

54. Nalimov, S.P., Todes, O.M. and Radin, S.I., J. Appl. Chem. USSR, 48, (1975), 2073 - 2077.

55. Nikolaev, P.I., Lyandres, S.E. and Vologodskii, L.B., Int. Chem. Eng. 15, (1975), 95 - 96.

56. Grimmett, E.S., A.I. Ch. E. J.,10, (1964), 717 - 722.

57. Wurster, D.E., J. Amer. Pharm. Ass., 48, (1959), 451 - 454.

58. Wurster, D.E., J. Amer. Pharm. Ass., 49, (1960), 82 - 84.

59. Singiser, R.E., Heiser, A.L. and Prillig, E.B., Chem. Eng. Prog. 62(6), (1966), 109 - 115.

60. Ormos, Z., Csukas, B. and Pataki, K., "Granulation and coating in a multicell fluidised bed", paper presented to Eng. Found. Conf. on Fluidisation, California, 1975.

61. Buckham, J.A., Ayers, A.L. and McBride, J.A., Chem. Eng. Prog. Symp. Ser., 62(65), (1966), 52 - 63.

62. Bakhshi, N.N. and Nihilani, A., Proc. of Int. Symp. on Fluidisation, Toulouse, (1973), 534 - 544.

63. Berquin, Y.F., Gen. Chim., 86, (1961), 45.

64. Uemaki, O. and Mathur, K.B., Ind. Eng. Chem. (Proc. Des. and Dev.), 15, (1976), 504 - 508.

65. Robinson, T. and Waldie, B., Trans. I. Chem. E., 57, (1979), 121 - 127.

66. Mann, U., Ind. Eng. Chem. (Proc. Des. and Dev.), 17, (1978), 103 - 106.

67. Hardesty, J.O., Chem. Eng. Prog. Symp. Ser., 60(48), (1964), 46 - 53.

68. Barlow, C.G., Chem. Engnr., July / August, (1968), CE196 - CE200.

69. Newitt, D.M. and Conway-Jones, J.M., Trans. I. Chem. E., 36, (1958), 422 - 442.

70. Capes, C.E. and Danckwerts, P.V., Trans. I Chem. E., 43, (1965), 116 - 123.

71. Kapur, P.C. and Fuerstenau, D.W., Ind. Eng. Chem. (Proc. Des. and Dev.), 5, (1966), 5 - 10.

72. Linkson, P.B., Glastonbury, J.R. and Duffy, G.J., Trans. I. Chem. E., 51, (1973), 251 - 259.

73. Sherrington, P.J., Chem. Engnr., July / August, (1968), CE201 - CE215.

74. Johnson, M.C.R., Rees, J.E. and Sendall, F., J. Pharm. Pharmacol., 27, (1975), 80P.

75. Davies, W.L. and Gloor, W.T., J. Pharm. Sci., 61, (1972), 618 - 622.

76. Davies, W.L. and Gloor, W.T., J. Pharm. Sci., 62, (1973), 170 - 171.

77. Randolph, A.D. and Larson, M.A., "Theory of particulate processes", Academic Press, 1971.

78. Shakhova, N.A., Yevdokimov, B.G. and Ragozina, N.M., Proc. Techn. Int., December, (1972), 946 - 947.

79. Grimmett, E.S., Chem. Eng. Prog. Ser., 62(67), (1966), 93 - 100.

80. Butensky, M. and Hyman, D., Ind. Eng. Chem. (Fundam.), 10, (1971), 212 - 219.

81. Capes, C.E., Germain, R.J. and Coleman, R.D., Ind. Eng. Chem. (Proc. Des. and Dev.), 16, (1977), 517 - 518.

82. Rumpf, H. and Schubert, H., J. Chem. Eng. Japan, 7, (1974), 294 - 298.

83. Pietsch, W.B., J. Eng. Ind. (Trans. A.S.M.E.), May, (1969), 435 - 449.

84. Pietsch, W.B. and Rumpf, H., Proc. Int. Coll. CNRS, Paris, (1966), 213 - 235.

85. Pietsch, W.B., Can. J. Chem. Eng., 47, (1969), 403 - 409.

86. Brook, D.B. and Marshall, K., J. Pharm. Sci., 57, (1968), 481 - 484.

87. Fairchild, H.J. and Michel, F., J. Pharm. Sci., 50, (1961), 966 - 969.

88. Ganderton, D. and Selkirk, A.B., J. Pharm. Pharmacol., 22, (1970), 345 - 353.

89. Harwood, C.F. and Pilpel, N., J. Pharm. Sci., 57, (1968), 478 - 481.

90. Gold, G., Duvall, R.N., Palermo, B.T. and Hurtle, R.L., J. Pharm. Sci. 60, (1971), 922 - 925.

91. Fonner, D.E., Banker, G.S. and Swarbrick, J., J. Pharm. Sci., 55, (1966), 181 - 186.

92. Marks, A.M. and Sciarra, J.J., J. Pharm. Sci., 57, (1968), 497 - 504.

93. Hunter, B.M., J. Pharm. Pharmacol., 25, (1973), 111 P.

94. Rowe, P.N., MacGillivray, H.J. and Cheesman, D.J., Trans. I. Chem. E., 57, (1979), 194 - 199.

95. Rowe, P.N., Chem. Eng. Sci., 28, (1973), 979 - 980.

96. Rowe, P.N. and Nienow, A.W., Powd. Tech., 15, (1976), 141 - 147.

97. Masters, K., "Spray Drying", 2nd Ed., George Godwin, 1976.

98. Allen T., "Particle Size measurement", 2nd Ed., Chapman and Hall, 1975.

99. Herdan, G., "Small particle statistics", Butterworths, 1960.

100. Weast, R.C., "Handbook of Chemistry and Physics", 55th Ed., CRC Press, 1974.

101. Leva, M.,"Fluidisation", McGraw-Hill, 1959.

102. Rowe, P.N., in "Fluidisation", Davidson, J.F. and Harrison, D., (Ed.), Academic Press, 1971.

103. Sokolovskii, A.A., Groshev, G.L. and Danov, S.M., Int. Chem. Eng., 11, (1971), 238 - 241.

104. Shakhova, N.A. and Minaev, G.A., Int. Chem. Eng., 13, (1973), 65 - 68.

105. Richardson, J.F. and Ayers, P.,Trans. I. Chem. E., 37, (1959), 314 - 322.

106. Kettenring, K.N., Manderfield, E.L. and Smith, J.M., Chem. Eng. Prog. 46, (1950), 193 - 145.

107. Kunii, D. and Levenspiel, O., "Fluidisation Engineering", John Wiley, 1969.

108. Brunauer, S., Emmett, P.H. and Teller, E., J. Amer. Chem. Soc., 60, (1938), 309 - 319.

109. Gregg, S.J. and Sing, K.S.W., "Adsorption, Surface area and Porosity", Academic Press, 1967.

110. Computer Library, Dept. of Chemical and Biochemical Engineering, University College London.

LIST OF SYMBOLS

| | | |
|---|---|---|
| $a$ | Thickness of growth layer (layered growth model) | m |
| $A$ | Bed cross-sectional area | $m^2$ |
| $A_s$ | Surface area of pores | $m^2$ |
| $A_z$ | Total particle surface area in evaporation zone available for heat transfer | $m^2$ |
| $b$ | Mass of binder in a single granule | kg |
| $B$ | Constant for Ostwald viscometer | $m^2\ s^{-2}$ |
| $c$ | Heat capacity | $J\ kg^{-1}\ K^{-1}$ |
| $\Delta c$ | Methanol vapour concentration difference (driving force for mass transfer) | - |
| $d$ | Diameter | m |
| $d_p$ | Particle diameter | m |
| $d^1$ | Diameter of particle with concentric growth layer (layered growth model) | m |
| $d_p$ (sv) | Surface-volume mean particle diameter | μm |
| $d_p$ (wm) | Weight-moment mean particle diameter | μm |
| $\delta d$ | Sieve size interval | m |
| $D$ | Bed diameter | m |
| $D_g$ | Granule diameter | m |
| $D_z$ | Diameter of evaporation zone | m |
| $E_i$ | Mass ratio of binder to initial particles for sieve fractions i = 1, 2, 3 ... | - |
| $f$ | Fraction of granule voids occupied by binder | - |
| $f_v$ | Volume shape factor | - |
| $F$ | Weight fraction of liquid in an agglomerate (Capes' model, Ch. 2). | - |
| $g$ | Ratio of granule diameter to initial particle diameter | - |
| $g$ | Accleration due to gravity (App. A) | $m\ s^{-2}$ |
| $G$ | Mass of a single granule | kg |

| | | |
|---|---|---|
| h | Particle to fluid heat transfer coefficient | $W\ m^{-2}\ K^{-1}$ |
| h | Height of liquid in capillary tube (App. A) | m |
| H | Fluidised bed height | m |
| $H_z$ | Height of evaporation zone | m |
| J | Absolute humidity | - |
| k | Ratio of void volume to solid volume in an agglomerate | - |
| k | Particle to fluid mass transfer coefficient | $m\ s^{-1}$ |
| K | Parameter in Capes' model (Ch. 2) | - |
| L | Length of viscometer capillary | m |
| m | Mass of a single initial particle | kg |
| m | Mass of liquid in capillary tube (App. A) | kg |
| M | Total mass of bed particles | kg |
| $M_b$ | Mass of binder | kg |
| n | Number of particles in a fluidised bed | - |
| n | Number of granules | - |
| dN | Number of particles in size interval $\delta d$ | - |
| NAR | Normalised air ratio (volumetric ratio of atomising air to liquid feed) | - |
| p | Mass of particles in a granule | kg |
| $\Delta p$ | Pressure drop across viscometer | Pa |
| P | Product discharge rate | $kg\ s^{-1}$ |
| PSD | Particle size distribution | - |
| q | Ratio of binder density to initial particle density (Ch. 3) | - |
| q | Rate of heat transfer | W |
| $q_w$ | Rate of heat input through bed wall | W |
| $q_L$ | Rate of heat losses | W |

| | | |
|---|---|---|
| $Q$ | Volumetric flowrate of fluidising gas | $m^3 s^{-1}$ |
| $Q(T_B)$ | Volumetric flowrate of fluidising gas at temperature $T_B$ | $m^3 s^{-1}$ |
| $Q_{mf}(T_B)$ | Volumetric flowrate of fluidising gas at minimum fluidising conditions and temperature $T_B$ | $m^3 s^{-1}$ |
| $r$ | Initial particle radius | m |
| $r$ | Capillary radius (App. A) | m |
| $R$ | Volumetric flowrate of solution | $m^3 s^{-1}$ |
| $R^1$ | Growth constant (Ch. 2) | $m s^{-1}$ |
| $R^{11}$ | Growth constant (Ch. 2) | $m^{-1}$ |
| $s$ | Dimensionless measure of withdrawal of binder from granule surface (agglomeration model) | - |
| $S$ | Surface area | $m^2$ |
| $t$ | Time | min |
| $t$ | Spraying time for short feed-time experiments (Ch. 4) | s |
| $T$ | Temperature | $^oC$ |
| $T_B$ | Nominal bed operating temperature | $^oC$ |
| $T_1$ | Room temperature | $^oC$ |
| $T_z$ | Average zone temperature | $^oC$ |
| $\Delta T$ | Temperature difference (driving force for heat transfer) | K |
| $U$ | Superficial gas velocity through fluidised bed | $m s^{-1}$ |
| $U_{mf}$ | Superficial gas velocity at minimum fluidising conditions | $m s^{-1}$ |
| $U(T_B)$ | Superficial gas velocity at temperature $T_B$ | $m s^{-1}$ |
| $U_{mf}(T_B)$ | Minimum fluidising velocity at temperature $T_B$ | $m s^{-1}$ |
| $v$ | Volume of feed, short feed-time experiments (Ch. 4) | $m^3$ |
| $V$ | Volume of solution in viscometer (App. A) | $m^3$ |
| $V$ | Volume of a particle | $m^3$ |
| $V_g$ | Envelope volume of a granule | $m^3$ |

| | | |
|---|---|---|
| $V_b$ | Volume of binder per particle | $m^3$ |
| $\Delta V$ | Volume difference | $m^3$ |
| $w_m$ | Rate of mass transfer (Ch. 7) | $m^3\ s^{-1}$ |
| $w$ | Feedrate of solution | $kg\ s^{-1}$, $m^3\ s^{-1}$ |
| $W$ | Mass of wet agglomerated particles | kg |
| $W_a$ | Mass flowrate of fluidising gas | $kg\ s^{-1}$ |
| $x_s$ | Mass fraction of solute in feed | - |
| $x_o$ | Methanol vapour concentration at particle surface | - |
| $x_\infty$ | Methanol vapour concentration in mixture of air and vapour | - |
| $y$ | Volumetric ratio of binder to particles in the bed | - |
| $Z$ | Bed hold-up | kg |

Greek symbols

| | | |
|---|---|---|
| $\beta$ | Ratio of initial particle diameter to granule diameter ( = 1 / g) | - |
| $\varepsilon$ | Voidage | - |
| $\theta$ | Intrinsic bridge strength | $Nm^{-2}$ |
| $\lambda$ | Latent heat of vaporisation (Ch. 2) | $J\ kg^{-1}$ |
| $\lambda$ | Volumetric fraction of voids in a mass of particles | - |
| $\mu$ | Viscosity | Pa s |
| $\rho$ | Density | $kg\ m^{-3}$ |
| $\rho_e$ | Envelope density | $kg\ m^{-3}$ |
| $\rho_B$ | Bulk density | $kg\ m^{-3}$ |
| $\sigma$ | Volumetric fraction of solids in a mass of particles | - |
| $\tau$ | Surface tension | $N\ m^{-1}$ |
| $\varphi_i$ | Combined mass sieve fractions i - 1, 2, 3 ... | - |
| $\Psi$ | Total strength of a granule | $N\ m^{-2}$ |

Subscripts

| | |
|---|---|
| a | Air |
| b | Binder |
| f | Fluid |
| g | Granule |
| i | Inlet |
| i | Integral number |
| j | Feed |
| L | Liquid |
| o | Outlet |
| p | Particle |
| s | Solids |
| v | Vapour |
| z | Zone |

# APPENDICES

## APPENDIX A PHYSICAL PROPERTIES OF PARTICLES, GRANULES AND SOLUTIONS

### Initial particle size and minimum fluidising velocity

Table A1 lists the mean particle diameters and minimum fluidising velocities of the particles used for granulation experiments.

Table A1 Mean particle diameter and minimum fluidising velocity

| | $d_p$ (sv) (μm) | $d_p$ (wm) (μm) | $U_{mf}$ ($ms^{-1}$. $10^2$) |
|---|---|---|---|
| alumina: | 272 ± 13 | 300 ± 12 | 4·7 ± 0·2 |
| small glass powder: | 270 ± 32 | 308 ± 19 | 7·4 ± 1·4 |
| large glass powder | 437 ± 18 | 471 ± 20 | 16·6 ± 1·3 |

The mass of particles charged to the bed at the beginning of an experiment was that required to give a packed depth of 0·12 m; 1·580 kg of alumina and 2·545 kg of glass powder.

The minimum fluidising velocity was determined in the usual way from a plot of bed pressure drop against superficial gas velocity through the bed. The bed was first vigorously fluidised for several minutes and the flow then reduced in stages and the pressure drop ($\Delta p$) recorded at each velocity. Pressure drop was measured with a simple probe which consisted of a metal tube 0·005 m in diameter with a wire gauze over one end, small enough to prevent the passage of particles. The other end of the tube was connected to one leg of a monometer. Fig. A1 shows a $U_{mf}$ plot for glass powder particles. By convention, minimum fluidising velocity is taken as the intersection of the pressure drop lines for fixed bed and fluidised bed respectively.

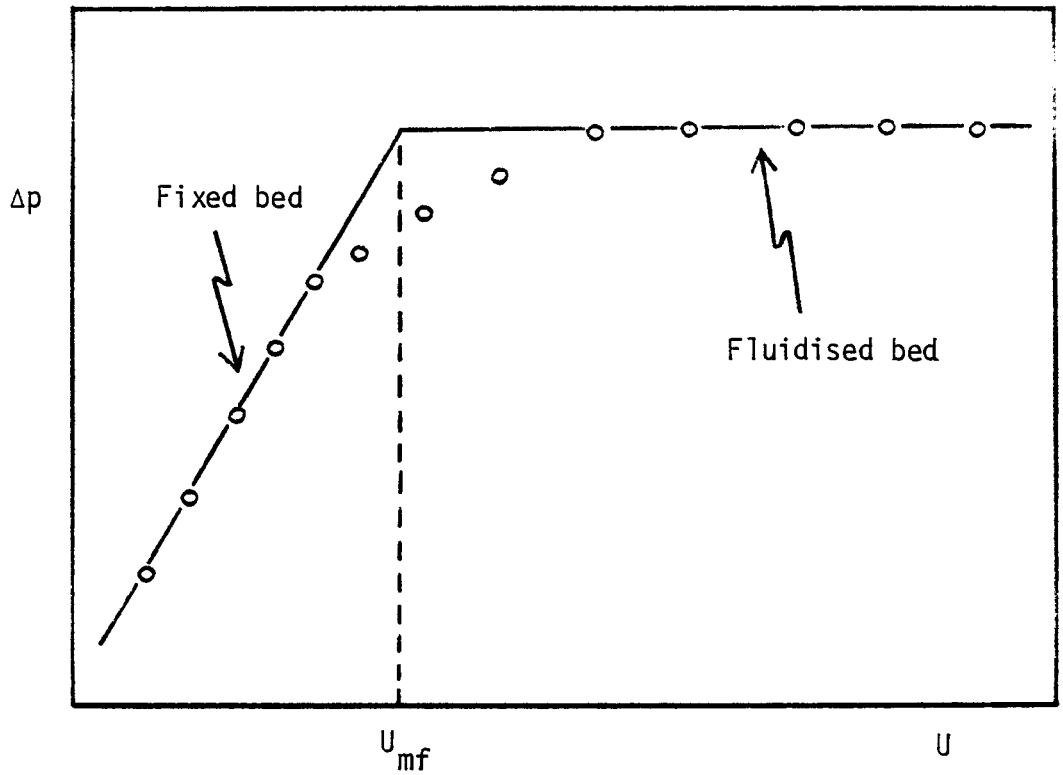


Fig. A1 Pressure drop / velocity curve to determine minimum fluidising velocity

Densities of initial particles

The material or real density ($\rho_p$) of glass powder was determined by measurements with a conventional specific gravity bottle, but the density of alumina cannot be measured in this way because of its porosity. Consequently the standard quoted[100] value for aluminium oxide has been taken for alumina. The envelope density ($\rho_e$) of alumina (i.e. that calculated from the mass of a particle and its volume if the pores were sealed at the external particle surface) was measured in a pyknometer, with mercury as the fluid. The envelope density for a non-porous solid

(e.g. glass powder) is the same as the material density. Bulk density ($\rho_B$) was measured by determining the packed volume of a sample of known weight in a graduated cylinder. The inter-particle voidage ($\varepsilon$) was calculated from Equ. A1.

$$\varepsilon = 1 - \frac{\rho_B}{\rho_e} \qquad \text{(A1)}$$

Table A2 Density and voidage of initial particles

| | $\rho_p$ | $\rho_B$ | $\rho_e$ | $\varepsilon$ |
|---|---|---|---|---|
| alumina: | 3·97 | 0·91 | 1·49 | 0·39 |
| small glass powder: | 2·20 | 1·28 | 2·20 | 0·42 |
| large small powder: | 2·20 | 1·28 | 2·20 | 0·45 |

Units of density are kg $m^{-3}$ x $10^{-3}$.

Porosity and internal surface area of alumina

A measure of the porosity of alumina was obtained by filling the pores with water and observing the increase in weight. The alumina was first soaked in distilled water overnight and then surface dried with absorbent paper and quickly weighed. The weight of absorbed water was measured by drying to constant weight in an oven, allowing the alumina to reach equilibrium moisture content at room temperature, and reweighing. Thus, using the real density of alumina and the density of water, a value for the porosity can be calculated. An average of three determinations gave the porosity to be 0·708 of the particle envelope volume.

The fraction of the porosity filled with benzoic acid (see Section 6.7.1) can be estimated using this value. The weight of a bed of alumina particles (envelope density, 1·490 x $10^3$ kg $m^{-3}$) is 1·580 kg. The total intra-particle porosity in the bed is therefore:

$$\frac{1{\cdot}58o \times 0{\cdot}708}{1{\cdot}49 \times 10^3} \ m^3$$

$$= 7{\cdot}507 \times 10^{-4} \ m^3$$

From Table 6.11, 0·389 kg of benzoic acid (real density, $1{\cdot}27 \times 10^3$ kg $m^{-3}$) was sprayed during the no-growth period. The volume of deposited benzoic acid is therefore:

$$\frac{0{\cdot}389}{1{\cdot}27 \times 10^3} \ m^3$$

$$= 3{\cdot}063 \times 10^{-4} \ m^3$$

Therefore the volume of porosity occupied is:

$$\frac{3{\cdot}063 \times 10^{-4}}{7{\cdot}507 \times 10^{-4}} \times 100 \ \%$$

$$= \underline{40{\cdot}8 \ \%}$$

The internal surface area of the alumina was determined by measuring the nitrogen adsorption isotherm and applying the method of Brunauer, Emmett and Teller, i.e. the B.E.T. equation.[108] A conventional pressure - volume apparatus[109] was used in which successive known amounts of gas are admitted to the adsorbent material, kept at a temperature of 77 K. The volume of adsorbed gas can then be calculated from the gas laws and from the pressure of unadsorbed gas remaining above the sample. It was not possible to measure the internal surface of benzoic acid impregnated alumina because under vacuum the benzoic acid sublimed and was lost from the sample. However, measurements were possible with carbowax impregnated alumina.

Density and shape factor of granules

An attempt to measure the density of glass powder / carbowax granules was made using a specific gravity bottle and a liquid, di-iso-propylether, in which carbowax did not dissolve. The resultant density was close to that of the constituent glass powder particles (see Section 6.3.3) and it can only be assumed that liquid seeped into the granule interior because of voids which were open to the exterior surface, giving a false value.

The volume shape factor of glass powder / carbowax agglomerates

(defined by Equ. 6.4) was determined by estimating the volume of the granule and dividing by the cube of an assumed diameter. The images of granules photographed on 35 mm film were projected by a microfilm reader and their outlines traced onto paper. Fig. A2 shows a typical outline. A PCD plotter was then used to transfer the coordinates of the outline onto paper tape. The granule volume was calculated (assuming it to be a body of revolution) by means of a computer program[110] and an IBM 360 / 65 digital computer. The second largest dimension (i.e. the sieve diameter) was measured from the outline in arbitrary units. (The volume was calculated in the same units.) Eight determinations were made giving $f_v$ to be: 0·34, 0·39, 0·37, 0·41, 0·40, 0·38, 0·46 and 0·52 with an arithmetic average of 0·41.

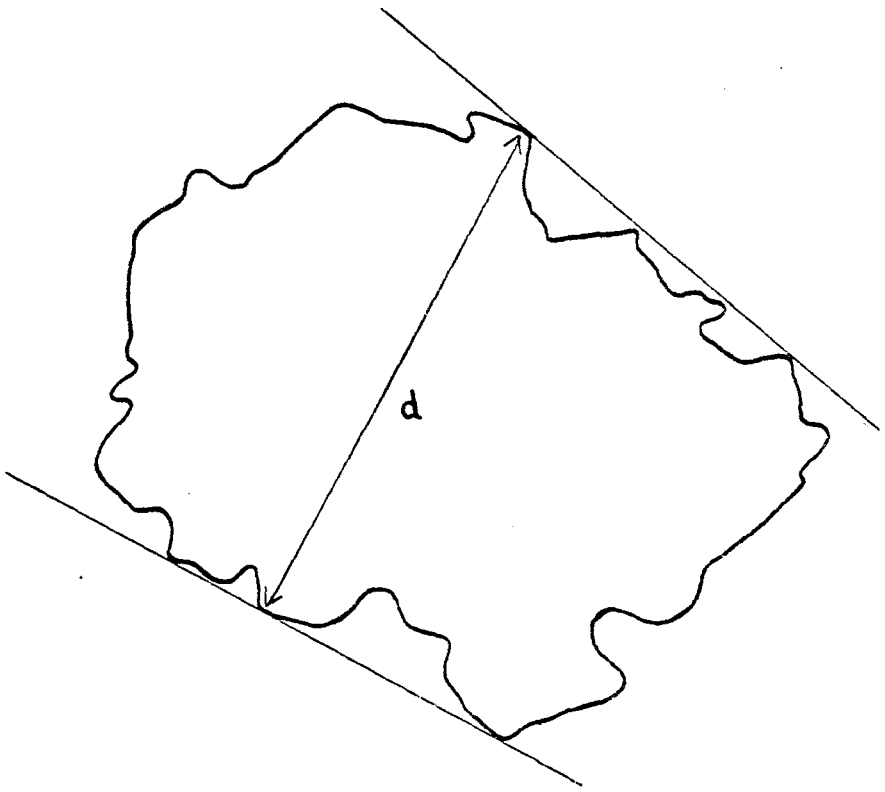


Fig. A2 Measurement of granule shape factor: outline of a typical granule

Physical properties of the binder solutions: viscosity, surface tension and density

The viscosities of solutions of benzoic acid in methanol and of carbowax in methanol were measured as a function of solute concentration, at 25° C and at 40° C, the latter being the nominal bed operating temperature for most of the granulation experiments. An Ostwald capillary tube viscometer was used for these measurements primarily because such apparatus restricts evaporation from volatile liquids and because the loss of fluid due to evaporation is less critical than in, for example, a concentric cylinder viscometer where end effects (possibly caused by evaporation) are important. An Ostwald viscometer is also simple to use and is adequate to demonstrate the difference in viscosity between the two fluids of interest here. The viscosity of a liquid is determined by measuring the time of flow t of a given volume of liquid V through a vertical capillary tube, under the influence of gravity. For an incompressible fluid, the rate of flow is given by the Poiseuille law:

$$\frac{dV}{dt} = \frac{\pi r^4 \Delta p}{8 \mu L} \qquad (A2)$$

where r and L are the radius and length respectively, of the capillary, and $\Delta p$ is the pressure drop across it.

$$\Delta p = \rho g L \qquad (A3)$$

and thus for a given V, Equ. A2 reduces to:

$$\frac{\mu}{\rho} = B t \qquad (A4)$$

where B is an apparatus constant determined by calibration with a liquid of known viscosity (in this case water) and $\rho$ is the liquid density.

The apparatus, which is illustrated in Fig. A3, was immersed in a constant temperature water bath fitted with glass sides. Sufficient solution was placed in the viscometer so that when it was drawn up above point X there was still liquid in the left-hand bulb. After releasing the suction the time of flow between points X and Y was measured with a

stop watch. This procedure was repeated twice, without refilling the viscometer, and the average of the three readings used to calculate the solution viscosity. Capillary tubes of larger radii were used for the more viscous solutions.

The surface tensions of the binder solutions were measured by the capillary tube method, in which the surface tension forces acting around the circumference of a liquid meniscus in a capillary tube are equated with the weight of the liquid column. The apparatus, shown in Fig. A4, consisted of a capillary tube C the end of which was submerged in a reservoir of solution, R. The position of the tube was adjusted so that the pin P just touched the liquid surface and the height of the bottom of the meniscus was then measured by a travelling microscope, TM. The position of the point P was also recorded and hence the height of the liquid column, h, could be determined.

If the liquid has a contact angle of zero, i.e. the liquid surface is a tangent to the inside of the tube, then the surface tension forces act vertically downwards and are exactly balanced by the weight of liquid in the tube. Hence:

$$2 \pi \tau = mg \qquad (A5)$$

where $\tau$ = surface tension, $r$ = radius of the tube and $m$ = the mass of liquid in the tube. But:

$$m = \pi r^2 h \rho \qquad (A6)$$

$$\text{therefore } \tau = \frac{r h g \rho}{2} \qquad (A7)$$

from which the surface tension is calculated. This method relies on the liquid contact angle being zero and also ignores the small mass of liquid above the bottom of the meniscus.

The solution densities were measured with $1{\cdot}0 \times 10^{-5}$ $m^3$ capacity specific gravity bottles. The densities of solutions of benzoic acid and of carbowax in methanol, as a function of concentration, are given

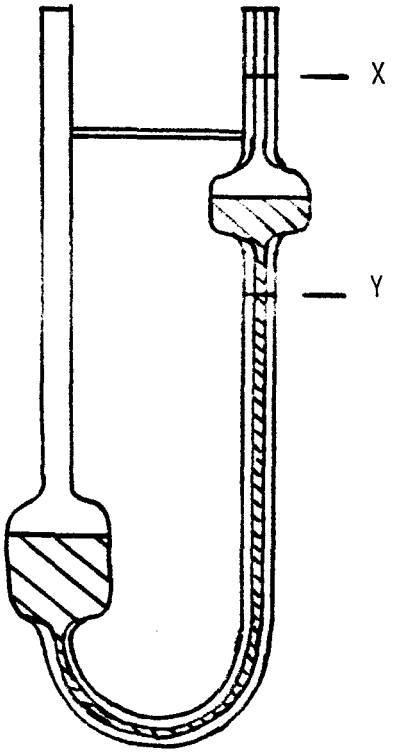


Fig. A3 Ostwald capillary tube viscometer

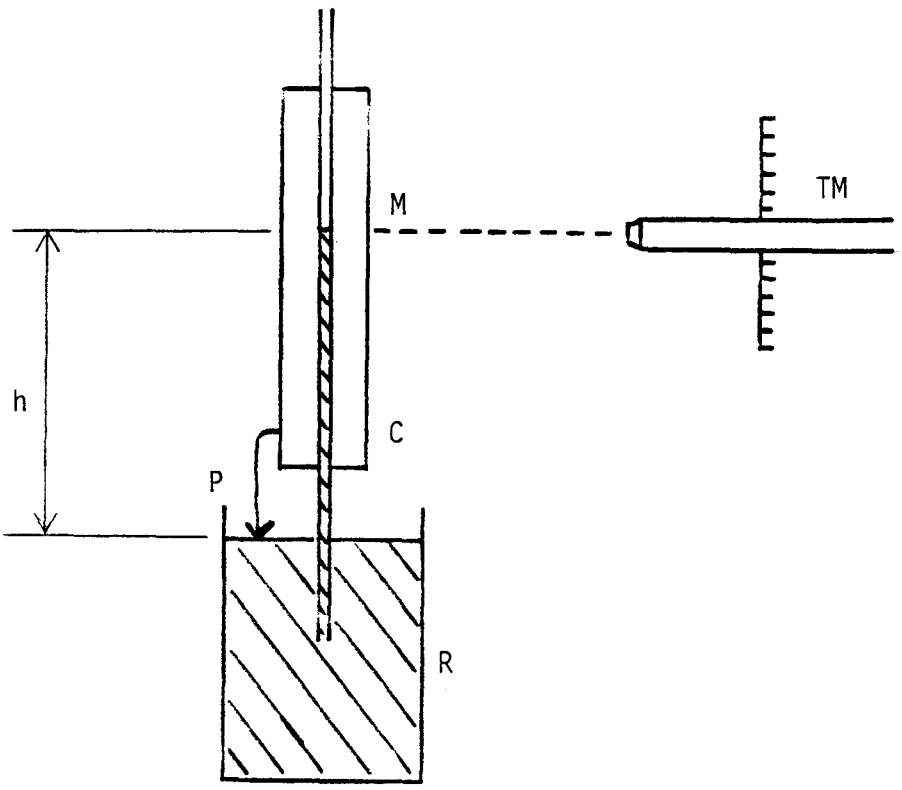


Fig. A4 Measurement of surface tension by the capillary tube method

in Table A3. The variation of solution viscosity with concentration is shown in Figs. A5 and A6 and surface tension as a function of concentration in Fig. A7.

Table A3 Densities of benzoic acid and carbowax solutions (in methanol)

| Binder concentration (wt. %) | Solution density (kg $m^{-3}$) at 25° C | |
|---|---|---|
| | Benzoic acid | Carbowax |
| 1·0 | - | 800·0 |
| 5·0 | - | 805·0 |
| 10·0 | 821·0 | 820·0 |
| 20·0 | 849·0 | 848·0 |
| 30·0 | 884·0 | 873·0 |
| 40·0 | 917·0 | - |
| 50·0 | - | 939·0 |
| 75·0 | - | 1030·0 |

The density of pure methanol at 20° C is 791·4 kg $m^{-3}$.

Densities of benzoic acid and carbowax

The density of carbowax (as it would form on a fluidised bed particle) was measured by taking a known weight of granular carbowax (as supplied) and melting it in a graduated cylinder by placing the cylinder in a laboratory oven at a temperature above 55° C (the approximate melting point). It was then left to cool and the volume occupied by the solidified carbowax was measured. The density was computed to be 1060·0 kg $m^{-3}$.

The density of benzoic acid is given[100] as 1266·0 kg $m^{-3}$.

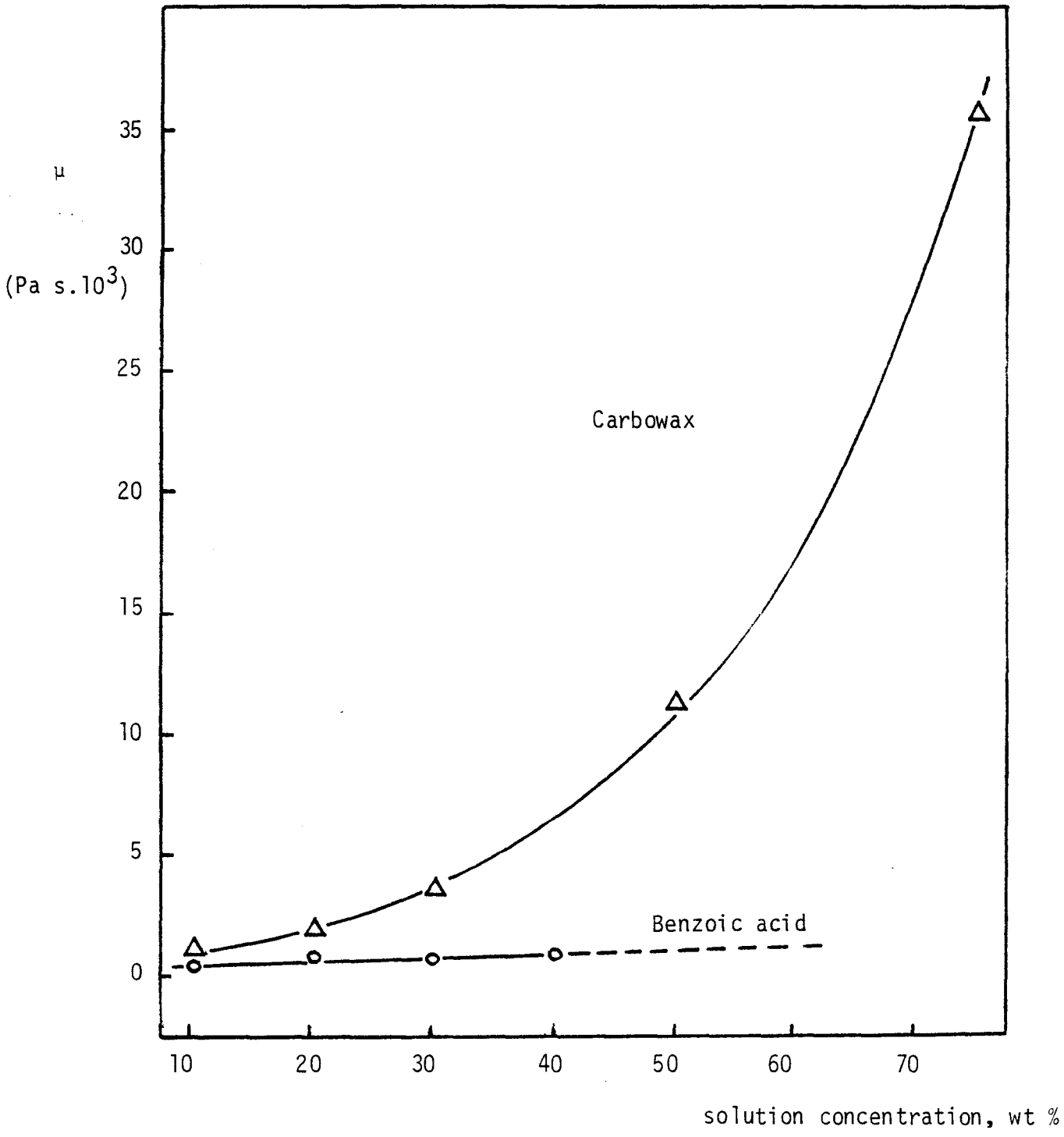


Fig. A5 Binder solution viscosity as a function of concentration at 40° C

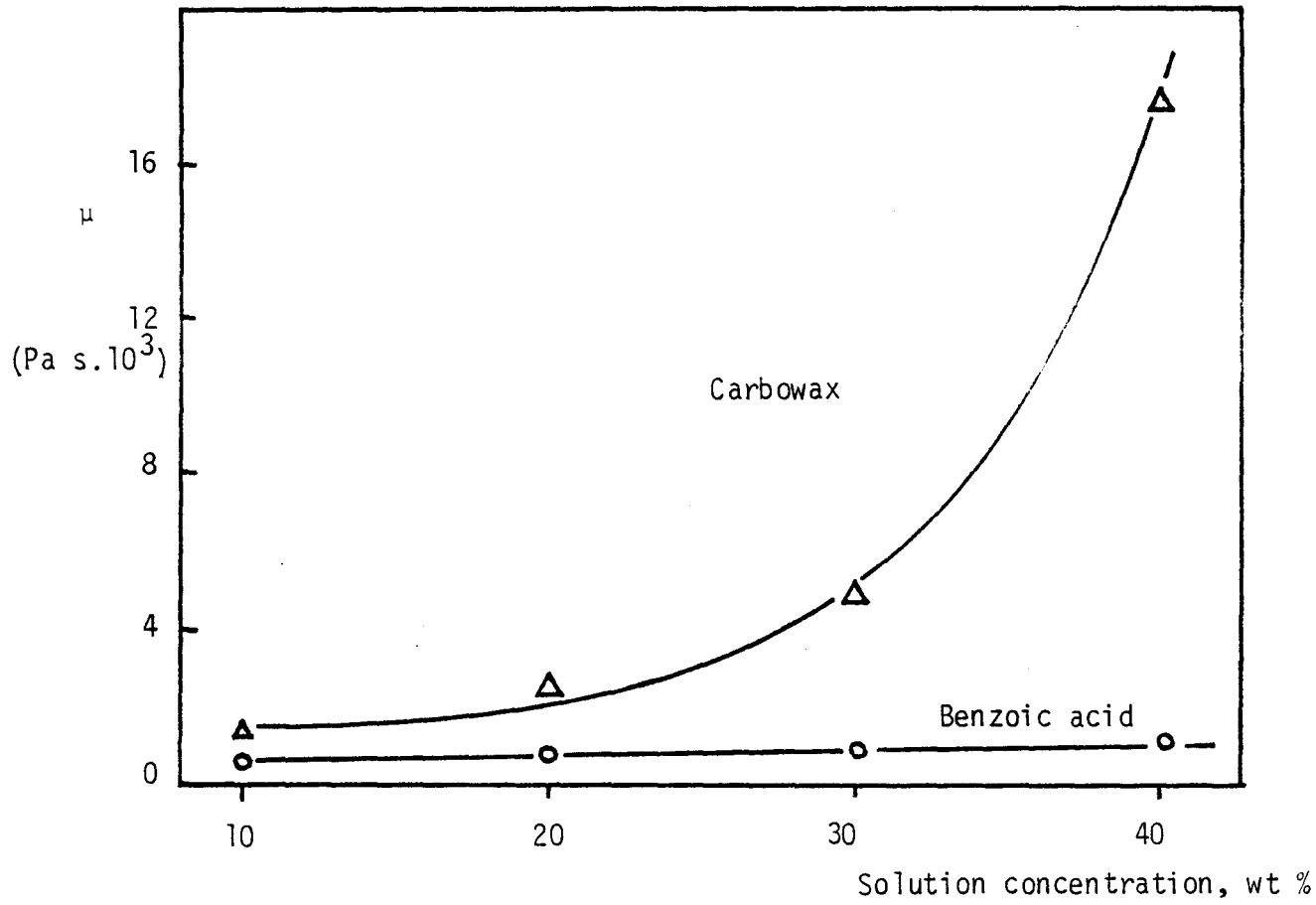


Fig. A6 Binder solution viscosity as a function of concentration at 25° C

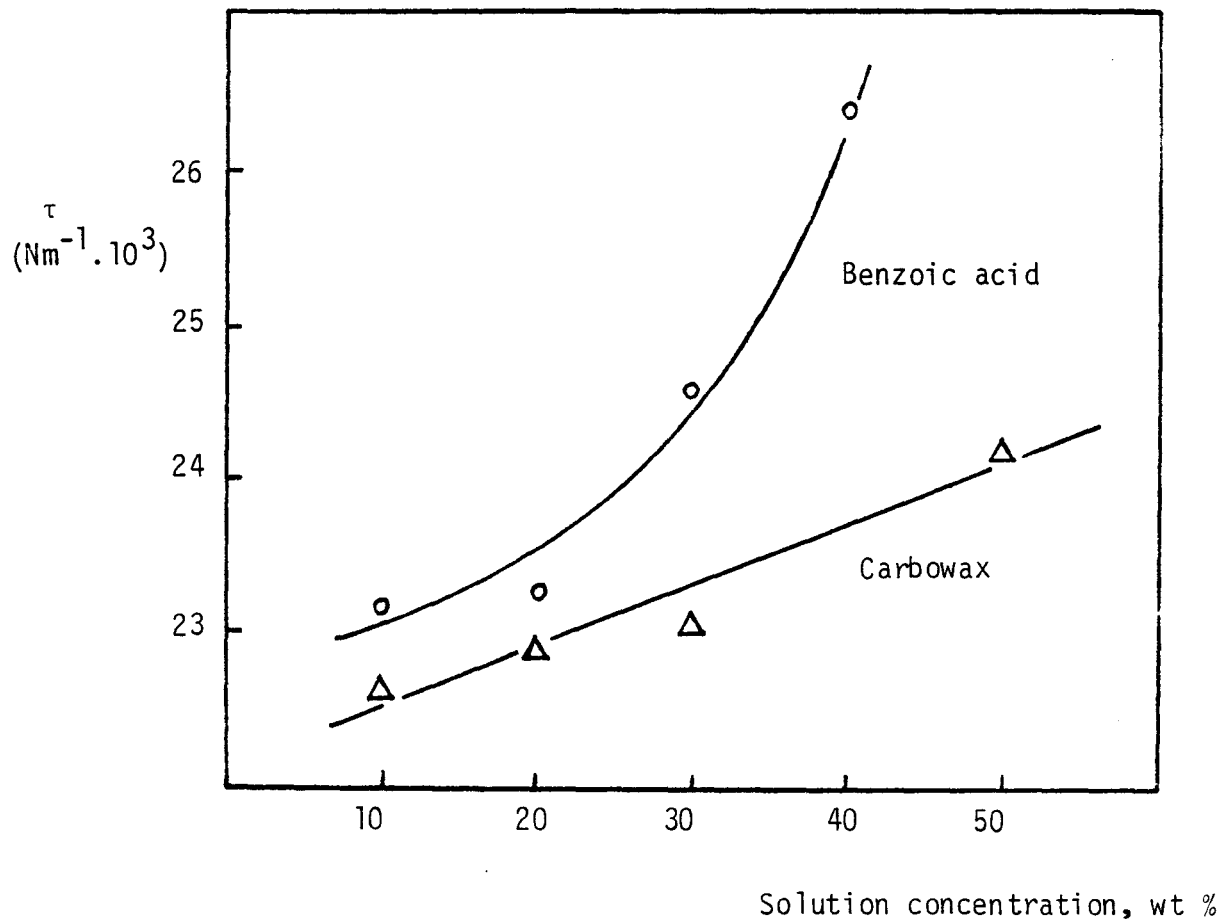


Fig. A7 Binder solution surface tension as a function of concentration at 22° C

## APPENDIX B DETAILS OF X-RAY EQUIPMENT

### Granulation experiments; evaporative conditions

The X-ray apparatus was supplied by Todd Research Ltd. and consisted of a Triton Mark IV generator (maximum output 1000 mA at 132 kV) coupled to a Mullard Guardian 150 tube. An X-ray beam was produced which passed through the fluidised bed and was intensified by a Phillips 0·23 m (9") diameter image intensifier with an average brightness intensification of 1000 times. A 35 mm Ariflex camera with a 0·05 m / f2 lens was used to expose Ilford HP5 film. The radiographic factors, which determine the exposure of the film, were found by trial and error. The values used were: 0·8 mAs, 800 mA, 75 kV giving a one millisecond pulse and a filming time of about five seconds.

### Ambient temperature experiments

The X-ray tube was a Machlett Dynamax Super 50 - 60 B with a Phillips 9 / 5 image intensifier (gain = 5000 times). A 16 mm Bolex cine camera (0·025 m / f1·4 lens) was used in addition to the 35 mm camera. The radiographic factors were: 0·8 mAs, 800 mA, 56 kV, a one millisecond pulse with a filming time of about eight seconds. For the 16 mm film: 1·6 mAs, 320 mA, 63 kV and a filming time of about ten seconds at 48 frames per second.

### Film analysis

A microfilm reader was used to study the 35 mm film, some still photographs are reproduced in Chapter Seven. The optical density of individual frames was determined with a Vitatron Densitometer. The 16 mm film was projected either at 16 or 2 frames per second and thus could be slowed down by up to 24 times.

## APPENDIX C SUPPLEMENTARY FIGURES TO CHAPTER SIX

Figs. C1 to C3 are agglomeration model plots for the different granulation conditions of Table 6.5. Fig. C4 shows that the existence of the no-growth period (see Section 6.7.1) is not a function of either excess gas velocity or of bed temperature.

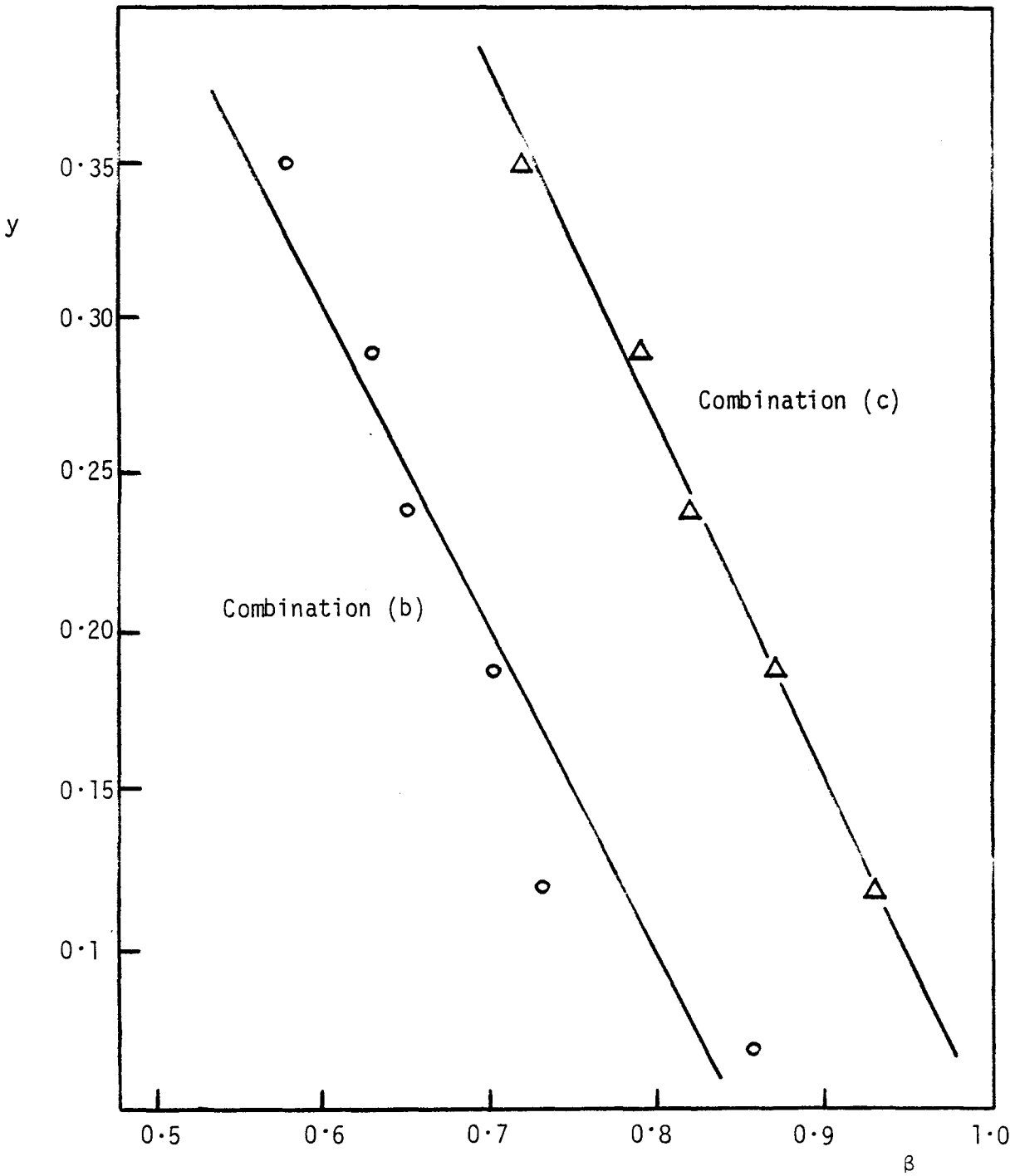


Fig. C1 Agglomeration model plot: glass powder, 1% carbowax, $U - U_{mf} = 0{\cdot}40\ ms^{-1}$

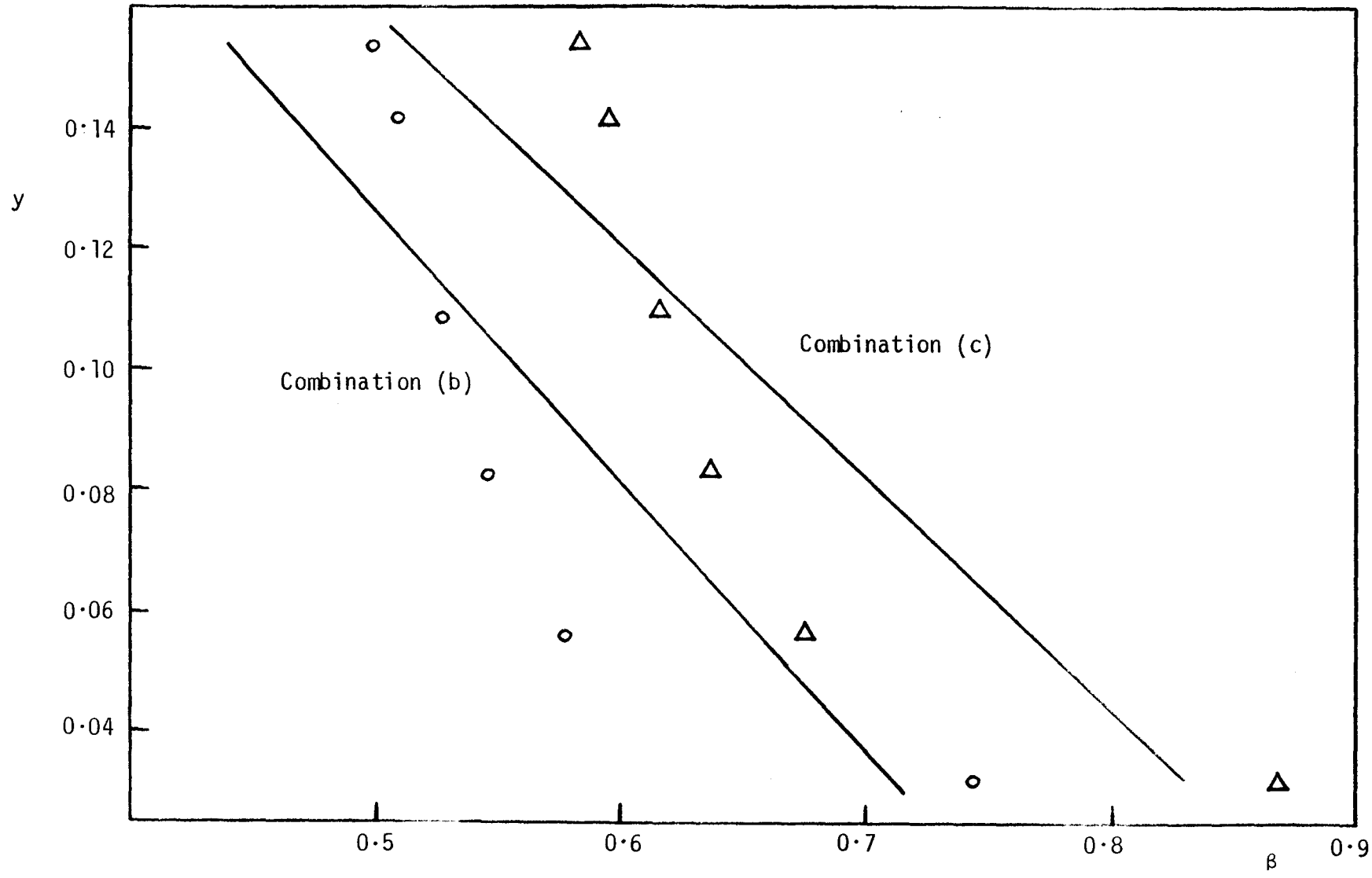


Fig. C2 Agglomeration model plot: glass powder, 5% carbowax, $\frac{U - U_{mf}}{} = 0{\cdot}65$ ms

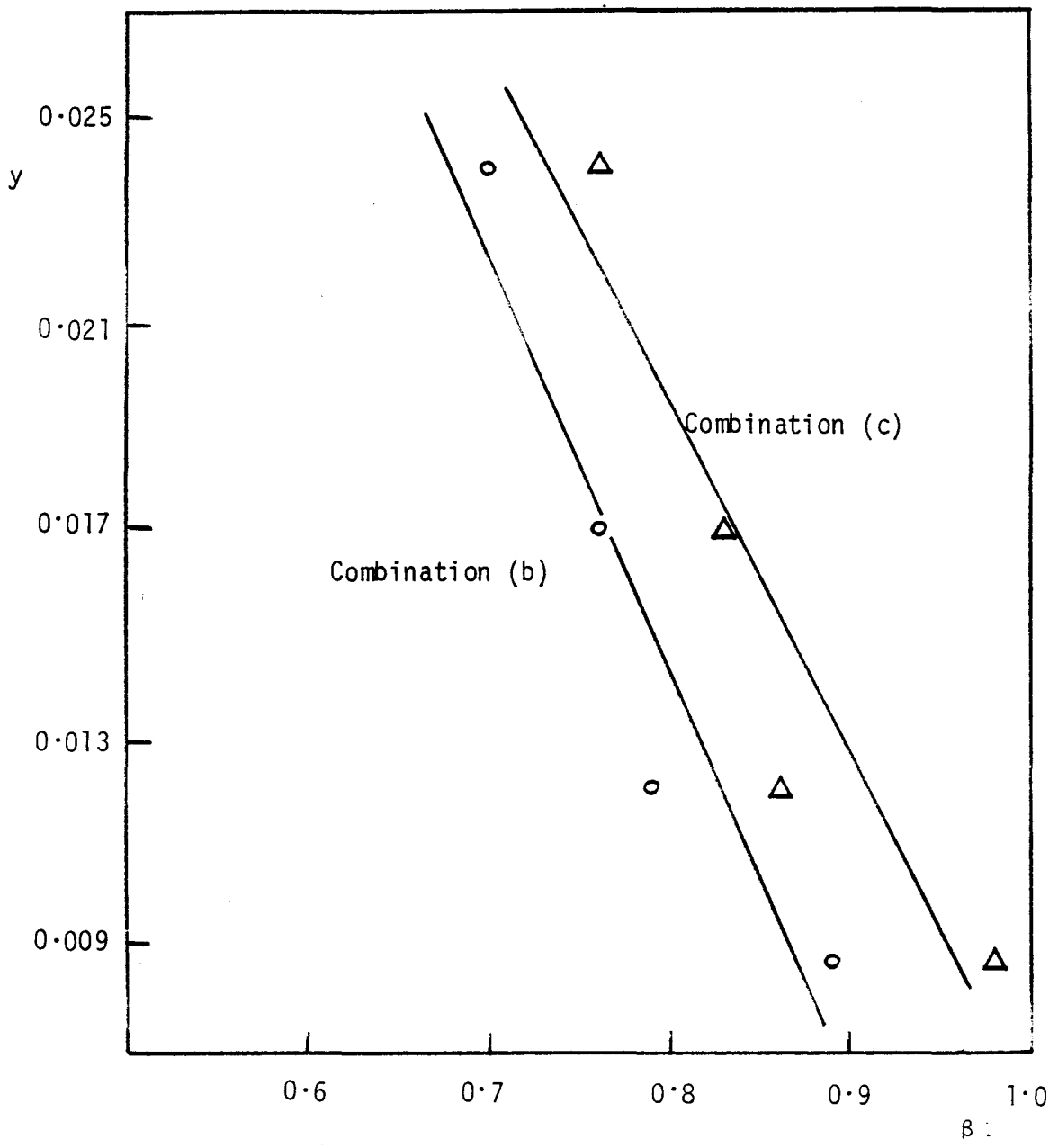


Fig. C3 Agglomeration model plot: glass powder, 5% carbowax, $U - U_{mf}$ = 0·525 $ms^{-1}$

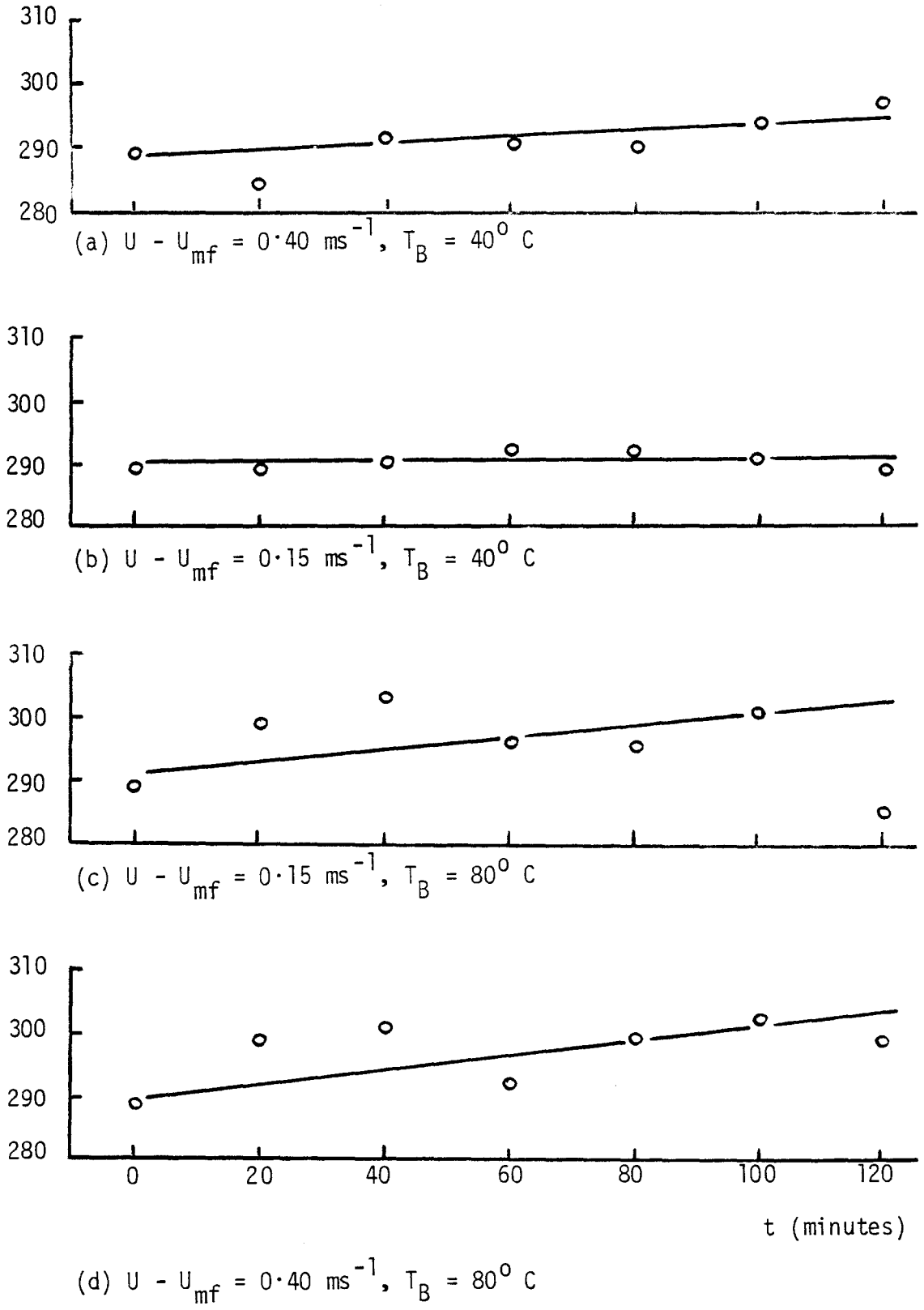


Fig. C4 No-growth period as a function of bed temperature and of gas velocity

## APPENDIX D HEAT AND MASS TRANSFER CALCULATIONS

### Calculation of total particle surface area available for heat transfer

If the total mass of particles in the bed is M, their density $\rho_p$ and their diameter is $d_p$, then the total number of particles in the bed is given by:

$$n = \frac{6M}{\pi\, d_p^3\, \rho_p} \qquad (D1)$$

The ratio of zone volume to bed volume is $D_z^2\, D_z \,/\, D^2\, H$ and the surface area of a single particle is $\pi\, d_p^2$, therefore the particle surface area in the zone is given by:

$$A_z = \frac{6M}{\pi\, d_p^3\, \rho_p} \cdot \frac{D_z^2\, H_z}{D^2\, H} \cdot \pi\, d_p^2 \qquad (D2)$$

and

$$A_z = \frac{6M\, D_z^2\, H_z}{d_p\, \rho_p\, D^2 H} \qquad (D3)$$

### Calculation of heat transfer coefficient

For the example of Fig. 7.7:

$$q = h\, A_z\, \Delta T \qquad (D4)$$

$$q = w\, \lambda \qquad (D5)$$

$w = 2{\cdot}1 \times 10^{-4}$ kg $s^{-1}$

$\lambda = 1{\cdot}14 \times 10^{6}$ J $hg^{-1}$

$A_z = 0{\cdot}464$ $m^2$

$\Delta T = (44 - 36) = 8$ K

$$\therefore\ h = \frac{2{\cdot}1 \times 10^{-4} \times 1{\cdot}14 \times 10^{6}}{0{\cdot}464 \times 8} \quad W\, m^{-2}\, K^{-1}$$

$$h = 64{\cdot}5 \ W\, m^{-2}\, K^{-1}$$

### Calculation of mass transfer coefficient

Mass transfer is assumed to take place between particles, whose surface is entirely covered by liquid methanol, and the surrounding mixture of air and methanol vapour in the zone. The mass transfer coefficient

is defined by:

$$w_m = k\, A_z\, \Delta c \qquad (D6)$$

The log mean concentration driving force ($\Delta c$) is calculated from the difference between the equilibrium partial pressure of methanol vapour at the liquid interface ($x_0$) and the partial pressure of the vapour in the zone ($x_\infty$). $x_0$ is equal to the vapour pressure of methanol divided by the total system pressure (= atmospheric) and $x_\infty$ is given by the volumetric fraction of vapour in the mixture of vapour, atomising air and fluidising air in the zone volume. Referring to Fig. D1, $\Delta c$ is defined by:

$$\Delta c = \frac{\Delta x_1 - \Delta x_2}{\ln (\Delta x_1 / \Delta x_2)} \qquad (D7)$$

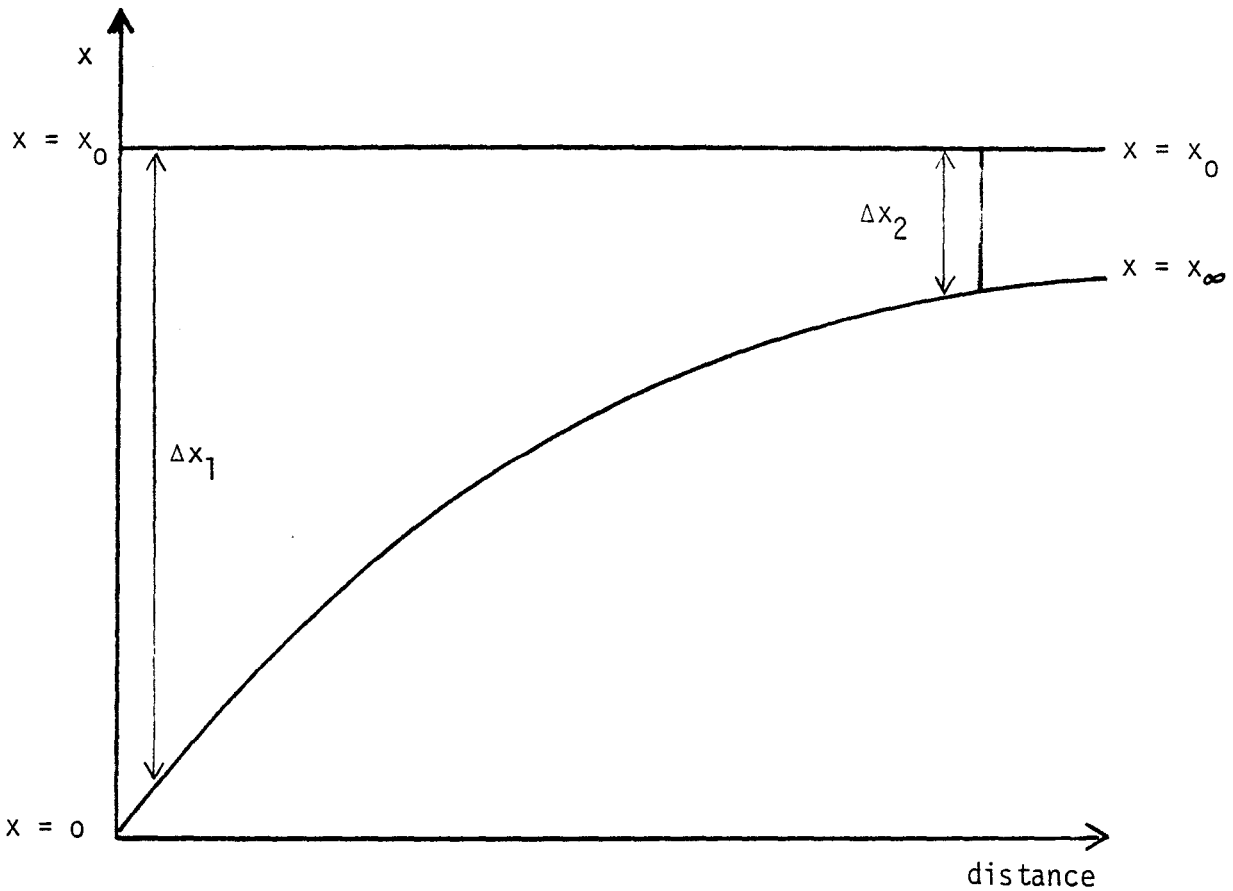


Fig. D1 Definition of log mean concentration difference

Thus, for the example of Fig. 7.7:

Vapour pressure of methanol at $44^{o}$ C = 306·6 mm Hg, therefore $x_o$ = 306·6 / 760·0 = 0·403.

atomising air flowrate = $1{\cdot}3 \times 10^{-4}$ $m^3 s^{-1}$

fluidising air flowrate through the zone = $4{\cdot}0 \times 10^{-4}$ $m^3 s^{-1}$

methanol vapour flow = $1{\cdot}7 \times 10^{-4}$ $m^3 s^{-1}$

$$\therefore \quad x_\infty = \frac{1{\cdot}7 \times 10^{-4}}{(1{\cdot}7 + 1{\cdot}3 + 4{\cdot}0) \times 10^{-4}}$$

$$= 0{\cdot}243$$

Therefore,

$$\Delta c = \frac{(0{\cdot}403 - 0) - (0{\cdot}403 - 0{\cdot}243)}{\text{In } (0{\cdot}403 / 0{\cdot}160)}$$

$$= 0{\cdot}263$$

$$w = 1{\cdot}7 \times 10^{-4} \ m^3 s^{-1}$$

therefore, substituting into Equ. D6;

$$k = \frac{1{\cdot}7 \times 10^{-4}}{0{\cdot}464 \times 0{\cdot}263} \quad ms^{-1}$$

$$= 1{\cdot}39 \times 10^{-3} \ ms^{-1}$$

6th IChemE Annual Research Meeting, UCL, London, April 1979

# A STUDY OF FLUID BED GRANULATION

by

P G Smith and A W Nienow*

## INTRODUCTION

Fluidised bed granulation is the term applied to a variety of processes including pharmaceutical granulation[1] and the drying of solutions.[2] Although some fundamental studies have been undertaken,[3] little has been published in the UK, save an extensive review.[4] In this study several bed particle/feed solution combinations have been used. Different binders dissolved in the feed solvent are responsible for different particle growth mechanisms.

## PRELIMINARY TESTS

Preliminary, short-time experiments showed that bed particle structure, gas velocity and the method and rate of feeding the solution were critical operating parameters. If the particles were porous (alumina), water evaporation rates of $9 \times 10^{-3}$ kg $s^{-1}m^{-2}$ could be sustained indefinitely whilst under otherwise identical conditions, non-porous particles (Ballotini) become "wet-quenched" and defluidisation resulted. In addition, a 10% sodium chloride solution sprayed at $1.8 \times 10^{-4}$ kg $s^{-1}$ onto alumina for 140 hours produced no significant change of particle size.

The need for careful positioning of the feed nozzle and a minimum level of atomisation was established. With the nozzle above the bed surface, spray drying of the atomised feed occurred as well as solute deposition (caking) on the spray nozzle and bed walls. These effects were eliminated when the nozzle was placed just below the bed surface. If the feed was not atomised at all, almost instantaneous wet-quenching occurred.

The importance of gas velocity was indicated by spraying 15% calcium chloride at room temperature into beds of alumina. Spraying was for very short time periods and at high rates in order to simulate the initiation of agglomeration. It was found that the mass of wet, aggregated material in the bed decreased markedly with increasing gas velocity.

## GRANULATION EXPERIMENTS

Current experiments are conducted in a 0.15 m diameter, open-topped, glass bed, with the particles being fluidised by electrically preheated air. Solution is fed via a metering pump and is sprayed into the bed by a twin-fluid atomising nozzle, positioned just below the fluidised bed surface. The change of particle size distribution with time is determined by sieving, over periods of time up to 10 hours. The quality of fluidisation during this period is also followed by visual observation and by temperature measurements.

## RESULTS AND DISCUSSION

### a) "Onion" Ring Growth

Using a bed of glass powder and a feed of $2.3 \times 10^{-5}$ kg $s^{-1}$ benzoic acid and dissolved in methanol (10% solution), an evaporation rate of $2.25 \times 10^{-4}$ kg $s^{-1}$ ($1.27 \times 10^{-2}$ kg $s^{-1}$ $m^{-2}$) has been sustained over a period of 3 hours at an excess gas velocity of 0.275 m $s^{-1}$, and for 10 hours at $U - U_{mf} = 0.525$ m $s^{-1}$. The weight-moment mean diameter, after 2 hours' operation, reached 895 μm and

*Department of Chemical and Biochemical Engineering, University College London

605 μm respectively, compared with an initial particle size of 295 μm. This effect of gas velocity is similar to that indicated by the short-time experiments.

Mass balances have established that up to 97% of the benzoic acid remains adhered to the bed particles and observations with an optical microscope show that the extent of particle-particle agglomeration, at for example $U - U_{mf}$ = 0.525 m $s^{-1}$, is very small. This suggests that a layering mechanism of growth is dominant and indeed the experimental results are in agreement with a simple model which assumes a uniform rate of binder deposition on uniformly sized spherical particles. Fig. 1 shows a plot of experimental surface-volume mean diameter and theoretical particle diameter (calculated from the binder input) respectively, against time.

With the benzoic acid/glass powder system a degree of agglomeration is observed at the lower gas velocities. If the extent of agglomeration, and hence particle size, is a function of excess gas velocity then it is to be expected that as the layering mechanism begins to predominate (at higher velocities) particle size will become independent of velocity. This is borne out by fig. 2, in which each point is the result of a separate experiment.

b) Growth by Agglomeration

Agglomeration of glass powder is observed to a much greater extent if carbowax is used in place of benzoic acid. This is shown by a comparison of particle size distributions, produced with the two binders, in fig. 4, and can also be clearly seen by low-power microscope observations. Mean particle diameters (weight-moment) after 2 hours, at a nominal $U - U_{mf}$ of 0.525 m $s^{-1}$, are 930 μm and 1900 μm with 1% and 5% carbowax solutions respectively. In the latter case it is necessary to periodically increase the gas flowrate to avoid wet-quenching and defluidisation.

c) Effect of particle porosites

Alumina, under the same conditions that produce growth with glass powder, remains unchanged for several hours and then undergoes rapid particle growth. The sudden change from zero to finite growth corresponds to a blocking of the pores with benzoic acid and confirms the importance of porosity indicated by the short-time experiments. Growth rates of alumina beyond this point are similar to those of the non-porous glass powder from time zero, as indicated in fig. 3.

REFERENCES


1. Davies and Gloor, J. Pharm. Sci., 60 (1971) 1869
2. Fukomoto et al., J. Nucl. Sci. Tech., 7 (1970) 137
3. Ormos et al., Hungarian J. Ind. Chem., 1 (1973) 307
4. Rowe and Nienow, 'State of the Art Report', SPS Harwell (1975)

FIG. 1

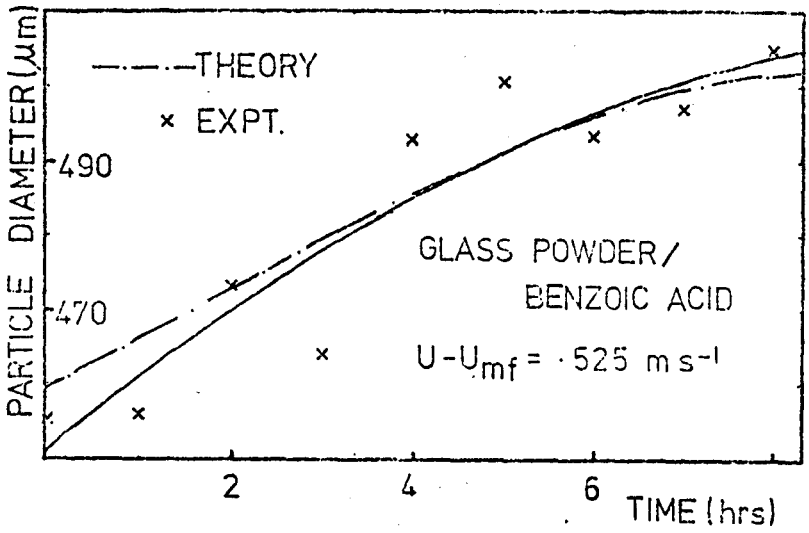


FIG. 2

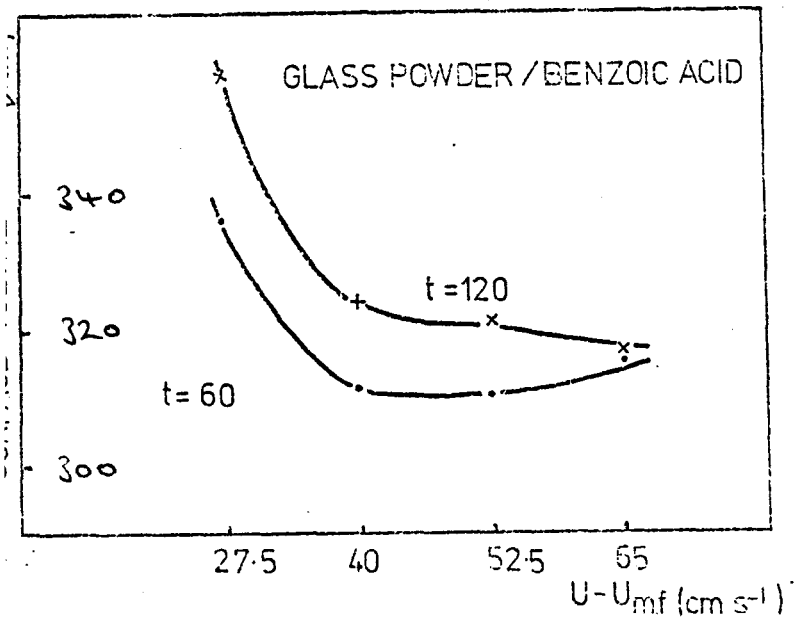


FIG. 3

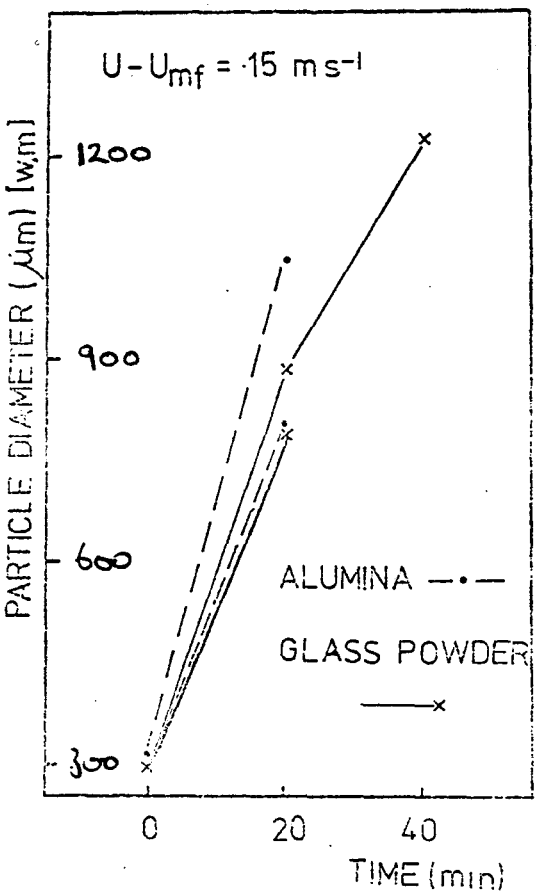


FIG. 4 (a)

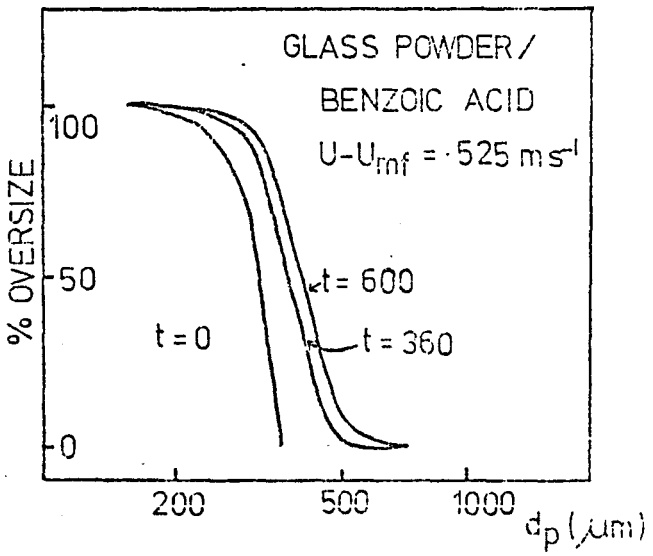


FIG 4 (b)